

Durham E-Theses

Sterically hindered chiral transition metal complexes

Brian Michael Bridgewater

How to cite:

Bridgewater, Brian Michael (1998) Sterically hindered chiral transition metal complexes. Doctoral thesis, Durham University.

Use policy

The full-text may be used and/or reproduced, and given to third parties in any format or medium, without prior permission or charge, for personal research or study, educational, or not-for-profit purposes provided that:

- a full bibliographic reference is made to the original source
- a <https://etheses.durham.ac.uk/id/eprint/5022/> is made to the metadata record in Durham E-Theses
- the full-text is not changed in any way

The full-text must not be sold in any format or medium without the formal permission of the copyright holders.

Please consult the [full Durham E-Theses policy](#) for further details.

Sterically Hindered Chiral Transition Metal Complexes

Brian Michael Bridgewater, B.Sc. (Dunelm)

Trevelyan College, University of Durham

The copyright of this thesis rests
with the author. No quotation
from it should be published
without the written consent of the
author and information derived
from it should be acknowledged.

A thesis submitted in part fulfillment of the requirements for the degree of Doctor of
Philosophy at the University of Durham.

October 1998


13 JAN 1999

STATEMENT OF COPYRIGHT

The copyright of this thesis rests with the author. No quotation from it should be published without his prior consent and information derived from it should be acknowledged.

DECLARATION

The work described in this thesis was carried out in the Department of Chemistry at the University of Durham between September 1995 and October 1998. All the work is my own, unless stated to the contrary, and it has not been submitted previously for a degree at this or any other University.

FINANCIAL SUPPORT

The Engineering and Physical Sciences Research Council (EPSRC) are gratefully acknowledged for providing a grant for the work described herein.

ABSTRACT

Sterically Hindered Chiral Transition Metal Complexes

Brian Michael Bridgewater
Trevelyan College

Michaelmas Term 1998
Submitted for Ph. D.

This thesis describes the synthesis, characterization and study of a series of organometallic compounds which all contain the same new ligand, 1-phenyl-3-methyl-4,5,6,7-tetrahydroindenyl. The ligand forms a chiral complex once coordinated, and is relatively bulky when compared with ligands such as cyclopentadienyl or 4,5,6,7-tetrahydroindenyl.

Chapter one of this thesis introduces cyclopentadienyl ligand chirality, cyclopentadienyl metal complex chirality and sterically demanding cyclopentadienyl systems. The synthesis and chemistry of tetrahydroindenes and some applications of chiral cyclopentadienyl metal complexes and their bulky analogues are also reviewed.

Chapter two describes modifications to a literature preparation of the tetrahydroindenone precursor of the new tetrahydroindenyl ligand which lead to higher yields. The synthesis of the ligand itself is described, as well as the synthesis of a benzyldiene-substituted hexahydroindene, which demonstrates a limitation in the flexibility of the synthetic route chosen. The synthesis, characterization and various properties of the following iron(II) compounds are discussed in chapter two; bis-1-phenyl-3-methyl-4,5,6,7-tetrahydroindenyl iron (II), **2.3**, 1-phenyl-3-methyl-4,5,6,7-tetrahydroindenyl iron(II) dicarbonyl dimer, **2.4**, and 1-phenyl-3-methyl-4,5,6,7-tetrahydroindenyl methyl dicarbonyl iron(II), **2.5**. For all these iron complexes, the solid state molecular structures and the absolute configuration of the chiral ligand were determined using single crystal X-ray diffraction. For **2.3** and **2.4**, three isomers are possible, two enantiomers that are collectively termed the *rac*-isomer and a third isomer, the *meso*-isomer. Cyclic voltammetric studies on **2.3** indicate that it has a reversible one electron oxidation at 0.187 V (with respect to a non-aqueous Ag/AgCl standard electrode). The difference between this and the reversible one electron oxidation for $(\eta\text{-C}_5\text{H}_5)_2\text{Fe}$ (with respect to the same standard) is -0.314 V, therefore **2.3** is shown to be much more easily oxidized than $(\eta\text{-C}_5\text{H}_5)_2\text{Fe}$. The solution-state infra-red spectrum of **2.4** is explained, with reference to a literature analysis of the unsubstituted analogue $[\text{CpFe}(\text{CO})_2]_2$. The steric forces present in the various molecular environments are discussed in connection with the degree of phenyl-ring tilt relative to the cyclopentadienyl mean plane and the deviation of the other cyclopentadienyl substituents away from the metal centre. Subsequent reactions of compounds **2.4** and **2.5** are described. Attempts to make linked analogues of the new ligand are summarized in chapter two.

In chapter three, two Zr(IV) compounds are prepared, bis (1-phenyl-3-methyl-4,5,6,7-tetrahydroindenyl) zirconium(IV) dichloride, **3.1**, and bis (1-phenyl-3-methyl-4,5,6,7-tetrahydroindenyl) dimethyl zirconium(IV), **3.2**. Upon crystallization, *rac*-**3.1** spontaneously resolves into crystals containing only one enantiomer. The similarities and differences in the spectroscopic data for the iron(II) compounds of chapter two and the zirconium(IV) compounds of chapter three are discussed and possible explanations offered. The solid state molecular structures of **3.1** and **3.2** were determined by single crystal X-ray diffraction. Experimental details are given in chapter four, whilst the characterizing data are presented in chapter five. Details of the X-ray structure determinations are given in Appendix A.

To my mum.

*“Tho’ much is taken, much abides; and tho’
We are not now that strength which in old days
Moved earth and heaven; that which we are, we are;
One equal temper of heroic hearts,
Made weak by time and fate, but strong in will
To strive, to seek, to find, and not to yield.”*

Alfred Lord Tennyson, *Ulysses*.

“Every time I learn something new,
it pushes some old stuff out of my brain.”

Homer Simpson

ACKNOWLEDGEMENTS

So many people to thank, and yet so little space. First and foremost I would like to thank Dr. Andrew Hughes for all his time and effort, for many enlightening discussions which always cover an incredibly diverse range of chemistry, for his boundless enthusiasm as a teacher, for allowing me to work with him in the first place and most importantly for having the patience to put up with me for three years despite a constant barrage of "Brian's dumb question of the day".

I am indebted to Prof. Judith Howard for all her time and patience in trying to teach this poor chemist the black arts that are crystallography, and for all her help, support and e-mails with regards to helping me get a job! My thanks go to all of the Durham crystallography group who virtually held my hand at the diffractometer whilst I tried to prove that you did actually need years of intensive training to collect data sets and solve structures, properly. Thank you most especially Janet, who has exhibited the patience of a saint in putting up with "Brian's dumb crystallography question of the day".

I wish to thank all the service personnel, technicians, cleaners and everyone else who keep the department running so smoothly and have helped to make my time here at Durham all the more pleasant, not least of whom are Ray and Gordon. Somehow managing to keep smiling even when presented with a vacuum line in substantially more pieces than when it left them, their help in building weird and wonderful apparatus for me has been invaluable and is greatly appreciated.

Now onto the lab-gang, or rather the section-gang, or even department-gang to include everyone who belongs. You all know who you are, and if I tried to thank you all by name I'd sure enough miss someone out and they'd get miffed. So instead I'll just thank you all together, for the laughs (lots), the tears (few), the pies (more) and the beers (some), and in the words of the unfortunately probably immortal Dr. (scary) P. Gemmell, in a very bad Japanese accent, "Don't be a stranger now." However, I must thank Andy "NMFAbba" Johnson individually, not for putting up with me in the lab, not even for buying me all those beers when I was skint, but for his cooking and his singing, without which I would never have learnt (in two opposing ways) the meaning of good food and good music.

Thank you Beth, without you this would never have been written.

Oh, and Rach, who would have believed it, aye?

CONTENTS

Chapter One: Introduction.....	1
1.1 Cyclopentadienyl metal chemistry.....	2
1.2 Chiral cyclopentadienyl metal complexes.....	3
1.2.1 Early work.....	3
1.2.2 Types of cyclopentadienyl metal complex chirality.....	4
1.2.2a Definitions.....	4
1.2.2a(i) Ligand derived chirality.....	4
1.2.2a(ii) Metal centred chirality.....	4
1.2.2a(iii) Ligand derived and metal centred chirality.....	4
1.2.2b Examples.....	5
1.2.2b(i) Ligand derived chirality.....	5
1.2.2b(ii) Metal centred chirality.....	5
1.2.2c(iii) Ligand derived and metal centred chirality.....	5
1.2.3 Types of cyclopentadienyl chirality.....	6
1.2.3a Definitions.....	6
1.2.3a(i) Homotopic ligands.....	7
1.2.3a(ii) Enantiotopic ligands.....	7
1.2.3a(iii) Diastereotopic ligands.....	7
1.2.3b Examples.....	7
1.2.3b(i) Homotopic ligands.....	7
1.2.3b(ii) Enantiotopic ligands.....	7
1.2.3b(iii) Diastereotopic ligands.....	8
1.2.4 Types of chiral cyclopentadienyl ligands.....	9
1.2.4a Monosubstituted cyclopentadienyls.....	9
1.2.4b Annulated cyclopentadienyls.....	10
1.2.4c Disubstituted cyclopentadienyl ligands.....	13
1.2.4d Bridged bis-cyclopentadienyls.....	14
1.2.5 Summary.....	15
1.3 Sterically demanding cyclopentadienyl metal complexes.....	16
1.3.1 Introduction.....	16
1.3.2 Alkyl-substituted cyclopentadienyl ligands.....	19
1.3.2.1 <i>Tert</i> -butyl substituted cyclopentadienyl ligands.....	19
1.3.2.2 Isopropyl substituted cyclopentadienyl ligands.....	23
1.3.2.3 Other alkyl substituents.....	26
1.3.3 Phenyl-substituted cyclopentadienyl ligands.....	26
1.3.4 Silyl-substituted cyclopentadienyl ligands.....	29
1.3.5 Summary.....	35
1.4 Tetrahydroindenones and Tetrahydroindenes.....	35
1.4.1 Introduction.....	35

1.4.2 Tetrahydroindenones.	38
1.4.2.1 Synthesis.	38
1.4.2.2 Nazarov cyclizations.	39
1.4.3 Tetrahydroindenes.	41
1.4.4 Summary.	44
1.5 Applications of Chiral Cyclopentadienyl Metal Complexes.	45
1.5.1 Introduction.	45
1.5.2 Catalytic enantioselective reactions.	45
1.5.2a Hydrogenation.	45
1.5.2b Epoxidation.	45
1.5.2c Alkene isomerisation.	46
1.5.2d Ketone Hydrosilylation.	46
1.5.2e Aldol reactions.	47
1.5.3 Catalytic stereoregular polymerizations.	47
1.5.4 Summary.	51
1.6 References.	51

Chapter Two: Iron(II) Complexes of the Cyclopentadienyl Analogue,

1-Phenyl-3-methyl-4,5,6,7-tetrahydroindenyl.	56
2.1 Introduction.	57
2.2 Ligand chemistry.	58
2.2.1 3-Methyl-2,3,4,5,6,7-hexahydroind-8(9)-en-1-one.	58
2.2.1a Synthesis.	58
2.2.1b Characterization.	59
2.2.1b(i) Nuclear magnetic resonance spectroscopy.	59
2.2.1b(ii) Infra-red spectroscopy.	59
2.2.2 1-Phenyl-3-methyl-4,5,6,7-tetrahydroindene.	61
2.2.2a Synthesis.	61
2.2.2b Characterization.	62
2.2.2b(i) Nuclear magnetic resonance spectroscopy.	62
2.2.2b(ii) Gas-chromatograph mass-spectrometry.	62
2.2.3 1-Benzylidene-3-methyl-2,3,4,5,6,7-hexahydroind-8(9)-ene.	64
2.2.3a Synthesis.	64
2.2.3b Characterization.	64
2.2.3b(i) Gas-chromatograph mass spectrometry (GC-MS).	64
2.2.3b(ii) Nuclear magnetic resonance spectroscopy.	64
2.2.4 Lithium 1-phenyl-3-methyl-4,5,6,7-tetrahydroindene, 2.1A.	67
2.2.5 Summary.	70
2.3 Bis-1-phenyl-3-methyl-4,5,6,7-tetrahydroindenyl iron (II).	70

2.3.1 Introduction.....	70
2.3.2 Discussion.	71
2.3.2a Synthesis.	71
2.3.2b Characterization.	71
2.3.2b(i) Infra-red spectroscopy.....	71
2.3.2b(ii) Nuclear magnetic resonance spectroscopy.	71
2.3.2b(iii) Mass spectrometry.	73
2.3.2b(iv) Powder and single crystal X-ray diffraction solid state molecular structure determination.	73
2.3.2b(v) Cyclic voltammetry.....	81
2.3.3 Summary.	83
2.4 1-Phenyl-3-methyl-4,5,6,7-tetrahydroindenyl iron(II) dicarbonyl dimer.....	83
2.4.1 Introduction.....	83
2.4.2 Discussion.	84
2.4.2a Synthesis.	84
2.4.2b Characterization.	84
2.4.2b(i) Infra-red spectroscopy.....	85
2.4.2b(ii) Nuclear magnetic resonance spectroscopy.	91
2.4.2b(iii) Single crystal X-ray diffraction solid state molecular structure determination.....	95
2.4.3 Summary.	102
2.5 1-Phenyl-3-methyl-4,5,6,7-tetrahydroindenyl methyl dicarbonyl iron(II).	102
2.5.1 Introduction.....	102
2.5.2 Discussion.	102
2.5.2a Synthesis.	102
2.5.2b Characterization.	103
2.5.2b(i) Infra-red spectroscopy.....	103
2.5.2b(ii) Nuclear magnetic resonance spectroscopy.	103
2.5.2b(iii) Single crystal X-ray diffraction solid state molecular structure determination.....	106
2.5.3 Summary.	111
2.6 Further work.....	111
2.6.1 Reaction of 2.4 with I ₂	111
2.6.2 Reaction of 2.5 with PPh ₃	112
2.6.3 The reaction of 1.12 with Li ₂ C ₂ B ₁₀ H ₁₀	114
2.7 Conclusions.	115
2.8 References.	117

Chapter Three: Zirconium(IV) Complexes Incorporating the Ligand

1-Phenyl-3-Methyl-4,5,6,7-Tetrahydroindenyl	121
3.1 Introduction	122
3.2 Bis (1-phenyl-3-methyl-4,5,6,7-tetrahydroindenyl) zirconium(IV) dichloride.	123
3.2.1 Introduction.....	123
3.2.2 Discussion.	123
3.2.2a Synthesis.	123
3.2.2b Characterization.	123
3.2.2b(i) Single crystal X-ray diffraction molecular structure determination.....	124
3.2.2b(ii) Nuclear magnetic resonance spectroscopy.	130
3.2.3 Summary.	134
3.3 Bis (1-phenyl-3-methyl-4,5,6,7-tetrahydroindenyl) dimethyl zirconium(IV).	134
3.3.1 Introduction.....	134
3.3.2 Discussion.	135
3.3.2a Synthesis.	135
3.3.2b Characterization.	135
3.3.2b(i) Nuclear magnetic resonance spectroscopy.	135
3.3.2b(ii) Single crystal X-ray diffraction solid state molecular structure determination.....	137
3.3.2b(iii) CHN analysis.....	141
3.3.3 Summary.	141
3.4 Conclusions.	141
3.5 References.	142
Chapter Four: Experimental Details	144
4.1 Experimental equipment and conditions.....	145
4.1.1 General experimental details.....	145
4.1.2 Instrumental methods.....	145
4.1.2a Spectroscopy, spectrometry and CHN analysis.	145
4.1.2b Cyclic voltammetry.....	145
4.1.2c X-ray diffraction crystallography.....	146
4.1.2c(i) Microcrystalline powder X-ray diffraction.....	146
4.1.2c(ii) Single crystal X-ray diffraction.	146
4.2 Preparations.....	147
4.2.1 Preparation of 3-methyl-2,3,4,5,6,7-hexahydroind-8(9)-en-1-one, 1.12.....	147
4.2.2 Preparation of 1-phenyl -3-methyl-4,5,6,7-tetrahydroindene, 2.1.....	148
4.2.2a Grignard method.	148

4.2.2b Phenyl lithium method.....	148
4.2.3 Preparation of 1-benzylidene-3-methyl-2,3,4,5,6,7-hexahydroind- 8(9)-ene, 2.2.....	149
4.2.4 Preparation of bis(1-phenyl-3-methyl-4,5,6,7-tetrahydroindenyl) iron(II), 2.3.	149
4.2.5 Preparation of 1-phenyl-3-methyl-4,5,6,7-tetrahydroindenyl dicarbonyl iron(II) dimer, 2.4.....	150
4.2.6 Preparation of 1-phenyl-3-methyl-4,5,6,7-tetrahydroindenyl methyl iron(II) dicarbonyl, 2.5.	150
4.2.7 Preparation of bis(1-phenyl-3-methyl-4,5,6,7-tetrahydroindenyl) zirconium(IV) dichloride, 3.1.	151
4.2.7 Preparation of rac-bis(1-phenyl-3-methyl-4,5,6,7-tetrahydroindenyl) dimethyl zirconium(IV), 3.2.....	151
4.3 References.....	151
Chapter Five: Characterizing Data.....	153
5.1 Data characterizing 3-methyl-2,3,4,5,6,7-hexahydroind-8(9)-en-1-one.....	154
5.2 Data characterizing 1-phenyl-3-methyl-4,5,6,7-tetrahydroindene, 2.1.....	154
5.3 Data characterizing 1-benzylidene-3-methyl-2,3,4,5,6,7-hexahydroind- 8(9)-ene, 2.2.	155
5.4 Data characterizing bis(1-phenyl-3-methyl-4,5,6,7-tetrahydroindenyl) iron(II), 2.3.....	155
5.5 Data characterizing 1-phenyl-3-methyl-4,5,6,7-tetrahydroindenyl iron dicarbonyl dimer, 2.4.....	158
5.6 Data characterizing 1-phenyl-3-methyl-4,5,6,7-tetrahydroindenyl methyl iron(II) dicarbonyl, 2.5.....	158
5.7 Data characterizing bis(1-phenyl-3-methyl-4,5,6,7-tetrahydroindenyl) zirconium dichloride, 3.1.....	159
5.7 Data characterizing bis(1-phenyl-3-methyl-4,5,6,7-tetrahydroindenyl) dimethyl zirconium(IV), 3.2.	159
5.8 Data obtained for reaction of 2.4 with I ₂	160
Appendix A: Crystallographic Data.....	161
A1 Crystallographic data for bis(1-phenyl-3-methyl-4,5,6,7-tetrahydroindenyl) iron(II), 2.3.....	162
A2 Crystallographic data for 1-phenyl-3-methyl-4,5,6,7-tetrahydroindenyl iron dicarbonyl dimer, 2.4.....	167

A3 Crystallographic data for 1-phenyl-3-methyl-4,5,6,7-tetrahydroindenyl methyl iron(II) dicarbonyl, 2.5.....	172
A4 Crystallographic data for bis(1-phenyl-3-methyl-4,5,6,7-tetrahydroindenyl) zirconium dichloride, 3.1.....	177
A5 Crystallographic data for bis(1-phenyl-3-methyl-4,5,6,7-tetrahydroindenyl) dimethyl zirconium(IV), 3.2.....	185
Appendix B: Courses, Lectures, Colloquia and Conferences Attended.....	194
B1 First Year Induction Courses: October 1995.....	195
B2 Examined Lecture Courses: October 1995 To April 1996.....	195
B3 Research Colloquia, Seminars And Lectures Organised By The Department Of Chemistry.....	196
B4 Conferences And Symposia Attended.....	199

LIST OF FIGURES

Chapter One

Fig. 1.1	Example of ligand derived chirality.	4
Fig. 1.2	Example of ligand derived and metal centred chirality.	6
Fig. 1.3	Free bond rotation rendering the substituted cyclopentadienyl ligand of titanocene 1.3 homotopic.	7
Fig. 1.4	The two faces of enantiotopic ligand 1.6 are related by a mirror plane.	8
Fig. 1.5	The <i>rac</i> - and <i>meso</i> -isomers of a linked bis-enantiotopic ligand metal complex.	8
Fig. 1.6	Camphor and diastereotopic ligand 1.7.	9
Fig. 1.7	Representation of a mono-substituted chiral cyclopentadienyl.	9
Fig. 1.8	Four stereoisomers of the 2-isopropyl-5-methylcyclohexyl moiety.	10
Fig. 1.9	The C_2 -symmetric di-phenyl bicyclo-[2.2.2]-octane substituted cyclopentadienyl, 1.9.	12
Fig. 1.10	Disubstituted enantiotopic planar cyclic polyenes and polyenyls, $R_1 \neq R_2$.	13
Fig. 1.11	A disubstituted non-enantiotopic planar polyene.	13
Fig. 1.12	Structures of $[(\eta-C_5H_5)_2GdCl]_4$ and $(\eta-C_5Me_5)_2HoCl.THF$.	18
Fig. 1.13	Two views of molecular structure of $C_5^1Pr_5^*$, indicating "paddle-wheel" type structure.	24
Fig. 1.14	The "gear-meshing" of all five isoalkyl groups of 1.10.	25
Fig. 1.15	Conformational directionality.	25
Fig. 1.16	Molecular structure of $[\eta-C_5(SiMe_2H)_5]Mn(CO)_3$ depicting the five membered ring in a "paddle-wheel" orientation.	31
Fig. 1.17	Molecular structures of $Fe[\eta-C_5(SiMe_3)_2H_3]_2$ and $Fe(\eta-C_5H_3^tBu_2)_2$.	32
Fig. 1.18	Molecular structure of $Fe[\eta-C_5(SiMe_3)_3H_2]_2$.	34
Fig. 1.19	1- R^1 -2- R^2 -3- R^3 -4,5,6,7-Tetrahydroindenyl.	36
Fig. 1.20	Spirolactones.	37
Fig. 1.21	Reaction of organic acids in PPA to generate acylium cation.	38
Fig. 1.22	Resonance stabilised oxocarbonium ion.	38
Fig. 1.23	A 3-hydroxypentadienylic cation.	40
Fig. 1.24	Solid state molecular structure of (R,R)-{Ti[(S,S)-2,3-butylene-1,1'-bis(4,5,6,7-tetrahydroindenyl)]Cl ₂ }.	41
Fig. 1.25	Solid state molecular structure of (R,S)-{Zr[(S,S)-2,3-butylene-1,1'-bis(4,5,6,7-tetrahydroindenyl)]Cl ₂ }	42
Fig. 1.26	Molecular structures of bis(1,3-dimethyl-4,5,6,7-tetrahydroindenyl) iron(II) and bis(1,2,3-trimethyl-4,5,6,7-tetrahydroindenyl) iron(II).	44
Fig. 1.27	Enantiomorphic site control producing isotactic (<i>pseudo</i> - C_2 -symmetric metal system, above) and syndiotactic (<i>pseudo</i> - C_5 -symmetric system, below) polymers.	50

Chapter Two

Fig. 2.1	¹³ C NMR spectrum of 1.12.	60
Fig. 2.2	The 40 different ways of placing two double bonds in the carbon skeleton of 2.1.	63
Fig. 2.3	Double resonance ¹ H NMR experiments on 2.2.	65
Fig. 2.4	Assigning R or S configuration to a planar-chiral metal-coordinated ligand.	69
Fig. 2.5	The <i>rac</i> - and <i>meso</i> -isomers of 2.3.	72
Fig. 2.6	¹³ C NMR spectrum showing assignments for 2.3C and "shadow" peaks of second isomer.	73
Fig. 2.7	Solid state molecular structure of the <i>meso</i> -isomer of 2.3.	74
Fig. 2.8	Experimental and calculated powder diffraction patterns of 2.3.	75
Fig. 2.9	Solid state molecular structure of 2.3, viewed along centroid-centroid axis.	76
Fig. 2.10	Solid state molecular structures of 2.a and 2.b, viewed along centroid-centroid axis.	76
Fig. 2.11	Solid state molecular structures of 2.c and 2.d, viewed along centroid-centroid axis.	77
Fig. 2.12	Key to Table 2.3.	79
Fig. 2.13	View of 2.3 depicting direction of phenyl ring twist.	81
Fig. 2.14	Cyclic voltammogram of 2.3 relative to that of ferrocene.	82
Fig. 2.15	Bis (1-methyl-4,5,6,7-tetrahydroindenyl) iron(II) and bis (4,5,6,7-tetrahydroindenyl) iron(II).	83
Fig. 2.16	The <i>cis</i> - and <i>trans</i> -isomers of 2.4.	84

Fig. 2.17	Portion of the solution-state infra-red spectrum of 2.4.	85
Fig. 2.18	Application of the symmetry operations of C_{2h} to a particular CO stretch in 2.4.	87
Fig. 2.19	Vibrations and symmetries for $\Gamma(\textit{trans})$.	88
Fig. 2.20	Vibrations and symmetries for $\Gamma(\textit{cis})$.	90
Fig. 2.21	A_1 symmetry stretch of the <i>cis</i> -isomer of 2.4.	91
Fig. 2.22	The <i>rac</i> - and <i>meso</i> -isomers of 2.4.	92
Fig. 2.23	^1H NMR spectrum of 2.4, assignments are in the text.	94
Fig. 2.24	Solid state molecular structure of the <i>meso</i> -isomer of 2.4.	96
Fig. 2.25	View of 2.4 along the centroid-centroid axis.	97
Fig. 2.26	Solid state molecular structures of $[(\eta\text{-C}_5\text{H}_5)\text{Fe}(\text{CO})]_2$ and $[(\eta\text{-C}_5\text{Me}_5)\text{Fe}(\text{CO})_2]_2$.	97
Fig. 2.27	Key to Tables 2.5 and 2.7.	98
Fig. 2.28	Solution state infra-red spectrum of 2.5.	104
Fig. 2.29	The ^1H NMR and $^{13}\text{C}\{^1\text{H}\}$ NMR spectra of 2.5	105
Fig. 2.30	Solid state molecular structure of 2.5.	107
Fig. 2.31	View of 2.5 showing the eclipsed methyl groups.	109
Fig. 2.32	Key to Table 2.10.	110
Fig. 2.33	Solution state infra-red spectrum of the product from the addition of I_2 to 2.4.	112
Fig. 2.34	Portion of ^1H NMR spectrum of product from the reaction of 2.5 with PPh_3 .	114
Fig. 2.35	Nucleophilic and electrophilic systems investigated as reagents in the synthesis of bis-tetrahydroindenyls.	116

Chapter Three

Fig. 3.1	Stereoisomers of 3.1.	124
Fig. 3.2	Solid state molecular structure of the <i>RR</i> -isomer of 3.1.	125
Fig. 3.3	Solid state molecular structure of $(\eta\text{-C}_5\text{H}_5)_2\text{ZrCl}_2$.	126
Fig. 3.4	Solid state molecular structure of the <i>R,R</i> -isomer of <i>rac</i> -bis(1-cyclohexyltetrahydroindenyl) zirconium dichloride	127
Fig. 3.5	Key to Table 3.2.	128
Fig. 3.6	View of molecular structure of 3.1 along centroid-centroid axis.	129
Fig. 3.7	Cyclohexyl substituent ring twist in 3.b.	130
Fig. 3.8	^1H - ^1H COSY spectrum of 3.1.	131
Fig. 3.9	^{13}C - ^1H HETCOR spectrum of 3.1.	131
Fig. 3.10	Solid state molecular structure of $(\eta\text{-C}_5\text{H}_5)_2\text{ZrMe}_2$.	137
Fig. 3.11	Solid state molecular structure of the <i>SS</i> -isomer of 3.2.	138
Fig. 3.12	View of molecular structure of 3.2 along centroid-centroid axis.	139
Fig. 3.13	Key to Table 3.5.	141

Chapter Four

Fig. 4.1	A Siemens SMART-CCD diffractometer.	147
----------	-------------------------------------	-----

LIST OF SCHEMES

Chapter One

Scheme 1.1	Hydrogenation of 2-phenyl-1-butene.	4
Scheme 1.2	Reaction of cyclopentadienyl molybdenum species with aldehyde.	6
Scheme 1.3	Synthesis of C ₂ -symmetric annulated cyclopentadienyl ligand 1.8.	11
Scheme 1.4	Diastereoselective cobalt mediated photolytic alkyne cyclizations to complexed cyclopentadienones.	12
Scheme 1.5	Disubstitution of cyclopentadienes using NaH and alkyl halides.	13
Scheme 1.6	Fulvenes as precursors to disubstituted cyclopentadienyls.	14
Scheme 1.7	Preparation of 2-methyl-5-ethylcyclopentadiene from a suitably substituted cyclopentenone.	14
Scheme 1.8	Reductive coupling of 2-substituted 6,6-dimethylfulvenes using Mg/CCl ₄ .	15
Scheme 1.9	Formation of silane linked cyclopentadienes.	15
Scheme 1.10	Alternative routes in the reaction of the cyclopentadienide anion with <i>tert</i> -butyl halides.	19
Scheme 1.11	Use of phase catalysis in preparation of <i>tert</i> -butyl substituted cyclopentadiene.	19
Scheme 1.12	Fulvenes in <i>tert</i> -butyl substituted cyclopentadienide anion synthesis.	20
Scheme 1.13	Products from reaction of ZrCl ₄ , Li(η-C ₅ H ₅) and Li(η-C ₅ R ^t BuH ₃).	20
Scheme 1.14	Isolated products of Friedel-Crafts alkylation of ferrocene with <i>tert</i> -butyl chloride.	21
Scheme 1.15	Reaction of Li(C ₅ H ₃ ^t Bu ₂) with FeCl ₂ under CO.	22
Scheme 1.16	Simultaneous deprotonation and alkylation of [Co(η-C ₅ Me ₅)(η-C ₅ H ₅)] ⁺ .	24
Scheme 1.17	Ion pair exchange.	25
Scheme 1.18	Routes to tetra- and penta-phenyl cyclopentadiene.	26
Scheme 1.19	Fe(η-C ₅ Ph ₅)(CO) ₂ Br as a starting material.	27
Scheme 1.20	Zwitterionic isomer of decaphenyl ferrocene and synthesis of [Fe(η-C ₅ Ph ₅)(η ⁶ -C ₆ H ₅)C ₅ HPh ₄] ⁺ .	28
Scheme 1.21	Selected reactions of [Ni(η-C ₅ Ph ₅)Br] ₂ .	28
Scheme 1.22	Formation of η-C ₅ Ph ₄ H within the coordination sphere of a molybdenum complex.	29
Scheme 1.23	Synthesis of silyl-substituted cyclopentadienyl ligands.	30
Scheme 1.24	Synthesis and reactions of Zr(ηC ₅ (SiMe ₃) ₂ H ₃) ₂ Cl ₂ .	33
Scheme 1.25	Reactions of the functional equivalent of Fe[η-C ₅ (SiMe ₃) ₃ H ₂]X.	35
Scheme 1.26	Synthesis of tetrahydroindenyls via hydrogenation of complexed indenyls.	36
Scheme 1.27	Sigmatropic rearrangement of spiro[4.4]nona-1,3-diene to 4,5,6,7-tetrahydroindene.	37
Scheme 1.28	One synthesis of pentamethylcyclopentadiene.	37
Scheme 1.29	Reaction of cyclohexene and crotonic acid in PPA to generate 3-methyl-2,3,4,5,6,7-hexahydroind-8(9)-en-1-one, 1.12.	38
Scheme 1.30	Nazarov cyclization of a divinyl ketone.	39
Scheme 1.31	Selected reagents capable of undergoing Nazarov cyclization.	40
Scheme 1.32	Nazarov cyclization products of cyclohexene with acrylic, crotonic and tiglic acid.	43
Scheme 1.33	Enantioselective hydrogenation of 2-phenyl-1-butene.	45
Scheme 1.34	Asymmetric catalytic epoxidation of alkenes.	46
Scheme 1.35	Asymmetric alkene isomerization.	46
Scheme 1.36	Hydrosilylation of ketones.	47
Scheme 1.37	Coupling reaction of ethyl pyruvate with 1-naphthol.	47

Chapter Two

Scheme 2.1	Preparation of 1.12 from crotonic acid and cyclohexene in PPA.	58
Scheme 2.2	Synthetic routes to 2.1.	61
Scheme 2.3	Formation of enolates versus coupling products using different aryl metal reagents.	62
Scheme 2.4	Formation of a single isomer of 2.2.	67
Scheme 2.5	Deprotonation of non-cyclopentadiene isomer of 2.1.	68
Scheme 2.6	Summary of chemistry in chapter two.	117

Chapter Three

Scheme 3.1	Summary of chemistry in chapter three.	142
------------	--	-----

ABBREVIATIONS

R	general alkyl group
Et	ethyl
Me	methyl
Ph	phenyl
^t Bu	<i>tert</i> -butyl
ⁿ Bu	<i>n</i> -butyl
ⁱ Pr	<i>iso</i> -propyl
Cp	η -C ₅ H ₅
L	general 2-electron ligand
X	general 1-electron ligand
PPA	poly phosphoric acid
MAO	methylaluminoxane
dmpe	1,2-bis(dimethylphosphino) ethane
THF	tetrahydrofuran
GC	gas chromatography
MS	mass spectrometry
EI	electron impact
IR	infra-red
w	weak
vs	very strong
NMR	nuclear magnetic resonance
s	singlet
d	doublet
m	multiplet
br	broad
ppm	parts per million
quat.	quaternary
$\Delta v_{1/2}$	width at half height
J	coupling constant
COSY	correlation spectroscopy
HETCOR	heteronuclear correlation spectroscopy
Red.	reducing agent
HOMO	highest occupied molecular orbital
LUMO	lowest unoccupied molecular orbital
CCD	charged-couple-device
P	polymer chain
IGLO	individual gauge of localized orbitals

Chapter One
Introduction.

1.1 Cyclopentadienyl metal chemistry.

Ever since the report of the synthesis of ferrocene by Kealy and Pauson in 1951 there has been great interest in cyclopentadienyl rings as organometallic ligands. Today they are one of the most important and widely used ligand systems in chemistry.¹ There are several reasons for this.

- (i) The η^5 -cyclopentadienyl unit attaches itself to the metal over three coordination sites with relatively strong metal-ligand bonding interactions.
- (ii) In the case of transition metal complexes the bonding interaction can be as high as 490 kJ mol^{-1} .²
- (iii) Cyclopentadienyl containing transition metal complexes are remarkably stable and inert to hydrolysis, even when the metal centres are in very high or very low oxidation states.³
- (iv) The geometry of the cyclopentadienyl coordination is predictable and gives rise to familiar structures such as tetrahedra or octahedra. In a small selection of cyclopentadienyl-metal complexes haptotropic shift (η^5 - η^3 - η^1) is observed, which distorts these familiar structures.⁴
- (v) A wide range of substituted cyclopentadienyl systems can be prepared. This is important in varying the steric and electronic properties of the ring, as well as being a means of introducing chirality into a complex.

A discussion of the methods used for incorporation of chirality and steric bulk will form the body of this chapter. There will be a section on the chemistry of cyclopentenones, a relevant synthetic precursor to substituted cyclopentadienes, and a section briefly describing some relevant areas of application of cyclopentadienyl metal complexes.

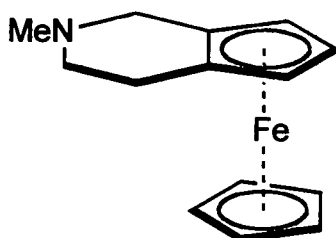
Mononuclear complexes, forming the majority of cyclopentadienyl containing transition metal species, exist in three main classes. Parallel metallocenes, (Cp_2M) , the structural analogues of ferrocene, are fairly limited in number, mainly on account of the limited number of combinations of M^{m+} and $(\text{Cp}_2)^{2-}$ giving rise to stable electron counts. Interest stems predominantly from electronic, magnetic and other physico-chemical measurements. Bent metallocenes, $(\text{Cp}_2\text{ML}_m\text{X}_n)$ where L is a two electron donor and X a one electron donor, are of greater importance and interest.⁵ The MCp_2 fragment is preserved as an organometallic template in most transition metal reactions, also their electronic structure has been thoroughly investigated and consistently established.⁶ They have proved very important in the development of early transition metal chemistry. The final group of mononuclear cyclopentadienyl complexes are the half-sandwich, or "piano-stool" complexes. Research into these complexes is developing rapidly and is of great interest. The multinuclear cyclopentadienyl complexes of interest to this work are the cyclopentadienyl carbonyl metal dimers, $[\text{CpM}(\text{CO})_n]_2$, these and relevant mononuclear species will be discussed further in chapters two and three.

1.2 Chiral cyclopentadienyl metal complexes.

For a molecule to be chiral the requirement is that it must belong to the point groups C_n or D_n , with C_1 being the most common.

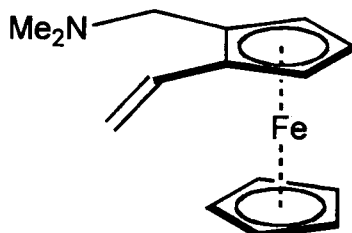
1.2.1 Early work.

Traditionally, the list of chiral ligands used in enantioselective synthesis as catalytic or stoichiometric mediators comprised phosphines, amines, imines and alcohols.⁷ However, chiral cyclopentadienyl systems has been known since 1958, when Hauser and co-workers treated 2-ferrocenylethylamine with formic acid (HCO_2H) and formaldehyde ($HCHO$) to give a bicyclic ferrocene derivative, 1.1.⁸



1.1

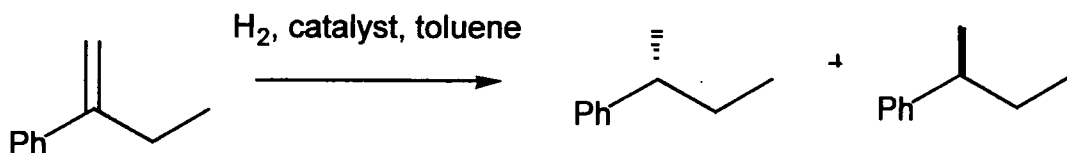
Reacting the methiodide salt of this product with potassium amide (KNH_2) caused ring opening. This resulted in the formation of the 1,2-disubstituted chiral ferrocene derivative 1-(N,N-dimethyl aminomethyl)-2-vinyl ferrocene, 1.2.



1.2

As with all new chemical systems, initial interest in chiral cyclopentadienyl species was primarily concerned with synthesis and the study of physical properties. It was not until 1979 that these chiral cyclopentadienyl complexes were applied in catalytic reactions.⁹ Kagan and co-workers noted how asymmetric hydrogenation using metal complexes of phosphines, amines and alcohols as catalysts had been the subject of intense research. However, little attention had been paid to the, by now, plentiful field of optically active hydrocarbon ligands, especially cyclopentadienyls, beyond noting that they had some catalytic activity when coordinated to certain metals. It was shown in Kagan's communication that the use of titanium(IV) complexes of menthyl- and neomenthyl-cyclopentadienyl ligands, 1.3, as homogeneous catalysts for the asymmetric hydrogenation of 2-phenyl-1-butene resulted in the (R)- or (S)-enantiomer predominating in the product (Scheme 1.1). The degree of enantiomeric excess

obtained, 15 %, although lower than desirable was comparable to that of the chiral phosphines which dominated research interests at that time.



Scheme 1.1 Hydrogenation of 2-phenyl-1-butene.

1.2.2 Types of cyclopentadienyl metal complex chirality.

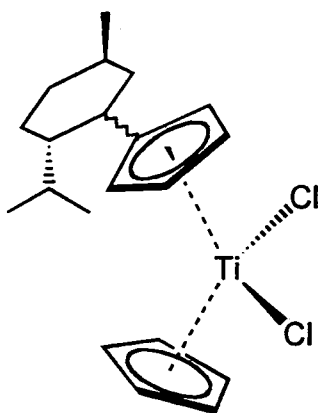
This section summarises the types of cyclopentadienyl ligands that give rise to chiral metallocenes, bent metallocenes and half-sandwich complexes.

1.2.2a Definitions.

There are three types of cyclopentadienyl metal complex chirality.

1.2.2a(i) Ligand derived chirality.

Where the coordinated cyclopentadienyl is chiral, discussed later, and the metal is non-stereogenic, the chirality is termed **ligand derived**. A stereogenic metal centre is one which has distinguishable ligands, such that the interchange of any two of the substituents leads to a stereoisomer. A stereoisomer possesses identical constitution, but differs in the spatial arrangement of its composite atoms.¹⁰



1.3

Fig. 1.1 Example of ligand derived chirality.

1.2.2a(ii) Metal centred chirality.

Where the coordinated cyclopentadienyl is achiral and the metal is stereogenic, the chirality is termed **metal centred**.

1.2.2a(iii) Ligand derived and metal centred chirality.

The metal complex possesses both **ligand derived** chirality and **metal centred** chirality when the coordinated cyclopentadienyl is chiral and the metal is stereogenic.

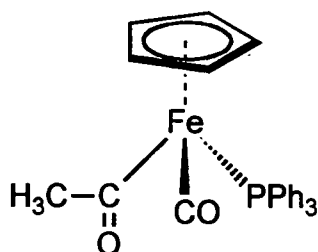
1.2.2b Examples.

1.2.2b(i) Ligand derived chirality.

The menthyl- and neomenthyl-cyclopentadienyl titanium(IV) species used by Kagan, **1.3**, possesses ligand derived chirality. The cyclopentadienyl group is rendered chiral by the substituent and the Ti metal centre is achiral (Fig. 1.1). This form of complex chirality is by far the most commonly encountered in cyclopentadienyl chemistry.

1.2.2b(ii) Metal centred chirality.

An example of a stereogenic metal centre coordinated to an achiral cyclopentadienyl ring is the organometallic acyl $\text{Fe}(\eta\text{-C}_5\text{H}_5)(\text{PPh}_3)(\text{CO})\text{COCH}_3$, **1.4**. Explored by Liebeskind and co-workers, **1.4** was used as a precursor for a "chiral enolate equivalent".¹¹ For reactions with alkylating agents, carbonyl compounds and imines, it has advantages over less flexible purely organic systems.

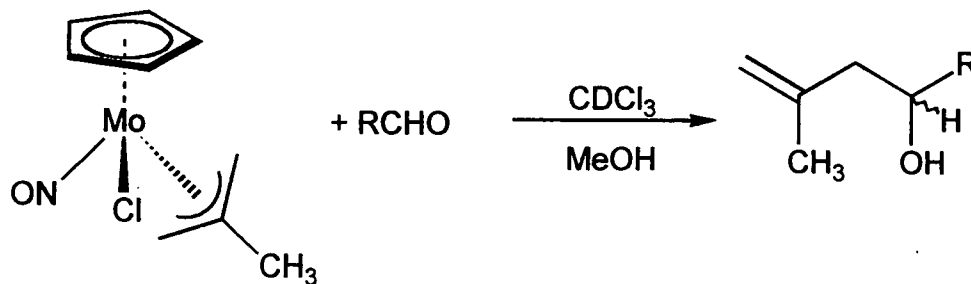


1.4

Metal based chiral systems can occur in a number of geometries inaccessible to organic compounds. Although compound **1.4** is four coordinate and tetrahedral (as features in chiral organic chemistry), five and six coordinate metal-centred chiral systems are also known, though less frequently used in enantioselective reactions.¹² Another advantage is the ability to alter the steric and electronic properties of the inducing chiral centre with greater variety than that of organic systems, simply by varying the ligands about the metal.

1.2.2c(iii) Ligand derived and metal centred chirality.

The third and final type of cyclopentadienyl metal complex chirality is a combination of the preceding two and comprises a stereogenic metal centre with one or more chiral ligands. Using NMR tube reactions, Faller and Linebarrier, treated the molybdenum complex $\text{Mo}(\eta\text{-C}_5\text{H}_5)(\text{NO})(\text{Cl})(\eta^3\text{-2-methylallyl})$ with an excess of an alkyl or aryl aldehyde to yield the corresponding homoallyl alcohols in high yields, 90 to 100%.¹³ (Scheme 1.2)



Scheme 1.2 Reaction of cyclopentadienyl molybdenum species with aldehyde.

To investigate the molybdenum complex's ability to enantioselectively generate the homoallyl alcohols, the neomenthyl substituted complex, **1.5**, was prepared, initially as a mixture of diastereomers (Fig. 1.2). This complex possesses both ligand derived and metal centred chirality.

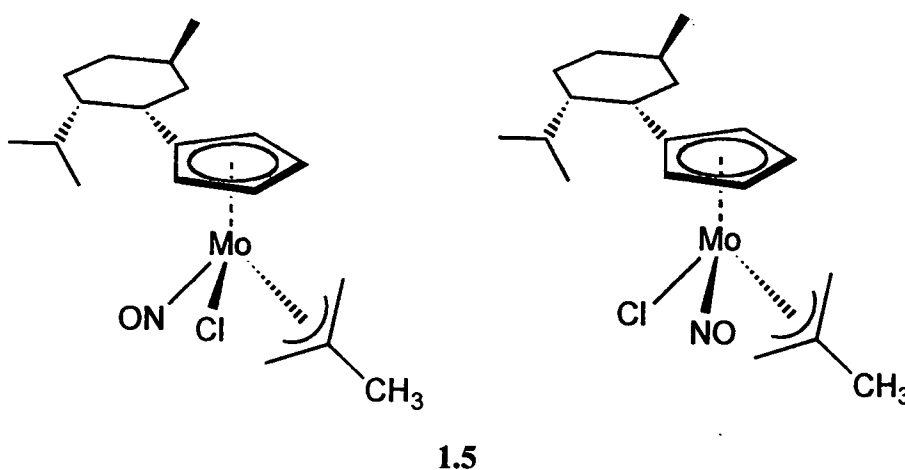


Fig. 1.2 Example of ligand derived and metal centred chirality.

The diastereomers formed are isolable with high diastereomeric excess, greater than 97% d.e., via fractional crystallization. This effectively resolves the metal centres. The condensations of benzaldehyde and propionaldehyde using resolved catalyst proceeded with 97% stereoselectivity. The enantioselectivity was independent of the nature of the aldehyde. The molybdenum chloride is an air stable compound that can be handled with no special precautions. This is not true of the main group organometallic reagents, allyl stannanes, allyl aluminiums and allyl boranes that had previously been used in these condensation reactions.

1.2.3 Types of cyclopentadienyl chirality.

Ligand derived chirality requires the planar cyclopentadienyl ring to be chiral in some manner. There are three ways the ligand may be optically active, which depend on how the two faces of the ligand are related to each other.

1.2.3a Definitions.

The following definitions apply to all ligands displaying "planar chirality", e.g. cyclopentadienyls, olefins and arenes.

1.2.3a(i) Homotopic ligands.

When the two faces of the chiral ligand are equivalent, either due to the presence of a C_2 -axis of symmetry, or due to free rotation between a chirality inducing substituent and the ring, the ligand is termed homotopic.

1.2.3a(ii) Enantiotopic ligands.

When the two faces of the chiral ligand are related by a mirror plane the ligand is termed enantiotopic.

1.2.3a(iii) Diastereotopic ligands.

When the two faces of the chiral ligand are not related by symmetry the ligand is termed diastereotopic.

1.2.3b Examples.

1.2.3b(i) Homotopic ligands.

An example of this has already been encountered in Kagan's titanium(IV) complex, **1.3**. The free rotation of the bond between the cyclopentadienyl moiety and the menthyl group renders the two faces of the ligand the same, and thus homotopic (Fig. 1.3). Cyclopentadienyl ligands with homotopic faces generate a single stereoisomer when metallated.

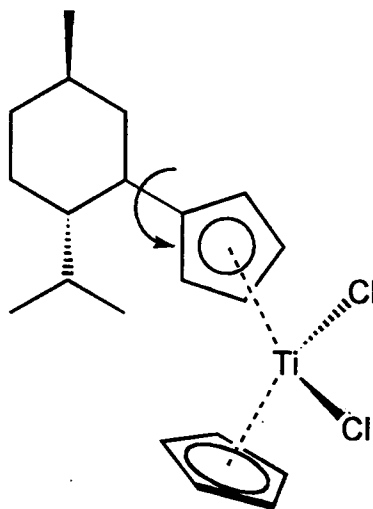


Fig. 1.3 Free bond rotation rendering the substituted cyclopentadienyl ligand of titanocene **1.3** homotopic.

1.2.3b(ii) Enantiotopic ligands.

Enantiotopic chirality exists when the two faces of the ligand are related by a mirror plane (Fig. 1.4). Enantiotopic ligands generate an enantiomeric mixture of complexes, but only when coordinated to an achiral metal fragment. In the work of Brintzinger, the ligand ethylene-bis(4,5,6,7-tetrahydro-1-indenyl), **1.6**, is enantiotopic.¹⁴

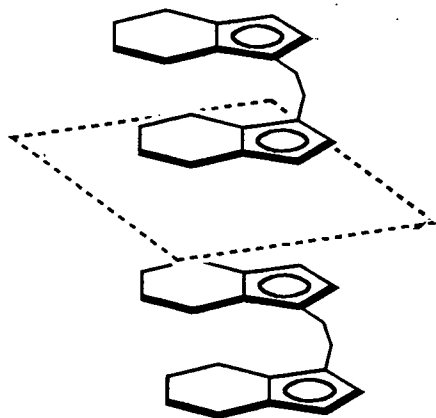


Fig. 1.4 The two faces of enantiotopic ligand 1.6 are related by a mirror plane.

Since both rings of the Brintzinger ligand 1.6 are coordinated to the same metal centre, once metallated each ring can be thought of as coordinating to a metal fragment rendered chiral by the other tetrahydroindenyl ring. Each ring of the metal-coordinated ligand has either a R or S configuration. This configuration is decided by viewing the ring of interest along the vector from the metal to the ring centroid and then ranking the ring substituents according to their Cahn-Ingold-Prelog priorities. The direction of travel from highest to lowest priority will be either clockwise or anti-clockwise, and the corresponding configuration R or S, respectively.¹⁵ Brintzinger's bis-tetrahydroindenyl titanium(IV) dichloride has three isomers, the RR, SS and SR. The presence of a mirror plane means that the RS and SR isomers are identical, and this achiral isomer is termed the mesomeric or *meso*-isomer. With the enantiomeric RR and SS isomers, termed the racemic or *rac*-isomers, the *meso*-isomer forms the final component of the diastereomeric mixture observed when two enantiotopic cyclopentadienyl, or the substituted analogue tetrahydroindenyl, ligands are coordinated to a chiral metal fragment (Fig. 1.5).

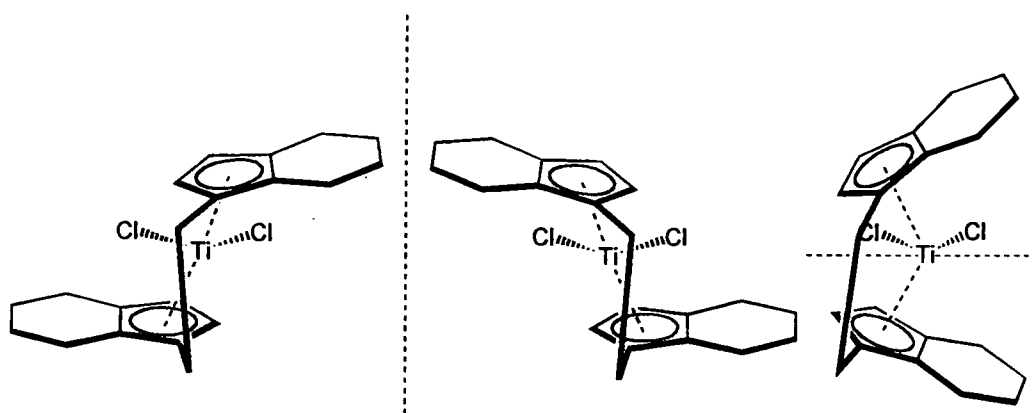


Fig. 1.5 The *rac*- and *meso*-isomers of a linked bis-enantiotopic ligand metal complex.

1.2.3b(iii) Diastereotopic ligands.

The final form of ligand derived chirality is where the faces of the cyclopentadienyl ligand are not related by symmetry and give a mixture of diastereomers when non-

selectively metallated. A non-chemical example of this type of planar chirality is the familiar human hand. The mixture of isomers obtained from non-selective metallation can be problematic and sometimes require difficult separations. However these ligand systems are quite common due to their facile preparation from enantiomerically enriched compounds that are naturally occurring. As well as the previously mentioned menthyl and neomenthyl substituents on cyclopentadiene (homotopic), molecules such as pulegone, camphor and tartrate are naturally derived chemicals used to synthesise substituted cyclopentadienyl ligands which are diastereotopic. Vollhardt and co-workers used camphor to synthesise the diastereotopic ligand **1.7** and study its ability, when coordinated in a titanium(IV) complex, to induce enantioselective control of the hydrogenation of 2-phenyl-1-butene.¹⁶



Fig. 1.6 Camphor and diastereotopic ligand **1.7**.

The readily available enantiomerically pure starting material and relatively simple synthesis of the cyclopentadienyl system were not the only reasons Vollhardt chose to use cyclopentadienyl ligands. It was observed that in the case of chiral chelating diphosphines efficient transfer of asymmetry in the hydrogenation reaction could be impeded by the lability of the phosphine ligands. The superior tenacity with which the η^5 -cyclopentadienyl unit attaches itself to a metal centre means that ligand lability is no longer a concern in the stereodifferentiation step. The bulk of **1.7** also helps maintain a rigid asymmetrical environment in which enantioselective hydrogenation can occur.

1.2.4 Types of chiral cyclopentadienyl ligands.

The methods used in synthesizing chiral cyclopentadienyl systems, whether they involve changing substituents on an achiral ring to induce chirality or building a chiral ring system from achiral or chiral acyclic precursors, are numerous. However, the resulting cyclopentadienyl systems themselves can be classified into broad groups of similar substitution.

1.2.4a Monosubstituted cyclopentadienyls.

The simplest of these groups and the logical starting point, are the mono-substituted chiral cyclopentadienyls (Fig. 1.7).

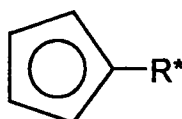


Fig. 1.7 Representation of a mono-substituted chiral cyclopentadienyl.

Monosubstituted cyclopentadienyls do not generate diastereomeric mixtures of complexes upon metallation. This is because they are homotopic ligands and capable of generating only one stereoisomer when metallated. Ligands like Kagan's menthyl system have the disadvantage of having the chirality inducing part of the ligand distant from the metal, which is commonly the stereodifferentiation centre in enantioselective reactions. As seen previously in 1.7, steric rigidity of the chiral environment of the metal complex is also important. Free rotation about the substituent-cyclopentadienyl ring bond, inherent in mono-substituted systems, prevents the formation of a rigid asymmetric environment. Menthyl and neomenthyl substituents are regularly used to induce chirality in cyclopentadienyl systems or to resolve chiral cyclopentadienyl metal complexes with metal centred chirality, as in compound 1.5 prepared by Faller and Linebarrier. Reaction of sodium cyclopentadienide with menthyl tosylate gives neomenthyl cyclopentadiene in a clean inversion (S_N2) reaction. The 2-isopropyl-5-methylcyclohexyl moiety, also known trivially as *para*-menthan-3-yl, has three positions on the cyclohexyl ring that are chiral, the 1-, 2- and 5-positions. Therefore, eight isomers are possible, (+)-(1S2R5S)- and (-)-(1R2S5R)-menthyl, (+)-(1S2S5R)- and (-)-(1R2R5S)-neomenthyl, (+)-(1S2R5R)- and (-)-(1R2S5S)-isomenthyl and (+)-(1R2R5R)- and (-)-(1S2S5S)-neoisomenthyl (Fig. 1.8).¹⁷

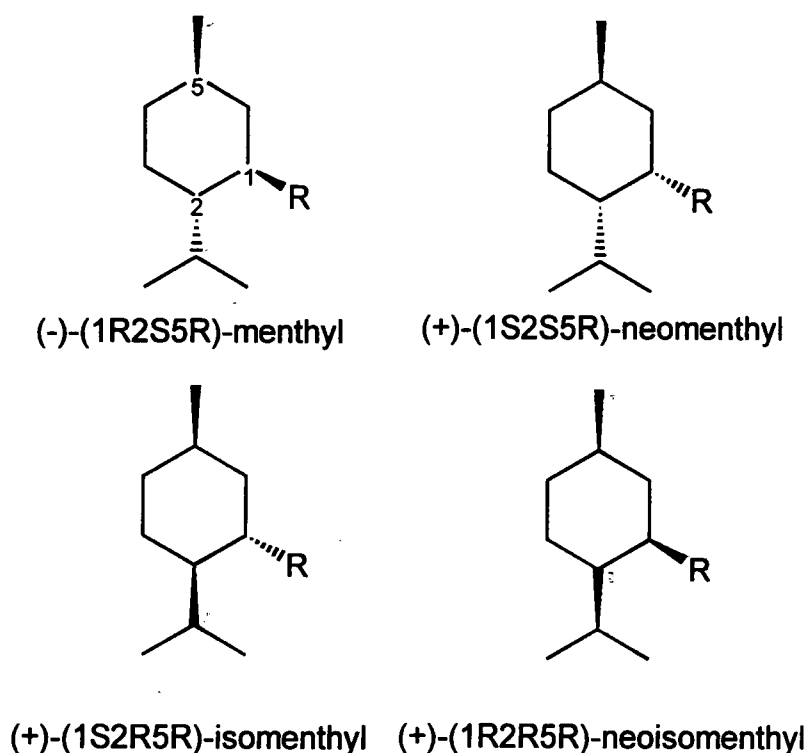
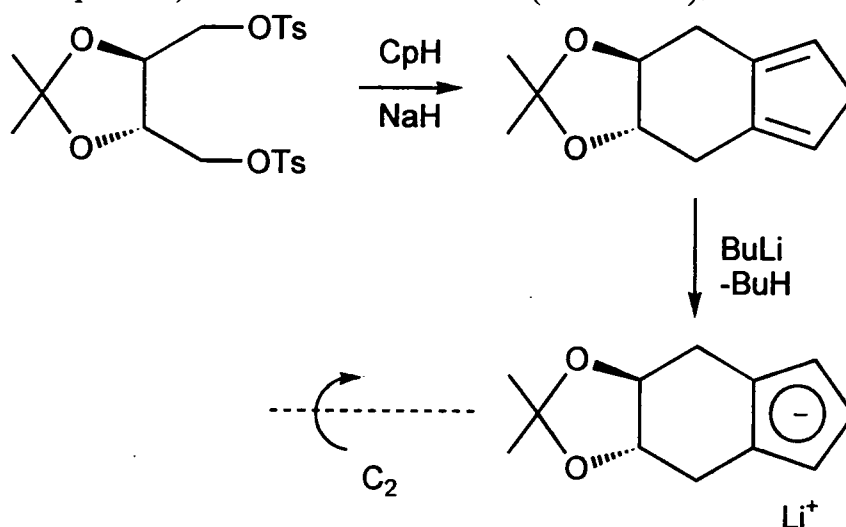


Fig. 1.8 Four stereoisomers of the 2-isopropyl-5-methylcyclohexyl moiety.

1.2.4b Annulated cyclopentadienyls.

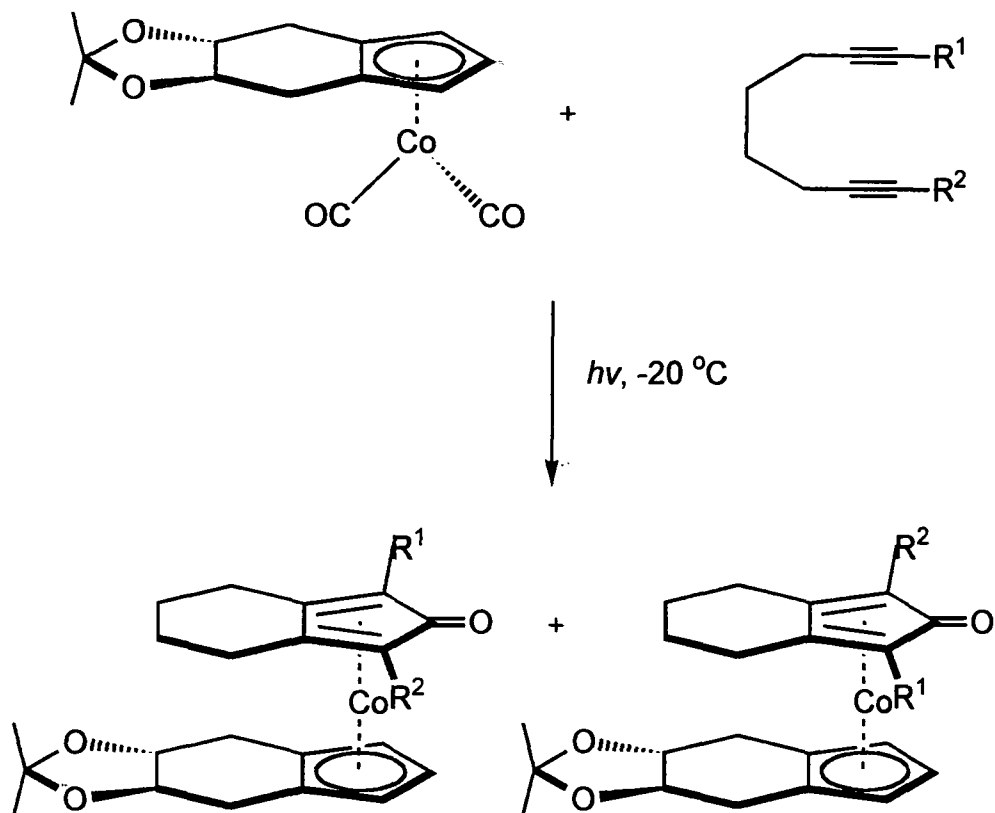
One method of holding the ligands in an asymmetric environment in the vicinity of a coordinated metal with more rigidity is to have the cyclopentadienyl substitution take the form of rings fused onto the cyclopentadienyl moiety. These are annulated

cyclopentadienes and form the second broad grouping of cyclopentadienyl substitution that can induce chirality. Brintzinger's bis-tetrahydroindenyl system, **1.6**, is an example of an enantiotopic annulated cyclopentadienyl, and also an example of the another category of cyclopentadienyl substitution, linked systems, which will be discussed later. Annulated systems can also be diastereotopic as can be seen in Vollhardt's camphor derived C_1 -symmetric ligand, **1.7**. The synthesis of this ligand is an example of ligand syntheses involving a cyclopentannulation sequence. A cyclopentadiene ring is formed at some point during the synthetic route and is not initially present. The other strategy for incorporating a cyclopentadienyl moiety into an annulated ligand system is by direct introduction of the five-membered ring to an appropriately functionalized substrate. This second strategy was utilised in the synthesis of the first published example of a C_2 -symmetric annulated cyclopentadiene, **1.8**, reported by Vollhardt.¹⁶ Due to its C_2 -symmetry, the homotopic ligand **1.8** circumvents the problem of diastereomeric mixtures upon metallation since both faces have the same configuration. The ligand was readily prepared from cyclopentadiene, excess sodium hydride and a commercially available bis(p-toluenesulphonate) ester derivative of tartrate (Scheme 1.3).



Scheme 1.3 Synthesis of C_2 -symmetric annulated cyclopentadienyl ligand **1.8**.

The titanocene dichloride derivative of **1.8** could not be synthesized, presumably due to the reactivity of the acid sensitive acetal. The dicarbonyl cobalt complex of **1.8** was synthesized by reaction with dicobalt octacarbonyl. The reaction used to test the stereoselectivity of this complex was the photolytic cyclization of alkynes to complexed cyclopentenones. No diastereoselection was observed between the possible diastereomeric products (Scheme 1.4).



Scheme 1.4 Diastereoselective cobalt mediated photolytic alkyne cyclizations to complexed cyclopentadienones.

The ligand **1.8** is a good example of how the distant location and nature of the asymmetry inducing part of the ligand can render it unsuitable as an enantioselective reagent when metallated. This is a common problem when relying on natural products or their derivatives for a source of chirality. An annulated system with C_2 -symmetry, possessing a rigid chiral environment about the metal, that is inherently chiral due to its structural nature rather than due to a chiral substituent, is far more effective. The first in this class of designed C_2 -symmetric ligands was also prepared by Vollhardt and co-workers.¹⁸ The di-phenyl bicyclo-[2.2.2]-octane substituted cyclopentadienyl, **1.9**, was prepared from achiral starting materials, and its titanocene dichloride complex was shown to be stereoselective as an asymmetric hydrogenation catalyst (Fig. 1.9).

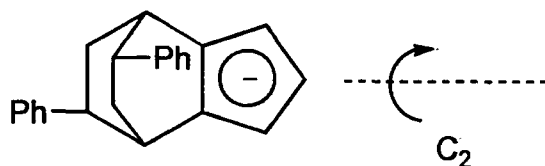


Fig. 1.9 The C_2 -symmetric di-phenyl bicyclo-[2.2.2]-octane substituted cyclopentadienyl, **1.9**.

Certain diastereomer resolution steps in the synthesis of **1.9** limit its large scale application and the versatility of the synthetic route. However, synthetic routes for a wide range of similar di-substituted bicyclo-[2.2.2]-octane cyclopentadienyl systems, which are all C_2 -symmetric, and their titanocene complexes, have since been reported.¹⁹

1.2.4c Disubstituted cyclopentadienyl ligands.

The minimum requirement for a planar cyclic polyene or polyenyl ligand to be enantiotopic is that it has two different substituents (Fig. 1.10). This is only true for planar cyclic polyene ligand systems such as arenes when the two positions on the ring of the substituents are not rendered equivalent by rotation about the ring-centroid metal axis, when coordinated (Fig. 1.11).

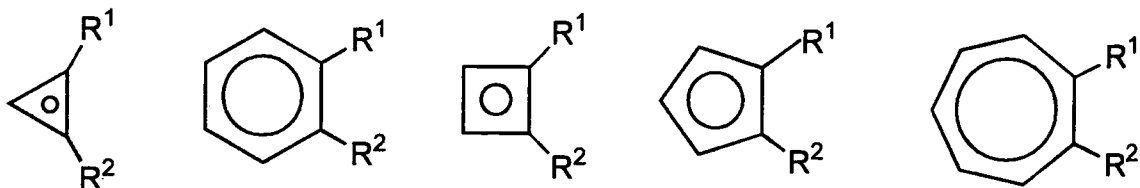


Fig. 1.10 Disubstituted enantiotopic planar cyclic polyenes and polyenyls,

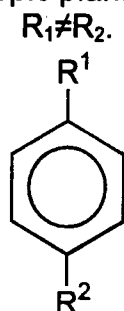
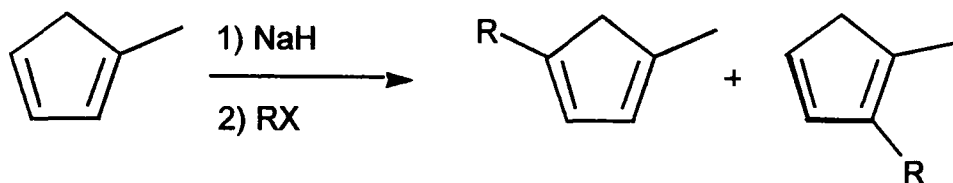


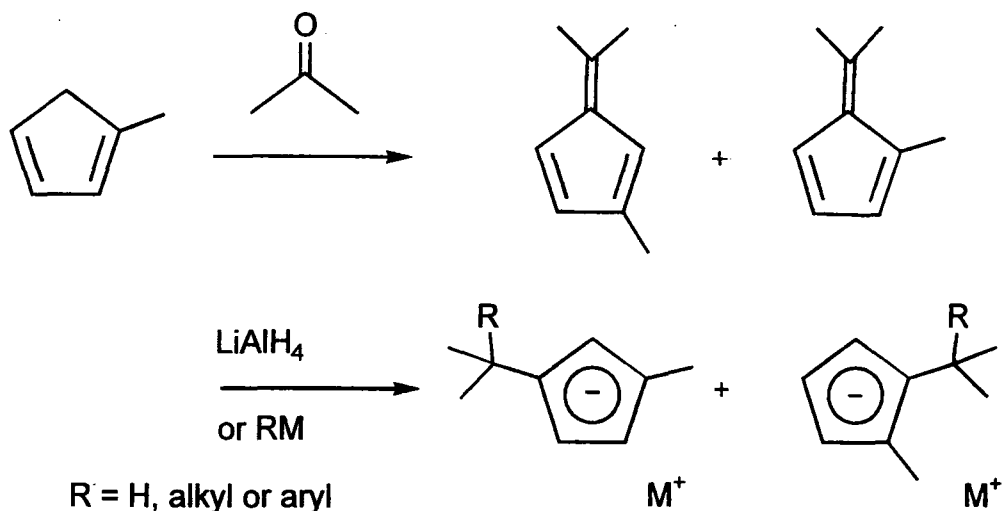
Fig. 1.11 A disubstituted non-enantiotopic planar polyene.

Disubstituted cyclopentadienyl ligands are readily prepared from the reaction of sodium hydride, monosubstituted cyclopentadienes and alkyl halides (Scheme 1.5).²⁰ This results in 1,2- and 1,3-disubstituted cyclopentadienes in roughly equal amounts, which can then be separated and converted into cyclopentadienyls for metallation.



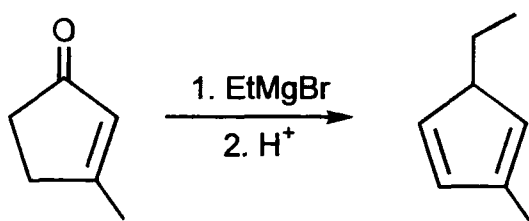
Scheme 1.5 Disubstitution of cyclopentadienes using NaH and alkyl halides.

The reaction of alkyl-substituted cyclopentadienes with acetone results in the formation of 1,2- and 1,3-isomers of alkyl(isopropylidene)cyclopentadiene.²¹ These fulvenes, the all carbon analogues of cyclopentadienones, can be separated using gas chromatography and then treated with metal alkyl, aryl or hydride reagents to form cyclopentadienyl species that can be directly metallated (Scheme 1.6).



Scheme 1.6 Fulvenes as precursors to disubstituted cyclopentadienyls.

The separate steps necessary for the multiple regioisomers formed in these reactions are undesirable. To synthesize only one regioisomer it is possible to use suitably functionalized cyclopentadienes, e.g. cyclopentenones. In 1958 Taylor reported the reaction of 3-methyl cyclopentenone with ethyl magnesium bromide. After acid promoted elimination of water the product was a single regioisomer, 2-methyl-5-ethylcyclopentadiene (Scheme 1.7).²² Cyclopentenones are a versatile route into substituted cyclopentadienyl chemistry and will be discussed later.

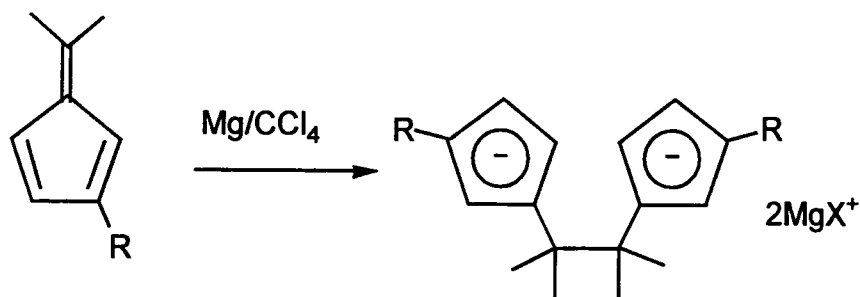


Scheme 1.7 Preparation of 2-methyl-5-ethylcyclopentadiene from a suitably substituted cyclopentenone.

1.2.4d Bridged bis-cyclopentadienyls.

For chiral cyclopentadienyl metal complexes to be efficient stereoselective mediators in asymmetric reactions, the source of chirality must be as close to the metal centre and as rigid as possible. Prevention of free rotation of substituents through increased bulk or annulation is one method. However, free rotation of the cyclopentadienyl ring in the complexes can also decrease the complex's efficiency as a chiral reagent. To prevent this ring rotation, linked bis-cyclopentadienyl systems have been prepared. These bis-cyclopentadienyl metal systems are termed *ansa*-metallocenes (*ansa*- coming from the Latin word for a bent handle attached at both ends). The *ansa*-metallocene of the Brintzinger ligand 1.6 has already been discussed. The first *ansa*-metallocene, C₂-symmetrical [η^5, η^5 -1,3-bis-(3-*tert*-butylcyclopentadienyl)propane]titanium(IV) dichloride was also prepared by Brintzinger and co-workers in 1979.²³ This involved the regioselective 1,3-alkylation of a hindered *tert*-butylcyclopentadienyl anion with 1,3-

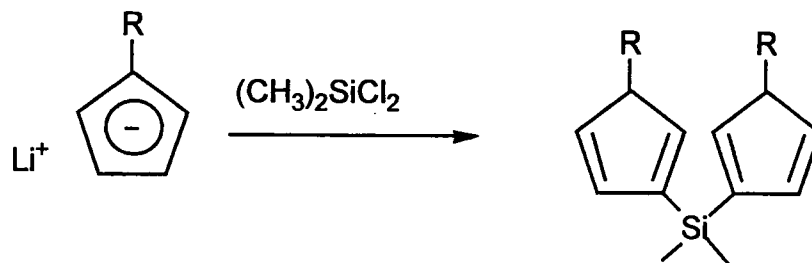
dibromopropane. For substituents smaller than isopropyl groups, increased formation of the 1,2-disubstituted products was observed. Other routes, reported by Brintzinger and co-workers, have since appeared for the preparation of linked cyclopentadienyl systems. Tetramethylethylene-bridged cyclopentadienyl magnesium chlorides can be prepared by reductive coupling of 2-substituted 6,6-dimethylfulvenes using Mg/CCl_4 (Scheme 1.8).²⁴ Brintzinger used these di-Grignards directly to prepare *ansa*-titanocenes and *ansa*-zirconocenes.



Scheme 1.8 Reductive coupling of 2-substituted 6,6-dimethylfulvenes using Mg/CCl_4 .

Dimethylsilane has been used to bridge substituted cyclopentadienes.²⁵ Brintzinger and co-workers prepared the *rac*- and *meso*- diastereomers of group IV metallocenes with dimethylsilanediyl bridged ligand frameworks. Addition of two equivalents of a substituted cyclopentadienyl lithium reagent to dimethyldichlorosilane gave silyl substitution at the least hindered position of the cyclopentadiene (Scheme 1.9). Deprotonation to form the bis-cyclopentadienyl was achieved by stirring the bis-cyclopentadiene with solid KH in a THF suspension.

The advantage of preparing silyl substituted ligands is that rapid sigmatropic shifts allow the silyl substituent to migrate around the ring to give the most thermodynamically stable isomer; typically the thermodynamics are driven by steric interactions.



Scheme 1.9 Formation of silane linked cyclopentadienes.

1.2.5 Summary.

Chiral cyclopentadienyl metal complexes have been known since 1959, but were not used as catalytic mediators in enantioselective reactions until 1979.

There are three types of cyclopentadienyl metal complex chirality. They are ligand derived, metal centred and combined ligand derived and metal centred chirality.

Ligand derived chirality exists in three forms, dependent on how the two faces of the ligand are related to each other. The three forms are homotopic, enantiotopic and diastereotopic chirality.

Although the range of chiral cyclopentadienyl compounds is very large, they can be discussed in broad groups of similar substitution, the most common of which are monosubstituted, annulated, disubstituted and bridged cyclopentadienyls.

1.3 Sterically demanding cyclopentadienyl metal complexes.

1.3.1 Introduction.

One of the reasons why cyclopentadienyl ligands are so widely used in transition metal chemistry is the wide variation possible with substitution of one or more of the hydrogen atoms in the C_5H_5 ring. As has already been discussed in section 1.2.4b, bulky substitution is essential for the incorporation of useful chirality, but other important considerations are the changes caused in the electronic properties and steric demand of the cyclopentadienyl ring. This is shown when considering the changes in structure and reactivity upon changing a $(\eta-C_5H_5)$ moiety to $(\eta-C_5MeH_4)$ and then to a $(\eta-C_5Me_5)$ moiety. The use of the methylcyclopentadienyl ligand does not have a profound effect on either structure or reactivity, the substitution by a single methyl group is insufficient. This substitution may however give improved solubility, better crystal packing (more ordered) leading to improved structure determinations, and the lowered symmetry provides a useful handle for NMR spectroscopy. However, the introduction of a pentamethyl cyclopentadienyl group permits the synthesis of a large number of new complexes with reactivity patterns unobserved for corresponding cyclopentadienyl analogues.²⁶ This may be due to the per-alkylated ligand being more electron donating and resulting in a more covalent metal-ligand interaction. This is revealed in the oxidation potentials, $E_{1/2}$, of the corresponding ferrocenes, which decrease by 0.047 V upon the introduction of an alkyl group, wherever it is introduced. Conversely the introduction of a phenyl group increases $E_{1/2}$ by 0.023 V.²⁷ Selected oxidation potentials for substituted ferrocenes are given in Table 1.1.²⁸ Alkyl substituents increase the tendency towards oxidation while phenyl groups reduce this tendency.

As well as an electronic reason for the dissimilar behaviour of $(\eta-C_5Me_5)$ complexes, sterically it may be due to the effective blocking of bimolecular reactions leading to lower molecular aggregates and/or coordinatively unsaturated species.²⁹ As yet it is impossible to say which, if either, of these factors plays the more important role in the chemistry of heavily substituted cyclopentadienyls.³⁰ The greater steric presence of substituted cyclopentadienyl ligands is certainly vital to the stabilisation of monomeric complexes of the lanthanides; this ability of bulky cyclopentadienyl ligands to stabilise organolanthanide complexes is of recent interest.³¹ These complexes can perform a wide variety of reactions with many substrates, however the large ionic radii of the lanthanides

combined with the electron deficiency and Lewis acidity of Cp_2LnR or Cp_2LnX , requires cyclopentadienyl based ligands that provide sufficient steric bulk to prevent metallocene oligomerisation. The most extensively used ligand is C_5Me_5 ; this is shown by the structures in Fig. 1.12.³² The tetrameric bis-cyclopentadienyl gadolinium complex, $[(\eta-C_5H_5)_2GdCl]_4$, and the monomeric bis-pentamethylcyclopentadienyl holmium complex, $(\eta-C_5Me_5)_2HoCl.THF$, can be compared, the size difference of the two lanthanides is not great, so the different structural motifs must be due to the greater steric demand of the $(\eta-C_5Me_5)$ ligands.

Compound	$E_{1/2}$ (V)
Fc (Ferrocene)	0.34
Me-Fc	0.28
1,1',2-Et ₃ -Fc	0.19
1,1',3-Et ₃ -Fc	0.20
1,1'-Me ₂ -2,2'-Et ₂ -Fc	0.16
1,1',2,2',3,3',4,4'-Et ₈ -Fc	-0.05
Ph-Fc	0.37
1,1'-Ph ₂ -Fc	0.39
1,2,4-Ph ₃ -Fc	0.42
1,1',3,3'-Ph ₄ -Fc	0.45
1,2,3,4-Ph ₄ -Fc	0.43

Table 1.1 Selected oxidation potentials for substituted ferrocene-ferrocinium couples.

This section will deal with the incorporation of substituents intended to increase the steric demand of coordinated cyclopentadienyl ligands, Okuda has reviewed this chemistry.³³ The two main methods for introducing substitution into cyclopentadienyl metal complexes have already been encountered. Functionalization of the already coordinated cyclopentadienyl ring occurred in the preparation of the first chiral cyclopentadienyl metal complex reported, ferrocene **1.2**. The second, and far more common, method is substitution of the ring prior to metallation, followed by reaction of the dienyl anion with a transition metal halide or carbonyl complex. Most of the complexes described in section 1.2 have been prepared this way. The bis-cyclopentadienyl Grignards in Scheme 1.8 are a good example of ring substitution generating the dienyl anion *in situ*, ready for transfer metallation. A third method, creating a specifically substituted cyclopentadienyl ligand from smaller carbon units such as alkylidynes and alkynes within the coordination sphere of the metal, is also known, but is not as widely applied as the preceding two.³⁴ Three types of bulky substituent will

be considered here. Firstly, alkyl substituents, of which *tert*-butyl and isopropyl are the most commonly used. These cyclopentadienes generally suffer from the formation of regioisomers during their synthesis and limitations on the number of bulky units that can be easily incorporated. The second type of bulky substituent is the phenyl group, C_6H_5 . This is widely used due to the ready availability of the synthetic precursor 2,3,4,5-tetraphenylcyclopentadienone, **1.11**. The third commonly used substituent is the silyl group, $SiMe_3$, which, due to silyltropic shifts in the preparation of the free ligand, does not suffer as many problems with regioisomerism.

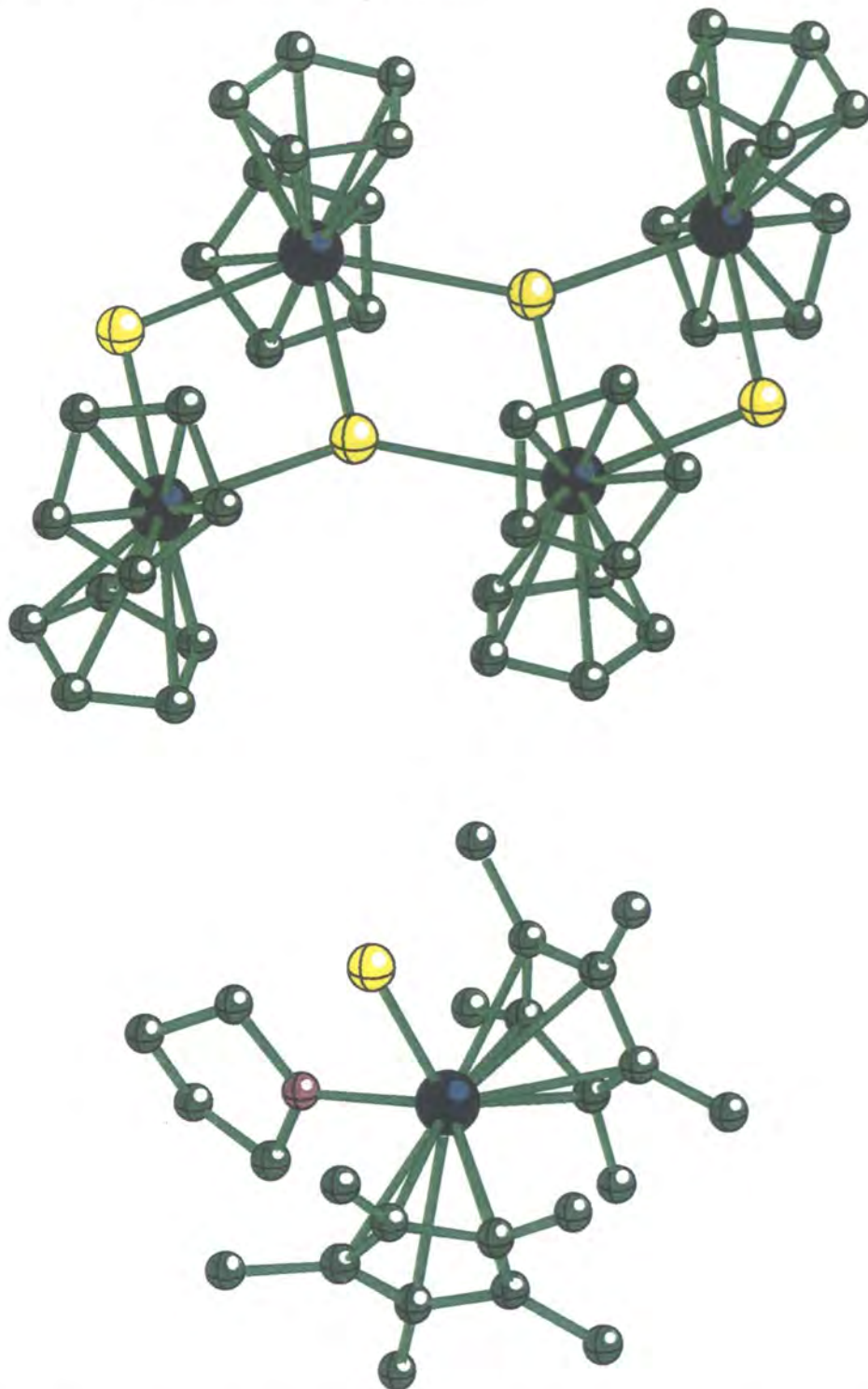
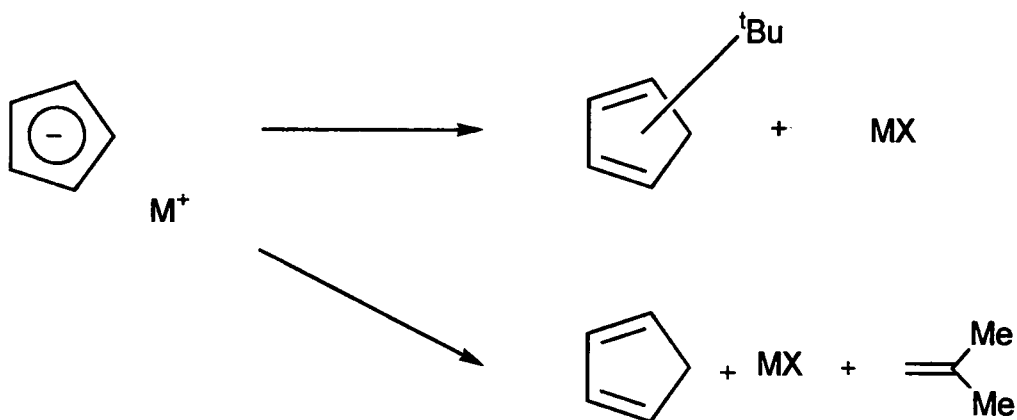


Fig. 1.12 Structures of $[(\eta-C_5H_5)_2GdCl]_2$ and $(\eta-C_5Me_5)_2HoCl \cdot THF$.

1.3.2 Alkyl-substituted cyclopentadienyl ligands.

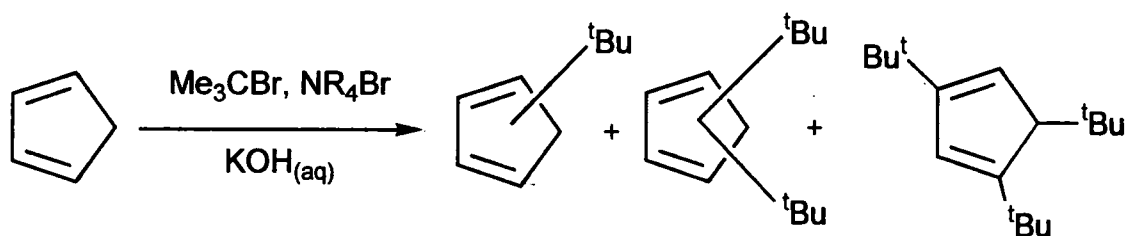
1.3.2.1 *Tert*-butyl substituted cyclopentadienyl ligands.

Initial reports of the synthesis of mono- and di-*tert*-butyl cyclopentadiene involved the reaction of a cyclopentadienide anion with *tert*-butyl halide. This nucleophilic attack competes with the elimination reaction that forms isobutene (Scheme 1.10).³⁵



Scheme 1.10 Alternative routes in the reaction of the cyclopentadienide anion with *tert*-butyl halides.

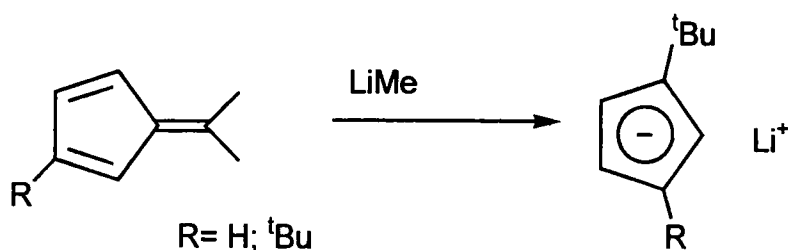
This results in low yields of the dialkyl substituted cyclopentadiene. The use of phase transfer catalysis by Leigh improved the yield of the mono- and disubstituted species, but yields for the trisubstituted product are still low due to steric interactions of adjacent *tert*-butyl groups (Scheme 1.11).³⁶ This was the first reported preparation of tri-*tert*-butyl cyclopentadiene and the first example of carbon alkylation under phase transfer conditions using a tertiary halide. Phase transfer catalysis removes the inconvenience of a reaction in a dry, inert atmosphere, in contrast to reactions involving cyclopentadienide anions. Only one isomer of tri-*tert*-butylcyclopentadiene is observed using this method, again due to steric interactions of adjacent *tert*-butyl groups. The predominance of the 1,3,5-isomer arises since it is the only arrangement that does not put *tert*-butyl groups on adjacent sp^2 carbons. Tetra-*tert*-butylcyclopentadiene has only ever been prepared in small amounts in connection with the synthesis of *tert*-butyltetrahedrane as part of a very long preparation.³⁷



Scheme 1.11 Use of phase catalysis in preparation of *tert*-butyl substituted cyclopentadiene.

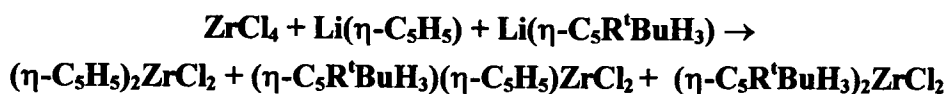
A measure of the steric effect of a substituent is the ligand cone angle, θ . Tolman calculated a value for $\eta\text{-C}_5\text{H}_5$ of 136° . Models for di- and tri-*tert*-butylcyclopentadienyls suggest that their cone angles may be 180° or more.³⁸

A method of preparing mono- and di-*tert*-butyl substituted cyclopentadienide anions directly is the use of suitable fulvenes, in a similar manner to those shown earlier in Scheme 1.5. Renault and co-workers added methyl lithium directly to 6,6-dimethyl fulvene and 2-*tert*-butyl-6,6-dimethyl fulvene.³⁹ This resulted in the desired mono- and disubstituted cyclopentadienide anions (Scheme 1.12). This removes the need for a separate cyclopentadienide anion formation step and the formation of regioisomers of the disubstituted species.



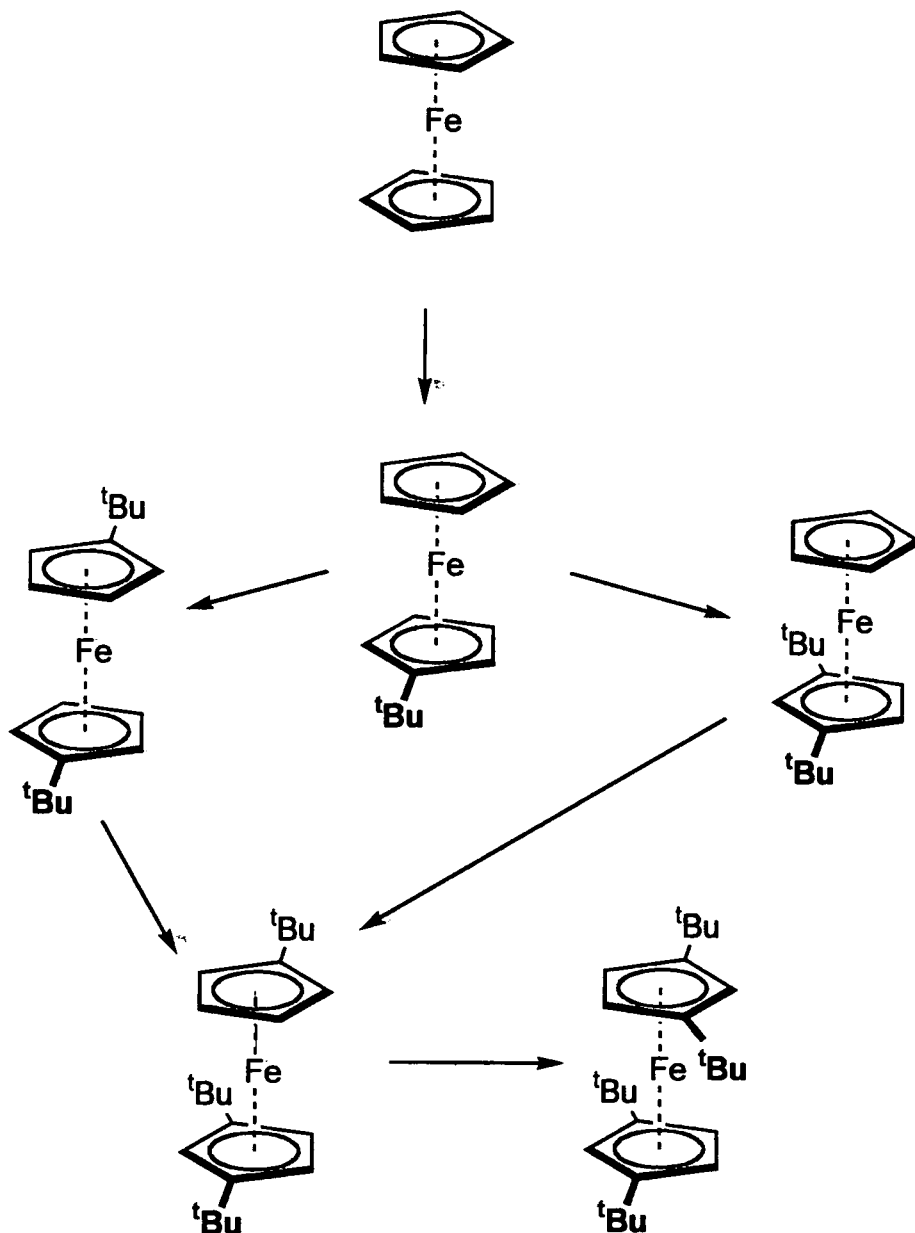
Scheme 1.12 Fulvenes in *tert*-butyl substituted cyclopentadienide anion synthesis.

Reaction between zirconium tetrachloride and the cyclopentadienide anions obtained from the fulvenes in Scheme 1.12, to prepare $(\eta\text{-C}_5\text{R}^t\text{BuH}_3)_2\text{ZrCl}_2$ was described. The complex $(\eta\text{-C}_5\text{R}^t\text{BuH}_3)(\eta\text{-C}_5\text{H}_5)\text{ZrCl}_2$ was prepared in the same way, as part of a mixture of products which required separation by chromatography (Scheme 1.13). Higher yields were obtained when the anions were reacted with $(\eta\text{-C}_5\text{H}_5)\text{ZrCl}_3 \cdot 2\text{THF}$.



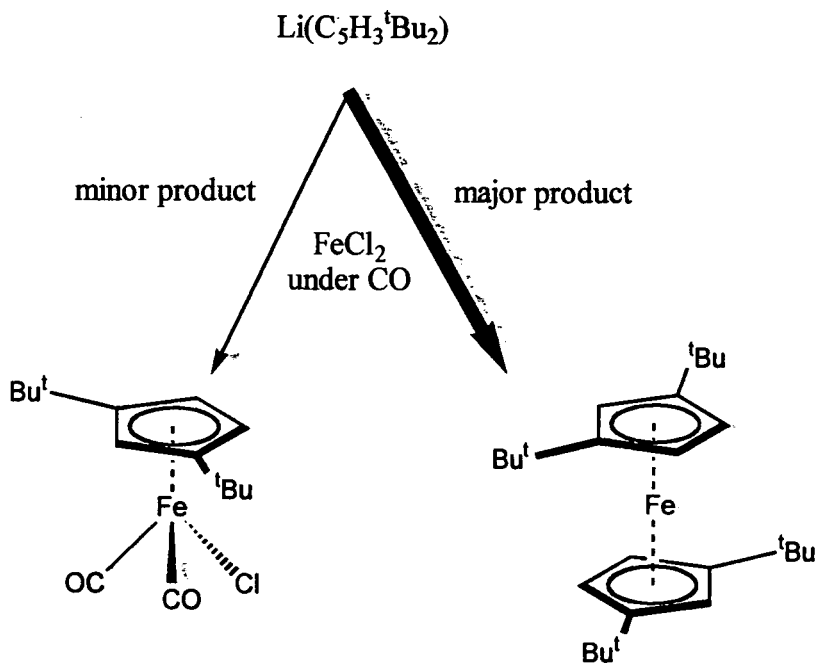
Scheme 1.13 Products from reaction of ZrCl_4 , $\text{Li}(\eta\text{-C}_5\text{H}_5)$ and $\text{Li}(\eta\text{-C}_5\text{R}^t\text{BuH}_3)$.

Using various Lewis and Brønsted acids as catalysts, up to two *tert*-butyl groups can be introduced into each ring via a Friedel-Crafts alkylation of the parent ferrocene $[\text{Fe}(\eta\text{-C}_5\text{H}_5)_2]$ (Scheme 1.14).³⁶ Alkylation of ferrocene with *tert*-butyl chloride under Friedel-Crafts conditions proceeds smoothly, and mono-, 1,1'-di-, 1,3-di-, 1,1',3-tri-, and 1,1',3,3'-tetra-*tert*-butyl ferrocenes can be isolated as crystalline products.



Scheme 1.14 Isolated products of Friedel-Crafts alkylation of ferrocene with *tert*-butyl chloride.

Preparation of half sandwich complexes with the $(\eta\text{-C}_5\text{H}_3\text{tBu}_2)$ ligand can be accomplished either by preformation of the parent diene or by substitution of a pre-coordinated cyclopentadienyl moiety. Okuda has reported a simple, though low yielding, method of synthesizing a half-sandwich iron complex incorporating $(\eta\text{-C}_5\text{H}_3\text{tBu}_2)$.⁴⁰ Reaction of the lithium salt of the relevant cyclopentadienide anion at low temperatures under CO with FeCl_2 , yields $\text{Fe}(\eta\text{-C}_5\text{H}_3\text{tBu}_2)(\text{CO})_2\text{Cl}$ in small amounts, the major product being the ferrocene (Scheme 1.15).



Scheme 1.15 Reaction of $\text{Li}(\text{C}_5\text{H}_3^t\text{Bu}_2)$ with FeCl_2 under CO.

A much higher yielding and simpler system in which the substituted cyclopentadienyl moiety is formed by substituting a pre-coordinated ring was reported by Hofmann and co-workers.⁴¹ Addition of *tert*-butyl bromide to $\text{Co}(\eta\text{-C}_5\text{H}_4^t\text{Bu})(\text{PMe}_3)_2$, followed by deprotonation with NaH, yielded the product $[\text{Co}(\eta\text{-C}_5\text{H}_3^t\text{Bu}_2)(\text{PMe}_3)_2]$. Attempts to introduce a third substituent by this method failed.

In general, the barrier to rotation about the metal-to-ring centroid in η^5 -cyclopentadienyl metal complexes is very small, for ferrocenes it is 8-21 kJ mol⁻¹.⁴² Estimated values for other metallocenes and for cyclopentadienyl metal carbonyls are of the same order of magnitude. In $[\text{Co}(\eta\text{-C}_5\text{H}_3^t\text{Bu}_2)(\text{PMe}_3)_2]$, ¹H and ¹³C NMR spectroscopy studies can detect two chemically non-equivalent *tert*-butyl groups, even up to temperatures of 100 °C. The two butyl groups in conjunction with the phosphine ligands must hinder rotation of the cyclopentadienyl ring. It was observed that the analogous isopropyl substituted compound does not possess inequivalent isopropyl groups, indicating an absence of the rotational barrier present in the *tert*-butyl substituted compound.

The metallocene dichloride of zirconium, $\text{Zr}(\eta\text{-C}_5\text{H}_3^t\text{Bu}_2)_2\text{Cl}_2$ has been prepared by Lemenovskii and co-workers.⁴³ The compound $\text{Zr}(\eta\text{-C}_5\text{H}_3^t\text{Bu}_2)_2\text{Cl}_2$ was obtained by the reaction of ZrCl_4 with $(\eta\text{-C}_5\text{H}_3^t\text{Bu}_2)\text{Li}$. Reduction of the metallocene dichloride with potassium sand in pentane gave the reduced Zr(III) species $\text{Zr}(\eta\text{-C}_5\text{H}_3^t\text{Bu}_2)_2\text{Cl}$.

Due to the difficulties involved in preparing the tri-*tert*-butyl cyclopentadienyl ligand, very few complexes incorporating it are known. The first transition metal complex known incorporating $\eta\text{-C}_5\text{H}_2^t\text{Bu}_3$ was $\text{Mo}(\eta\text{-C}_5\text{H}_2^t\text{Bu}_3)(\text{CO})_3\text{CH}_3$, reported by Sitzmann in 1990.⁴⁴ Molybdenum hexacarbonyl and $(\eta\text{-C}_5\text{H}_2^t\text{Bu}_3)\text{Li}$ were refluxed for 18 h in THF, followed by the addition of MeI. As demonstrated here, homoleptic metal carbonyls are a useful synthetic starting point for the coordination of bulky

cyclopentadienyl ligands that can prove difficult to coordinate by other methods, especially per-phenyl substituted systems, see section 1.3.3.

1.3.2.2 Isopropyl substituted cyclopentadienyl ligands.

Multiple isopropyl substituted cyclopentadienes can be easily synthesized using the same alkylation of the cyclopentadienide anion with alkyl bromide used in *tert*-butyl substitution chemistry. The decreased steric demand of the isopropyl group means that tetra-isopropyl cyclopentadiene can be readily prepared in good yield. However, the substituent is still sufficiently bulky to cause poor yields in the synthesis of penta-isopropyl cyclopentadiene. Sitzmann has prepared the bis-tetra-isopropyl-cyclopentadienyl ferrocene, $\text{Fe}(\eta\text{-C}_5\text{H}^i\text{Pr}_4)_2$.⁴⁵ Starting from di-isopropyl cyclopentadiene, tri- and tetra-isopropyl cyclopentadienes can be synthesized by deprotonation with sodium amide and then by alkylation with 2-bromopropane; typically tetra-isopropyl cyclopentadienyl sodium and a 1:4 mixture of 1,2,3- and 1,2,4-tri-isopropyl cyclopentadienyl sodium are isolated. Reaction of FeCl_2 with $2(\eta\text{-C}_5\text{H}^i\text{Pr}_4)\text{Na}$ produced the ferrocene. However, the reaction of FeCl_2 with $\text{C}_5^i\text{Pr}_5\text{Na}$ does not yield a ferrocene derivative, but instead the stable radical, $\text{C}_5^i\text{Pr}_5^\bullet$, is isolated.⁴⁶ The bulky isopropyl substituents interfere with the formation of a sandwich structure. In the crystal the cyclopentadienyl units are packed to give a "metal-free polydecker". This radical is the first cyclopentadienyl radical characterised by X-ray structure analysis. The isopropyl groups are arranged in a "paddle-wheel" like arrangement around the five membered ring (Fig. 1.13).

In the crystal, half of the lattice sites are occupied by radicals with an opposite arrangement of the isopropyl groups. This is a form of prochirality and will be discussed later in an example of a coordinated $(\eta\text{-C}_5^i\text{Pr}_5)$ ring. In the analogous phenyl substituted system $\text{C}_5\text{Ph}_5\text{Na}$, a stable pentaphenyl cyclopentadienyl radical can also form when condensation reactions are attempted with metal halides.⁴⁷

Gloaguen and Astruc reported the first penta-isopropyl cyclopentadienyl complex, $[\text{Co}(\eta\text{-C}_5^i\text{Pr}_5)(\eta\text{-C}_5\text{H}_5)]^+$, **1.10**, prepared by the elegant simultaneous deprotonation and alkylation of $[\text{Co}(\eta\text{-C}_5\text{Me}_5)(\eta\text{-C}_5\text{H}_5)]^+$ (Scheme 1.16).⁴⁸ This was a development of a synthesis for per-alkyl substituted arene ligands, in which the per-alkyl complexes $[\text{Fe}(\eta\text{-C}_5\text{H}_5)(\text{C}_6(\text{CH}_2\text{R})_6)]^+$ (R = Me; Ph) are synthesized by reacting $[\text{Fe}(\eta\text{-C}_5\text{H}_5)(\text{C}_6\text{Me}_6)]^+$ with $^t\text{BuOK}$ and RX (X = Cl; Br).⁴⁹ Similarly, $[\text{Fe}(\eta\text{-C}_5\text{H}_5)(1,3,5\text{-C}_6\text{H}_3^i\text{Bu}_3)]^+$ is available from $[\text{Fe}(\eta\text{-C}_5\text{H}_5)(1,3,5\text{-C}_6\text{H}_3\text{Me}_3)]^+$ via multiple deprotonations and alkylations

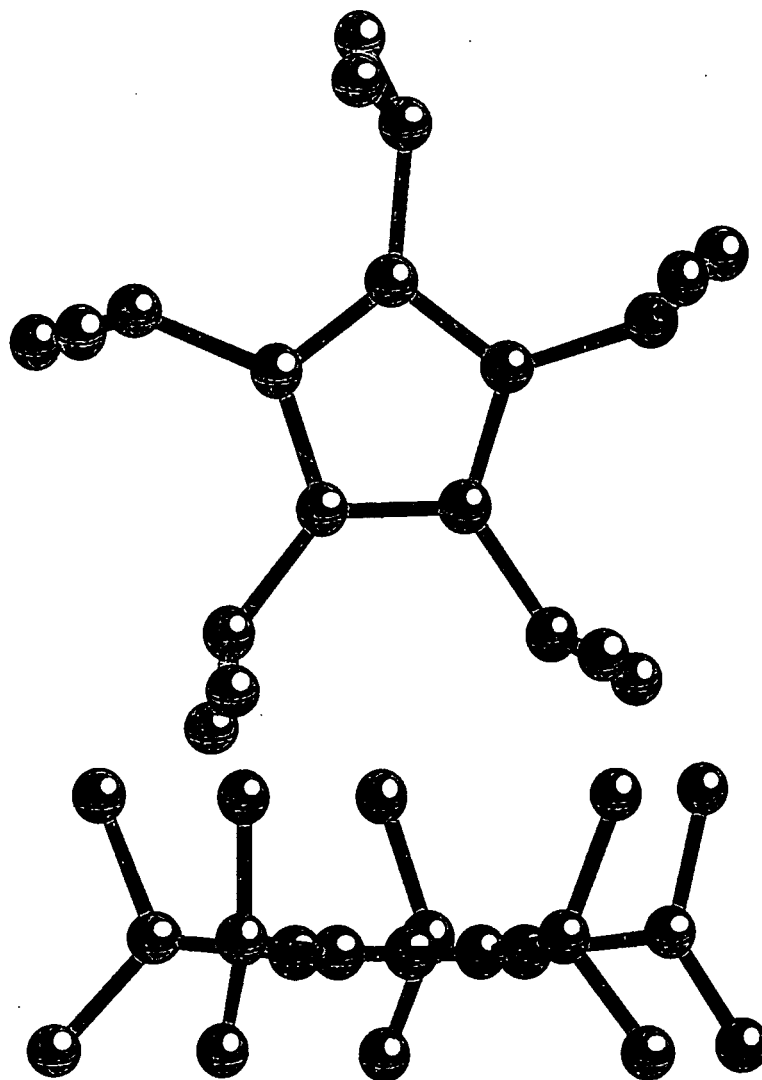
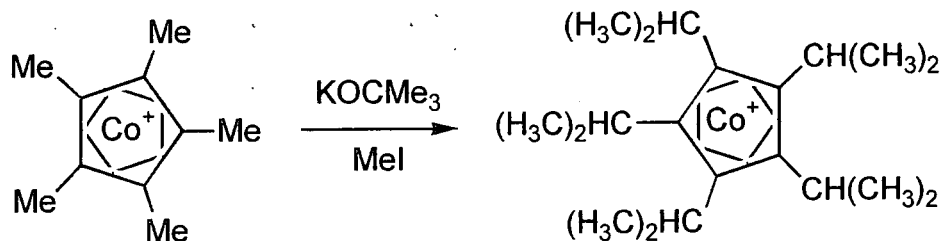
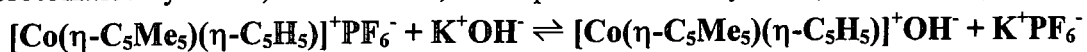


Fig. 1.13 Two views of molecular structure of $C_5Pr_5^+$, indicating "paddle-wheel" type structure.



Scheme 1.16 Simultaneous deprotonation and alkylation of $[Co(\eta-C_5Me_5)(\eta-C_5H_5)]^+$.

Extension of the alkylation to EtI is impossible using $tBuOK$ because the dehydrohalogenation of RX is faster than the deprotonation of the sandwich complex. However, the reaction works if KOH is used instead of $tBuOK$ and the reaction is performed with EtI as the solvent. Ion pair exchange provides the driving force for deprotonation by naked, reactive OH^- , in the phase transfer system (Scheme 1.17).



Scheme 1.17 Ion pair exchange.

At room temperature the ($\eta\text{-C}_5^i\text{Pr}_5$) complex **1.10** shows a rigid chiral conformation of the per-alkyl cyclopentadienyl ligand due to the “gear-meshing” of all five isoalkyl groups in such a manner that all methine protons point in the same direction (Fig. 1.14).

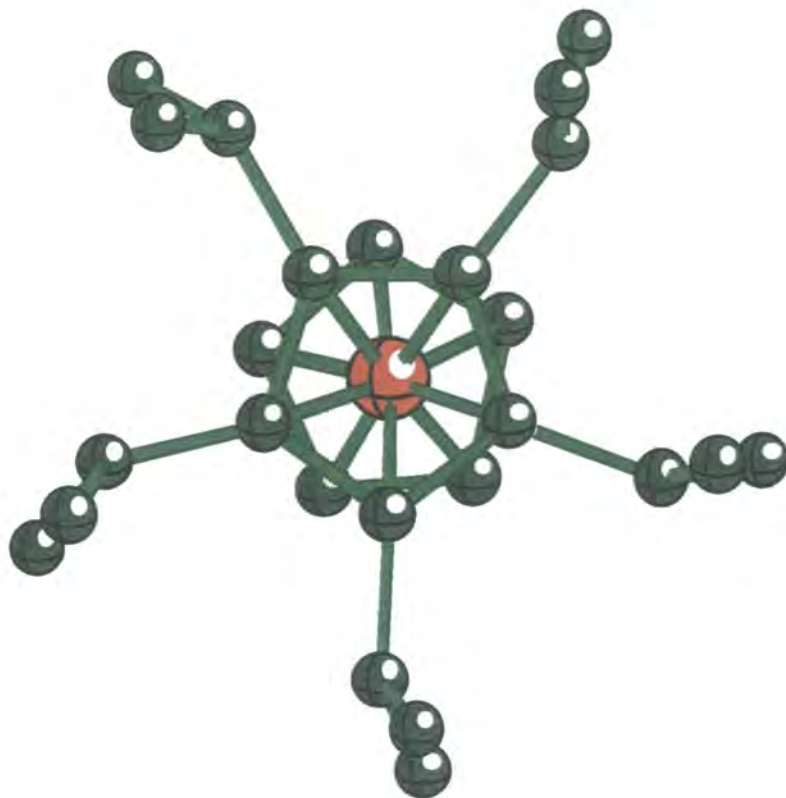


Fig. 1.14 The “gear-meshing” of all five isoalkyl groups of **1.10**.

This orientation causes a chirality that was first observed in hexa-substituted benzene derivatives.⁵⁰ This form of chirality is termed conformational directionality and it can be thought of as the same chirality present in a propeller (Fig. 1.15).

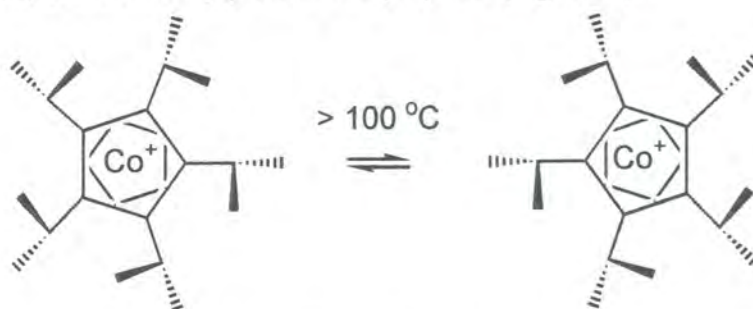


Fig. 1.15 Conformational directionality.

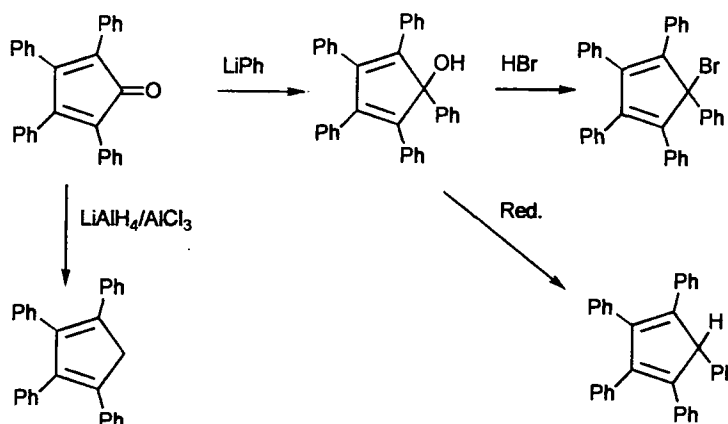
There are few other $\eta\text{-C}_5^i\text{Pr}_5$ containing complexes, but they too show this conformational directionality.⁴⁴ In all cases the two stereoisomers racemize at temperatures above 100 °C.

1.3.2.3 Other alkyl substituents.

Many other alkyl substituted cyclopentadienyl ligands exist, with varying degrees of steric demand, ease of synthesis and ease of metallation. The most common alkyl derivative is the methyl group in $\eta\text{-C}_5\text{Me}_5$. However, compared with *tert*-butyl and isopropyl groups, its steric demand is low. Other groups of interest in the literature that are relevant to $\eta\text{-C}_5\text{H}_n\text{R}_m$ chemistry are the benzyl, ethyl, trifluoromethyl and carbomethoxy groups.⁵¹ The electron withdrawing nature of multiple CF_3 groups renders groups such as $[\text{C}_5(\text{CF}_3)_4\text{H}]^-$ poor ligands with weak metal-ligands bonds. No reaction occurs between the tetrakis(trifluoromethyl) cyclopentadienide salt, $[\text{C}_5(\text{CF}_3)_4\text{H}]^-\text{Me}_4\text{N}^+$ and metal halides, owing to the low nucleophilicity of the anion. Reaction with the solvated metal cation $[(\eta\text{-C}_5\text{Me}_5)\text{Ru}(\text{MeCN})_3]^+\text{O}_3\text{SCF}_3^-$, however, resulted in quantitative formation of the mixed ruthenocene $[\text{Ru}(\eta\text{-C}_5(\text{CF}_3)_4\text{H})(\eta\text{-C}_5\text{Me}_5)]$. As an electron poor cyclopentadienyl ligand $[\text{C}_5(\text{CO}_2\text{Me})_5]^-$ has been extensively studied and its coordination chemistry has been comprehensively reviewed.^{51d}

1.3.3 Phenyl-substituted cyclopentadienyl ligands.

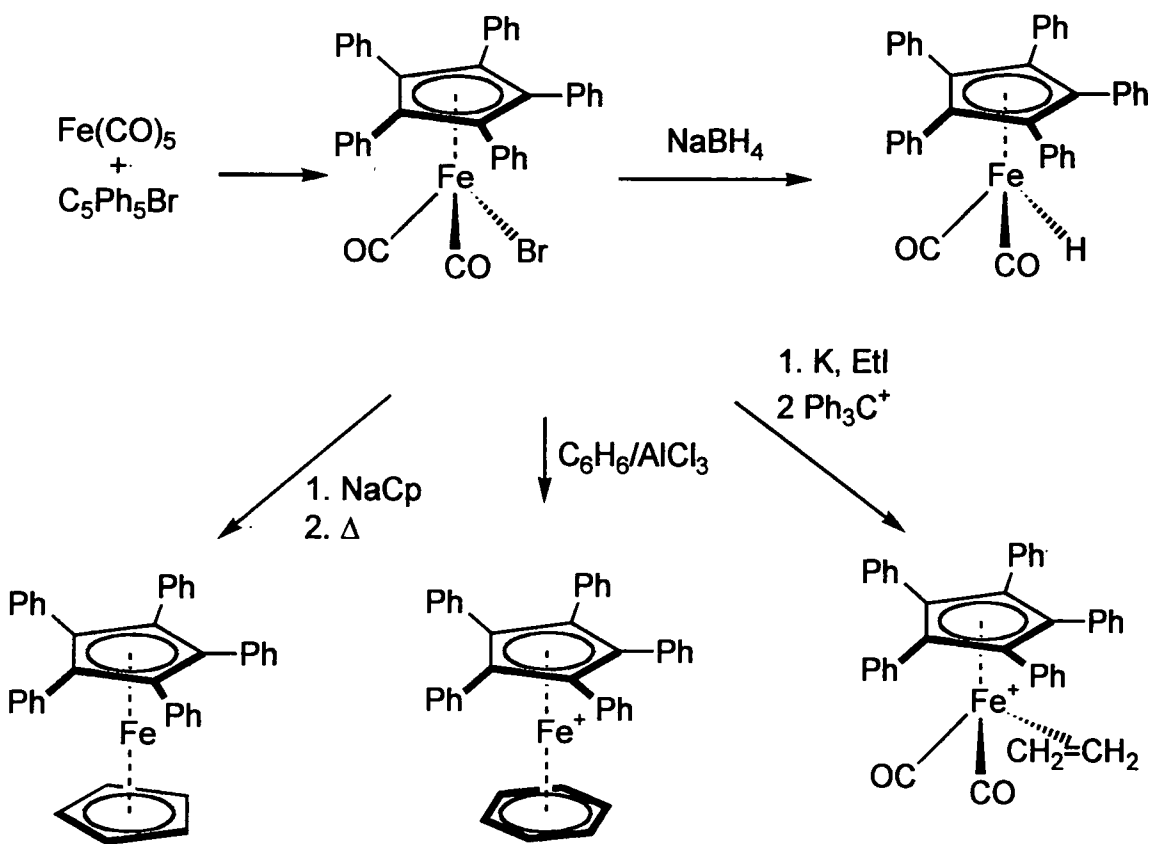
Substituted cyclopentadienyl ligands containing phenyl groups have been systematically used in transition metal chemistry since the work of Pauson in 1954.⁵² Tetracyclone, tetraphenyl cyclopentadienone, **1.11**, and a large number of both symmetrical and unsymmetrical analogues can be readily prepared.⁵³ From this easily synthesized compound $\text{C}_5\text{Ph}_4\text{H}$ can be prepared by reduction with $\text{LiAlH}_4/\text{AlCl}_3$ in high yields and $\text{C}_5\text{Ph}_5\text{Br}$, a useful $\eta\text{-C}_5\text{Ph}_5$ precursor, by reaction with phenyl lithium and HBr (Scheme 1.18).⁵⁴ It is also possible to reduce the product of the dienone and phenyl lithium reaction to form $\text{C}_5\text{Ph}_4\text{H}_2$.



Scheme 1.18 Routes to tetra- and penta-phenyl cyclopentadiene.

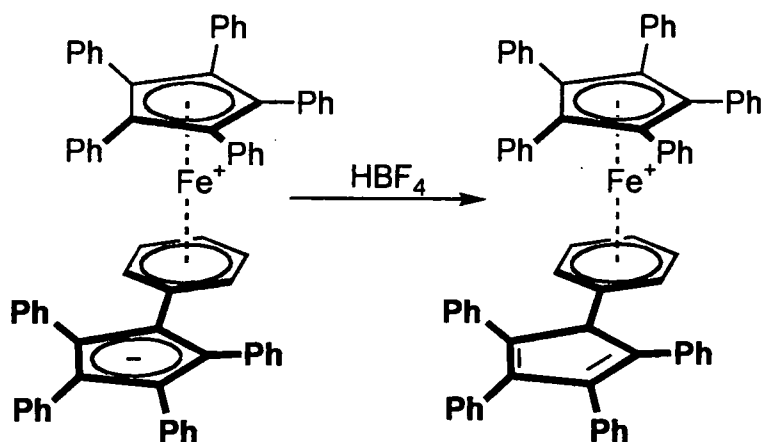
One of the earliest examples of the formation of a cyclopentadienyl ligand within the coordination sphere of a transition metal was the preparation of $\text{Fe}(\eta\text{-C}_5\text{HPh}_4)(\eta\text{-C}_5\text{H}_5)$ by Nakamura and Hagihara.^{54b} Diphenyl acetylene was reacted with $\text{Fe}(\eta\text{-C}_5\text{H}_5)(\text{CO})_2\text{CH}_3$ to give $\text{Fe}(\eta\text{-C}_5\text{HPh}_4)(\eta\text{-C}_5\text{H}_5)$. A number of $(\eta\text{-C}_5\text{Ph}_5)$ complexes that cannot be prepared by conventional means due to the formation of a stable radical, (see section 1.3.2.2), have been prepared using this synthetic route and diphenyl acetylene.⁵⁵

There are other reasons why few (η -C₅Ph₅) complexes have been reported. Those that have been prepared are frequently insoluble in commonly used solvents and have low volatility, they also have particularly uninformative ¹H and ¹³C NMR spectra. The only efficient way of introducing a (η -C₅Ph₅) ligand appears to be the oxidative addition of bromopentaphenyl cyclopentadiene to homoleptic carbonyl compounds. Masters and co-workers reacted C₅Ph₅Br with Fe(CO)₅ to afford dark red needles of Fe(η -C₅Ph₅)(CO)₂Br in good yield.⁵⁶ Conformational directionality is not observed as the phenyl rings are not all twisted out of the C₅-plane by the same amount. A number of compounds have since been synthesized using this "piano-stool" complex as a starting material (Scheme 1.19).⁵⁷



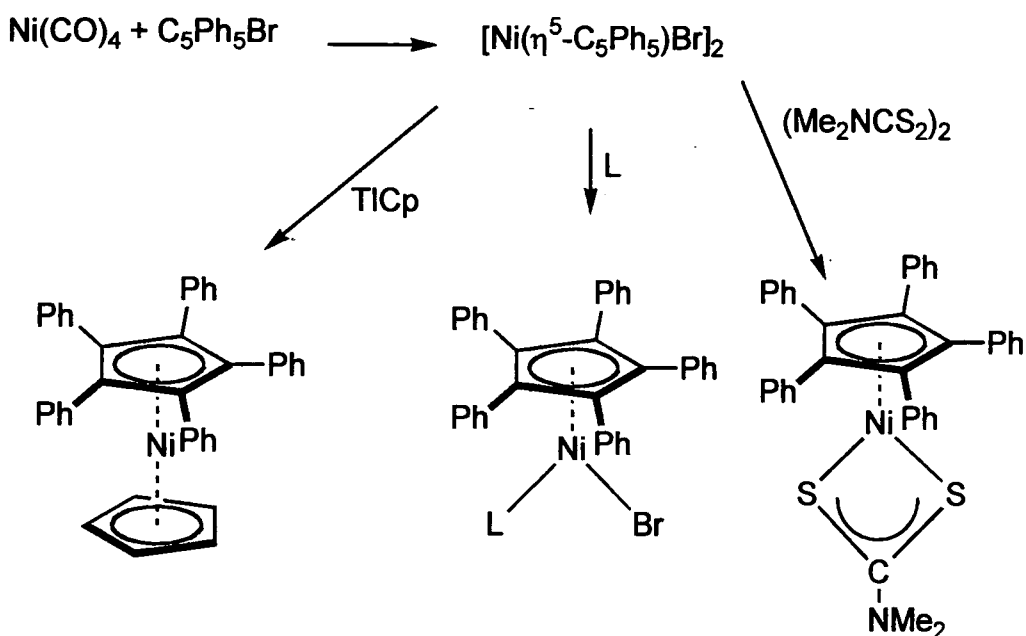
Scheme 1.19 Fe(η -C₅Ph₅)(CO)₂Br as a starting material.

The (η -C₅H₅) analogues of the complexes in Scheme 1.19 are kinetically very active, however the (η -C₅Ph₅) ligand renders the complexes shown kinetically inert. Masters and co-workers also synthesized an unusual zwitterionic isomer of decaphenyl ferrocene by refluxing C₅Ph₅Br, zinc and Fe(CO)₅ in benzene.⁵⁸ Using spectroscopic and electrochemical data a structure was deduced in which the Fe(η -C₅Ph₅) fragment is coordinated to one of the five phenyl groups in the second C₅Ph₅ ligand in an η^6 -fashion. Upon protonation of this zwitterionic species with HBF₄ the cation [Fe(η -C₅Ph₅)(η^6 -C₆H₅C₅HPh₄)]⁺ was produced (Scheme 1.20).



Scheme 1.20 Zwitterionic isomer of decaphenyl ferrocene and synthesis of $[\text{Fe}(\eta\text{-C}_5\text{Ph}_5)((\eta^6\text{-C}_6\text{H}_5)\text{C}_5\text{HPh}_4)]^+$.

Reactions of the bromide, $\text{C}_5\text{Ph}_5\text{Br}$, with $[\text{Co}(\text{CO})_4]^-$ or $\text{Co}_2(\text{CO})_8$, and with $\text{Ni}(\text{CO})_4$ have also been reported.⁵⁹ In the case of $\text{Ni}(\text{CO})_4$ the reaction forms $[\text{Ni}(\eta\text{-C}_5\text{Ph}_5)\text{Br}]_2$. This is a versatile starting material for the synthesis of half-sandwich complexes containing the $\text{Ni}(\eta\text{-C}_5\text{Ph}_5)$ fragment (Scheme 1.21).

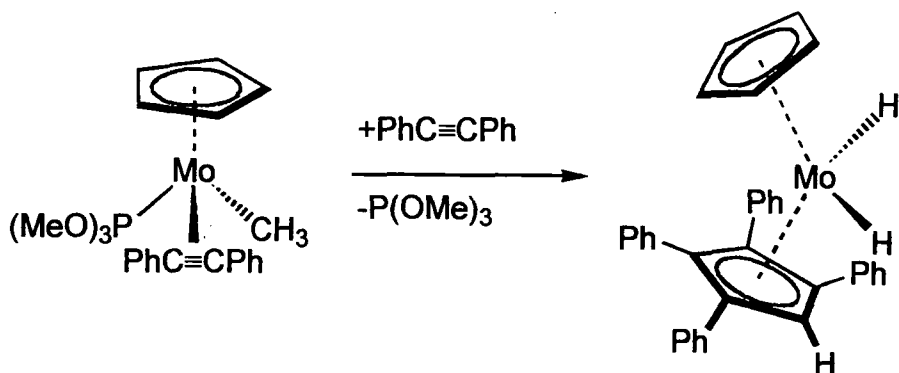


Scheme 1.21 Selected reactions of $[\text{Ni}(\eta\text{-C}_5\text{Ph}_5)\text{Br}]_2$.

Due to difficulties encountered with the pentaphenyl cyclopentadienyl ligand, the ligand $(\eta\text{-C}_5\text{Ph}_4\text{H})$ is more frequently used. The ferrocene $\text{Fe}(\eta\text{-C}_5\text{Ph}_4\text{H})_2$ is readily obtained from FeCl_2 and $\text{Li}(\text{C}_5\text{Ph}_4\text{H})$. Electron spectroscopic and electrochemical data are consistent with the slightly electron withdrawing property of the phenyl groups.⁵⁶ The analogous metallocenes of V, Cr, Co and Ni have all been prepared by reacting the metal halide with $\text{K}(\text{C}_5\text{Ph}_4\text{H})\cdot(\text{THF})_{1/2}$.⁶⁰

The titanocene chloride, $\text{Ti}(\eta\text{-C}_5\text{Ph}_4\text{H})_2\text{Cl}$, was prepared from TiCl_3 and $\text{K}(\text{C}_5\text{Ph}_4\text{H})$, and then oxidized with AgCl to give $\text{Ti}(\eta\text{-C}_5\text{Ph}_4\text{H})_2\text{Cl}_2$.⁶¹

An example of the rare formation of substituted cyclopentadienyl ligands within the coordination sphere of a metal is the synthesis of the tetraphenyl molybdenocene dihydride $\text{Mo}(\eta\text{-C}_5\text{Ph}_4\text{H})(\eta\text{-C}_5\text{H}_5)\text{H}_2$ by addition of diphenylacetylene to $\text{Mo}(\eta\text{-C}_5\text{H}_5)[\text{P}(\text{OMe})_3](\text{PhCCPh})\text{CH}_3$, followed by elimination of $\text{P}(\text{OMe})_3$, resulted in the desired product (Scheme 1.22).⁶²

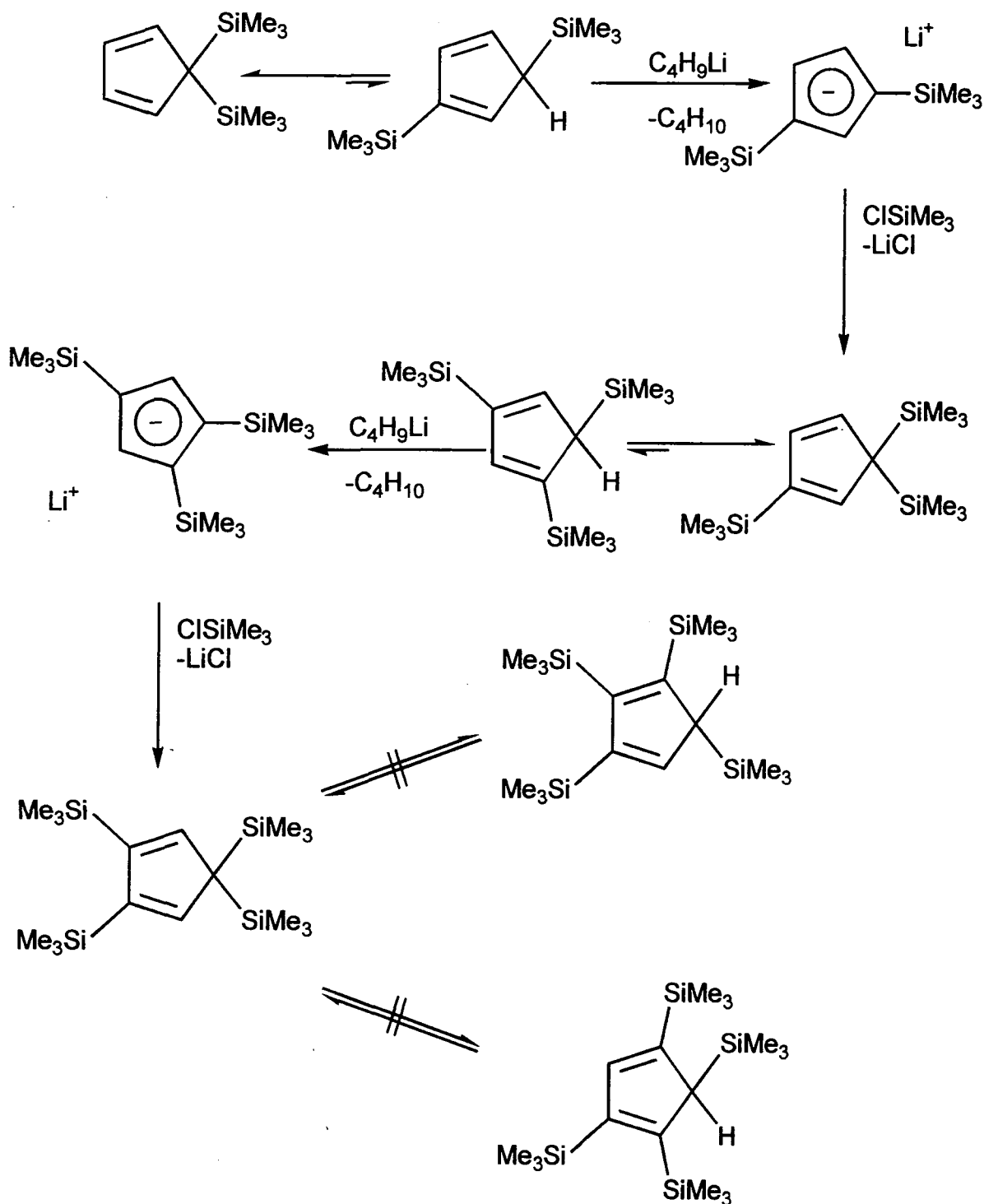


Scheme 1.22 Formation of $\eta\text{-C}_5\text{Ph}_4\text{H}$ within the coordination sphere of a molybdenum complex.

1.3.4 Silyl-substituted cyclopentadienyl ligands.

Cyclopentadienes with up to four trimethylsilyl groups can be prepared simply from cyclopentadiene via repeated metallation with *n*-butyllithium and treating the resulting cyclopentadienide anion with chlorotrimethylsilane.⁶³ For up to three trimethylsilyl groups the problem of regioisomers does not occur due to the trimethylsilyl-substituted cyclopentadienes being rendered fluxional by proto- and sila-tropic shifts.⁶⁴ The reason that multiply trimethylsilyl substituted cyclopentadienes can be prepared more easily than their *tetra*-butyl substituted analogues is the longer cyclopentadiene carbon-silicon bond. This results in a decrease in the adjacent substituent steric interaction.

In bis-, tris- and tetrakis-trimethylsilyl substituted cyclopentadienes, the isomers with two silyl substituents on the sp^3 carbon exist preferentially. However, upon deprotonation with *n*-butyllithium the thermodynamically most favourable anion is formed (Scheme 1.24). Metallation of bis-trimethylsilyl cyclopentadiene, which exists preferentially as the 5,5-isomer, selectively forms the 1,3-substituted anion. Tris-trimethylsilyl cyclopentadiene, which is mainly found as the 2,5,5-isomer, gives the 1,2,4-substituted anion. However, tetrakis-trimethylsilyl cyclopentadiene, found as the 2,3,5,5-isomer, is not fluxional due to the steric repulsion of trimethylsilyl groups on adjacent sp^2 carbons. Therefore, it cannot be deprotonated to form the cyclopentadienide anion.



Scheme 1.23 Synthesis of silyl-substituted cyclopentadienyl ligands.

Although no tetrakis- or pentakis-trimethylsilyl cyclopentadienyl transition metal complexes have been prepared, Sunkel and Hofmann have used a novel synthetic method to synthesize the first π -complex of a cyclopentadienyl ligand with five silyl substituents.⁶⁵ Starting from $(\eta-C_5Br_5)Mn(CO)_3$, the per-brominated analogue of cymantrene, $(\eta-C_5H_5)Mn(CO)_3$, the complex $[\eta-C_5(SiMe_2H)_5]Mn(CO)_3$ was prepared by a series of halogen-lithium exchange reactions, followed by silylation with $SiMe_2HCl$. The solid state molecular structure of this compound shows the same highly symmetrical

"paddle-wheel" orientation of the five silyl groups around the C₅-ring found previously in the isopropyl groups of penta-isopropyl cyclopentadienyl complexes (Fig. 1.16).

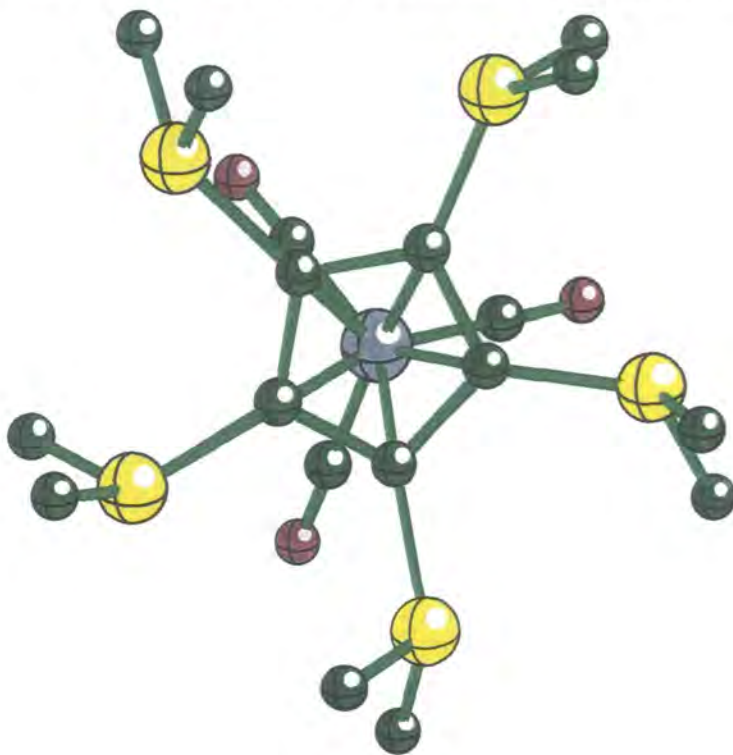


Fig. 1.16 Molecular structure of $[\eta\text{-C}_5(\text{SiMe}_2\text{H})_5]\text{Mn}(\text{CO})_3$ depicting the five membered ring in a "paddle-wheel" orientation.

Trimethylsilyl substituted cyclopentadienyl ligands are not as strongly electron donating as those with alkyl substituents. Electrochemical and spectroscopic studies have shown that trimethylsilyl groups on the cyclopentadienyl ligand can be characterized as weakly electron withdrawing.⁶⁶ The effects are small and any difference between the coordination chemistry of $(\eta\text{-C}_5\text{H}_5)$ or $(\eta\text{-C}_5\text{Me}_5)$ and multiply silyl substituted cyclopentadienyl ligands can be attributed to predominantly steric effects.

Mono and 1,1'-bis-trimethylsilyl ferrocene were synthesized in 1960 from $\text{Fe}(\eta\text{-C}_5\text{H}_5)_2$.⁶⁷ In 1978 1,1',3,3'-tetrakis-trimethylsilyl ferrocene was reported.⁶⁸ The reaction of the lithium salt of the cyclopentadienide anion gave the desired substituted ferrocene as an air- and moisture-stable crystalline product. The isolation of a small amount of $\text{Fe}[\eta\text{-C}_5(\text{SiMe}_3)_2\text{H}_3](\text{CO})_2\text{Cl}$ when the complexation reaction was performed at low temperatures under CO is thought to provide evidence of a stepwise coordination of the two $[\eta\text{-C}_5(\text{SiMe}_3)_2\text{H}_3]$ ligands.⁶⁹ X-ray structural analysis of $\text{Fe}[\eta\text{-C}_5(\text{SiMe}_3)_2\text{H}_3]_2$ shows the five membered rings adopting a fully eclipsed conformation so that the two pairs of trimethylsilyl groups are interlocked, a similar conformation is found in the X-ray structural analysis of $\text{Fe}(\eta\text{-C}_5\text{H}_3^t\text{Bu}_2)_2$ (Fig. 1.17).

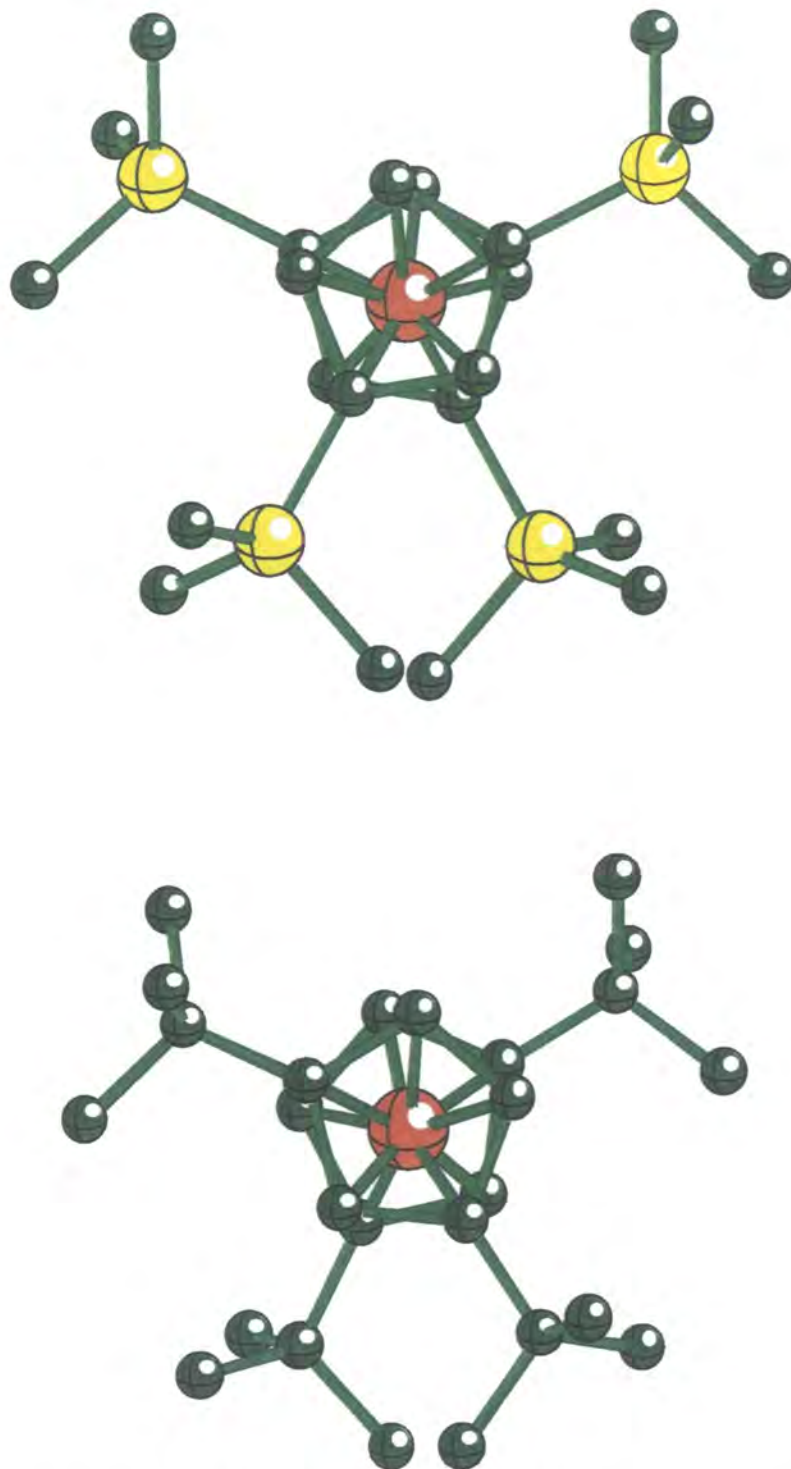
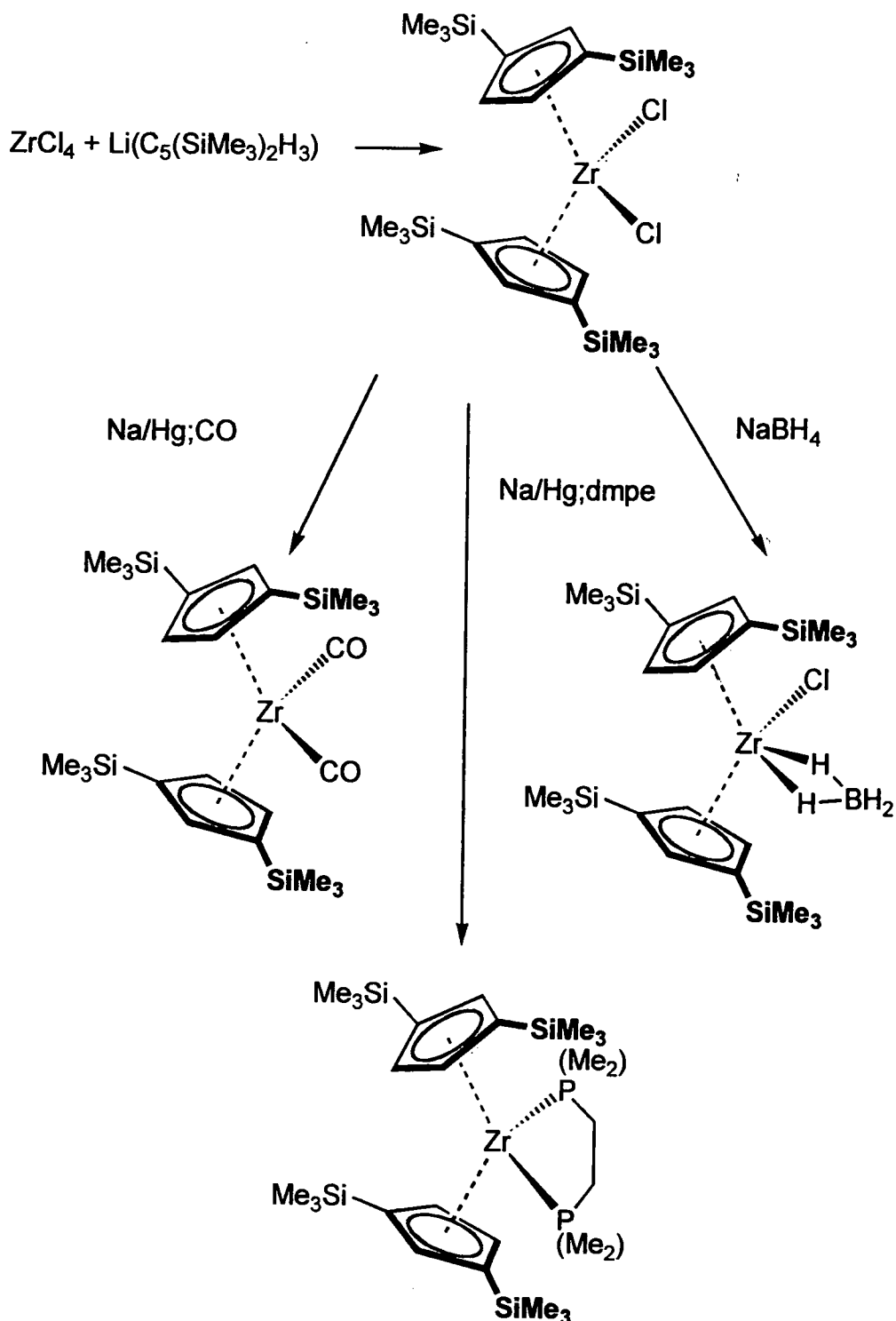


Fig. 1.17 Molecular structures of $\text{Fe}[\eta\text{-C}_5(\text{SiMe}_3)_2\text{H}_3]_2$ and $\text{Fe}(\eta\text{-C}_5\text{H}_3^i\text{Bu}_2)_2$.

The zirconocene dichloride, $\text{Zr}[\eta\text{-C}_5(\text{SiMe}_3)_2\text{H}_3]_2\text{Cl}_2$ has been prepared by Lappert and co-workers, and is a versatile starting material for a variety of complexes (Scheme 1.24).⁷⁰ Reduction of the zirconocene dichloride with sodium amalgam gave the dimeric complex $\{\text{Zr}[\eta\text{-C}_5(\text{SiMe}_3)_2\text{H}_3]_2\text{Cl}\}_2$.⁷¹ Reduction with the amalgam under CO gave the dicarbonyl $\text{Zr}[\eta\text{-C}_5(\text{SiMe}_3)_2\text{H}_3]_2(\text{CO})_2$ and in the presence of 1,2-bis(dimethylphosphino)ethane, dmpe, gave $\text{Zr}[\eta\text{-C}_5(\text{SiMe}_3)_2\text{H}_3]_2(\text{dmpe})$.⁷² Treatment of the original metallocene with NaBH_4 gave a complex with a η^2 -bonded BH_4 ligand, $\text{Zr}[\eta\text{-C}_5(\text{SiMe}_3)_2\text{H}_3]_2\text{Cl}(\text{BH}_4)$.⁷³



Scheme 1.24 Synthesis and reactions of $\text{Zr}(\eta\text{-C}_5(\text{SiMe}_3)_2\text{H}_3)_2\text{Cl}_2$.

The reaction of $\text{Li}[\eta\text{-C}_5(\text{SiMe}_3)_3\text{H}_2]$ with FeBr_2 gives 1,1',2,2',4,4'-hexakis-trimethylsilyl ferrocene, $\text{Fe}[\eta\text{-C}_5(\text{SiMe}_3)_3\text{H}_2]_2$, in low yields.⁷⁴ Okuda has discovered at low temperatures a highly reactive, thermally labile intermediate with one $[\eta\text{-C}_5(\text{SiMe}_3)_3\text{H}_2]$ unit per iron centre.⁷⁵ Despite the reactivity of this species, the low yield of the ferrocene is thought to be due to the difficulty in attaching the second $[\eta\text{-C}_5(\text{SiMe}_3)_3\text{H}_2]$ ligand at the iron centre due to the extreme bulk of this ligand. The sandwich structure determined using X-ray structural analysis showed a congested molecule with an average iron-ring distance of 2.082 Å, a ring tilt of 6.1° and the conformation shown in Fig. 1.18.

One pair of trimethylsilyl groups are eclipsed so as to enable the other two pairs to be fully staggered.

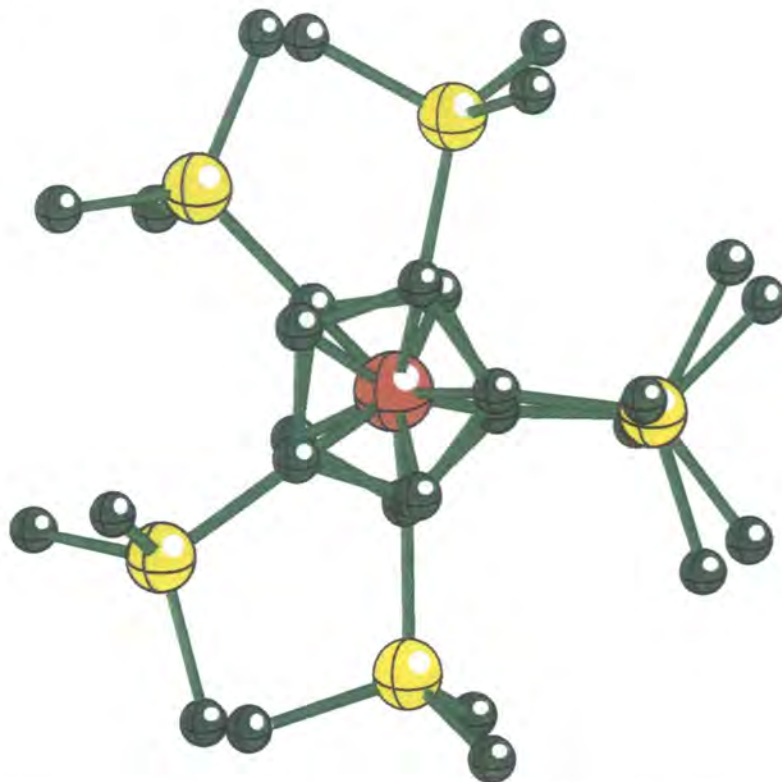
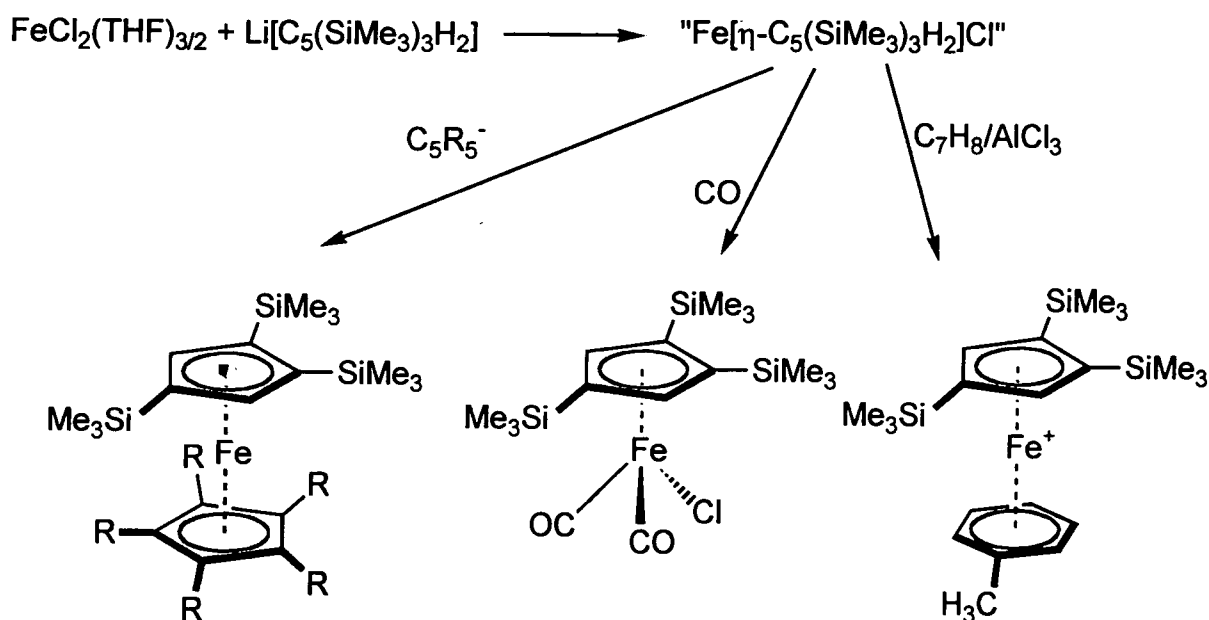


Fig. 1.18 Molecular structure of $\text{Fe}[\eta\text{-C}_5(\text{SiMe}_3)_3\text{H}_2]_2$.

The reactive intermediate discovered by Okuda behaves as a functional equivalent of the 14-electron half-sandwich fragment $\text{Fe}[\eta\text{-C}_5(\text{SiMe}_3)_3\text{H}_2]\text{X}$ (Scheme 1.25). It can be trapped with the two electron donor CO to give the complex $\text{Fe}[\eta\text{-C}_5(\text{SiMe}_3)_3\text{H}_2](\text{CO})_2\text{X}$.⁷⁵ In the presence of AlCl_3 and an arene such as toluene it gives rise to the formation of the mixed sandwich complex $\{\text{Fe}[\eta\text{-C}_5(\text{SiMe}_3)_3\text{H}_2](\eta\text{-C}_6\text{H}_5\text{CH}_3)\}^+$.⁷⁶ Other cyclopentadienyl transfer reagents such as $\text{Na}(\eta\text{-C}_5\text{H}_5)$ or $\text{Li}(\eta\text{-C}_5\text{Me}_5)$, when reacted with the intermediate, generate mixed ferrocene derivatives $\text{Fe}[\eta\text{-C}_5(\text{SiMe}_3)_3\text{H}_2](\eta\text{-C}_5\text{H}_5)$ and $\text{Fe}[\eta\text{-C}_5(\text{SiMe}_3)_3\text{H}_2](\eta\text{-C}_5\text{Me}_5)$.⁷⁷

Unlike the ferrocene the cobaltocene analogue, $\text{Co}[\eta\text{-C}_5(\text{SiMe}_3)_3\text{H}_2]_2$, and the nickelocene analogue, $\text{Ni}[\eta\text{-C}_5(\text{SiMe}_3)_3\text{H}_2]_2$, are easily prepared.⁷⁸ In the case of the nickelocene the intermediate with one $[\eta\text{-C}_5(\text{SiMe}_3)_3\text{H}_2]$ ligand per nickel atom, probably an analogue of $[\text{Ni}(\eta\text{-C}_5\text{Ph}_5)\text{X}]_2$, was trapped via the isolation of the phosphine complex, $\text{Ni}[\eta\text{-C}_5(\text{SiMe}_3)_3\text{H}_2](\text{PPh}_3)\text{Cl}$.

Winter and co-workers have prepared 1,1',2,2',4,4'-hexakis-trimethylsilyl zirconocene dichloride by reacting tris-trimethylsilyl cyclopentadienyl lithium with zirconium tetrachloride. ¹³C NMR spectroscopic measurements have indicated that the complex shows hindered rotation of the cyclopentadienyl ligand with a barrier to rotation of 46.1kJ mol^{-1} .⁷⁹



Scheme 1.25 Reactions of the functional equivalent of $\text{Fe}[\eta\text{-C}_5(\text{SiMe}_3)_3\text{H}_2]\text{X}$.

1.3.5 Summary.

Substitution of cyclopentadienyl rings can affect the electronic and physical properties of the complexes they are part of. The most commonly used alkyl substituents are *tert*-butyl groups, of which up to three can be relatively easily placed on a cyclopentadienyl ring, and isopropyl groups, where up to four can be easily substituted onto the cyclopentadienyl ring, although pentaisopropyl cyclopentadienyl complexes are known. Tetra- and penta-phenyl substituted cyclopentadienyl complexes are known. Pentaphenylcyclopentadienyl rings are difficult to coordinate to metals unless homoleptic carbonyls are used as the metal source. Although up to four trimethylsilyl groups can be put on a cyclopentadiene ring, no tetrakis-trimethylsilyl cyclopentadienyl transition metal complexes have been prepared. Steric interactions between adjacent SiMe_3 groups on a cyclopentadienyl ring are less than that for adjacent CMe_3 groups due to the longer cyclopentadienyl carbon-silicon bond length.

1.4 Tetrahydroindenones and Tetrahydroindenes.

1.4.1 Introduction.

The substituted analogues of the annulated cyclopentadienyl ligand 4,5,6,7-tetrahydroindenyl are of interest as bulky, prochiral ligands in a variety of transition metal complexes (Fig. 1.19). One such example is ethylene-bis- η -tetrahydroindenyl-zirconium dichloride which is used as a precursor to highly active soluble Ziegler-Natta catalysts for the preparation of polypropylene, (see section 1.5.2).⁸⁰

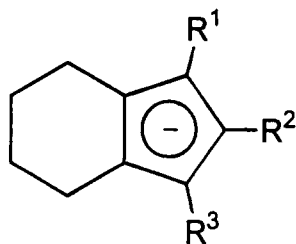
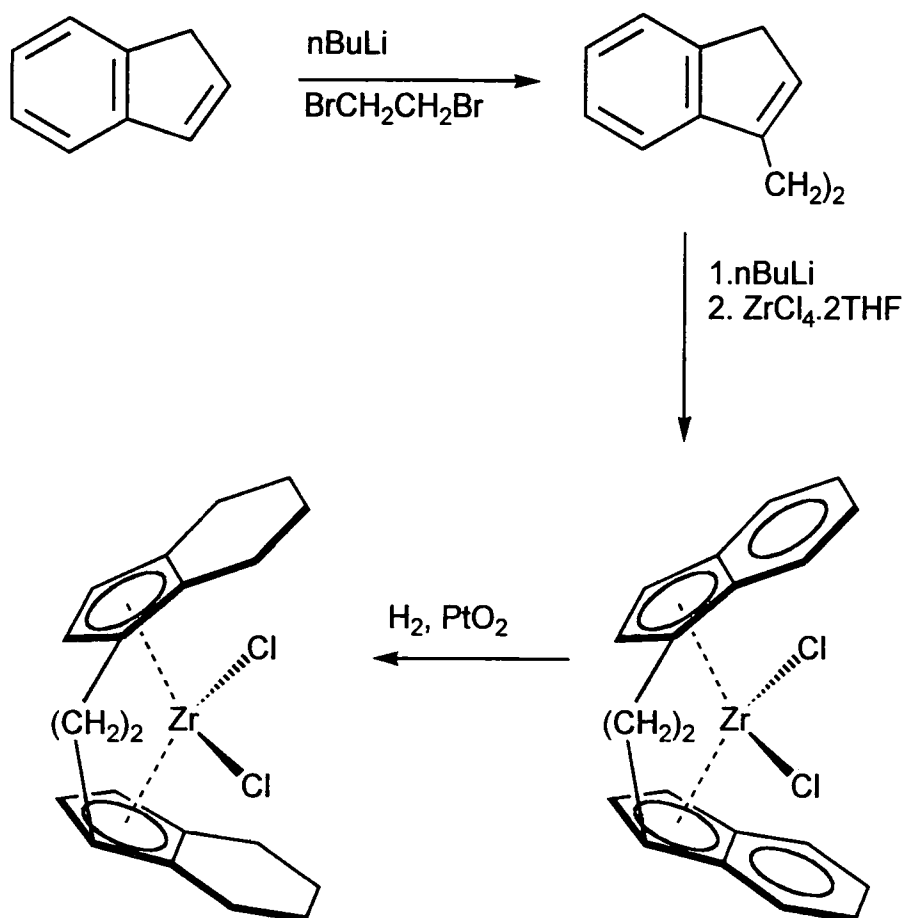


Fig. 1.19 1-R¹-2-R²-3-R³-4,5,6,7-Tetrahydroindenyl.

Initial methods of preparing tetrahydroindenyl ligands involved hydrogenation of the six membered aromatic ring of the corresponding complexed indenyl ligand (Scheme 1.26).⁸¹



Scheme 1.26 Synthesis of tetrahydroindenyls via hydrogenation of complexed indenyls.

Alternative methods of preparing tetrahydroindenones involve multi-step organic reactions from starting materials that are either commercially available or easily synthesized. However, the routes to the final tetrahydroindenones have little adaptability, leading to a limited variety of substituted ligands. Herrmann and co-workers synthesized tetrahydroindenones and their cyclopentylidene analogues via the rearrangement of spiro lactones, (Fig. 1.20) which can be made from commercially available oxiranes.⁸² The tetrahydroindenones prepared were precursors for ligands of neodymium and zirconium complexes of the type $(\eta\text{-C}_5\text{R}_5)_2\text{ZrCl}_2$, $[(\eta\text{-C}_5\text{R}_5)_2\text{NdCl}]_2$ and $(\eta\text{-C}_5\text{R}_5)_3\text{Nd}$.

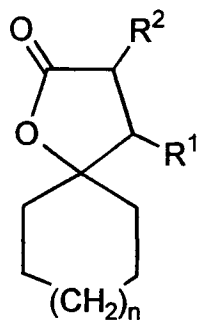
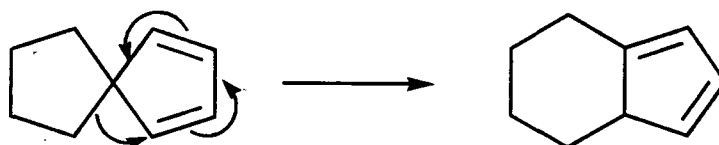


Fig. 1.20 Spirolactones.

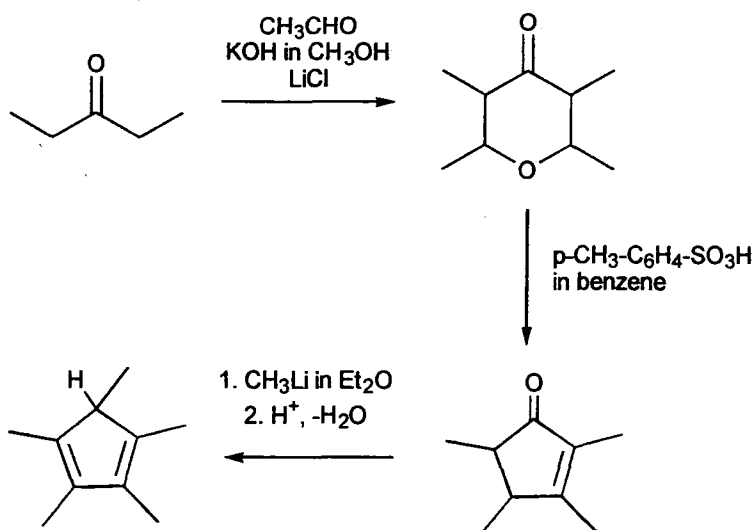
Yang and co-workers used a known, facile sigmatropic rearrangement of spiro[4.4]nona-1,3-diene to construct tetrahydroindene (Scheme 1.27).⁸³



Scheme 1.27 Sigmatropic rearrangement of spiro[4.4]nona-1,3-diene to 4,5,6,7-tetrahydroindene.

Although this avoids the preparation and catalytic hydrogenation of the indenyl complexes, the synthetic route has limited flexibility and can only produce a small range of substituted cyclopentadienes.

Nile and co-workers have reported the synthesis of 4,5,6,7-tetrahydroindene and its 1-methyl-, 1,3-dimethyl- and 1,2,3-trimethyl- congeners via the methylation of the corresponding cyclopentenones.⁸⁴ Cyclopentenones, and tetrahydroindenones, through their α,β -unsaturated ketone functionality, represent a versatile and facile route into substituted cyclopentadiene chemistry. The ubiquitous substituted cyclopentadiene, pentamethylcyclopentadiene, is commonly prepared via a cyclopentenone (Scheme 1.28).⁸⁵ This section will discuss the synthesis of tetrahydroindenones via a particular cyclization and the tetrahydroindenones derived from them.



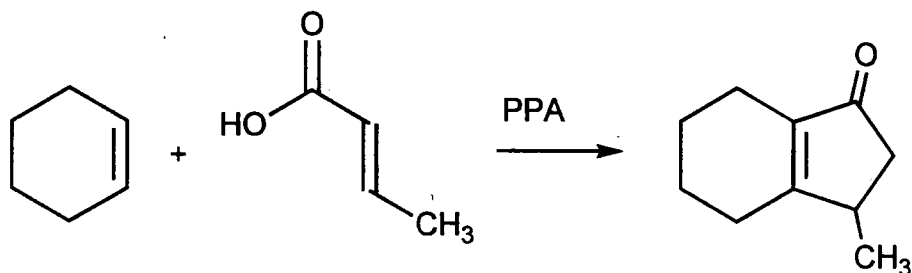
Scheme 1.28 One synthesis of pentamethylcyclopentadiene.

1.4.2 Tetrahydroindenones.

1.4.2.1 Synthesis.

Nile and co-workers used a preparation reported by Dev to synthesize 3-methyl-2,3,4,5,6,7-hexahydroind-8(9)-en-1-one, **1.12** (Scheme. 1.30).⁸⁶

In the work of Dev, the direct generation of substituted cyclopentenones via the acylation of cycloalkenes with suitable unsaturated acids in the presence of polyphosphoric acid, PPA, was investigated. Nile used cyclohexene and crotonic acid to generate his cyclopentenone system.



Scheme 1.29 Reaction of cyclohexene and crotonic acid in PPA to generate 3-methyl-2,3,4,5,6,7-hexahydroind-8(9)-en-1-one, **1.12**.

Dev explains how PPA is active for various acid-catalysed transformations and cyclizations due to the polar phosphorus pentoxide unit made available in the ionising medium (Fig. 1.21).

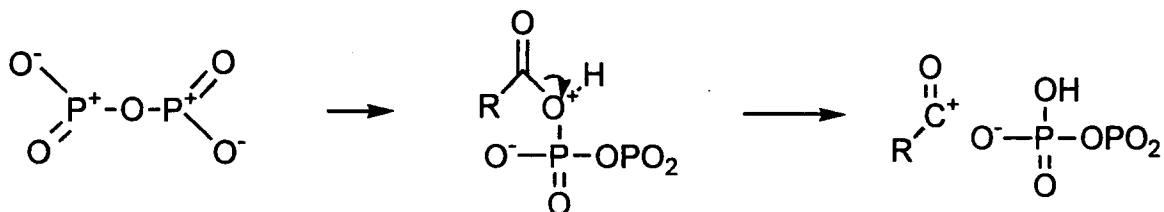


Fig. 1.21 Reaction of organic acids in PPA to generate acylium cation.

The dissolution of organic acids in PPA leads rapidly and reversibly to the formation of the preliminary coordination complex shown in Fig. 1.21. The complex is rapidly stabilised by the electron-interactions shown in Fig. 1.21 to give the acylium cation.

In the case of crotonic acid the oxocarbenium ion is stabilised by the resonance shown in Fig. 1.22.

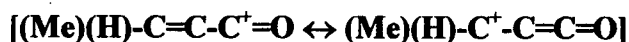
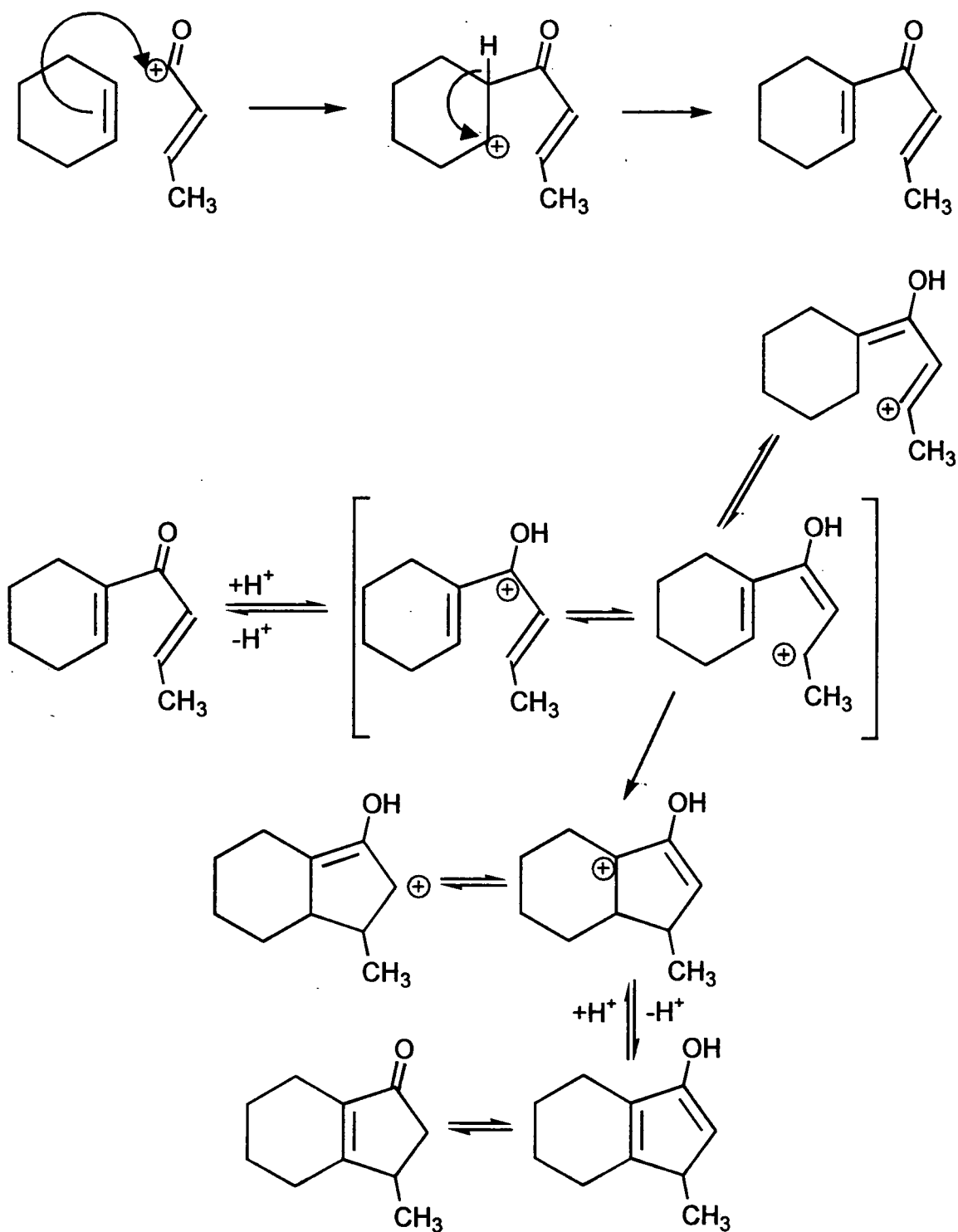


Fig. 1.22 Resonance stabilised oxocarbenium ion.

The cation generated attacks the olefinic linkage in cyclohexene, which stabilises itself by the elimination of a proton to yield the divinyl ketone. The divinyl ketone then undergoes ring closure as shown in Scheme 1.30 to yield the corresponding cyclopentenone. The cyclization pathway described is termed a Nazarov cyclization.



Scheme 1.30 Nazarov cyclization of a divinyl ketone.

1.4.2.2 Nazarov cyclizations.

Whilst studying the formation of allyl vinyl ketones by the mercuric ion and acid-catalysed hydration of dienyne in the 1950's, Nazarov and his co-workers discovered a secondary reaction to form 2-cyclopentenones.⁸⁷ Nazarov initially formulated a direct acid-catalysed closure of the allyl vinyl ketones and demonstrated the preparation of 2-

cyclopentenones from these precursors in dozens of cases. In 1952, Braude and Coles suggested the presence of carbocations as intermediates and demonstrated that the formation of 2-cyclopentenones actually proceeds via the α,α' -divinyl ketones.⁸⁸ A broader definition of the Nazarov cyclization includes a wide variety of precursors that under specific reaction conditions also produce 2-cyclopentadienones via divinyl ketones or their functional equivalents. It is the structural variety of precursors that lends versatility to the Nazarov cyclization. The essential structural feature for the Nazarov cyclization is a 3-hydroxypentadienylic cation (Fig. 1.23). Nazarov cyclizations have been reviewed.⁸⁹

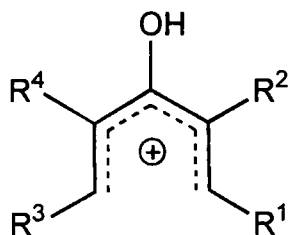
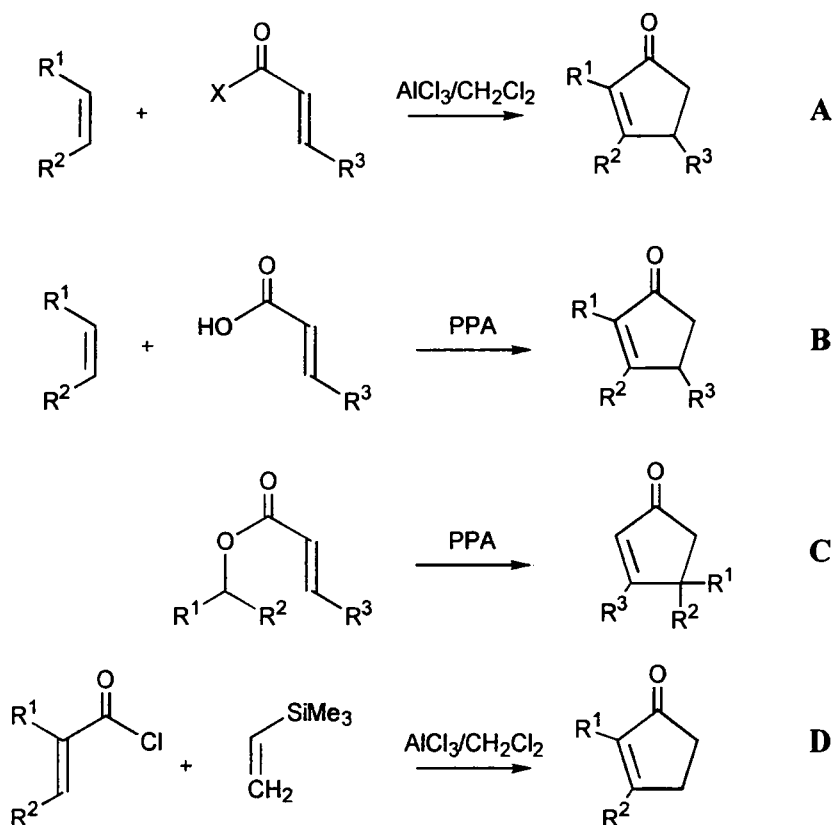


Fig. 1.23 A 3-hydroxypentadienylic cation.

Any substrate that can form this intermediate can potentially undergo Nazarov cyclization. Proven substrate systems include: olefins and α,β -unsaturated acyl chlorides and bromides (Scheme 1.31A),⁹⁰ olefins and α,β -unsaturated acids (Scheme 1.31B);⁹¹ α,β -unsaturated esters (Scheme 1.31C),⁹² vinyl silanes and α,β -unsaturated acyl chlorides (Scheme 1.31D).⁹³



Scheme 1.31 Selected reagents capable of undergoing Nazarov cyclization.

1.4.3 Tetrahydroindenenes.

The work of Collins and co-workers demonstrates that tetrahydroindenyls can be prepared from the parent indenyls using catalytic hydrogenation, see Scheme 1.26. Bosnich and co-workers prepared the ligand (S,S)-2,3-butylene-1,1'-bis(indene) from diindenyl magnesium and the dimesylate of (R,R)-2,3-butanediol.⁹⁴ Reaction of the dilithium salt of (S,S)-2,3-butylene-1,1'-bis(indenide) with $\text{TiCl}_4 \cdot 2\text{THF}$ in THF under high dilution conditions, to prevent the formation of oligomeric by-products, gave $\{\text{Ti}[(\text{S,S})\text{-2,3-butylene-1,1'-bis(indenyl)}]\text{Cl}_2\}$. Upon catalytic reduction with PtO_2/H_2 , $\{\text{Ti}[(\text{S,S})\text{-2,3-butylene-1,1'-bis(4,5,6,7-tetrahydroindenyl)}]\text{Cl}_2\}$ was formed as a mixture of isomers. The isomers consisted of the [R,R-(S,S)], [S,S-(S,S)] and [R,S-(S,S)] diastereomers. Upon irradiation, a photostationary state consisting of 85% of the [R,R-(S,S)] isomer and 15% of the [R,S-(S,S)] isomer was obtained. (R,R)- $\{\text{Ti}[(\text{S,S})\text{-2,3-butylene-1,1'-bis(4,5,6,7-tetrahydroindenyl)}]\text{Cl}_2\}$ was isolated and its crystal structure determined using X-ray diffraction (Fig. 1.24).

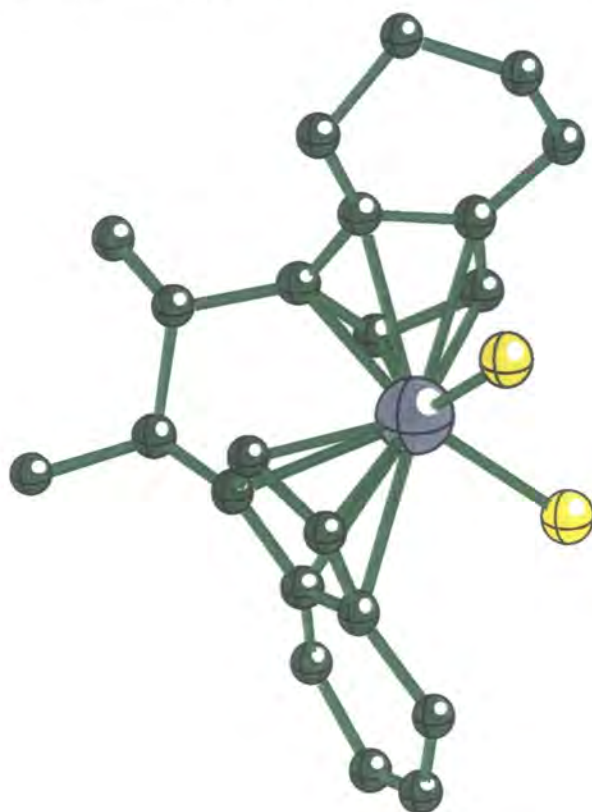


Fig. 1.24 Solid state molecular structure of (R,R)- $\{\text{Ti}[(\text{S,S})\text{-2,3-butylene-1,1'-bis(4,5,6,7-tetrahydroindenyl)}]\text{Cl}_2\}$.

The corresponding zirconium complexes were obtained in low yield. There is a strong kinetic preference for the (R,S)- $\{\text{Zr}[(\text{S,S})\text{-2,3-butylene-1,1'-bis(4,5,6,7-tetrahydroindenyl)}]\text{Cl}_2\}$ isomer, which was isolated and its structure also determined using X-ray diffraction (Fig. 1.25). The photostationary state was different from that of the titanocene analogue, consisting of a mixture of the [R,R-(S,S)] and [S,S-(S,S)] diastereomers.

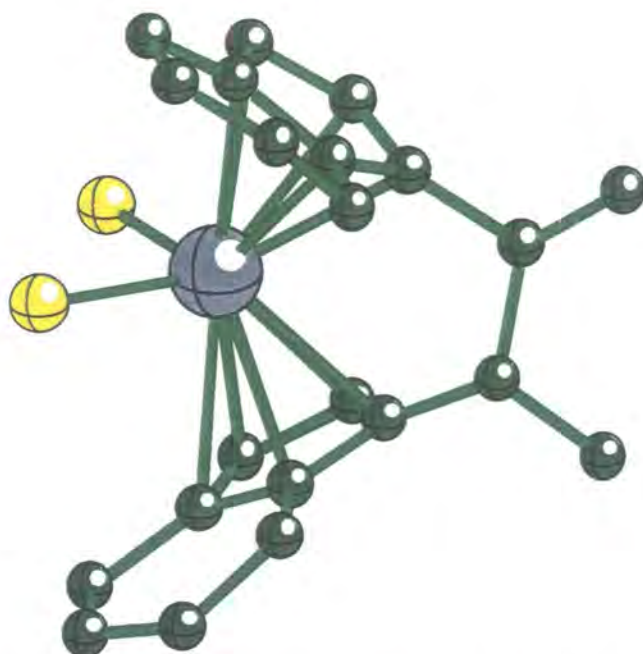


Fig. 1.25 Solid state molecular structure of (R,S)-{Zr[(S,S)-2,3-butylene-1,1'-bis(4,5,6,7-tetrahydroindenyl)]Cl₂}

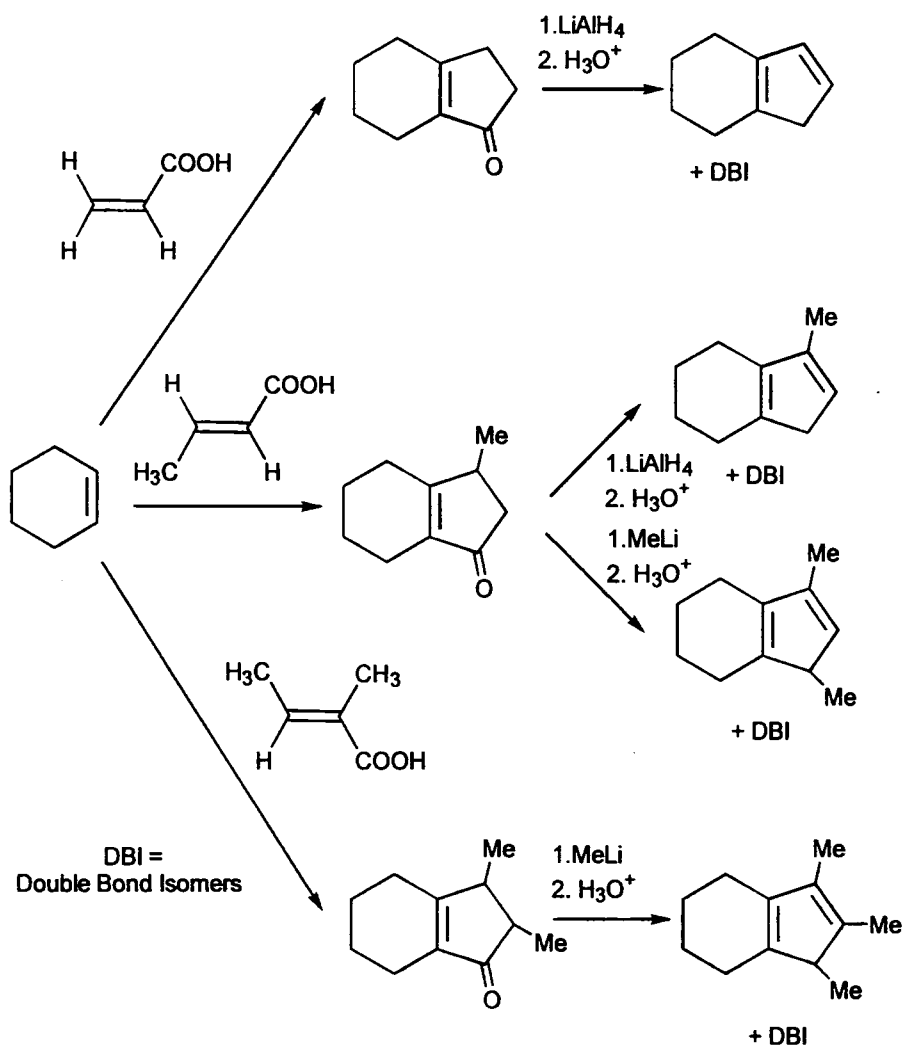
Catalytic hydrogenation of a complexed indenyl is a very inflexible route that limits the synthesis of an extensive range of tetrahydroindenide complexes, especially those containing any moieties that are sensitive to hydrogenation.

As mentioned earlier cyclopentenones are easily prepared using the method of Dev via a Nazarov cyclization. The starting materials, crotonic acid, tiglic acid, acrylic acid and polyphosphoric acid are all commercially available. The ketones generated are treated with LiAlH₄ or MeLi to give allylic alcohols that are dehydrated *in situ* using HCl (Scheme 1.32). Para-toluene sulphonic acid can also be used to dehydrate allylic alcohols to give cyclopentadienes.⁹⁵ The addition-dehydration process yields the desired tetrahydroindenes. Analysis by gas-chromatography indicates that tetrahydroindenes are formed as mixtures of isomers.

Nile synthesized the ferrocenes of each of the tetrahydroindenyl ligands by treating FeCl₂ with a tetrahydroindenide lithium or bis-tetrahydroindenide magnesium reagent, generated *in situ*. However, yields were low and Nile suggests this may be due to some of the double bond isomers formed not having sufficiently acidic hydrogens to be deprotonated when reacted with ⁿBuLi or (ⁿBu)₂Mg, see section 2.2.2.

Using X-ray structural analysis the cyclopentadienyl rings of bis(1,3-dimethyl-4,5,6,7-tetrahydroindenyl) iron and bis(1,2,3-trimethyl-4,5,6,7-tetrahydroindenyl) iron were observed to be in different conformations (Fig. 1.26). The rings in the dimethyl derivative were staggered as in Fe(η-C₅Me₅)₂ and Fe(η-C₅Me₄H)₂.⁹⁶ The cyclohexylidene rings are *trans* to one another with the steric bulk of the substituents causing the carbons of the two methyl groups and the two carbons of the cyclohexylidene ring adjacent to the cyclopentadienyl ring to deviate from the plane of

the five membered ring by an average of 0.057 Å. $\text{Fe}(\eta\text{-C}_5\text{Me}_5)_2$ and $\text{Fe}(\eta\text{-C}_5\text{Me}_4\text{H})_2$ show similar distortions with average deviations of 0.064 Å and 0.060 Å respectively. In the trimethyl tetrahydroindenyl ferrocene the cyclopentadienyl rings and cyclohexylidene rings are eclipsed. The carbons of the three methyl groups and two adjacent cyclohexylidene carbons deviate from the plane with an average deviation of 0.118 Å. Nile describes this greater deviation as being caused by the more severe steric interactions in the trimethylated ferrocene due to the eclipsed conformation. However, the iron atom-cyclopentadienyl centroid distance is 1.669 Å which is similar to that for the dimethylated ferrocene, 1.662 Å.



Scheme 1.32 Nazarov cyclization products of cyclohexene with acrylic, crotonic and tiglic acid.

The differing conformations between the two ferrocenes are not as important as might be thought. Almenningen and co-workers have estimated the stability of the favoured staggered conformation for $\text{Fe}(\eta\text{-C}_5\text{Me}_5)_2$ to be only 4.2 kJ mol⁻¹ relative to the eclipsed form.⁹⁷ Therefore the different conformations for the bis-tetrahydroindenyl ferrocenes prepared by Nile can probably be explained by small forces in crystal packing, perhaps caused by interlocking of the puckered cyclohexylidene rings in the trimethylated ferrocene.

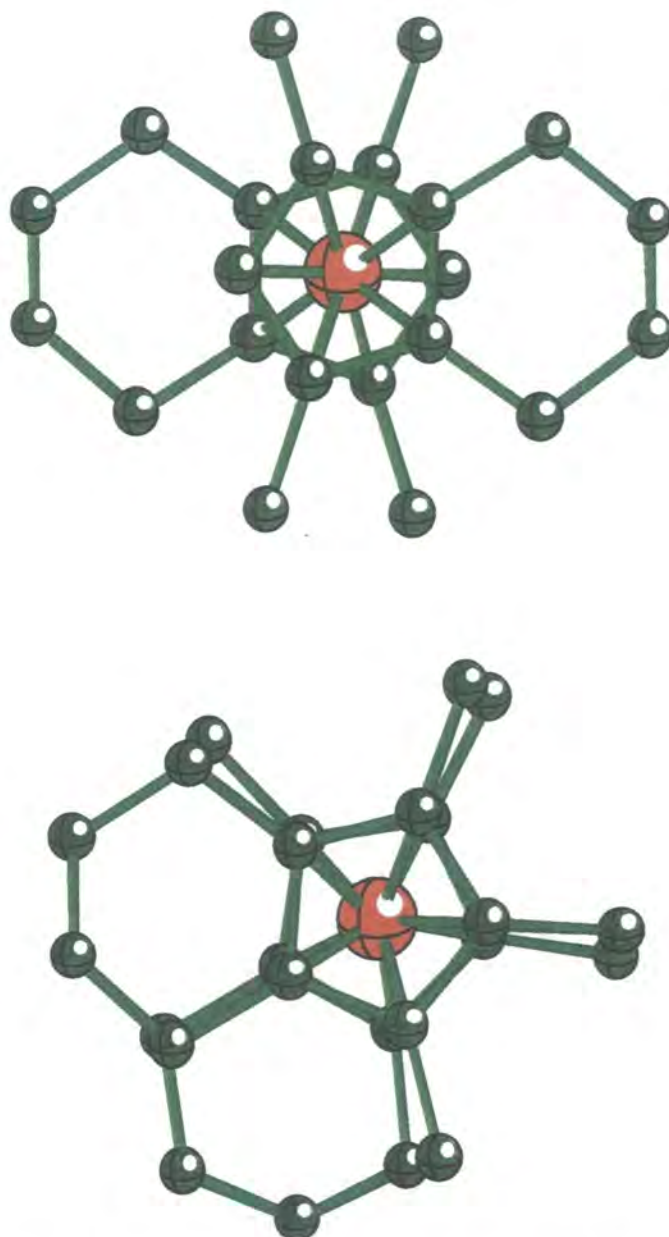


Fig. 1.26 Molecular structures of bis(1,3-dimethyl-4,5,6,7-tetrahydroindenyl) iron(II) and bis(1,2,3-trimethyl-4,5,6,7-tetrahydroindenyl) iron(II).

1.4.4 Summary.

Substituted tetrahydroindenyls are of interest as bulky, chiral ligands. Initial methods of preparation involved catalytic hydrogenation of pre-complexed indenyl analogues. Subsequent synthetic methods involved multi-step syntheses with little adaptability that led to a limited variety of ligand systems. Nile and co-workers have used a two step synthesis derived from the work of Dev to prepare methylated tetrahydroindenes. The tetrahydroindene intermediate is prepared by a Nazarov cyclization and has potential synthetic versatility due to its α,β -unsaturated ketonic functionality. A wide variety of tetrahydroindenones can be prepared due to the wide range of precursors that can undergo Nazarov cyclization. The essential structural feature of a Nazarov cyclization is a 3-hydroxypentadienylic cation.

1.5 Applications of Chiral Cyclopentadienyl Metal Complexes.

1.5.1 Introduction.

There are three main areas in which chiral cyclopentadienyl complexes are of use as enantioselective mediators:

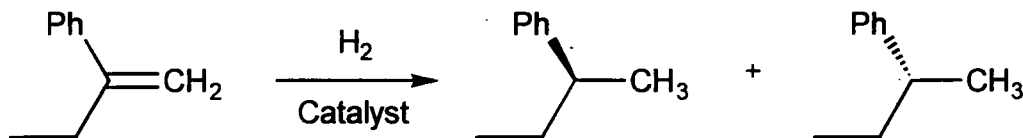
- 1) stoichiometric diastereoselective reactions;
- 2) catalytic enantioselective reactions;
- 3) catalytic polymerization of alkenes into stereoregular polymers.

The catalytic reactions combine the reactivity of transition metal complexes with the ability to repeatedly and consistently propagate asymmetry with great efficacy. At present, interest in stoichiometric diastereoselective reactions is substantially less than that for catalytic systems, but will probably grow as the need for resolution of racemic cyclopentadienyl complexes grows. An example of stoichiometric diastereoselective reactions is the work of Faller and Linebarrier with neomenthyl derivatives of chiral cyclopentadienyl molybdenum complexes in section 1.2.2b(iii). The catalytic systems will be discussed in further detail in this section.

1.5.2 Catalytic enantioselective reactions.

1.5.2a Hydrogenation.

Enantioselective hydrogenation of simple alkenes was the first published example of a chiral cyclopentadienyl mediated reaction (Scheme 1.1). The work of Kagan with enantiomerically pure menthyl- or neomenthyl-substituted titanocene dichlorides has already been discussed in section 1.2.1. The application of chiral cyclopentadienyl metal complexes as mediators for the hydrogenation of 2-phenyl-1-butene remains widespread, as it is one of the most common methods for ascertaining the ability of a new ligand to induce asymmetry into a complex (Scheme 1.33). The most selective chiral metallocene catalyst for the hydrogenation of 2-phenyl-1-butene to date (95% e.e. with 25 turnovers at $-78\text{ }^{\circ}\text{C}$, 68% e.e. with 100 turnovers at $25\text{ }^{\circ}\text{C}$) is the titanocene dichloride of the diphenyl bicyclo-[2.2.2]-octane-fused cyclopentadienyl ligand shown earlier in Fig. 1.9.

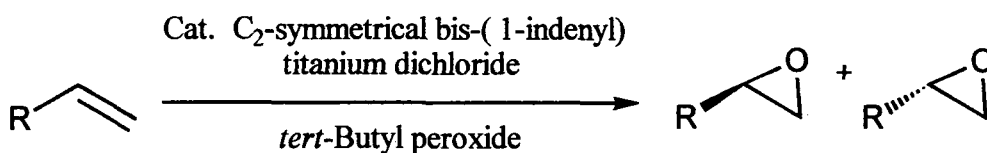


Scheme 1.33 Enantioselective hydrogenation of 2-phenyl-1-butene.

1.5.2b Epoxidation.

Although titanocene dichloride, $(\eta\text{-C}_5\text{H}_5)_2\text{TiCl}_2$, in solution does not show any activity in the epoxidation of alkenes, the use of polymer-bound titanocene does cause the epoxidation to proceed catalytically.⁹⁸ Coletti and Halterman have reported the only example of using chiral cyclopentadienyl metal catalysts for asymmetric epoxidation

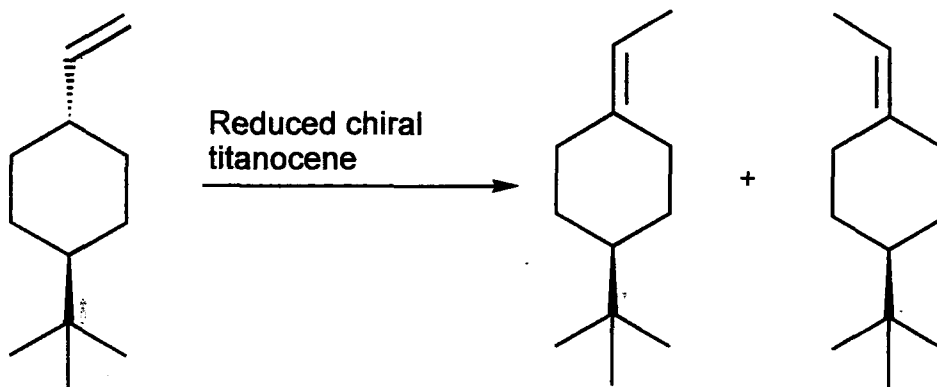
(Scheme 1.34).⁹⁹ They describe the use of a C₂-symmetrical bis-(1-indenyl) titanium dichloride as a catalyst for the asymmetric epoxidation of alkenes in the presence of *tert*-butyl hydroperoxide, although with only moderate activity (40-60 turnovers) and enantioselectivity (12-22% e.e.).



Scheme 1.34 Asymmetric catalytic epoxidation of alkenes.

1.5.2c Alkene isomerisation.

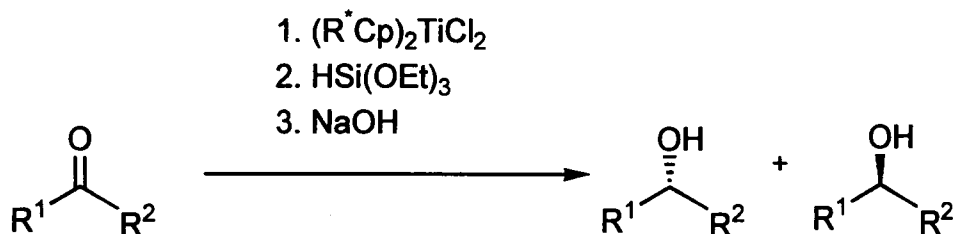
Treatment of (η-C₅H₅)₂TiCl₂ at elevated temperatures with LiAlH₄ partially reduces the complex to give an unidentified titanium species that can insert into an allylic C-H bond to generate an intermediate π-allyltitanium hydride species which can undergo reductive elimination to give the free isomerized alkene.¹⁰⁰ Chen and Halterman have reported the enantioselective isomerization of the *meso*-vinylcyclohexane shown in Scheme 1.35 into the chiral ethylenecyclohexane in the presence of a reduced *ansa*-bis(indenyl)-titanium dichloride. The catalyst gave 80% e.e. with 50 turnovers at 23 °C.¹⁰¹



Scheme 1.35 Asymmetric alkene isomerization.

1.5.2d Ketone Hydrosilylation.

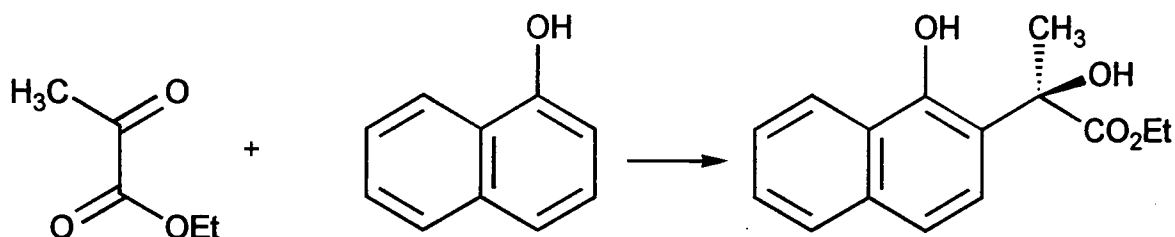
After Buchwald's reported use of (η-C₅H₅)₂TiCl₂ as a catalyst for the hydrosilylation of ketones, followed by hydrolysis of the silyl ether formed to generate a secondary alcohol, Chen and Halterman examined the reduction using chiral bis(cyclopentadienyl)- and *ansa*-bis(indenyl) titanium dichlorides as catalysts.¹⁰² (Scheme 1.36) The enantioselectivities of the reaction were low (1-20%).



Scheme 1.36 Hydrosilylation of ketones.

1.5.2e Aldol reactions.

Erker and co-workers have reported the use of a chiral cyclopentadienyl zirconium trichloride complex incorporating a C_2 -symmetrical tetrasubstituted cyclopentadienyl system derived from camphor as an effective enantioselective mediator in the aldol-like carbon-carbon coupling reaction of 1-naphthol with ethylpyruvate to give good yields of the chiral acetate shown in Scheme 1.37 (27-80% e.e. depending on reaction temperature).



Scheme 1.37 Coupling reaction of ethyl pyruvate with 1-naphthol.

1.5.3 Catalytic stereoregular polymerizations.

Alkene polymerization is one of the most important catalytic reactions in commercial use. The Ziegler-Natta catalysts, for which Ziegler and Natta won the Nobel Prize in 1963, account for millions of tons of polyethylene and polypropylene annually. The best known catalysts are $TiCl_3/Et_2AlCl$ and variants, which are heterogeneous catalysts, polymerization occurring at crystal defects where Ti is coordinatively unsaturated. $TiCl_3/Et_2AlCl$ is active at 25 °C and 1 atm, in contrast with thermal polymerization which occurs in the absence of catalyst at 200 °C and 100 atm. Metallocene catalysts have been used to produce polyolefins commercially since the early 1990's, but the application of group 4 metallocenes as Ziegler-Natta catalysts for the polymerization of alkenes have been known since 1957.¹⁰³ Ewen first reported the efficacy of chiral group 4 metallocenes as mediators of the stereoregular polymerization of α -olefins.¹⁰⁴ He employed a C_2 -symmetric ethanobridged-indenyl-titanocene/MAO system as an effective homogeneous isospecific propylene polymerization catalyst (Fig. 1.27).

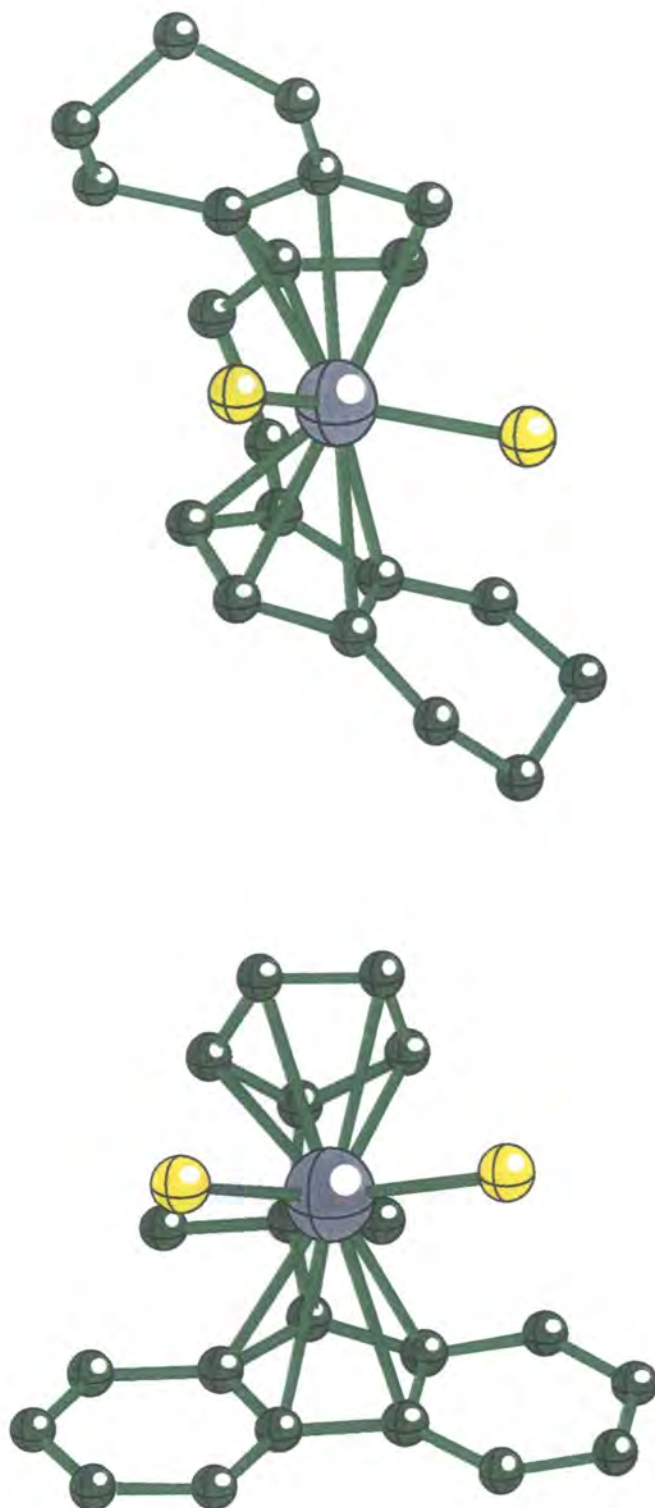


Fig. 1.27 Molecular structures of C_2 - and C_s -symmetric metallocenes.

There are five potential variations in the tacticity of polypropylene (PP), three are considered the "main" types (Fig. 1.28). These three structural forms occur due to the different positions of the pendant structural group relative to the main polymer chain, and each form results in very different properties.¹⁰⁵

In isotactic PP the pendant methyl groups are all on one side of the polymer chain or molecule. This structure does not allow chains to crystallize in a planar zigzag form, but instead a helix is formed with three molecules per turn of the helix. Commercial grades

of PP are usually in the order of 90-95% isotactic. A higher isotactic index leads to higher crystallinity and so higher stiffness, tensile strength and hardness.

In the case of syndiotactic PP, the methyl groups alternate in order on either side of the molecule. This results in less crystallization because the pendant groups sterically hinder the formation of the helical structures.

The third form, atactic PP, is random in order. It is therefore an amorphous polymer with very little strength and of little commercial value.

The remaining two varieties are really sub-classes of the first two. Stereoblock is an isotactic polymer where isotactic blocks of the opposite configuration are present. Hemiisotactic is where every other stereocentre has the same configuration, stereocentres in-between have completely random stereochemistry.

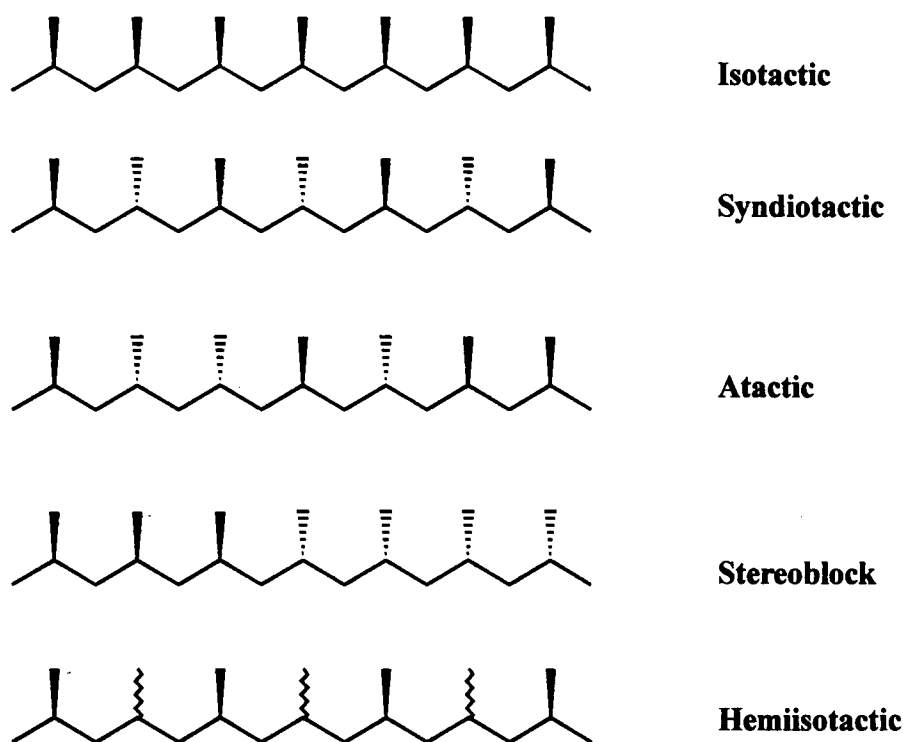


Fig. 1.28 Different types of polymer tacticity.

Ewen also reported diphenyl titanocene as affording isotactic polypropylene, though with a different microstructure and at low temperatures, which is unusual as unsubstituted, achiral titanocenes more commonly produce atactic polypropylene. Both of the systems described by Ewen gave predominantly isotactic polypropylene. However, the microstructure of the polymer synthesized using the chiral metallocene as a mediator was consistent with that obtained via an enantiomorphic site-control mechanism (predominantly isotactic) and the microstructure of the polymer prepared using diphenyl titanocene as a catalyst had a microstructure consistent with that obtained via a chain-end-control mechanism (predominantly stereoblock). With site-control the orientation of olefin insertion is dependent on the chiral-influence of the cavity surrounding the coordination site at the metal (Fig. 1.29). In the case of C_2 -symmetric complexes the

handedness of the cavity does not change whichever side of the complex the olefin approaches from, so each monomer unit is oriented the same way upon insertion forming isotactic polymers. In the case of the achiral C_3 -symmetric metallocene, also discussed by Ewen, the cavities on either side of the molecule are of opposite handedness so monomer units insert with alternately opposite conformation, leading to syndiotactic polymer (Fig. 1.27, molecular structure of C_3 -symmetric metallocene, zirconocene depicted as molecular structure of C_3 -symmetric titanocene unavailable; Fig. 1.29, olefin polymerization using a C_3 -symmetric system). Insertion of unfavourably aligned olefins does not affect the overall tacticity of the polymer because subsequent insertions are dependent on the nature of the cavity surrounding the olefin coordination site at the metal. In chain-end-control polymerization the orientation of the previously inserted olefin is what decides the conformation, upon insertion, of the next olefin coordinating to the metal complex.

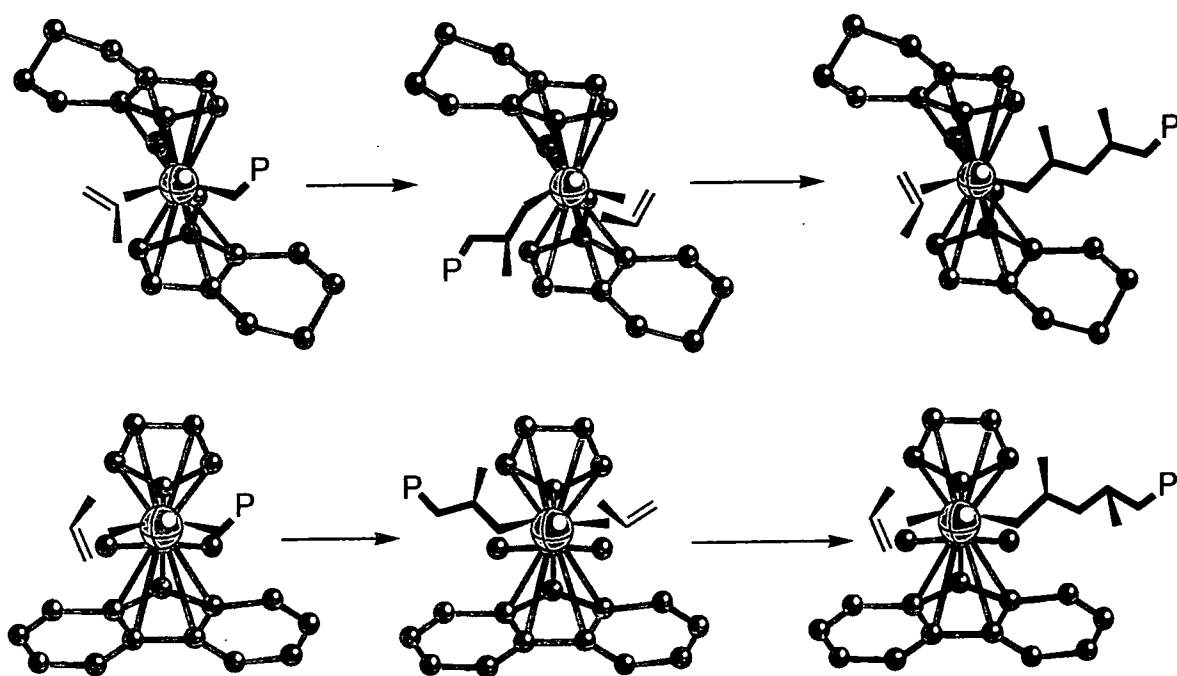


Fig. 1.29 Enantiomorphic site control producing isotactic (*pseudo-C₂*-symmetric metal system, above) and syndiotactic (*pseudo-C₃*-symmetric system, below) polymers.

The systems explored by Ewen were predominantly titanocenes and their indenyl analogues, Kaminsky and Brintzinger have used ethanobridged bis-(tetrahydro-1-indenyl) zirconium dichlorides to give highly isotactic polypropylene with high molecular weight and narrow molecular weight range.¹⁰⁶ These catalytic studies have been largely limited to ring-bridged bis(indenyl) and bis(tetrahydroindenyl) group 4 complexes and other axially symmetric metallocenes. The syntheses of these ligands generally produce substantial quantities of the undesirable *meso*-isomer, requiring tedious separation of the *rac*-isomer. If a single enantiomer of the *rac*-isomer is required additional

functionalization and separation are required. In catalytic polymerization of propene enantiomerically pure catalysts are not required since the polymer produced has *meso*-symmetry and is essentially achiral. To avoid the necessity of removing unwanted achiral *meso*-isomers Marks and co-workers have synthesized chiral group 4 and lanthanide metallocenes with C_1 -symmetry which, when combined with a variety of cation forming co-catalysts, are highly active ethylene and isospecific propylene polymerization catalysts.¹⁰⁷ Marks also reports significant counteranion effects which offer additional control of polymer microstructure and molecular weight.

1.5.4 Summary.

Chiral cyclopentadienyl metal complexes have been applied to a small number of reactions that have already been shown to be mediated by achiral cyclopentadienyl complexes. Mediation can be stoichiometric or catalytic. Catalytic systems are more extensively researched at the moment, the most comprehensively studied are stereoregular polymerizations. Other catalytic enantioselective reactions include hydrogenation, epoxidation, alkene isomerization, ketone hydrosilylation and aldol reactions.

1.6 References.

- 1 T. J. Kealy and P. L. Pauson, *Nature*, 1951, 168.
- 2 D. B. Jacobson and B. S. Freiser, *J. Am. Chem. Soc.*, 1985, **107**, 7399.
- 3 J. E. Ellis, *Adv. Organomet. Chem.*, 1990, **31**, 1.
- 4 J. M. O'Connor and C. P. Casey, *Chem. Rev.*, 1987, **87**, 307.
- 5 M. L. H. Green, *J. Organomet. Chem.*, 1995, **500**, 127.
- 6 J. W. Lauher and R. Hoffman, *J. Am. Chem. Soc.*, 1976, **98**, 1729.
- 7 R. L. Halterman, *Chem. Rev.*, 1992, **92**, 965.
- 8 D. Lednicer and C. R. Hauser, *J. Org. Chem.*, 1959, **24**, 43.
- 9 E. Cesarotti, R. Ugo and H. B. Kagan, *Angew. Chem., Int. Ed. Engl.*, 1979, **18**, 779.
- 10 A. D. McNaught and A. Wilkinson, *International Union of Physical and Applied Chemistry, Compendium of Chemical Terminology*, Blackwell, Oxford, 1997, edn. 2.
- 11 L. S. Liebeskind, M. E. Welker and R. E. Fengl, *J. Am. Chem. Soc.*, 1986, **108**, 6328.
- 12 H. Brunner, *Adv. Organomet. Chem.*, 1980, **18**, 151 and references therein.
- 13 J. W. Faller and D. L. Linebarrier, *J. Am. Chem. Soc.*, 1989, **111**, 1937.
- 14 F. R. W. P. Wild, L. Zsolnai, G. Huttner and H. H. Brintzinger, *J. Organomet. Chem.*, 1982, **232**, 233.
- 15 C. M. Haar, C. L. Stern and T. J. Marks, *Organometallics*, 1996, **15**, 1765.
- 16 R. L. Halterman and K. P. C. Vollhardt, *Organometallics*, 1988, **7**, 883.
- 17 J. J. Buckingham, *Dictionary of Natural Products*, Chapman and Hall, London, 1994, vol. 4.

- 18 R. L. Halterman, K. P. C. Vollhardt, M. E. Welker, D. Bläser and R. Boese, *J. Am. Chem. Soc.*, 1987, **109**, 8105.
- 19 Z. Chen and R. L. Halterman, *Synlett*, 1990, 103.
- 20 a) M. Hoch, A. Duch and D. Rehder, *Inorg. Chem.*, 1986, **25**, 2907;
b) D. Rehder, M. Hoch and M. Link, *Organometallics*, 1988, **7**, 233.
- 21 a) J. Besancon, S. Top, *J. Organomet. Chem.*, 1977, **79**, 5471;
b) J. Besancon, S. Top, J. Tirouflet, *J. Organomet. Chem.*, 1975, **281**, 135.
- 22 D. A. H. Taylor, *J. Chem. Soc.*, 1958, 4779.
- 23 H. Schnutenhaus and H. H. Brintzinger, *Angew. Chem., Int. Ed. Engl.*, 1979, **18**, 777.
- 24 S. Gutmann, P. Burger, H. U. Hund, J. Hofmann and H. H. Brintzinger, *J. Organomet. Chem.*, 1989, **369**, 343.
- 25 H. Wiesenfeldt, A. Reinmuth, E. Barsties, K. Evertz and H. H. Brintzinger, *J. Organomet. Chem.*, 1989, **369**, 359.
- 26 R. B. King and M. B. Bisnette, *J. Organomet. Chem.*, 1967, **8**, 287.
- 27 N. J. Long, *Metallocenes*, Blackwell Science, Oxford, 1998, ch. 2, p. 59.
- 28 G. Wilkinson, *Comprehensive Organometallic Chemistry: the Synthesis, Structures and Reactions of Organometallic Compounds*, Pergamon, Oxford, 1982, vol.4, p. 481.
- 29 a) P. M. Maitlis, *Acc. Chem. Res.*, 1978, **11**, 301;
b) P. T. Wolzcanski and J. E. Bercaw, *Acc. Chem. Res.*, 1980, **13**, 121;
c) S. J. McLain, J. Sancho and R. R. Schrock, *J. Am. Chem. Soc.*, 1979, **101**, 5451.
- 30 H. Y. Liu, K. Eriks, A. Prock and W. P. Giering, *Organometallics*, 1998, **9**, 1758.
- 31 Y. Li, P.F. Fu and T.J. Marks, *Organometallics*, 1994, **13**, 439.
- 32 a) W. Lamberts, B. Hessner and H. Lueken, *Inorg. Chim. Acta*, 139, **215**, 1987;
b) H. Schumann, J. Loebel, D van der Helm and M. B. Hossain, *Z. Naturforsch., Teil B*, 1988, **43**, 323.
- 33 J. Okuda, *Topics in Current Chemistry*, 1991, **160**, 97.
- 34 R. R. Schrock, S. F. Pedersen, M. R. Churchill and J. W. Ziller, *Organometallics*, 1984, **3**, 1574.
- 35 R. Riemschneider, *Z. Naturforsch.*, 1963, **B 18**, 641.
- 36 T. Leigh, *J. Chem. Soc.*, 1964, 3294.
- 37 G. Maier, S. P. Friem, U. Schäfer, K. D. Malsch and R. Matusch, *Chem. Ber.*, 1981, **114**, 3965.
- 38 C. A. Tolman, *Chem. Rev.*, 1977, **77**, 313.
- 39 P. Renault, G. Tainturier and B. Gautheron, *J. Organomet. Chem.*, 1978, **148**, 35.
- 40 J. Okuda, *J. Organomet. Chem.*, 1990, **385**, C39.
- 41 W. Hofmann, W. Buchner and H. Werner, *Angew. Chem., Int. Ed. Engl.*, 1977, **16**, 795.

- 42 M. Rosenblum, *Chemistry of the Iron group metallocenes, Part I*, Wiley-Interscience, New York, 1965, p.45
- 43 I. F. Urazowski, V. I. Ponomaryev, I. E. Nifantev and D. A. Lemenovskii, *J. Organomet. Chem.*, 1989, **368**, 287.
- 44 H. Sitzmann, *Chem. Ber.*, 1990, **123**, 2311.
- 45 H. Sitzmann, *J. Organomet. Chem.*, 1988, **354**, 203.
- 46 H. Sitzmann and R. Boese, *Angew. Chem., Int. Ed. Engl.*, 1991, **30**, 971.
- 47 K. Ziegler and B. Schnell, *Justus Liebigs Ann. Chem.*, 1925, **445**, 266.
- 48 B. Gloaguen and D. Astruc, *J. Am. Chem. Soc.*, 1990, **112**, 4607.
- 49 D. Astruc, *Acc. Chem. Res.*, 1986, **19**, 377.
- 50 H. Schuster, W. Weissensteiner and K. Mislow, *J. Am. Chem. Soc.*, 1986, **108**, 6661.
- 51 a) H. Schumann, C. Janiak, R. D. Kohn, J. Loebel and A. Dietrich, *J. Organomet. Chem.*, 1989, **365**, 137;
 b) R. R. Schrock, S. F. Pedersen, M. R. Churchill and J. W. Ziller, *Organometallics*, 1984, **3**, 1574;
 c) M. J. Burk, A. J. Arduengo, J. C. Calabrese and R. L. Harlow, *J. Am. Chem. Soc.*, 1989, **111**, 8938;
 d) M. I. Bruce and A. H. White, *Aust. J. Chem.*, 1990, **43**, 949.
- 52 P. L. Pauson, *J. Am. Chem. Soc.*, 1954, **76**, 2187.
- 53 M. A. Oglarusso, M. G. Romanelli and E. I. Becker, *Chem. Rev.*, 1965, **65**, 293.
- 54 a) M. P. Cava and K. J. Narasimhan, *J. Org. Chem.*, 1969, **34**, 3641;
 b) A. Nakamura and N. Hagihara, *J. Chem. Soc. Japan*, 1963, **84**, 344;
 c) F. Feher, M. Green and G. A. Orpen, *J. Chem. Soc., Chem. Commun.*, 1986, 291.
- 55 M. L. Listeman and R. R. Schrock, *Organometallics*, 1985, **4**, 74.
- 56 L. D. Field, T. W. Hambley, C. M. Lindall and A. F. Masters, *Polyhedron*, 1989, **8**, 2425.
- 57 P. Brégaint, J. R. Hammon and C. Lapinte, *J. Organomet. Chem.*, 1990, **328**, C 25.
- 58 K. N. Brown, L. D. Field, P.A. Lay, C. M. Lindall and A. F. Masters, *J. Chem. Soc., Chem. Commun.*, 1990, 408.
- 59 a) W. Kläui and L. Ramacher, *Angew. Chem., Int. Ed. Engl.*, 1986, **25**, 97;
 b) N. G. Connelly and S. J. Raven, *J. Chem. Soc., Dalton Trans.*, 1986, 1613;
 c) N. G. Connelly, S. J. Raven and W. E. Geiger, *J. Chem. Soc., Dalton Trans.*, 1987, 467;
 d) N. G. Connelly, W. E. Geiger, G. A. Lane, S. J. Raven and P. H. Rieger, *J. Am. Chem. Soc.*, 1986, **108**, 6219;
 e) U. Kölle, B. Fuss, F. Khouzami and J. Gersdorf, *J. Organomet. Chem.*, 1985, **290**, 77;
 f) U. Kölle and F. Khouzami, *Angew. Chem., Int. Ed. Engl.*, 1980, **19**, 640.
- 60 M. P. Castellani, S. J. Geib, A. L. Rheingold and W. C. Trogler, 1987, *Organometallics*, 1987, **6**, 1703.

- 61 M. P. Castellani, S. J. Geib, A. L. Rheingold and W. C. Trogler, *Organometallics*, 1987, **6**, 2524.
- 62 F. Feher, M. Green and G. A. Orpen, *J. Chem. Soc., Chem. Commun.*, 1986, 291.
- 63 P. Jutzi and R. Sauer, *J. Organomet. Chem.*, 1973, **50**, C29.
- 64 P. Jutzi, *Chem. Rev.*, 1986, **86**, 983.
- 65 K. Sunkel and J. Hofmann, *Organometallics*, 1992, **11**, 3923.
- 66 J. Okuda, R. W. Albach and E. Herdtweck, *Polyhedron*, 1991, **10**, 1741.
- 67 M. D. Rausch, M. Vogel and H. Rosenberg, *J. Org. Chem.*, 1957, **22**, 900.
- 68 G. A. Tolstikov, M. S. Miftakhov and Y. B. Monakov, *Zh. Obshch. Khim.*, 1976, **46**, 1778.
- 69 J. Okuda and E. Herdtweck, *J. Organomet. Chem.*, 1989, **373**, 99.
- 70 A. Antiñolo, M. F. Lappert, A. Singh, D. J. W. Winterborn, L. M. Engelhardt, C. L. Raston, A. H. White, A. J. Carty and N. J. Taylor, *J. Chem. Soc., Dalton Trans.*, 1987, 1463.
- 71 A. Antiñolo, M. F. Lappert, G. A. Lawless and H. Oliver, *Polyhedron*, 1989, **8**, 1882.
- 72 A. Antiñolo, M. F. Lappert and D. J. W. Winterborn, *J. Organomet. Chem.*, 1984, **272**, C37.
- 73 A. Antiñolo, G. S. Bristow, G. K. Campbell, A. W. Duff, P. B. Hitchcock, R. A. Kamarudin, M. F. Lappert, R. J. Norton, N. Sarjudeen, D. J. W. Winterborn, J. L. Atwood, W. E. Hunter and H. Zhang, *Polyhedron*, 1989, **8**, 1601.
- 74 M. S. Miftakhov and G. A. Tolstikov, *Zh. Obshch. Khim.*, 1976, **46**, 930.
- 75 J. Okuda, *J. Organomet. Chem.*, 1987, **333**, C41.
- 76 J. Okuda, *J. Organomet. Chem.*, 1989, **375**, C13.
- 77 J. Okuda and E. Herdtweck, *Chem. Ber.*, 1988, **121**, 1899.
- 78 a) J. Okuda, *Chem. Ber.*, 1990, **123**, 87.
b) J. Okuda, *J. Organomet. Chem.*, 1988, **353**, C1.
- 79 C. H. Winter, D. A. Dobbs and X. X. Zhan, *J. Organomet. Chem.*, 1991, **403**, 145.
- 80 F. W. R. P. Wild, L. Zsolnai, G. Huttner and H. H. Brintzinger, *J. Organomet. Chem.*, 1982, **232**, 233;
b) F. W. R. P. Wild, M. Wasiucionek, G. Huttner and H. H. Brintzinger, *J. Organomet. Chem.*, 1985, **288**, 63.
- 81 S. Collins, B. A. Kuntz, N. J. Taylor and D. G. Ward, *J. Organomet. Chem.*, 1988, **342**, 21.
- 82 W. A. Herrmann, R. Anwender, H. Riepl, W. Scherer and C. R. Whitaker, *Organometallics*, 1993, **12**, 4342.
- 83 Q. Yang and M. D. Jensen, *Synlett*, 1996, **6**, 563.
- 84 a) R. N. Austin, T. J. Clark, T. E. Dickson, C. M. Killian, T. A. Nile, D. J. Schabacker and A. T. McPhail, *J. Organomet. Chem.*, 1995, **491**, 11;
b) R. N. Austin, T. J. Clark, T. E. Dickson, C. M. Killian and T. A. Nile, *J. Organomet. Chem.*, 1995, **498**, C31.

- 85 F. X. Kohl and P. Jutzi, *J. Organomet. Chem.*, 1983, **243**, 119.
- 86 S. Dev, *J. Ind. Chem.*, 1957, **34**, 169.
- 87 I. N. Nazarov, I. I. Zaretskaya and T. I. Sorkina, *J. Gen. Chem. USSR*, 1960, **30**, 765.
- 88 E. A. Braude and J. A. Coles, *J. Chem. Soc.*, 1952, 1430.
- 89 C. Santelli-Rouvier and M. Santelli, *Synthesis*, 1983, 427.
- 90 a) S. Hacini, R. Pardo and M. Santelli, *Tet. Lett.*, 1979, 4553;
b) N. Jones and H. T. Taylor, *J. Chem. Soc.*, 1959, 4017.
- 91 S. Dev, *J. Ind. Chem.*, 1957, **34**, 169.
- 92 J. M. Conia and M. L. Lriverend, *Tet. Lett.*, 1968, 2101.
- 93 F. Cooke, R. Moerck, J. Schwindeman and P. Magnus, *J. Org. Chem.*, 1980, **45**, 1046.
- 94 A. L. Rheingold, N. P. Robinson, J. Whelan and B. Bosnich, *Organometallics*, 1992, **11**, 1869.
- 95 S. C. Yoon, T. K. Han, B. W. Woo, H. Song, S. I. Woo and J. T. Park, *J. Organomet. Chem.*, 1997, **534**, 81.
- 96 a) D. P. Freyberg, J. L. Robbins, K. N. Raymond and J. C. Smart, *J. Am. Chem. Soc.*, 1979, **101**, 892;
b) Y. T. Struchkov, V. G. Andrianov, T. N. Sal'nikova, I. R. Lyatitov and R. R. Materikova, *J. Organomet. Chem.*, 1978, **148**, 213.
- 97 A. Almenningen, A. Haaland, S. Samdal, J. Brunvoll, J. L. Robbins and J. C. Smart, *J. Organomet. Chem.*, 1973, **60**, 287.
- 98 C. P. Lau, B. H. Chang, R. H. Grubbs and C. H. Brubaker Jr., *J. Organomet. Chem.*, 1981, **214**, 325.
- 99 S. Coletti and R. L. Halterman, *Tet. Lett.*, 1992, **33**, 1005.
- 100 H. Lehmkuhl and Y. Qian, *Chem. Ber.*, 1983, **116**, 2437.
- 101 Z. Chen and R. L. Halterman, *J. Am. Chem. Soc.*, 1992, **114**, 2276.
- 102 a) S. C. Berk, K. A. Kreutzer and S. L. Buchwald, *J. Am. Chem. Soc.*, 1991, **113**, 5093;
b) R. L. Halterman, *Chem. Rev.*, 1992, **92**, 965.
- 103 G. Natta, P. Pino, G. Mazzanti and U. Giannini, *J. Am. Chem. Soc.*, 1957, **79**, 2975.
- 104 J. A. Ewen, *J. Am. Chem. Soc.*, 1984, **106**, 6355.
- 105 M. Lee, *Chem. Br.*, 1998, **34**, 22.
- 106 W. Kaminsky, K. Külper, H. H. Brintzinger and F. R. P. Wild, *Angew. Chem., Int. Ed. Engl.*, 1985, **24**, 507.
- 107 M. A. Giardello, M. S. Eisen, C. L. Stern and T. J. Marks, *J. Am. Chem. Soc.*, 1995, **117**, 12114.

Chapter Two
Iron(II) Complexes of the Cyclopentadienyl Analogue,
1-Phenyl-3-methyl-4,5,6,7-tetrahydroindenyl.

2.1 Introduction.

As outlined in the introductory chapter the cyclopentadienyl ring plays an important part in organotransition-metallic chemistry. This is primarily due to the ease of synthesis of complexes incorporating one or more cyclopentadienyl rings and the wide variation possible in the steric and electronic properties of these complexes associated with substitution on the ring.¹ The most extensively used substituted ligand is C_5Me_5 , but other systems include the indenyl and 4,5,6,7-tetrahydroindenyl ligands.

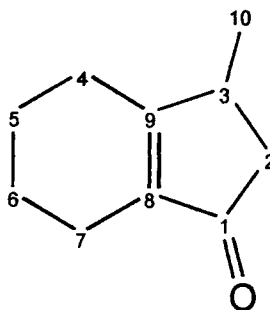
Nile and co-workers have reported the synthesis of alkylated 4,5,6,7-tetrahydroindenes via methylation of the corresponding cyclopentenones.² The synthesis of these cyclopentenones and subsequent methylation provides a route to 4,5,6,7-tetrahydroindenes which is significantly more facile and versatile than the previous method of hydrogenating the relevant complexed indenyl ligands. In this chapter the synthesis and complexation of a more sterically demanding 4,5,6,7-tetrahydroindene, 1-phenyl-3-methyl-4,5,6,7-tetrahydroindene, **2.1**, is reported. The ketone precursor to this ligand is one prepared by Nile, 3-methyl-2,3,4,5,6,7-hexahydroind-8(9)-en-1-one, **1.12**, although a slightly modified synthesis of **1.12** is reported here. The Nazarov cyclization used to synthesize **1.12** is a commonly employed route to cyclopentenones and cyclopentadienes.³

Of as much importance as its steric requirements is the pro-chiral nature of the anion of **2.1**. This pro-chiral character means that when complexed in a metallocene-type compound the cyclopentadienyl ligands will have enantiotopic faces, labelled R and S. The assignment of R and S configurations is discussed in this chapter, as well as the implications of coordinating pro-chiral ligands with respect to the formation of isomeric transition metal complexes.

The preparation of the organotransition metal complexes bis(1-phenyl-3-methyl-4,5,6,7-tetrahydroindenyl) iron(II), **2.3**, 1-phenyl-3-methyl-4,5,6,7-tetrahydroindenyl iron(II) dicarbonyl dimer, **2.4**, and 1-phenyl-3-methyl-4,5,6,7-tetrahydroindenyl methyl iron(II) dicarbonyl, **2.5**, are reported in this chapter and data characterizing the complexes are discussed.

2.2 Ligand chemistry.

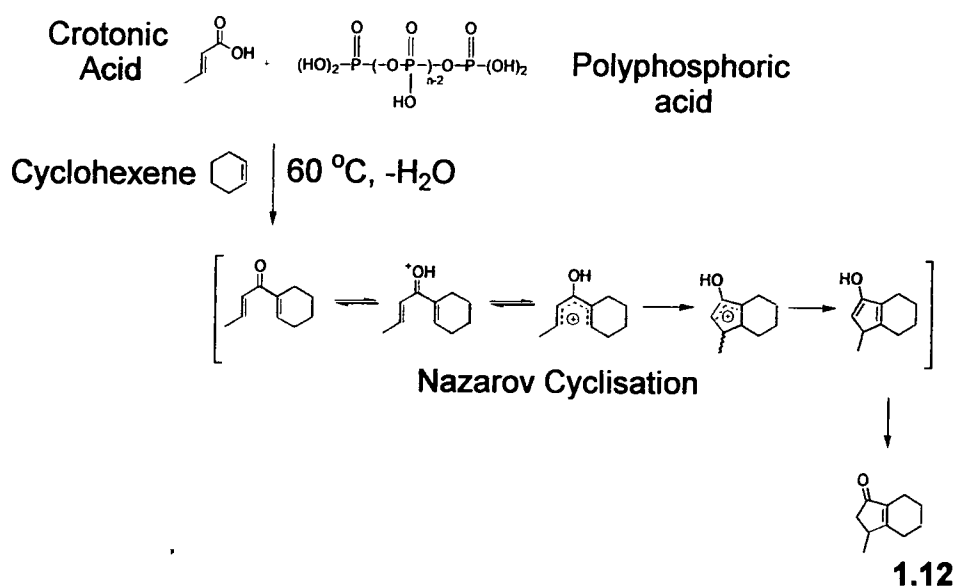
2.2.1 3-Methyl-2,3,4,5,6,7-hexahydroind-8(9)-en-1-one.



1.12

2.2.1a Synthesis.

The tetrahydroindenone, 3-methyl-2,3,4,5,6,7-hexahydroind-8(9)-en-1-one, **1.12**, was prepared via a Nazarov cyclization (Scheme 2.1). The method used was a slight variation on that previously reported. Cyclohexene was added slowly to a mechanically stirred mixture of crotonic acid (2-butenic acid) and polyphosphoric acid (PPA) maintained at 60 °C. Mechanical stirring was essential for efficient mixing. The mixture was stirred at 60 °C for 2 h and then the PPA was decomposed with sodium hydroxide overnight. The organic extracts were washed with ammonia solution and brine. After drying and concentration, distillation of the crude oil resulted in **1.12** in moderate yield (55 %).



Scheme 2.1 Preparation of **1.12** from crotonic acid and cyclohexene in PPA.

Following the work of Dev, Nile and co-workers prepared **1.12** from crotonic acid and cyclohexene in 36% yield, using hot PPA as the reaction medium. The method of Dev

involves the combination of all reactants in cold PPA followed by heating at 60 °C for 30 min. In the improved synthesis reported here, it was observed that by preheating crotonic acid in PPA to 60 °C and then adding the cyclohexene, the yield of the reaction is increased to 55%. This is presumably due to the presence of the resonance stabilized oxocarbenium ion, see section 1.4.2, in high concentration which promotes the reaction of the cycloalkene to form the required pentadienylic intermediate for Nazarov cyclization, instead of unwanted by-products formed by reaction with the hot PPA medium. Also, the amount of PPA used can be as little as 20% of that used by Dev and Nile, without appreciable decrease in yield of the ketone. There are two possible reasons for this.

- Firstly, the PPA may be acting as a catalytic medium for formation of the oxocarbenium ion, so the equivalents of PPA present can be greatly decreased without unfavourable decrease in the formation of the ion.
- Secondly, unwanted by-products are probably due to reaction between the cycloalkene and the PPA medium. Increasing the amount of the oxocarbenium ion relative to the PPA present probably decreases the amount of unwanted products formed in much the same way as pre-forming the ion before introduction of the alkene does.

Care must be taken to thoroughly wash the organic extracts with ammonia solution, and with the distillation of the product to prevent contamination by unreacted crotonic acid. In a later report Niles and co-workers warn of the possibility of an exothermic initiation in their ketone synthesis that requires thermal quenching with ice-water. Even after multiple repetitions, slow addition of the cycloalkene to the hot mixture of crotonic acid and PPA never initiated violently enough to warrant quenching.

2.2.1b Characterization.

Characterization was by ^1H NMR, ^{13}C NMR and infra-red spectroscopy and mass spectrometry.

2.2.1b(i) Nuclear magnetic resonance spectroscopy.

The ^1H NMR spectrum consists mainly of a series of overlapping, unassignable, multiplets due to the CH_2 and CH protons, however there is a distinctive doublet at $\delta = 1.11$ ppm which is assigned to the methyl protons; the ten peaks in the ^{13}C NMR spectrum are easily assigned (Table 2.1 and Fig. 2.1).

2.2.1b(ii) Infra-red spectroscopy.

The infra-red spectrum shows a distinctive CO stretch at 1700 cm^{-1} and a $\text{C}=\text{C}$ stretch at 1647 cm^{-1} . Initially the CO stretch seems higher than expected for conjugated ketone carbonyl group stretches.⁴ However, when the CO stretches of cyclohexanone, 1715 cm^{-1} , and cyclopentanone, 1745 cm^{-1} , are compared it can be seen that confining

within a strained cyclic system shifts the carbonyl stretch to higher wave numbers due a forced change in the hybridisation of the carbonyl carbon.⁴

δ , ppm	Assignment
19.2	CH ₃
20.4	CH ₂
22.1	CH ₂
22.6	CH ₂
26.4	CH ₂
36.7	CH ₂
43.9	CH
138.3	quat. C
177.9	quat. C
208.7	quat. C

Table 2.1 Assignments for the ¹³C NMR spectrum of 1.12.

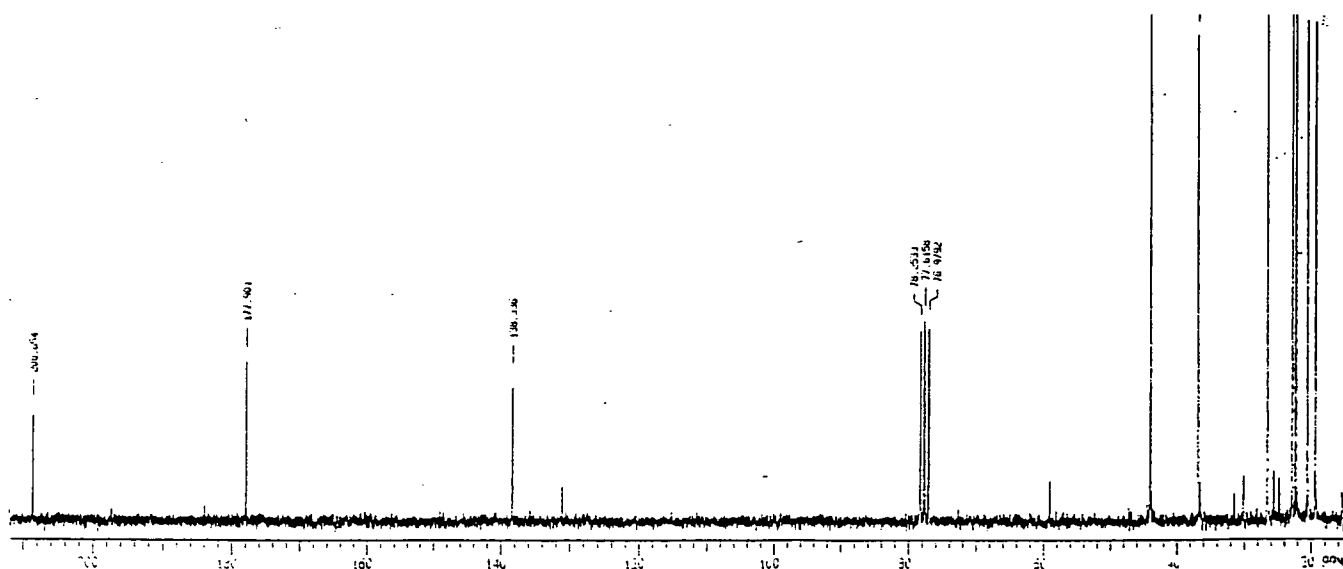
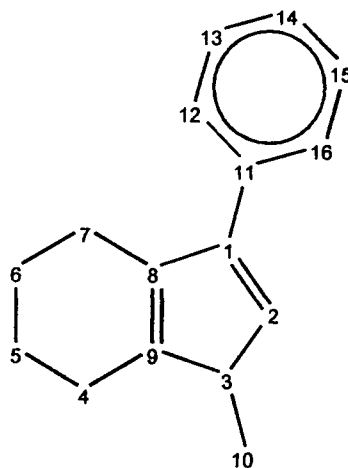


Fig. 2.1 ¹³C NMR spectrum of 1.12.

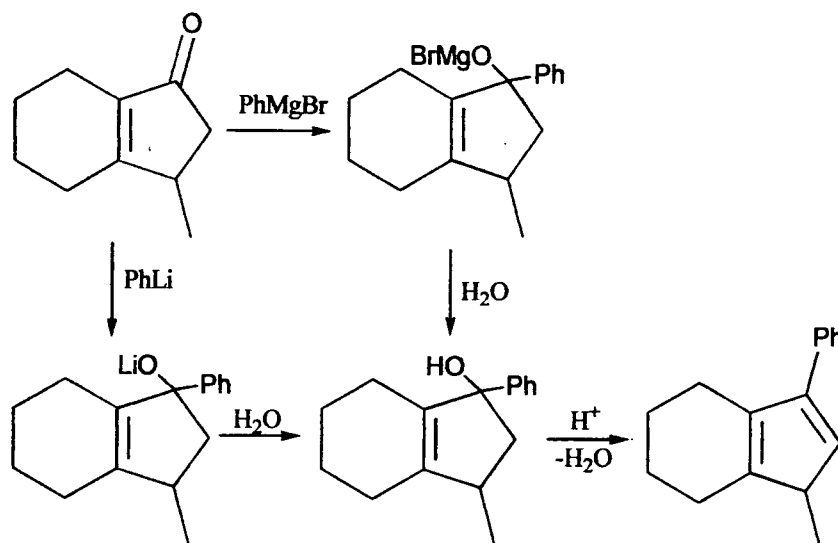
2.2.2 1-Phenyl-3-methyl-4,5,6,7-tetrahydroindene.



2.1

2.2.2a Synthesis.

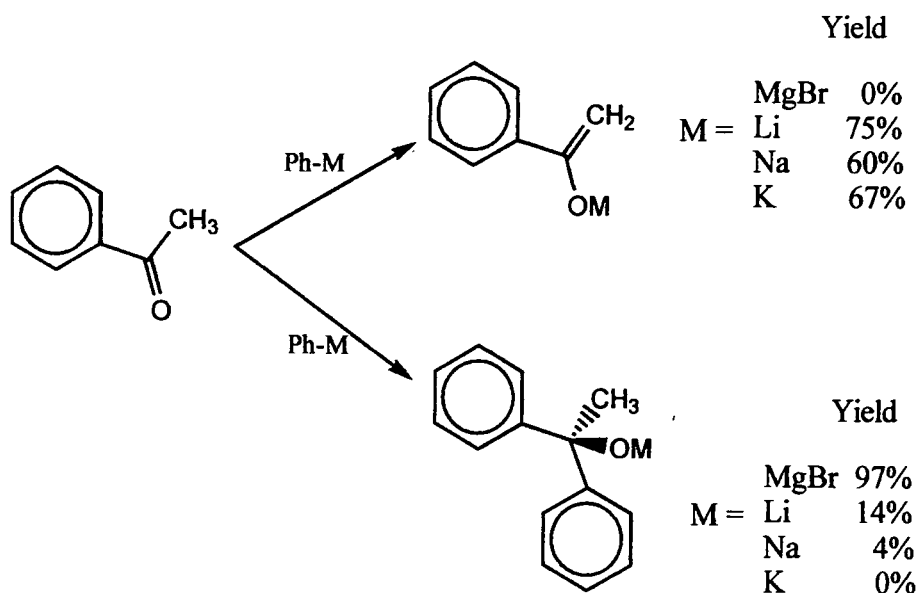
The tetrahydroindene, 1-phenyl-3-methyl-4,5,6,7-tetrahydroindene, **2.1**, can be prepared by the reaction of **1.12** with phenyl magnesium bromide or phenyl lithium. The synthetic method is the same in both cases (Scheme 2.2). After careful distillation of the crude product, **2.1** was afforded in moderate yield (52%) when phenyl magnesium bromide was used as the source of the phenyl moiety, but in a much lower yield when phenyl lithium was used (25%).



Scheme 2.2 Synthetic routes to **2.1**.

The effect of the metal in the organometallic reagent upon coupling reactions of this kind has been studied by Schlosser and co-workers.⁵ Schlosser reported that when aryl lithium reagents are used instead of aryl Grignards the poorer yields are due to the

preferential formation of enolates rather than the desired coupling products (Scheme 2.3).



Scheme 2.3 Formation of enolates versus coupling products using different aryl metal reagents.

The major source of product loss in the preparation of **2.1** was through pyrolysis of the diene in the distillation flask. Attempts to purify **2.1** by column chromatography resulted in very low yields and substantial decomposition of **2.1** on the chromatography support. Flash distillation resulted in contamination of **2.1** by **1.12**.

2.2.2b Characterization.

Characterization was attempted by ^1H and ^{13}C NMR spectroscopy and gas-chromatograph-mass spectrometry.

2.2.2b(i) Nuclear magnetic resonance spectroscopy.

Both the ^1H and ^{13}C spectra were unassignable due to the presence of multiple double bond isomers.

2.2.2b(ii) Gas-chromatograph mass-spectrometry.

The gas-chromatograph-mass spectrometry (GC-MS) data indicated the presence of four isomers with $m/z = 210$ [M^+]. On the gas-chromatograph trace one of the peaks is significantly broader than the others, possibly indicating the presence of two species exiting the gas-chromatograph within the resolution of the instrument. Although only five species with mass 210 are observed (assuming the broad peak is due to two isomers), there are, in theory, forty ways of placing two double bonds into the carbon skeleton of **2.1** (Fig. 2.2).

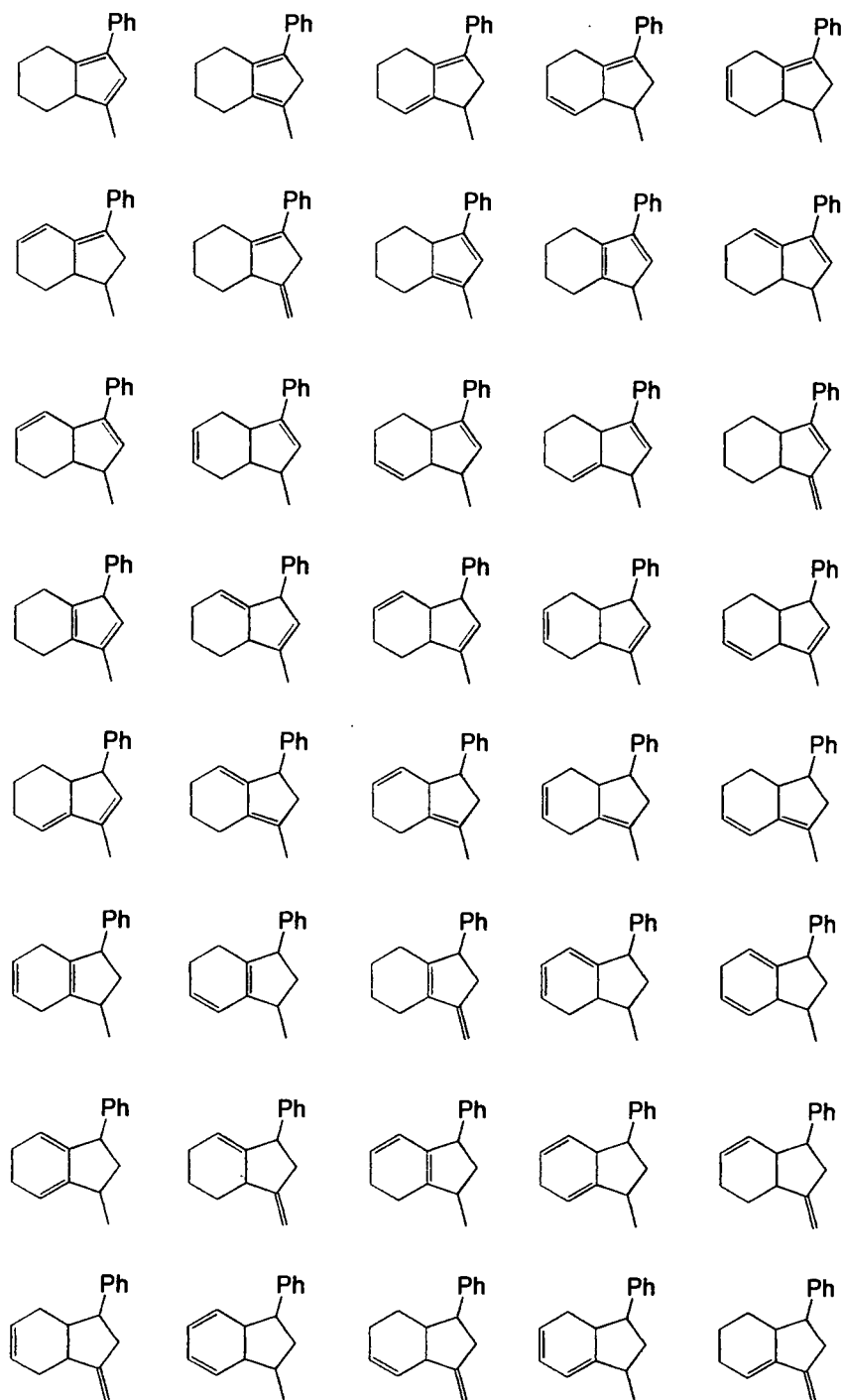


Fig. 2.2 The 40 different ways of placing two double bonds in the carbon skeleton of **2.1**.

Very few of the structures shown in Fig. 2.2 can be made by the synthetic route shown in Scheme 2.2, those that can are due to stabilization by extended conjugation through the molecule and the mechanism through which the dienes are formed from the ketone starting material via an enol intermediate. The isomers of the product formed, **2.1**, can not be categorically assigned structures in which all the double bonds are endocyclic with regards to the five membered ring, i.e. cyclopentadiene structures, using the characterization data obtained. However, further reactions of the product are described

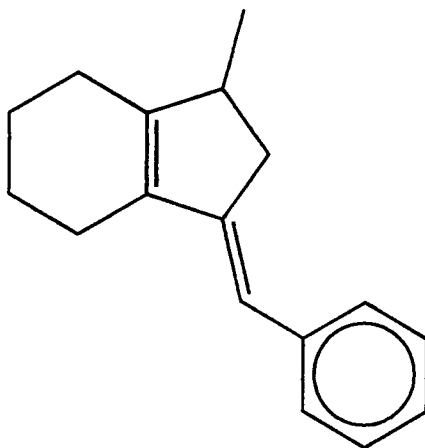
in this chapter and chapter three. These reactions render complexes containing the deprotonated η^5 -tetrahydroindenyl form of **2.1**. This strengthens the argument for assigning a cyclopentadiene structure to at least some of the isomers present in the product.

2.2.3 1-Benzylidene-3-methyl-2,3,4,5,6,7-hexahydroind-8(9)-ene.

A wide range of substituted cyclopentadienes can be envisaged by varying the Grignard used in the reaction with **1.12**. However, one limitation is illustrated by the use of benzyl Grignard, PhCH_2MgBr .

2.2.3a Synthesis.

The reaction of **1.12** with benzyl Grignard proceeded in the same manner as for the synthesis of **2.1**. However, characterization of the distilled product revealed it to be the single isomer 1-benzylidene-3-methyl-2,3,4,5,6,7-hexahydroind-8(9)-ene, **2.2**. In the acid catalysed elimination part of the reaction the second double bond is generated exocyclic to the five membered ring, giving a benzylidene substituted cyclopentene.



2.2

2.2.3b Characterization.

Characterization was by ^1H and ^{13}C NMR spectroscopy and GC-MS.

2.2.3b(i) Gas-chromatograph mass spectrometry (GC-MS).

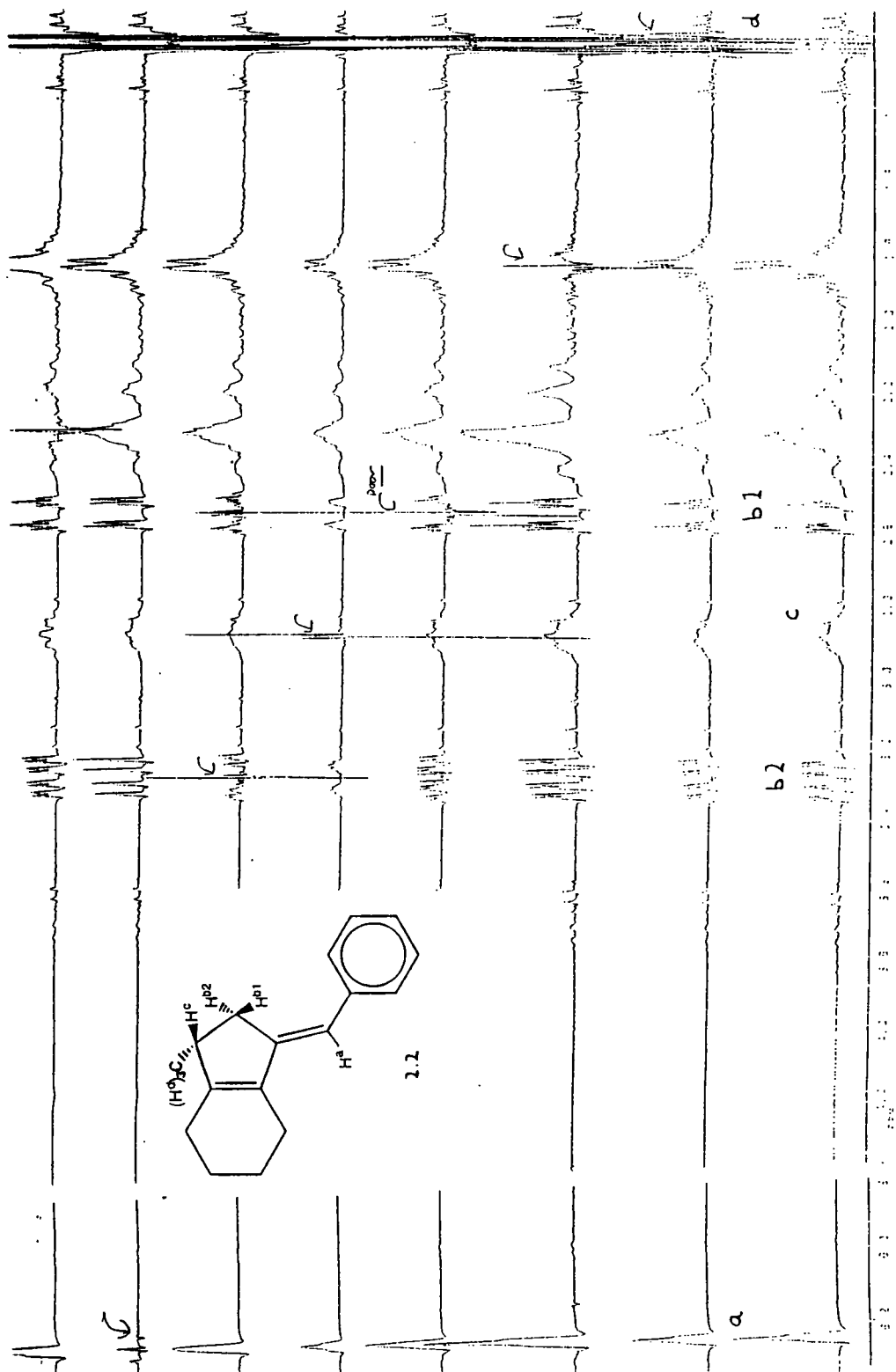
GC-MS revealed the presence of predominantly one product with $m/z = 224$ [M^+], minor peaks in the gas-chromatograph trace all had $m/z = 224$ [M^+] possibly indicating the presence of small amounts of endo-cyclic isomers.

2.2.3b(ii) Nuclear magnetic resonance spectroscopy.

The ^{13}C NMR spectrum was readily assigned. The ^1H NMR spectrum consisted of a series of multiplets; coupling constants could be extracted which enabled the

identification of a single isomer of 2.2. A series of double-resonance ^1H NMR experiments were performed in which each multiplet was irradiated in turn and the effect upon the other multiplets observed (Fig. 2.3). This enabled specific assignment of peaks to ring and substituent protons.

Fig. 2.3 Double resonance ^1H NMR experiments on 2.2.

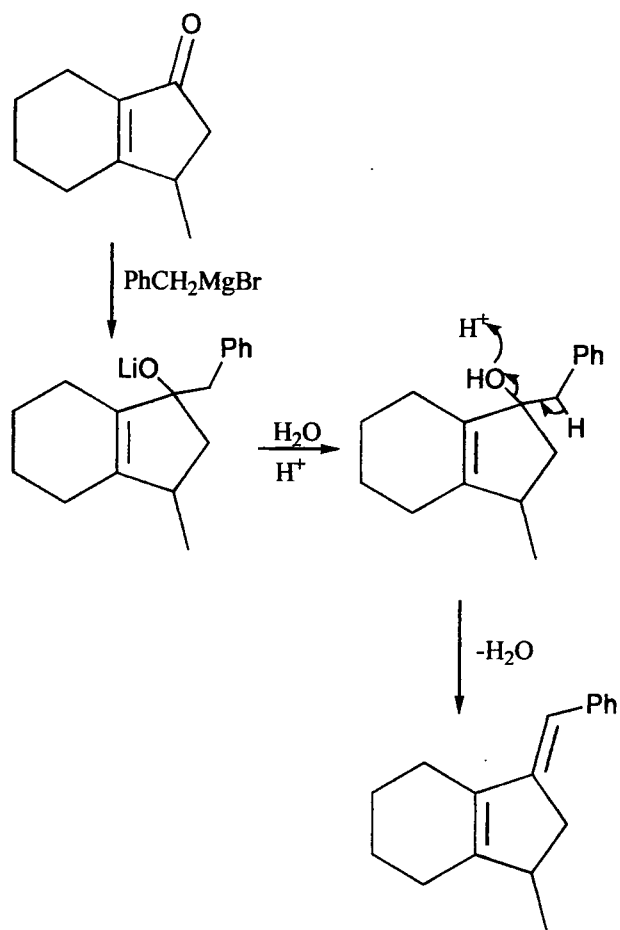


- The broad singlet at $\delta = 6.16$ ppm is assigned to the vinylic proton of the benzylidene group (H^a). When it was irradiated the multiplets at $\delta = 3.18$ ppm and 2.44 ppm both collapsed to form two doublets of doublets; these multiplets at $\delta = 3.18$ ppm and $\delta = 2.44$ ppm are thus assigned to the CH_2 protons of the five membered ring (H^{b1} and H^{b2}). When each of these multiplets was irradiated the other multiplet showed signs of partial collapse.
- The broad multiplet at $\delta = 2.80$ ppm is assigned to the CH proton of the five membered ring (H^c). When irradiated the doublets assigned to H^{b1} and H^{b2} both collapsed to give broad doublets and the doublet at $\delta = 1.15$ ppm collapsed to give a singlet, though this is not clear in Fig. 2.3.
- The two broad regions between $\delta = 1.4$ ppm and $\delta = 2.2$ ppm are assigned to the CH_2 protons of the six membered ring. No appreciable change was noticed in any other features of the spectra when they were irradiated.
- The sharp doublet at $\delta = 1.15$ ppm is assigned to the methyl group protons (H^d). When irradiated no change was observed in any other features of the spectra, though the multiplet assigned to H^c is sufficiently broad to mask the expected collapse.

Unambiguous assignment of the multiplet at $\delta = 3.18$ ppm to H^{b2} , the proton in a transoid arrangement with H^c , was achieved using the coupling patterns for the multiplets assigned to H^{b1} and H^{b2} .

- H^{b1} and H^{b2} couple to each other with a coupling constant of $J = 17.5$ Hz and to H^a with a coupling constant of $J = 2.5$ Hz.
- The coupling to H^a is the same for both H^{b1} and H^{b2} due to H^a lying in the plane of the five membered ring and being equi-distant from both protons.
- Although the coupling is masked by broadness in the singlet at $\delta = 6.16$ ppm, the 2.5 Hz coupling constant can be assigned to this coupling by the disappearance of the 2.5 Hz coupling upon irradiation of the singlet.
- It is apparent that H^{b1} and H^{b2} both couple to H^c as both multiplets collapsed when the broad multiplet assigned to H^c was irradiated.
- The multiplet at $\delta = 2.44$ ppm appears as a doublet of triplets rather than the expected doublet of doublet of doublets because two of the coupling constants (to H^c and H^a) are approximately equal (2.5 Hz), within the resolution of the 1H NMR spectrum.
- The multiplet at $\delta = 3.18$ ppm has the expected appearance of a doublet of doublet of doublets with three distinct coupling constants; the coupling to H^c has a constant $J = 7.5$ Hz.
- Using the Karplus⁶ relationship the higher coupling, $J = 7.5$ Hz, can be assigned to the coupling between H^c and the CH_2 on the five membered ring in a transoid orientation to it, H^{b2} .

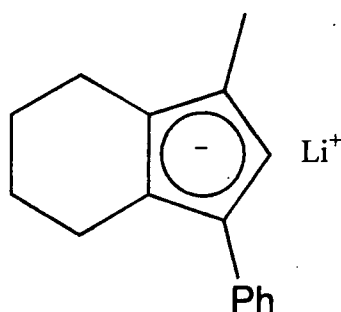
The dominance of this particular isomer of **2.2** is almost certainly due to the stabilisation gained by the extended conjugation present through the two double bonds and the phenyl ring (Scheme 2.4).



Scheme 2.4 Formation of a single isomer of **2.2**.

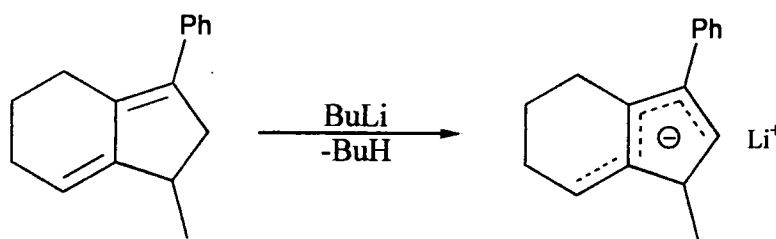
2.2.4 Lithium 1-phenyl-3-methyl-4,5,6,7-tetrahydroindene, **2.1A**.

As has already been mentioned in chapter one, lithium salts of cyclopentadienide anions are useful reagents in the preparation of transition metal complexes containing cyclopentadienyl ligands. The salt **2.1A** is readily prepared and isolated by addition of *n*-butyl lithium to **2.1** in diethyl ether or petroleum solutions, followed by filtration and washing with diethyl ether to remove unreacted *n*-butyl lithium and diene. The pale yellow solid is very air and moisture sensitive and insoluble in common NMR spectroscopy solvents, rendering characterization impossible.



2.1A

Nile and co-workers used THF solutions of their tetrahydroindenides, either lithium tetrahydroindenide or magnesium bis-tetrahydroindenide, prepared *in situ* to synthesize a range of ferrocenes. Nile reports low yields for these compounds and suggests this might be due to certain double bond isomers formed having insufficiently acidic hydrogens to be removed by the *n*-butyl lithium or dibutyl magnesium. Alternatively, when isomers with double bonds exo-cyclic to the five membered ring are considered, assuming they can be deprotonated, the tetrahydroindenyl formed would not possess a cyclopentadienyl ring capable of η^5 -coordination (Scheme 2.5). In combination with Nile's suggestion and the effects of steric hindrance during coordination reactions, this may explain low yields in metallocene preparations. The presence of exo-cyclic isomers would certainly affect the efficient synthesis of compounds prepared from the diene rather than a dienide salt. Compounds such as the tetrahydroindenyl iron dicarbonyl dimer discussed later in this chapter are prepared in this manner by reaction of the diene with homoleptic transition metal carbonyls.



Scheme. 2.5 Deprotonation of non-cyclopentadiene isomer of 2.1.

The 1-phenyl-3-methyl-4,5,6,7-tetrahydroindenide anion is planar and pro-chiral. As mentioned in chapter one, coordination to a metal generates a metal-cyclopentadienyl complex in which the metal-coordinated ligand has either an R or S configuration. This is decided by viewing the ring along the vector from the metal to the ring centroid and then ranking the substituents according to the Cahn-Ingold-Prelog priorities used for pseudo-tetrahedral chiral carbon atoms in standard organic chemistry (Fig. 2.4). The direction of travel from highest to lowest priority will be either clockwise or anti-clockwise, and the corresponding configuration R or S respectively.⁷

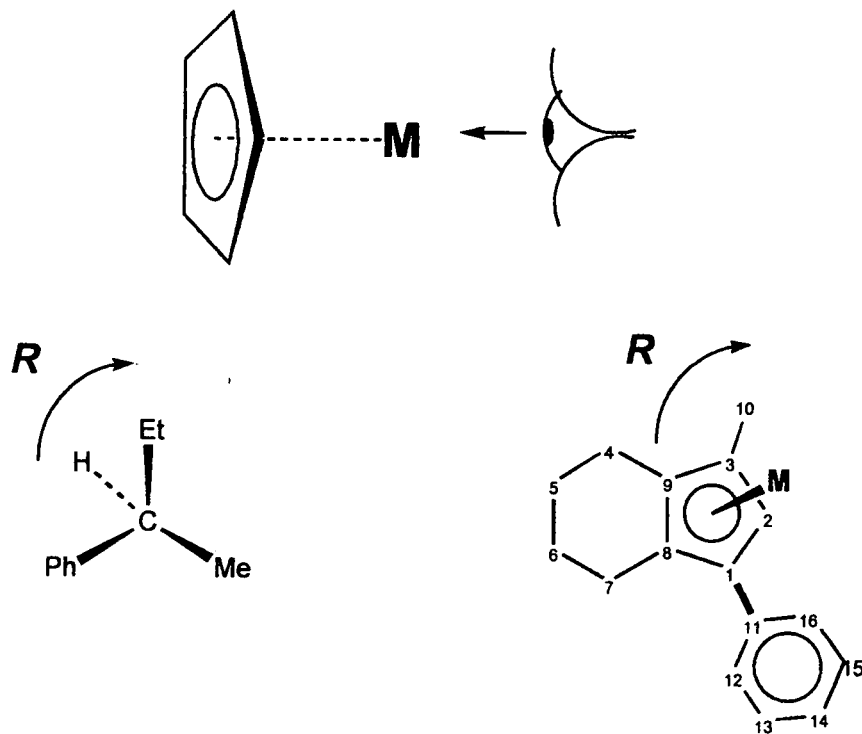


Fig. 2.4 Assigning R or S configuration to a planar-chiral metal-coordinated ligand.

If a single tetrahydroindenyl moiety is coordinated to one metal, then two isomers are possible (R and S). These isomers are enantiomers of each other, have identical physical properties and are indistinguishable by spectroscopic means. The absolute configuration of a particular enantiomer, if not present in a racemic mixture, can be individually identified by single crystal X-ray diffraction structural analysis or by circular dichroism measurements.

If a bis-tetrahydroindenyl complex (metallocene) is synthesized, then three isomers (RR, SS and SR) are possible. The RR and SS isomers are enantiomers of each other, have identical physical properties and are indistinguishable by spectroscopic means. These enantiomers are usually referred to collectively as the *rac*-isomer. The presence of a molecular inversion centre or mirror plane, which are both symmetry elements capable of turning one configuration into the other, means that the apparently different RS and SR compounds are identical, and compose only one achiral isomer, the *meso*-isomer. The *meso*-isomer has different physical properties to the *rac*-isomer and is distinguishable from it by spectroscopic means, e.g. NMR spectroscopy. The three isomers all possess identical constitution but only two are interconvertible via a single symmetry operation to the whole molecule; this means they form a diastereomeric mixture.

2.2.5 Summary.

The tetrahydroindenone **1.12** has been prepared in higher yields than has previously been reported in the literature, by appropriate modifications of earlier synthetic methods. The substituted cyclopentadiene **2.1** has been prepared and is present as at least four isomers, although characterization by spectroscopic and spectrometric means cannot identify specific isomers. The product formed contains a phenyl group at the 1-position and a methyl group at the 3-position. Assuming the isomers present are analogous to cyclopentadiene they contain fused cyclohexyl rings as well. The lithium tetrahydroindenide salt of **2.1**, **2.1A**, can be isolated, but is very sensitive to air and water. The compound **2.2** was prepared by the use of benzyl Grignard rather than phenyl Grignard and is present as a single isomer with a double bond exo-cyclic to the five membered ring, forming a benzylidene substituent at the 1-position due to extended conjugation through the molecule. A bis-tetrahydroindenyl complex synthesized from **2.1** or its tetrahydroindenide anion has three possible stereoisomers, the RR, SS, and RS.

2.3 Bis-1-phenyl-3-methyl-4,5,6,7-tetrahydroindenyl iron (II).

2.3.1 Introduction.

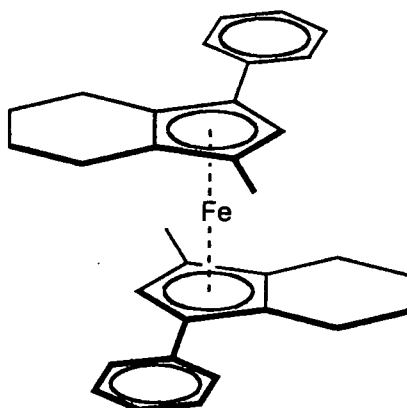
Ferrocene, $(\eta\text{-C}_5\text{H}_5)_2\text{Fe}$, was first reported in 1951 by Kealy and Pauson as a product from the reaction of cyclopentadienyl magnesium bromide in benzene with anhydrous iron(III) chloride in ether, dicyclopentadienyl was the expected product;⁸ since then there has been an enormous amount of research into ferrocene and analogous metallocenes. Despite ferrocene's now considerable age, research into and involving ferrocene and its analogues grows every year, with new applications being continually found. A survey of the Science Citation Index between the years of 1995 and 1998, using the word "ferrocene" as a search parameter, produced 1544 citations, 325 so far in 1998 alone. Over the same three year range the search parameter "olefin+polymerization" produced only 895 citations. The ferrocene publications span an incredibly wide and diverse field of chemistry for ferrocene and its analogues, including their application in microelectrodes, heterobimetallic complex syntheses, organic syntheses, flame retardant materials, alcohol biosensors, propellants, cytotoxicity in human cell tissue, liquid crystal systems and novel redox chemistry.⁹

In this section the synthesis and characterization of a sterically hindered ferrocene with two stereogenic centres is discussed together with some of its properties.

2.3.2 Discussion.

2.3.2a Synthesis.

The ferrocene, bis-1-phenyl-3-methyl-4,5,6,7-tetrahydroindenyl iron (II), **2.3**, was prepared via the addition of FeCl_2 to two equivalents of the tetrahydroindenide anion **2.1A**. Recrystallization of the crude product from petroleum ether gave a small crop (10% yield) of orange crystals. Further solid was isolated from the petroleum solution in moderate yields as an orange microcrystalline powder (20 % yield, 30 % total yield).



2.3

2.3.2b Characterization.

Three samples of **2.3** were characterized, namely the crude reaction mixture, **2.3A**, the first crop of crystalline material, **2.3B**, and a second crop of microcrystalline powder, **2.3C**. Characterization was by ^1H NMR, ^{13}C NMR (in C_6D_6) and solid state infra-red spectroscopy, mass spectrometry ($m/z = 474$ [M^+]), cyclic voltammetry and powder X-ray diffraction using **2.3C**, and ^1H NMR spectroscopic analysis of **2.3A**. CHN analysis was performed using **2.3C**. The crystals of sample **2.3B** were of sufficient crystallinity and size for solid state structural analysis by single crystal X-ray diffraction.

2.3.2b(i) Infra-red spectroscopy.

The solid state infra-red spectrum of **2.3** contains sufficient bands in all regions to make accurate assignment impossible. However, there are four summation bands at 1949 cm^{-1} , 1881 cm^{-1} , 1812 cm^{-1} and 1751 cm^{-1} which are indicative of the presence of a mono-substituted arene, in this case a phenyl ring.¹⁰

2.3.2b(ii) Nuclear magnetic resonance spectroscopy.

Three stereoisomers of **2.3** are possible (Fig. 2.5).

- The RR and SS isomers are enantiomers of each other, not distinguishable by spectroscopic means and will be collectively referred to as the *rac*-isomer.

- The RS isomer possesses a molecular inversion centre at the iron atom, rendering the SR isomer identical and will be referred to as the *meso*-isomer.

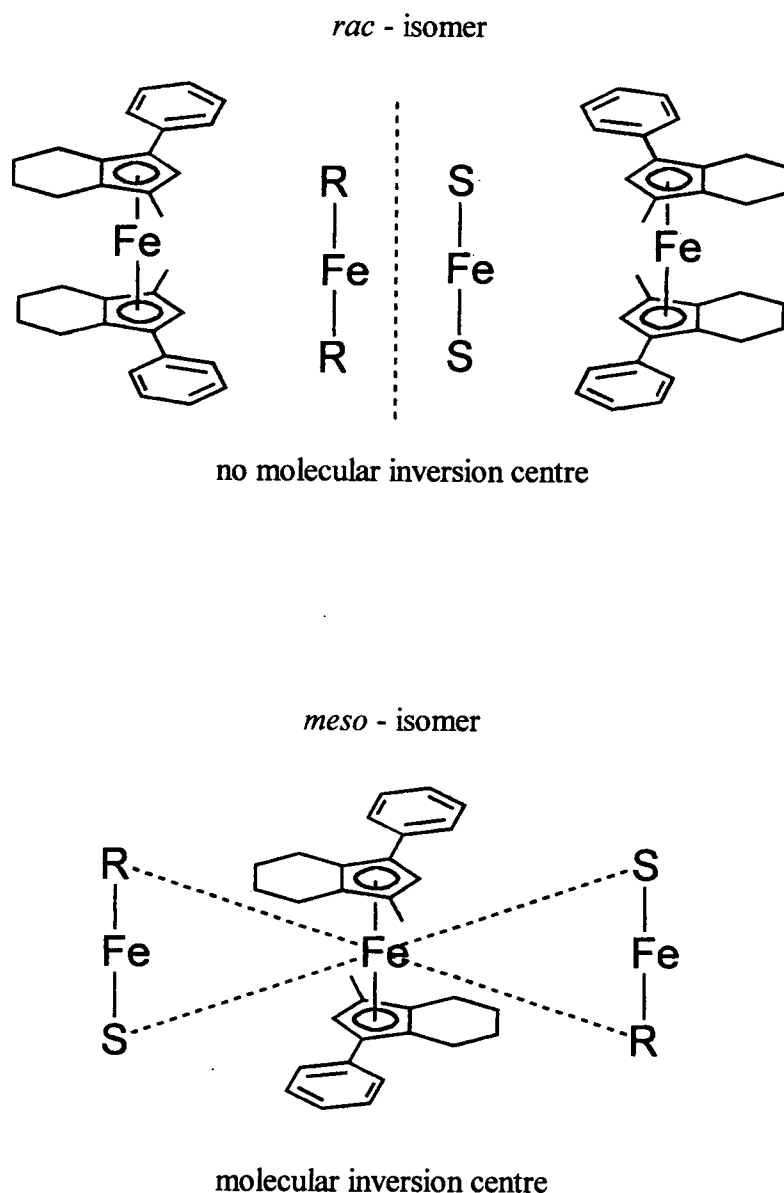
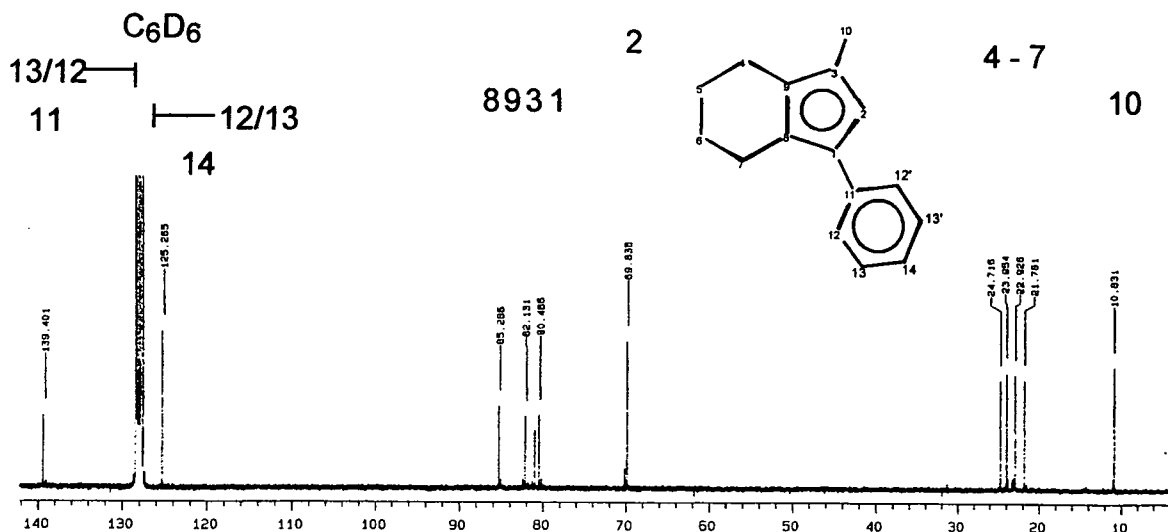


Fig. 2.5 The *rac*- and *meso*-isomers of **2.3**.

The ^1H NMR spectrum of sample **2.3A** shows two sharp resonances at $\delta = 3.77$ ppm and $\delta = 3.80$ ppm which are assigned to the CH protons of the five membered rings in the *rac*- and *meso*-isomers. The ^1H and ^{13}C NMR spectra of sample **2.3C** indicate the presence of predominantly one isomer. Each peak has a very small "shadow" peak at its base due to the other isomer (Fig. 2.6).



The ^{13}C NMR spectrum of bis(1-phenyl-3-methyl-4,5,6,7-tetrahydroindenyl) iron(II).

Fig. 2.6 ^{13}C NMR spectrum showing assignments for **2.3C** and "shadow" peaks of second isomer.

In the ^1H NMR spectrum the singlet at $\delta = 3.77$ ppm is the predominant peak and the singlet at $\delta = 3.80$ is the "shadow" peak.

The $^{13}\text{C}\{^1\text{H}\}$ NMR spectrum of the bulk microcrystalline product possesses a distinctive and characteristic singlet at $\delta = 70.3$ ppm, which is assigned to the CH carbon of the five-membered ring.

Neither the ^{13}C nor the ^1H chemical shifts of the CH group differ greatly from those observed for ferrocene; ^1H $\delta = 4.04$ ppm; ^{13}C $\delta = 68.2$ ppm.¹¹

2.3.2b(iii) Mass spectrometry.

Data obtained from mass spectrometry indicate that $m/z = 474$ [M^+].

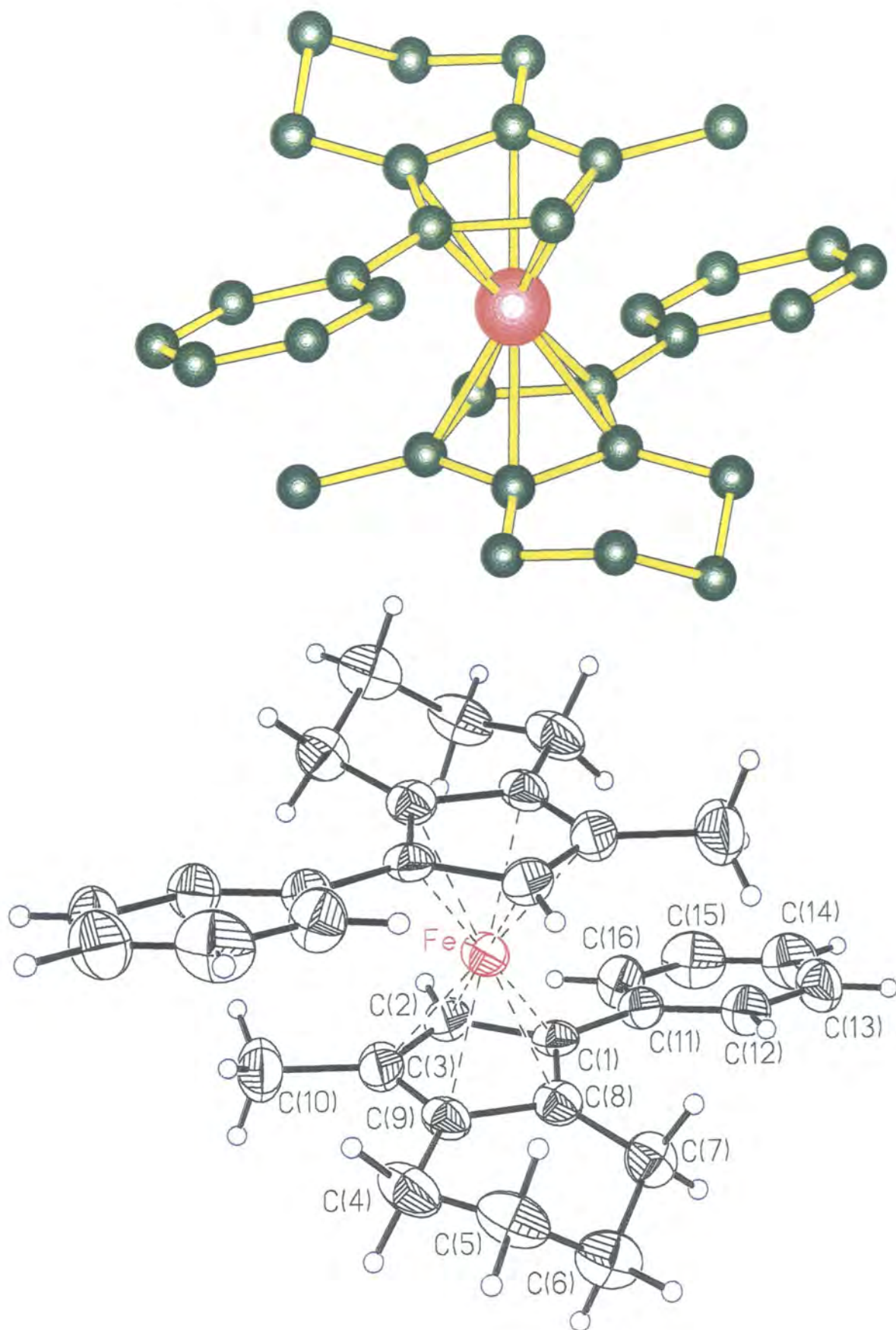
Using spectroscopic and spectrometric methods alone it is not possible to say which isomer is present in sample **2.3C**, or if the initial crop of **2.3B** is the same isomer.

2.3.2b(iv) Powder and single crystal X-ray diffraction solid state molecular structure determination.

The crystals obtained in sample **2.3B** were of sufficient crystallinity and size for a single crystal X-ray diffraction experiment to be performed. Data were collected (5882 reflections collected, 1974 independent, 1935 used for structure solution) at -123 °C and solved using the SHELXTL software suite. The ferrocene crystallizes in the space group $\text{P}2_1/\text{c}$. The iron atom is located on a crystallographic inversion centre. As the *meso*-isomer of **2.3** must possess a molecular inversion centre at the iron atom, the

meso-configuration can automatically be assigned to the isomer of ferrocene **2.3** used in the single crystal diffraction experiment (Fig. 2.7).

Fig 2.7 Solid state molecular structure of the *meso*-isomer of **2.3**.



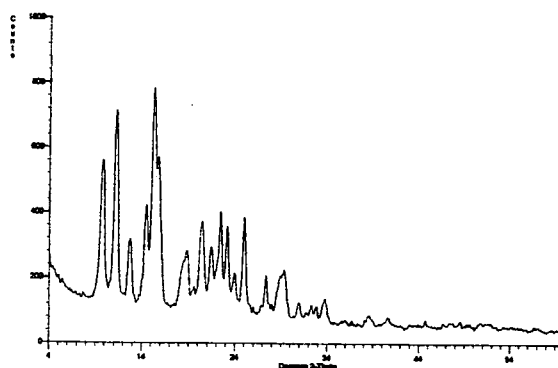
Using the XPOW program from the SHELXTL series it is possible to calculate a theoretical powder diffraction pattern for the *meso*-isomer of **2.3** used in the single crystal experiment.

A powder X-ray diffraction experiment was performed on the bulk powder sample of **2.3**.

The X-ray powder diffraction pattern of the bulk sample was compared with the X-ray powder diffraction pattern calculated for **2.3** from the data obtained in the single crystal diffraction experiment.

As can be seen in Fig. 2.8 the powder patterns are the same (the calculated and experimentally derived powder diffraction patterns are reproduced in chapter five more clearly). Therefore, the bulk material, sample **2.3C**, characterised by ^{13}C and ^1H NMR spectroscopy has the same structure as that determined for the single crystal, from sample **2.3B**, namely the *meso*- isomer. The *rac*-isomer is considerably more soluble in the liquors than the *meso*-isomer and has not been isolated as a pure material.

Experimentally obtained X-ray powder diffraction pattern of **2.3**, from bulk sample **2.3C**.



Calculated X-ray powder diffraction pattern of **2.3**, from solid state structure data. Crystal from sample **2.3B**.

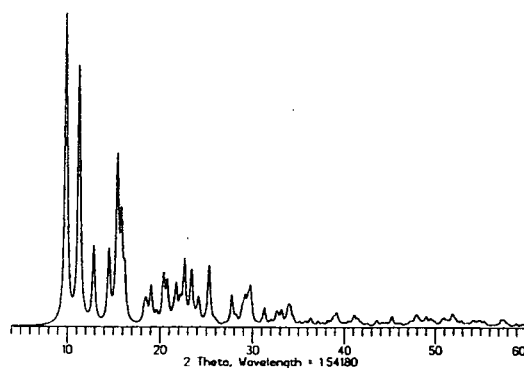


Fig. 2.8 Experimental and calculated powder diffraction patterns of **2.3**.

The asymmetric unit of the crystal structure of **2.3** consists of only one half of the molecule. The other half is generated by the inversion centre at the iron atom. This has two consequences with regards to the configuration of the molecular structure.

- In the solid state **2.3** exists in a configuration that results in the minimum steric interaction between the substituents on the two cyclopentadienyl rings, this is called a distal configuration.¹²
- The two five membered rings are staggered in **2.3** (Fig. 2.9), as are those in $(\eta\text{-C}_5\text{Me}_5)_2\text{Fe}$, **2.a** (Fig. 2.10), $(\eta\text{-C}_5\text{Me}_4\text{H})_2\text{Fe}$, **2.b** (Fig. 2.10), and bis(1,3-dimethyl-4,5,6,7-tetrahydroindenyl) iron(II), **2.c** (Fig. 2.11). In bis(1,2,3-trimethyl-4,5,6,7-tetrahydroindenyl) iron(II), **2.d** (Fig. 2.11), the five membered rings are eclipsed.^{2, 13}

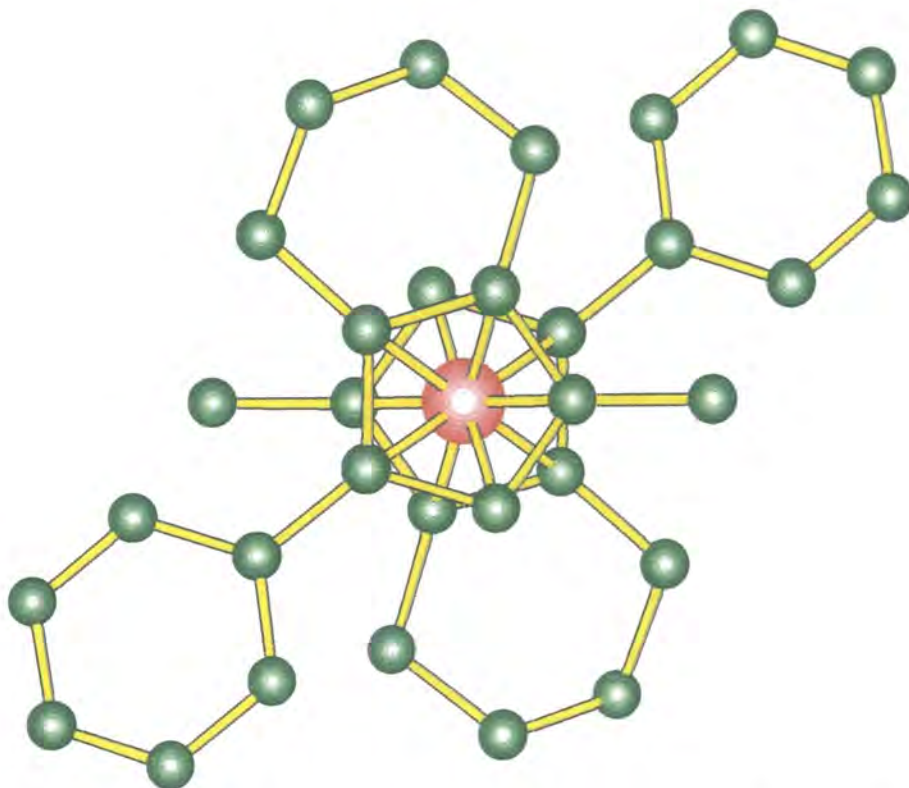


Fig. 2.9 Solid state molecular structure of **2.3**, viewed along centroid-centroid axis.

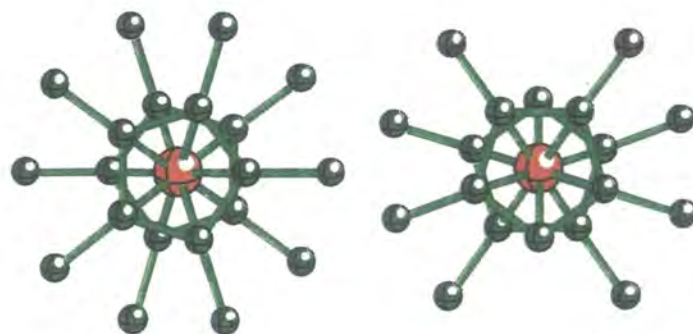


Fig. 2.10 Solid state molecular structures of **2.a** and **2.b**, viewed along centroid-centroid axis.

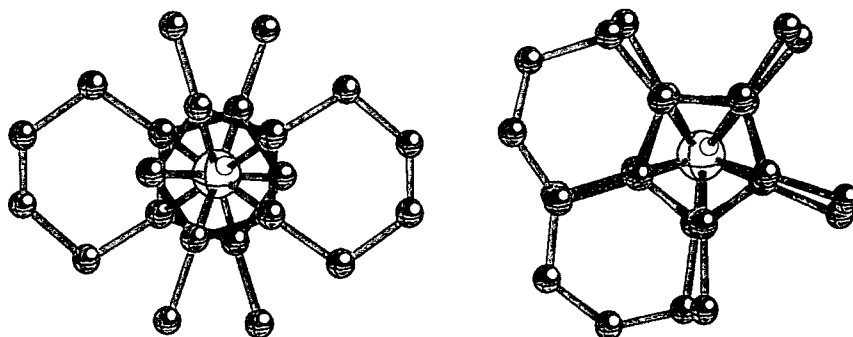


Fig. 2.11 Solid state molecular structures of **2.c** and **2.d**, viewed along centroid-centroid axis.

Various data can be extracted from the molecular structure obtained for **2.3**; a selection is tabulated in Table 2.2 with comparative values for **2.a**, **2.b**, **2.c** and **2.d**.

Distance, Å	Average Fe-C(ring)	Average C(ring)-C(ring)	C(ring)-C(methyl)
2.3	2.067(5)	1.428(7)	1.517(7)
2.a	2.064(3)	1.419(2)	1.502(3)
2.b	2.054(3)	1.428(4)	1.496(6)
2.c	2.050(4)	1.411(6)	1.504(8)
2.d	2.062(4)	1.424(5)	1.495(6)

Table 2.2 Selected bond distances for **2.3** and comparative data for **2.a**, **2.b**, **2.c** and **2.d**.

- The average Fe-C(ring) distance in **2.3** is slightly longer than values for **2.b** and **2.c**, but comparable in length with values for **2.a** and **2.d**.
- The average C(ring)-C(ring) distance in **2.3** is comparable with **2.a**, **2.b**, **2.c** and **2.d**.
- The C(ring)-C(methyl) distance in **2.3** is longer than the average distances in **2.a**, **2.b**, **2.c**, and **2.d**.

The C(ring)-C(phenyl) distance in **2.3** is 1.474 (7) Å, significantly shorter than the C(ring)-C(methyl) distance. This is not unexpected and reflects the difference between a sp^2 - sp^2 and a sp^2 - sp^3 bond; the conjugation between the five membered and six membered π -aromatic systems strengthening the C(ring)-C(phenyl) bond. This "smearing" of electron density out of the cyclopentadienyl ring is shown to be only a very minor contributor, if at all, in increasing the iron atom-cyclopentadienyl centroid distance, by comparing the smaller values for **2.a** and **2.b**, 1.657 Å in both cases, with those of **2.3**, 1.672 Å, **2.c**, 1.662 Å, and **2.d**, 1.669 Å. The major factor affecting the metal-ring distance is obviously the inherent steric bulk of the tetrahydroindenyl ligands. Although there is a small decrease in values going from **2.3** to **2.d** to **2.c**, the significance of this trend must be considered in light of the precision of the structure

determinations. Of the 1186 ferrocenes on the Cambridge Structural Database (CSD), only 63 have a longer iron atom-cyclopentadienyl centroid distance.

It seems appropriate at this point to discuss why certain distances extracted from molecular structures determined by diffraction experiments are quoted with estimated standard deviations (e.s.d.) and others are not. Using present day computational methods, the calculation of e.s.d.'s for bond lengths and bond angles is a relatively trivial matter. Sometimes an e.s.d. for a torsion angle can also be calculated, though with greater difficulty due to it itself being derived from the series of e.s.d.'s for the multiple atomic coordinates concerned within it. The determination of the e.s.d. associated with an atom-ring centroid distance however is computationally non-trivial, and sufficiently difficult as to remain unconsidered in mainstream chemical literature. For this reason no e.s.d.'s are reported here for atom ring centroid distances, angles whose e.s.d. calculation would involve the use of an atom-ring centroid distance e.s.d. or to torsion angles involving these atom-ring centroid angles.

The cyclopentadienyl ring in **2.3** is not perfectly planar and has the following deviations from the mean plane (Å): C(1) -0.006; C(2) 0.004; C(3) 0.000; C(8) 0.006; C(9) -0.004. The steric bulk of the substituents causes the carbons of the methyl group, the phenyl group and cyclohexyl ring adjacent to the five membered ring to deviate from the mean plane of the cyclopentadienyl ring in the direction away from the iron. The cyclohexenyl ring is puckered with average C-C bond distances of 1.527 (8) Å with the following deviations from the mean cyclopentadienyl plane (Å, positive deviation indicates deviation away from the iron atom): C(4) 0.013; C(5) -0.246; C(6) 0.607; C(7) 0.143. The *ipso*-carbon of the phenyl group and the carbon of the methyl group deviate by 0.082 Å and 0.076 Å from the mean plane of the cyclopentadienyl ring respectively. Carbon atom deviation from the mean plane of the cyclopentadienyl ring in **2.3** is summarised in Table 2.3.

Initially it may seem strange that the phenyl group does not deviate away from the plane much more than the methyl group. Also the carbon of the cyclopentadienyl ring bonded to the phenyl group deviates towards the iron rather than away as might be expected so as to alleviate steric interactions of the bulkier phenyl ring. In fact the whole cyclopentadienyl ring tilts towards the iron on the phenyl "side" of the ligand; this is clearly shown in the iron atom-cyclopentadienyl ring carbon distances (Å): C(1) 2.054(5); C(2) 2.070(5); C(3) 2.087(5); C(8) 2.066(5); C(9) 2.058(5). These apparent anomalies can be explained by considering what type of substituents the phenyl and methyl groups are.

Carbon atom	Deviation from C ₅ -plane (Å)
1 (ring C)	-0.006
2 (ring C)	0.004
3 (ring C)	0.000
8 (ring C)	0.006
9 (ring C)	-0.004
4 (C9-CH ₂)	0.013
7 (C8-CH ₂)	0.143
10 (methyl C)	0.076
11 (<i>ipso</i> -phenyl C)	0.082

Table 2.3 Carbon atom deviation from the mean plane of the cyclopentadienyl ring in **2.3**.

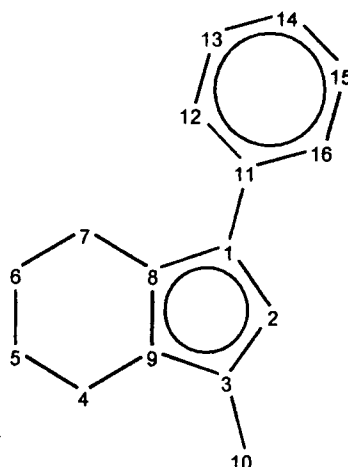


Fig. 2.12 Key to Table 2.3.

The steric influence the methyl group exerts on its immediate environment can be thought of as basically spherical, equal in all directions. Some relief from steric pressure can be achieved through adjustment of the relative positions of the methyl hydrogens. In the structure of **2.3** two of the methyl hydrogens (freely refined in structure solution) are oriented towards the iron and the other ligand. The difference between this and an orientation with one hydrogen pointing "in" towards the iron and other ligand is probably negligible in terms of steric demand. Without an effective bond-rotation mechanism to relieve steric strain the only options remaining to the methyl group are bending of the C(ring)-C(methyl) bond, out of the cyclopentadienyl plane, away from the iron and deviation of the cyclopentadienyl carbon bonded to the methyl group so as to disrupt the planarity of the cyclopentadienyl ring.

The steric influence the phenyl group exerts on its immediate environment can be thought of as more "plate"- or "donut"-like. The ability to rotate about the C(ring)-C(phenyl) bond adds another dimension to the phenyl group's ability to relieve steric pressure in the molecule. In **2.3**, this twisting moves the phenyl ring out of the vicinity of the cyclohexyl ring adjacent to it. As there is only a hydrogen on the other side of the phenyl ring to the cyclohexyl group, the most favourable direction of the twist away from the adjacent cyclohexyl carbon will be dictated by the new interactions created between the phenyl ring and the other tetrahydroindenyl ligand. Due to the symmetry of the molecule, bond deviations for one ligand are identical for the other. The methyl group deviates further from the iron, and, hence, the other ligand, than the cyclohexenyl carbon adjacent to it does. Therefore, the most favourable twisting of the phenyl group should "point" it towards the methyl carbon and away from the cyclohexyl carbon on the second tetrahydroindenyl ligand. As can be seen from the molecular structure of **2.3** this is indeed what happens (Fig. 2.13, side on view of **2.3**, with iron removed for clarity; the carbons of one phenyl group and opposing methyl and cyclohexenyl carbons are rendered in blue.).

Excessive phenyl-ring rotation would reduce the efficacy of the conjugation of the two 6π -aromatic rings by decreasing the overlap of the two π -systems. This may act as a limiting influence on the ability of phenyl-ring rotation to reduce steric pressure in the ligand.

It may be possible to assess the degree of steric interaction in the complexed tetrahydroindenyl ligand by the amount the phenyl ring rotates about the C(cyclopentadienyl ring)-C(phenyl ring) bond. However, a problem with this exists in that ring rotation is not the only mechanism of steric strain relief in evidence for the phenyl ring. The phenyl ring deviates from planarity with the cyclopentadienyl ring due to the "bending" of the ring away from the cyclopentadienyl mean plane. Combined with the deviation of the cyclopentadienyl ring itself from planarity, this means that four discreet torsion angles can be extracted from the molecular structure of **2.3** to describe the rotation of the phenyl ring. If this rotation is to be used to assess the relative steric strain present in the ligand's environment in different complexes, then the "bending" must be comparable in each case and either a single torsion angle must be defined, although this may be affected by deviations in a single cyclopentadienyl ring bond, or the dihedral angle between the cyclopentadienyl and phenyl rings (or rather their mean planes) used instead. For **2.3** and the other complexes described here the dihedral angle is used, and in the case of **2.3** it is 17.9° .

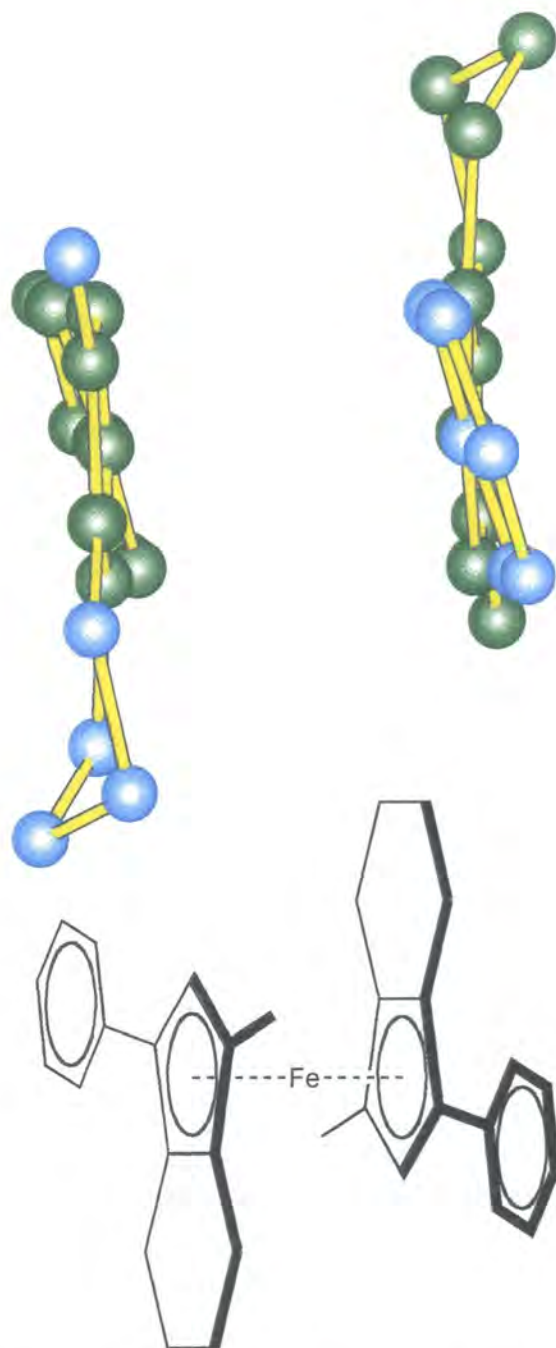


Fig. 2.13 View of **2.3** depicting direction of phenyl ring twist.

2.3.2b(v) Cyclic voltammetry.

In order to investigate the electronic properties of **2.3**, the electro-chemistry of **2.3** was investigated by cyclic voltammetry in acetonitrile using a Ag/AgCl non-aqueous reference electrode as a reference and lithium perchlorate as the supporting electrolyte. The ease of oxidation of substituted ferrocenes relative to ferrocene, as discussed in section 1.3.1, can be expressed in terms of $\Delta E_{1/2}$, which is the difference between $E_{1/2}$ for the substituted ferrocene and ferrocene itself. A value for $E_{1/2}$ of 0.187 V was measured for $(\eta\text{-C}_5\text{H}_5)_2\text{Fe}$, and a value of -0.127 V for **2.3**, giving a value for $\Delta E_{1/2}$ of -0.314 V. The cyclic voltammogram of **2.3** relative to that of ferrocene is shown in Fig. 2.14 (*x*-axis shifted by -187 mV due to software rendering artifact for double plots).

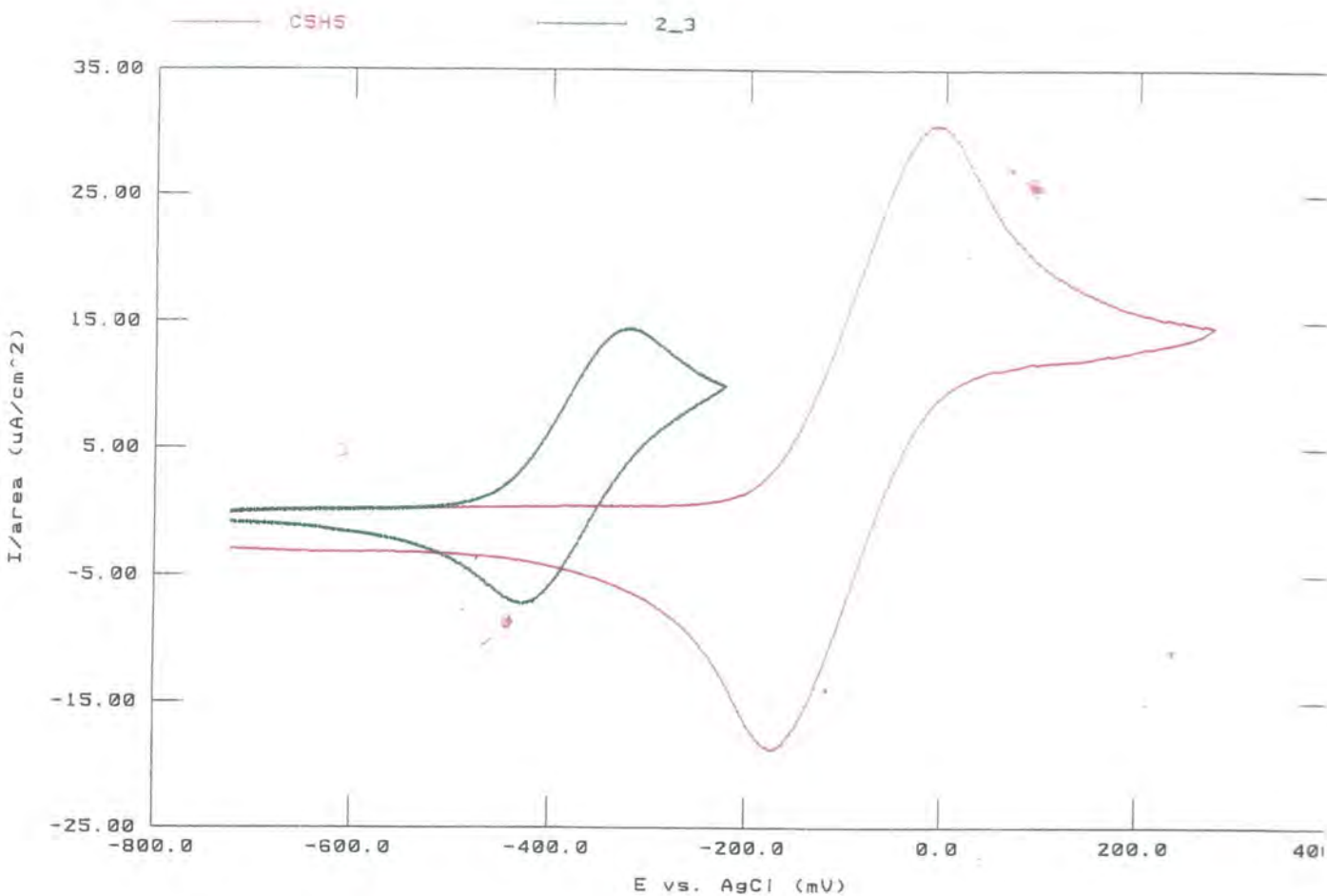


Fig. 2.14 Cyclic voltammogram of **2.3** relative to that of ferrocene.

As mentioned earlier, $E_{1/2}$ decreases upon the introduction of an alkyl group, and increases when a phenyl substituent is introduced. Therefore, the value of $\Delta E_{1/2}$ for **2.3** would be expected to be less negative than that for a ferrocene with three alkyl substituents on each cyclopentadienyl ring and more negative than a ferrocene with only two alkyl substituents per cyclopentadienyl ring. As predicted the value of $\Delta E_{1/2}$ for **2.3** is less negative than the value of $\Delta E_{1/2}$ for bis (1-methyl-4,5,6,7-tetrahydroindenyl) iron(II) (three alkyl substituents per cyclopentadienyl ring, Fig. 2.15), -0.340 V, and more negative than the value of $\Delta E_{1/2}$ for bis (4,5,6,7-tetrahydroindenyl) iron(II) (two alkyl substituents per cyclopentadienyl ring, Fig. 2.15), -0.249 V. This means **2.3** is harder to oxidize than the former, easier to oxidize than the latter and that all three are much more easily oxidized than ferrocene.

The range of travel of the trace in the y-direction of the cyclic voltammogram is a function of concentration; the cyclic voltammogram is smaller vertically for **2.3** than for ferrocene due to its lower solubility in acetonitrile.

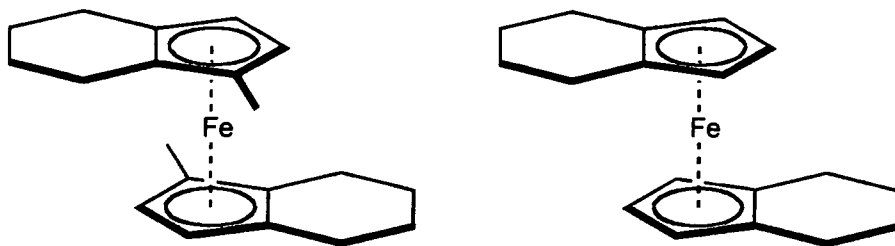


Fig. 2.15 Bis (1-methyl-4,5,6,7-tetrahydroindenyl) iron(II) and bis (4,5,6,7-tetrahydroindenyl) iron(II).

2.3.3 Summary.

The bulky ferrocene, **2.3**, has been prepared. The reaction produces two isomers, the chiral (RR-/SS-)*rac*-isomer and the achiral (RS-/SR-)*meso*-isomer. The achiral isomer is less soluble in hexanes than the chiral isomer and has been isolated as a pure solid and characterized by various techniques, including powder X-ray diffraction. The achiral species crystallizes in the space group $P2_1/c$, with the molecular inversion centre of the molecule coincident with a crystallographic inversion centre. In the solid state the *meso*-isomer is sterically crowded, resulting in deviation of the cyclopentadienyl ring substituents from the mean plane of the five membered ring away from the iron atom and the second tetrahydroindenyl ligand. The deviation of the phenyl group is reduced by its ability to twist to relieve steric pressure. The dihedral angle of the phenyl and cyclopentadienyl mean planes is 17.9° and the iron atom-cyclopentadienyl centroid distance is 1.672 \AA . Cyclic voltammetric measurements show how **2.3** is more easily oxidized than ferrocene, this is due to the inductive effect of the alkyl substituents on the tetrahydroindenyl ligands. As opposed to **2.3**, there are no ferrocenes in the literature that contain both alkyl and aryl substituents on the cyclopentadienyl rings.

2.4 1-Phenyl-3-methyl-4,5,6,7-tetrahydroindenyl iron(II) dicarbonyl dimer.

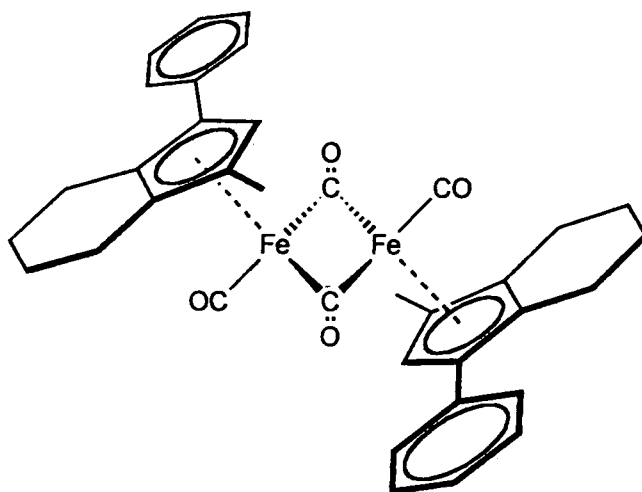
2.4.1 Introduction.

Isolated first as an intermediate in the synthesis of ferrocene, $[(\eta\text{-C}_5\text{H}_5)\text{Fe}(\text{CO})_2]_2$ and its analogues are commonly found as a by-product of many organo-iron compound syntheses.¹⁴ These dimers are precursors to mono-nuclear iron compounds, usually prepared by cleavage with iodine, to form $\text{CpFe}(\text{CO})_2\text{I}$, or sodium amalgam, to form the extremely nucleophilic anion $\text{CpFe}(\text{CO})_2^-$.¹⁵ The photochemistry of cyclopentadienyl dicarbonyl iron dimers is of continuing interest.¹⁶

2.4.2 Discussion.

2.4.2a Synthesis.

The cyclopentadienyl iron dicarbonyl dimer, 1-phenyl-3-methyl-4,5,6,7-tetrahydroindenyl iron(II) dicarbonyl dimer, **2.4**, was prepared by addition of **2.1** to di-iron nonacarbonyl, $\text{Fe}_2(\text{CO})_9$, followed by reflux in toluene for 24 h. Extraction of the crude reaction mixture with toluene, reduction of solvent volume under reduced pressure and filtration gave **2.4** as a black powder in low to moderate yields (typically 25 %). Recrystallization from acetonitrile gave dark red-brown crystals of **2.4** suitable for single crystal X-ray diffraction structural analysis.



2.4

2.4.2b Characterization.

Characterization was by ^1H NMR, ^{13}C NMR and solution (dichloromethane) state infrared spectroscopy, mass spectrometry ($m/z = 642 [\text{M}^+]$), single crystal X-ray diffraction and CHN analysis. *Cis*- and *trans*-isomers are possible for **2.4** as shown in Fig. 2.16.

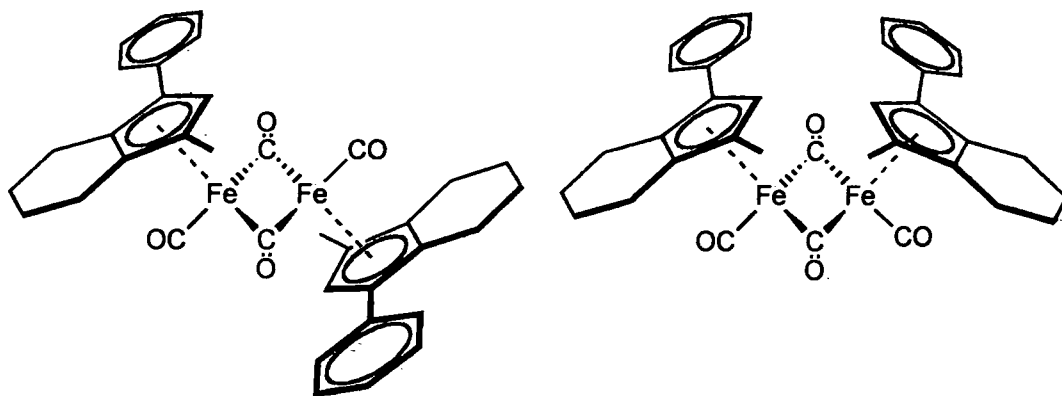


Fig 2.16 The *cis*- and *trans*-isomers of **2.4**.

2.4.2b(i) Infra-red spectroscopy.

The solution state infra-red spectrum of **2.4** has three strong bands (band A at 1761 cm^{-1} , band C at 1934 cm^{-1} and band D at 1974 cm^{-1}) and a weak shoulder (band B at 1796 cm^{-1}) between 1500 cm^{-1} and 2000 cm^{-1} (Fig. 2.17).

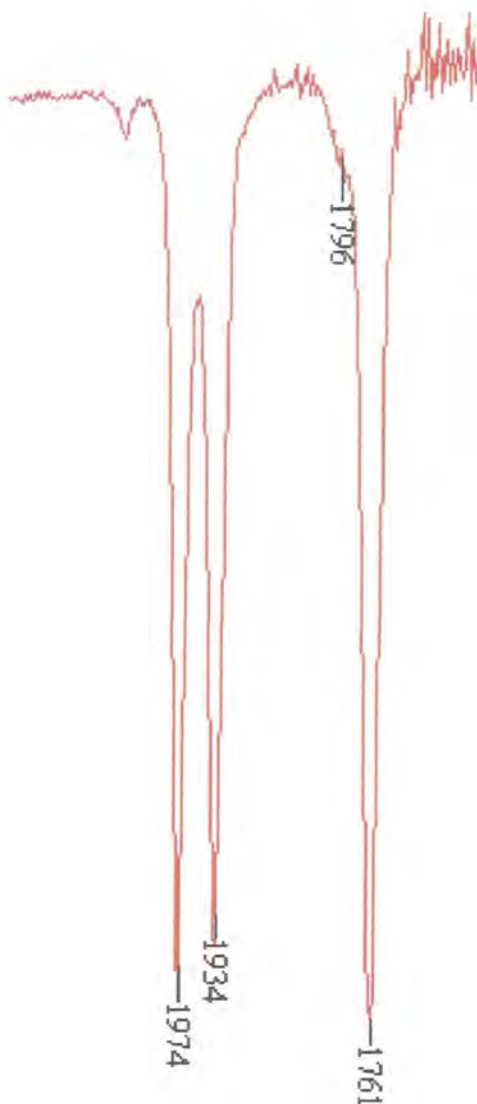


Fig. 2.17 Portion of the solution-state infra-red spectrum of **2.4**.

In the infra-red data analysis that follows the simplification is made that the tetrahydroindenyl ligand is rotating rapidly about the ligand-metal axis. The molecule thus has time-averaged C_{2h} symmetry in the *trans*-form or C_{2v} symmetry in the *cis*-form.

The behaviour for the totally symmetric carbonyl stretch for the *trans*-isomer under the symmetry elements of C_{2h} was examined: for example, under i none of the of the carbonyls remain superimposed on themselves, whilst the operations C_2 and σ_h leave two unchanged vectors. The carbonyl vectors give the representation $\Gamma(\textit{trans})$ in the point group character table (Table 2.4). The representation $\Gamma(\textit{trans})$ reduces to $2A_g + A_u + B_u$.

C_{2h}	E	C_2	i	σ_h		
A_g	1	1	1	1	R_z	x^2, y^2, z^2, xy
B_g	1	-1	1	-1	R_x, R_y	yz, zx
A_u	1	1	-1	-1	z	
B_u	1	-1	-1	1	x, y	
$\Gamma(trans)$	4	2	0	2	=	$2A_g + A_u + B_u$

Table 2.4 Character table for the point group C_{2h} .

Thus, four carbonyl stretches are expected, two with A_g symmetry, one with A_u symmetry and one with B_u symmetry.

To determine which symmetry representation is appropriate to a particular vibration, the symmetry operations of C_{2h} are applied to a diagram in which the motions of the atoms are represented by arrows (Fig. 2.18).

The necessary information conveyed by the transformation matrix which expresses the result of the operation on the motion represented by the arrows is contained in the **character** of the matrix. The character (χ) is derived as the trace (sum of diagonal elements) of the transformation matrix. In the case of C_{2h} (and C_{2v}) each symmetry operation will either leave the motion unchanged or reverse its direction. Hence, the transformation matrices are simply +1 or -1, respectively.

In the case of the vibration depicted in Fig. 2.18 The identity operator, E , leaves the motion unchanged, so $\chi_v(E)$ is +1. Equally, operation of the C_2 rotation axis leaves all arrows unmoved, so $\chi_v(C_2)$ is +1. Operation of the inversion centre, i , reverses the arrows of the bridging carbonyls, so $\chi_v(i)$ is -1. Finally, operation of the mirror plane, σ_h , also reverses the bridging carbonyl arrows, so $\chi_v(\sigma_h)$ is -1. The representation for this vibration is

$$\Gamma_v = \begin{matrix} & E & C_2 & i & \sigma_h \\ & +1 & +1 & -1 & -1 \end{matrix}$$

and it can be deduced that the vibration is of symmetry A_u .

The character table for C_{2h} shows that the z axis also has A_u symmetry, so the A_u symmetry vibration in Fig. 2.18 will give a dipole change along z , and will be infra-red active (i.e. give rise to a band in the infra-red spectrum). As will the B_u symmetry vibration, but not the two A_g symmetry vibrations.

The vibrations and the corresponding symmetries for the representation $\Gamma(trans)$ are given in Fig. 2.19.

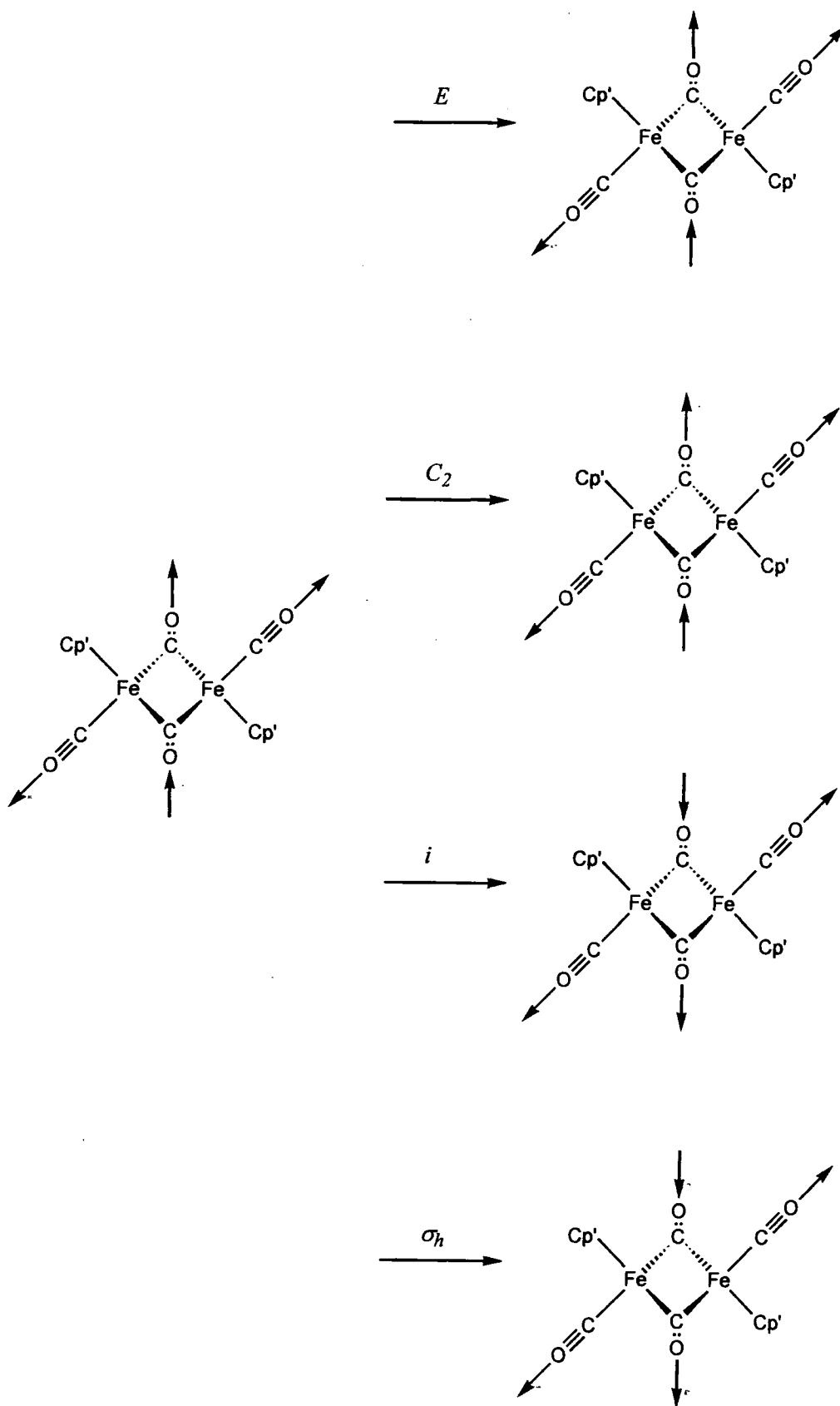


Fig 2.18 Application of the symmetry operations of C_{2h} to a particular CO stretch in 2.4.

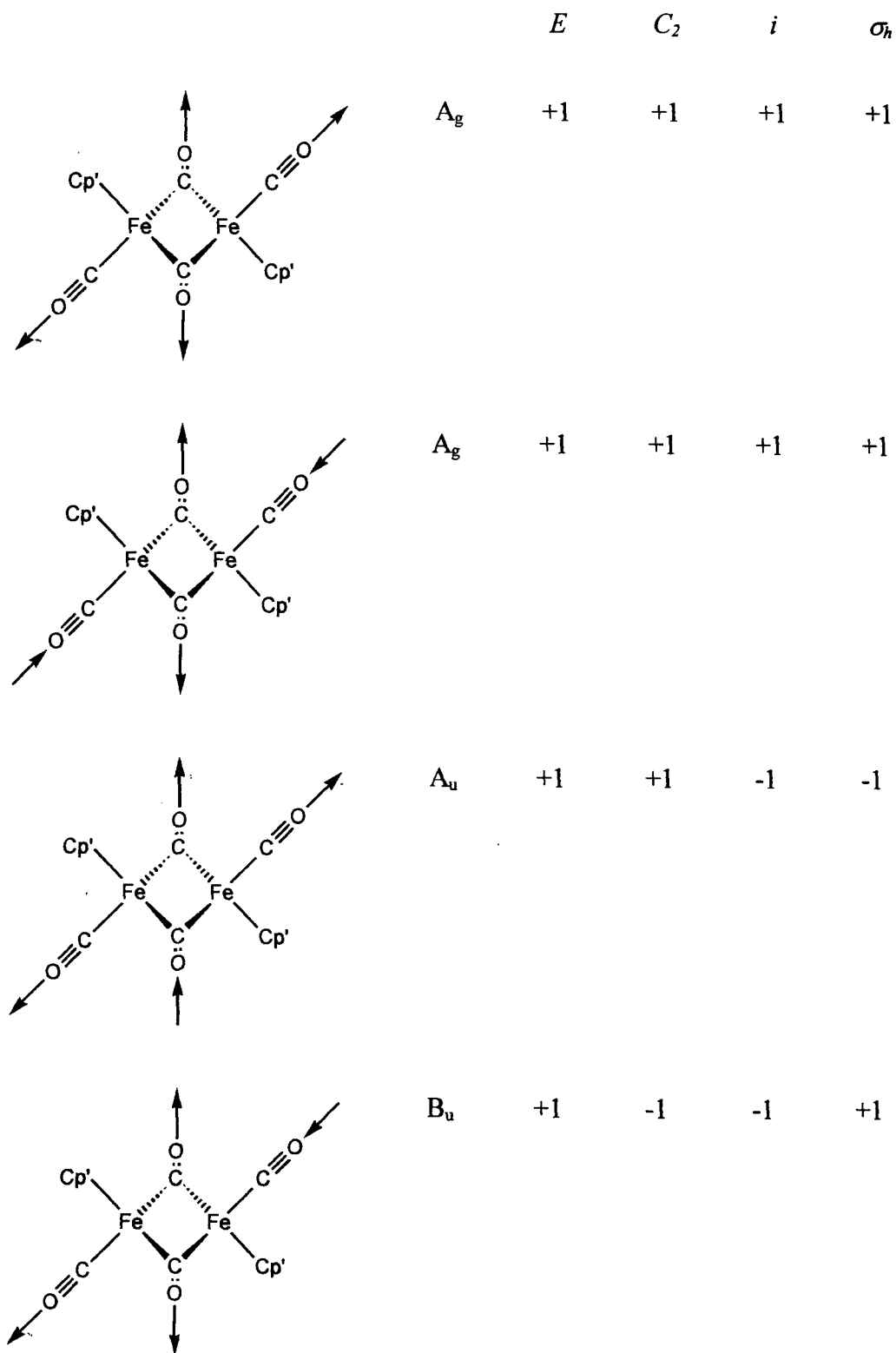


Fig. 2.19 Vibrations and symmetries for $\Gamma(\text{trans})$.

The behaviour for the totally symmetric carbonyl stretch for the *cis*-isomer under the symmetry elements of C_{2v} was examined in the same manner. The carbonyl vectors give the representation $\Gamma(cis)$ in the character table (Table 2.5). This reduces to $2A_1+B_1+B_2$.

C_{2v}	E	C_2	$\sigma_v(xz)$	$\sigma_v(yz)$		
A_1	1	1	1	1	z	x^2, y^2, z^2
A_2	1	1	-1	-1	R_z	xy
B_1	1	-1	1	-1	x, R_y	zx
B_2	1	-1	-1	1	y, R_x	yz
$\Gamma(cis)$	4	0	2	2	=	$2A_1+B_1+B_2$

Table 2.5 Character table for the point group C_{2v} .

The vibrations and the corresponding symmetries for the representation $\Gamma(cis)$ are shown in Fig. 2.20.

The character table for C_{2v} shows that the x axis has B_1 symmetry, the y axis B_2 symmetry and the z axis A_1 symmetry. Therefore, all four vibrations in Fig. 2.20 will be infra-red active.

From these two analyses the following information can be obtained.

- The *trans*-isomer has two symmetry permitted infra-red active vibrational modes.
- The *cis*-isomer has four symmetry permitted infra-red active vibrational modes.

Since the observed solution state infra-red spectrum has three very strong stretching bands (A, C and D) and a weak shoulder (B) in the carbonyl stretching frequency region it would initially seem sensible to assign the structure present in solution to the seemingly sterically unfavourable *cis*-isomer.

However, in work reported by Manning, the infra-red spectrum of $[(\eta-C_5H_5)Fe(CO)_2]_2$, which has three strong bands and a weak shoulder analogous to that of 2.4, shows splitting of the bands analogous to bands A and C when recorded in certain solvents.¹⁷ This indicates the presence of more than one species in solution. Manning also describes how bands A, C and D have varying relative intensities in different solvents due to the formation one isomer or the other being more favourable in these solvents. The more polar a solvent, the greater the preference for the polar *cis*-isomer; in less polar solvents the non-polar *trans*-isomer is favoured.

Following the assignments of Manning, the carbonyl band pattern for the infra-red spectrum of 2.4 can be assigned as follows.

- Band A is assigned to the A_u symmetry stretch of the *trans*-isomer and the B_1 symmetry stretch of the *cis*-isomer.

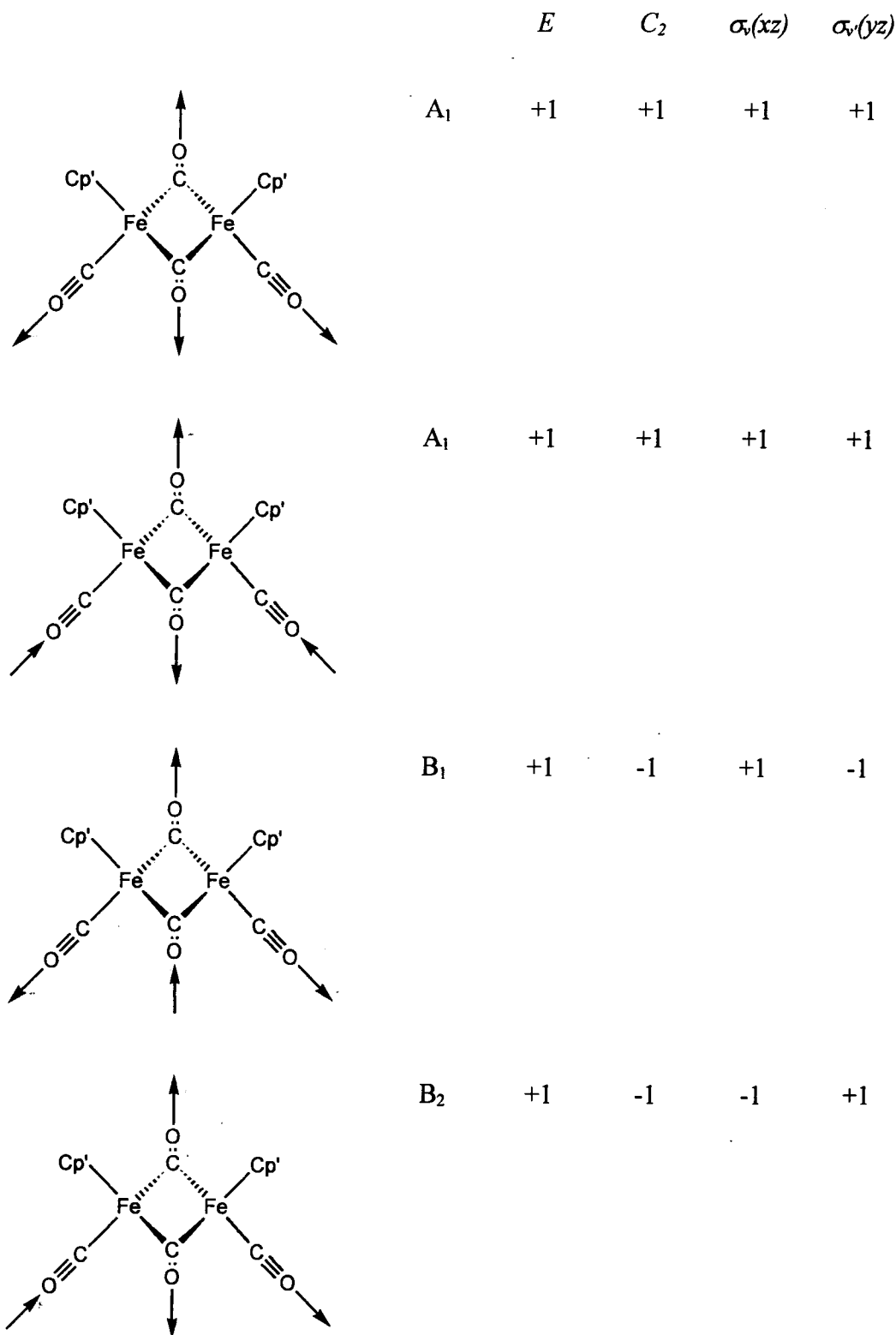


Fig. 2.20 Vibrations and symmetries for $\Gamma(cis)$.

- Band B is assigned to the A_1 symmetry stretch of the *cis*-isomer shown in Fig. 2.21. Band B is weak due to both bridging vibrations moving *anti* to the terminal vibrations. That is to say when the terminal vibrations vibrate away from the molecule, the bridging vibrations vibrate towards the molecule. Hence, the

magnitude of the dipole moment change, the property of a vibration that is responsible for its intensity, is always kept small and the resulting infra-red band weak.

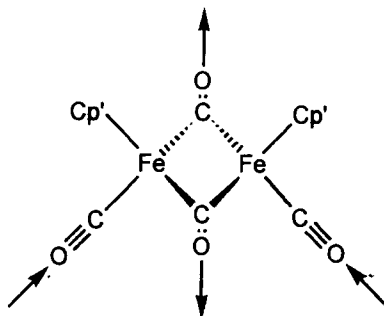


Fig. 2.21 A_1 symmetry stretch of the *cis*-isomer of **2.4**.

- Band C is assigned to the B_u symmetry stretch of the *trans*-isomer and the B_2 symmetry stretch of the *cis*-isomer.
- Band D is assigned to the remaining A_1 symmetry stretch of the *cis*-isomer.

The bulky tetrahydroindenyl ligand possesses insufficient steric demand to prevent formation of the *cis*-isomer in solution. The importance of having five substituents on both five membered rings in order to sterically inhibit the formation of the *cis*-isomer even in polar solvents has been shown nicely by McArdle and co-workers via infra-red studies of $[(\eta-C_5Me_5)Fe(CO)_2]_2$, **2.e**, and $(\eta-C_5Me_5)(\eta-C_5Me_4H)Fe_2(CO)_4$, **2.f**.¹⁸ In apolar solvents only two bands are seen in the carbonyl stretching region of the infra-red spectrum of **2.f**, due to the A_u and B_u symmetric vibrational modes of the *trans*-isomer and indicating its sole presence in solution. However, in acetonitrile the three strong bands indicative of a *cis*-/*trans*-mixture are observed. In the case of **2.e** only two bands are seen regardless of solvent polarity. Five substituents on each ring are crucial in achieving a steric limit to *cis*- $[(\eta-C_5R_5)Fe(CO)_2]_2$ complexes in solution.

2.4.2b(ii) Nuclear magnetic resonance spectroscopy.

On the NMR timescale the *trans*-isomer and the *cis*-isomer cannot be distinguished, at room temperature, due to rapid interconversion of the two. This illustrates the fact that the IR-timescale allows two species to be observed whilst the slower NMR timescale allows only a time-averaged view of the isomers. Different chemical shifts have been reported by Gansow and co-workers, for the carbonyl carbons of the two isomers of the dimer, $[(\eta-C_5H_5)Fe(CO)_2]_2$, using variable temperature ^{13}C NMR spectroscopy to "freeze-out" the isomerization.¹⁹

As for **2.3** three stereoisomers of **2.4** are possible (Fig. 2.22).

- The RR and SS isomers, which will be collectively referred to as the *rac*-isomer.
- The RS isomer which will be referred to as the *meso*-isomer.

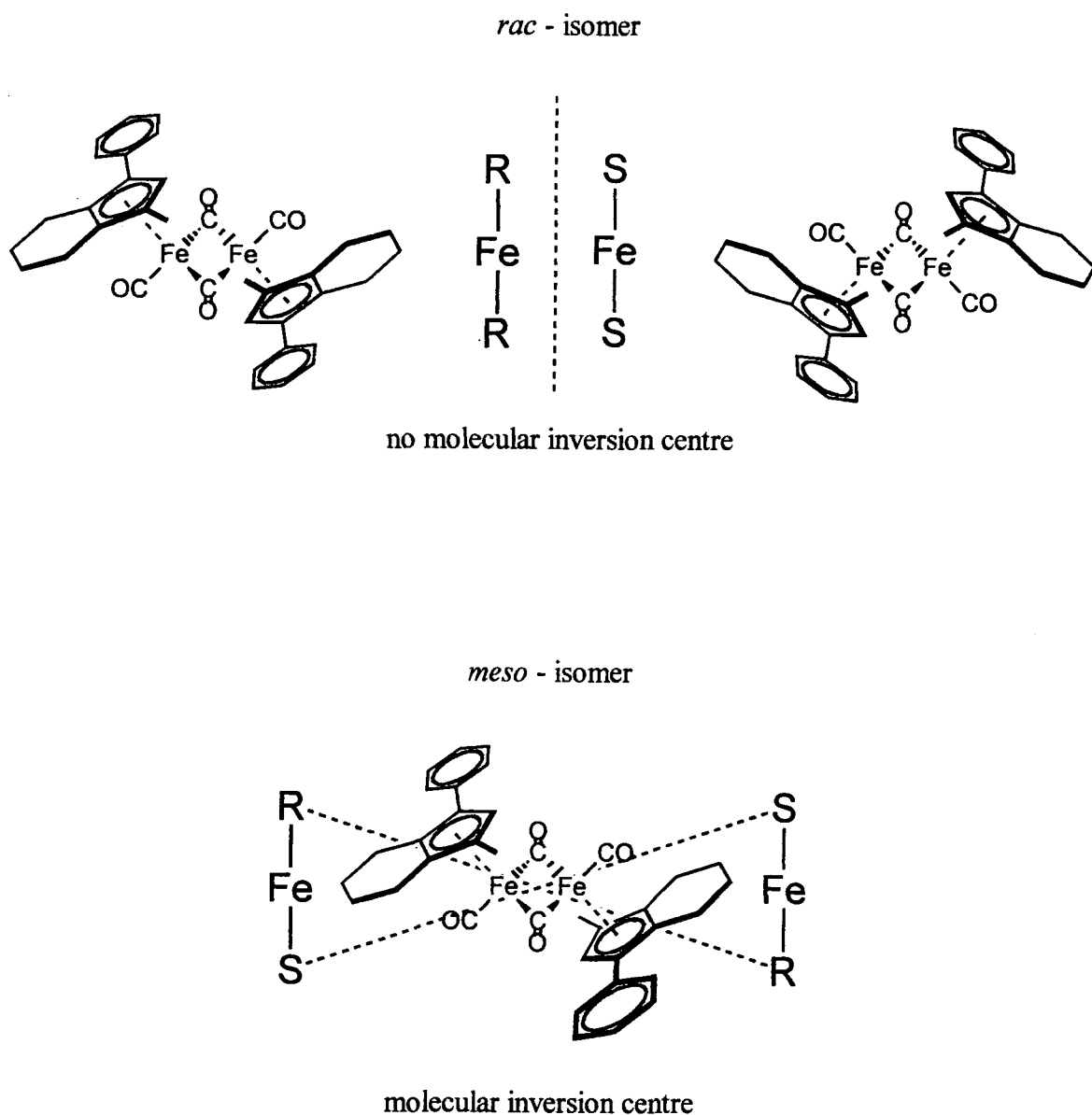


Fig. 2.22 The *rac*- and *meso*-isomers of **2.4**.

It has proven difficult to obtain high quality ^1H or ^{13}C NMR spectroscopic data for **2.4**, since even samples prepared under strictly anaerobic conditions from freshly crystallized material give rise to a broad cyclopentadienyl C-H resonance ($\Delta\nu_{1/2} = 80$ Hz) in the ^1H NMR spectrum, although the resonances due to other protons remote from the iron are sharp.

Very careful sample preparation was necessary to prepare a sample from which it was possible to obtain a $^{13}\text{C}\{^1\text{H}\}$ NMR spectrum in which the organic ligand resonances could be assigned; even in this sample the carbonyl resonances were not observed and certain resonances behaved other than might have been expected.

These NMR spectral characteristics are probably due to oxidation or some other decomposition process in solution, giving rise to traces of paramagnetic impurities. However, the presence of paramagnetic impurities might be expected to aid observation

of the carbonyl resonances by providing a quicker relaxation pathway and reducing the carbonyl carbon's relaxation time; indeed the addition of paramagnetic material is a commonly used NMR technique in aiding the observation of carbonyl resonances. Also the presence of paramagnetic material might be expected to broaden all proton resonances in the ^1H NMR spectrum not just those of the protons near the iron atoms. There are other possible reasons for the difficulty in obtaining satisfactory NMR spectroscopic data. It is possible that an equilibrium exists in solution between the di-iron dimer and either a paramagnetic 17 electron monomer or the 32 electron molecule, $\text{Cp}'_2\text{Fe}_2(\eta\text{-CO})_3$, and CO. The dimer-monomer equilibrium is well documented in group 6 chemistry for $[(\eta\text{-C}_5\text{Me}_5)\text{M}(\text{CO})_3]_2$ ($\text{M} = \text{Cr}, \text{Mo}, \text{W}$).²⁰ The existence of the 17 electron monomeric species $(\eta\text{-C}_5\text{H}_5)\text{Fe}(\text{CO})_2$ is also known; this has been observed in solutions at room temperature by employing fast time-resolved infra-red spectroscopy after flash photolysis of $[(\eta\text{-C}_5\text{H}_5)\text{Fe}(\text{CO})_2]_2$, the Fe-Fe bond homolysis is promoted by visible light.²¹ Using flash photolysis the 32 electron species $(\eta\text{-C}_5\text{H}_5)_2\text{Fe}_2(\text{CO})_3$ has been reported to be much longer lived than the 17 electron monomer.²² Although these species are short lived in the $(\eta\text{-C}_5\text{H}_5)$ species, there is literature evidence that substitution of cyclopentadienyl rings can dramatically increase the stability of otherwise highly reactive photochemically induced intermediates in cyclopentadienyl dicarbonyl iron(II) chemistry. Baird and co-workers have reported the proclivity of per-aryl substituted cyclopentadienyl dicarbonyl iron(II) dimers to undergo, spontaneous, thermal homolysis to the 17-electron monomers.^{22b,c} Sitzmann and co-workers have reported the synthesis and characterization of penta-iso-propyl cyclopentadienyl dicarbonyl iron(II) dimer.^{22d}

The ^1H NMR spectrum of **2.4** was assigned as follows.

- Five overlapping multiplets between $\delta = 1.14$ ppm and 2.18 ppm which are assigned to six of the CH_2 protons of the six membered ring.
- Two doublets of doublets of doublets at $\delta = 2.92$ ppm ($J = 16$ Hz, 10 Hz and 6 Hz) and 2.74 ppm ($J = 16$ Hz, 5 Hz and 5 Hz) which are assigned to two protons of the CH_2 groups in the 4 or 7 positions of the six membered ring.
- A slightly broad singlet at $\delta = 1.65$ ppm which is assigned to the protons of the methyl group.
- A very broad singlet at $\delta = 3.75$ ppm which is assigned to the proton of the CH group in the five membered ring.
- A series of multiplets at $\delta = 7.11$ ppm to 7.43 ppm which are assigned to the phenyl group protons.

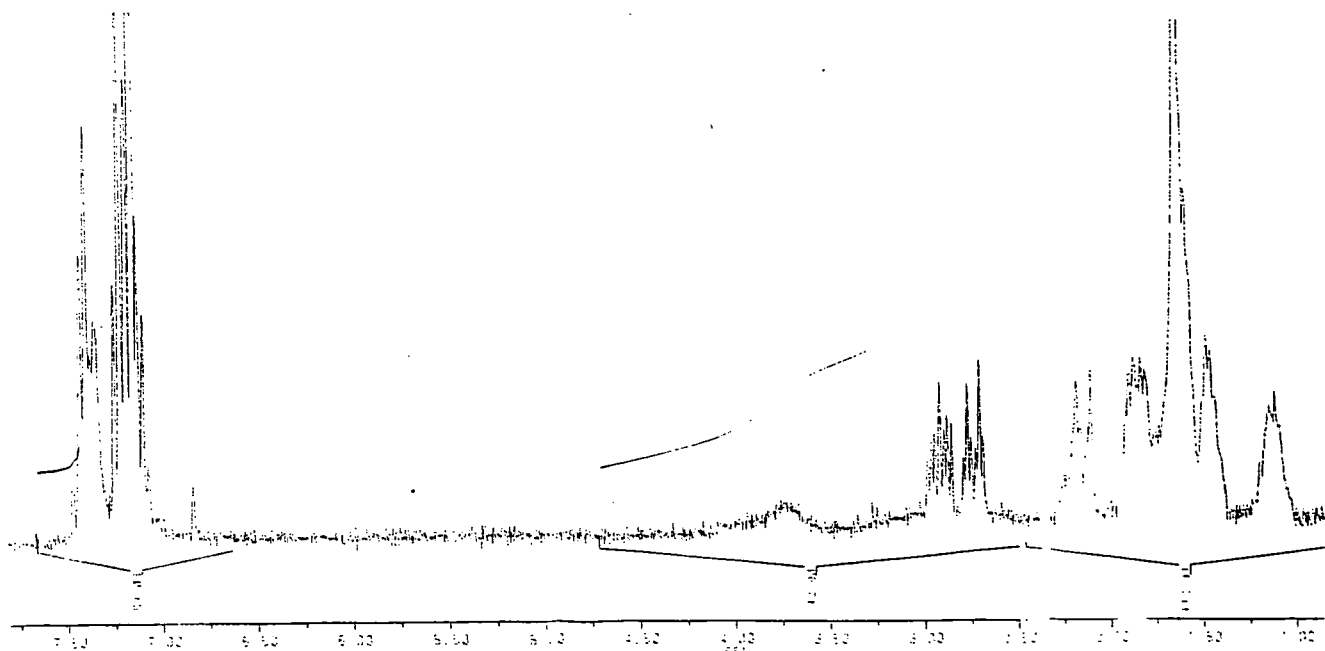


Fig. 2.23 ^1H NMR spectrum of **2.4**, assignments are in the text.

The $^{13}\text{C}\{^1\text{H}\}$ NMR spectrum of **2.4** was a close match to that of **2.3**, as expected. The resonances assigned to the methyl group carbon, the phenyl group carbons, the quaternary carbons and the CH_2 carbons for **2.3** were all present in the ^{13}C NMR spectrum of **2.4**. However, no resonance was observed in the $^{13}\text{C}\{^1\text{H}\}$ NMR spectrum of **2.4** that could be assigned to the CH carbon of the five membered ring, no resonances were observed that could be assigned to the carbonyl carbons and, in contrast to the ^{13}C NMR spectra of **2.2** and **2.3**, two of the resonances observed for the CH_2 groups are very strong and two very weak.

Due to the wide range of relaxation times which exists for ^{13}C nuclei in different environments, comparisons of intensities (or areas) between different carbon resonances is not practicable; this is not the case in ^1H NMR spectroscopy where integration of peak areas is a valuable tool. However, as shown in the ^{13}C NMR of **2.2** and **2.3**, similarly substituted carbon nuclei in the same molecule usually have comparable intensities. The absence of a resonance in the ^{13}C NMR spectrum of **2.4** that could be assigned to the CH carbon of the five membered ring is presumed to be due to whatever causes the broadening of the resonance assigned to the proton attached to this carbon.

The presence of only one set of resonances in the ^1H NMR spectrum for the methyl, phenyl and tetrahydro backbone indicates that the isolated material for **2.4** consists of

only one isomer, but does not distinguish between a di-iron dimer containing a molecular inversion centre (*meso*) and one containing a two-fold rotation axis (*rac*), such a distinction needs to be made by other techniques. The NMR spectrum of the crude, unrecrystallized, material is considerably broader than that of the isolated material and cannot be used to determine the *rac*-/*meso*-isomer ratio prior to recrystallization.

2.4.2b(iii) Single crystal X-ray diffraction solid state molecular structure determination.

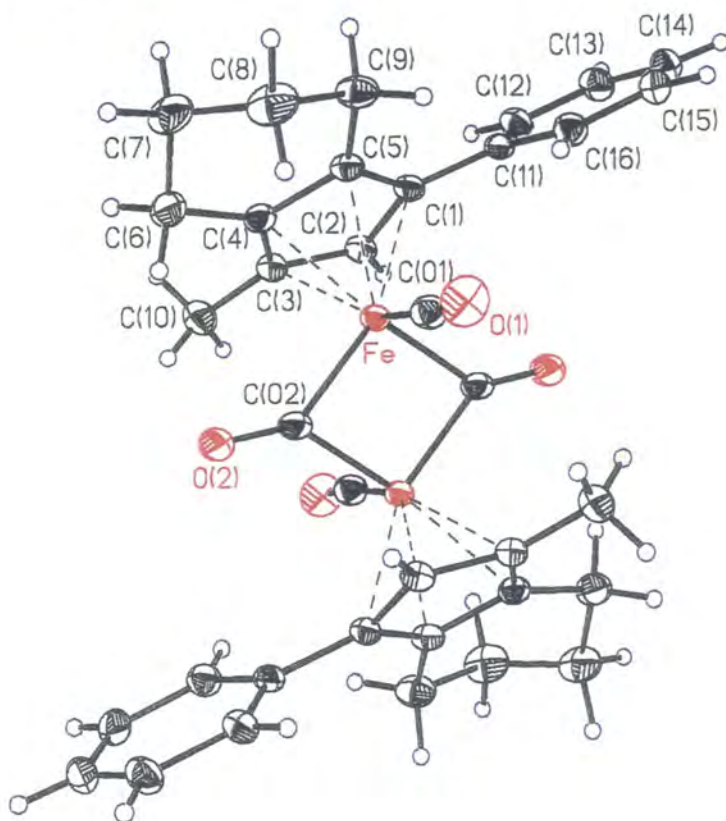
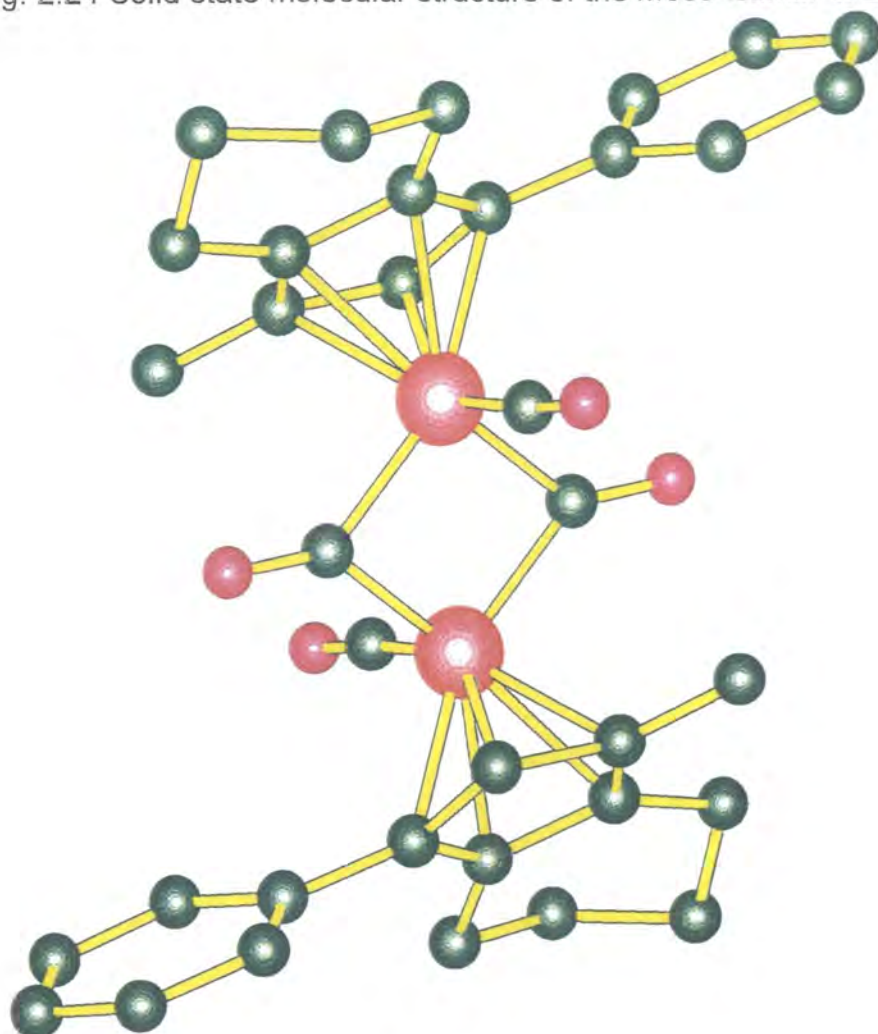
The crystalline material used for spectroscopic analysis contained crystals of suitable quality for a single crystal X-ray diffraction experiment to be performed. Data were collected (14599 reflections collected, 3961 independent, 3949 used for structure solution) at -123 °C and solved using the SHELXTL software suite. The dimer crystallizes from acetonitrile in the space group $P2_1/c$. A crystallographic inversion centre is located midway between the two iron atoms. As the *meso*-isomer of **2.4** must possess a molecular inversion centre midway between the two iron atoms, the *meso*-configuration can automatically be assigned to the isomer of dimer **2.4** used in the single crystal diffraction experiment (Fig. 2.24).

The asymmetric unit of the crystal structure of **2.4** consists of only half the molecule; the other half is generated by the crystallographic inversion centre midway between the iron atoms. This has two consequences with regards to the molecular structure.

- In the solid state RS-**2.4** exists in the *trans*-form in a configuration that results in the minimum steric interaction between the substituents on the two cyclopentadienyl rings, this is called a distal configuration. As the cyclopentadienyl centroid-iron axes are not coincident in **2.4** the distal configuration is best viewed along the centroid-centroid axis (Fig. 2.25).
- When viewed along the centroid-centroid axis, as in Fig. 2.25, the two five membered rings are staggered, a direct consequence of the crystallographic symmetry. This is also the case in $[(\eta-C_5H_5)Fe(CO)_2]_2$, **2.g** (Fig. 2.26), and $[(\eta-C_5Me_5)Fe(CO)_2]_2$, **2.e** (Fig. 2.26).²³ In **2.e** a C(ring)-CH₃ bond eclipses the terminal carbonyl ligand coordinated to the iron which is coordinated to the cyclopentadienyl ring of the methyl group. In **2.4** the C(ring)-CH₃ bond does not eclipse the corresponding terminal carbonyl, but a C(ring)-CH₂ bond does. However, in **2.g** no C(ring)-H bonds eclipse the corresponding carbonyl.

Various data can be extracted from the molecular structure obtained for **2.4**; these are summarised in Table 2.5 along with comparative data for **2.g** and **2.e**.

Fig. 2.24 Solid state molecular structure of the *meso*-isomer of 2.4.



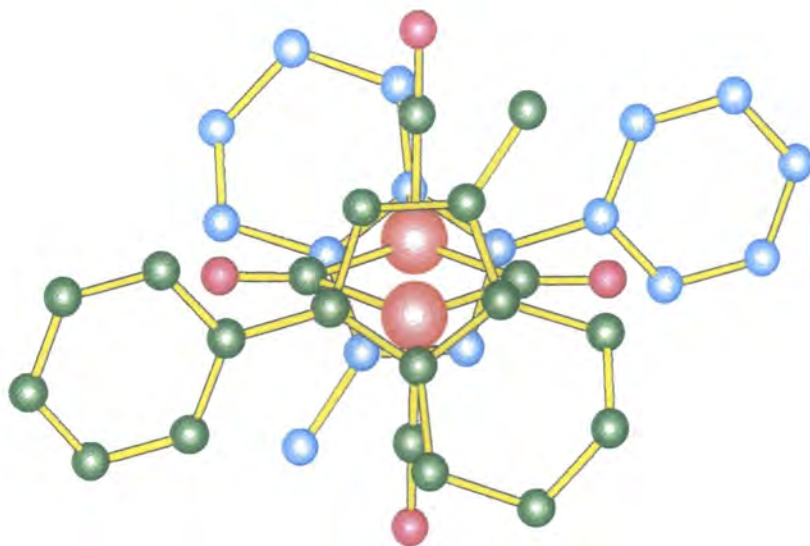


Fig. 2.25 View of **2.4** along the centroid-centroid axis.
 (Carbons of rearmost tetrahydroindenyl ligand rendered in blue for clarity.)

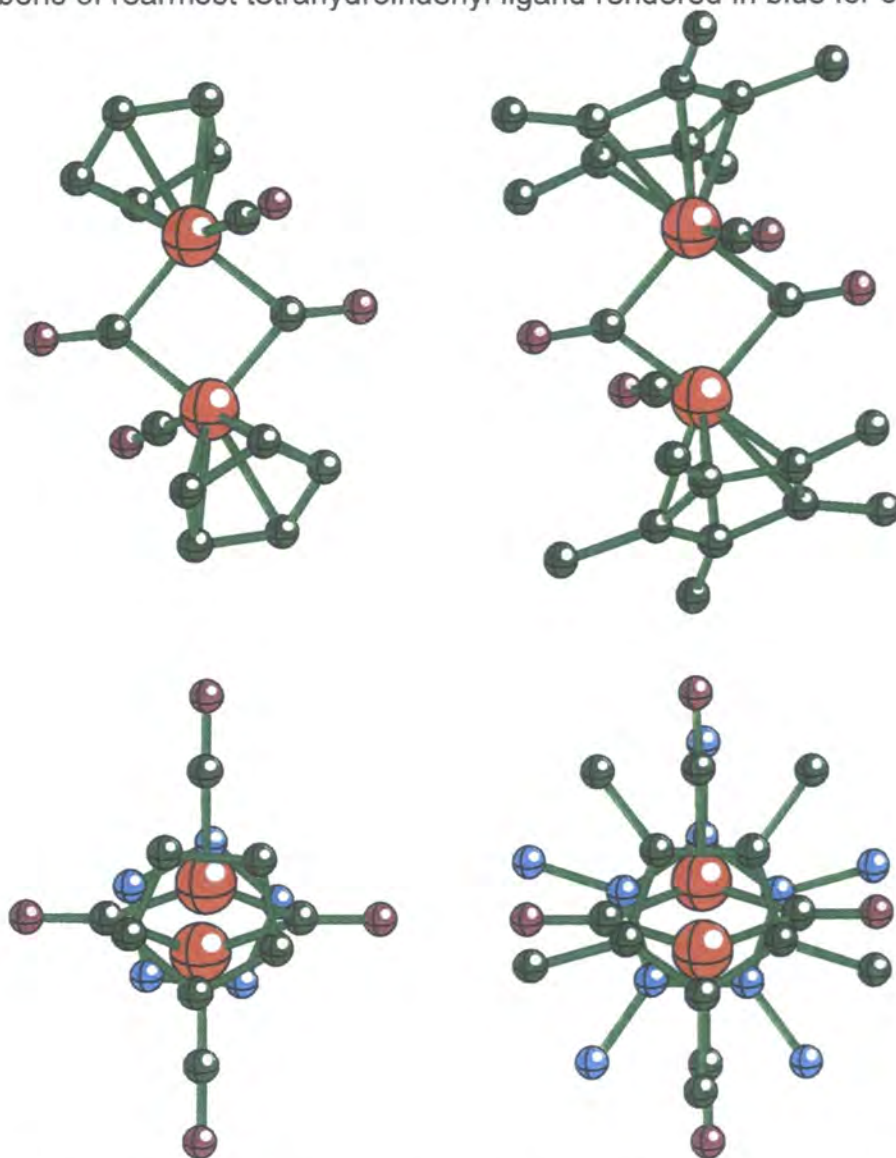


Fig. 2.26 Solid state molecular structures of $[(\eta\text{-C}_5\text{H}_5)\text{Fe}(\text{CO})_2]_2$ and $[(\eta\text{-C}_5\text{Me}_5)\text{Fe}(\text{CO})_2]_2$.

Distance (Å) or Angle (°)	2.4	2.g [(η -C ₅ H ₅)Fe(CO) ₂] ₂	2.e [(η -C ₅ Me ₅)Fe(CO) ₂] ₂
Fe-Fe'	2.5541(5)	2.534(2)	2.560(1)
Average Fe-C(ring), [Range]	2.143(1) [2.104(1)-2.188(1)]	2.106(7) [2.082(7)-2.121(8)]	2.142(2) [2.115(2)-2.162(2)]
Fe-Centroid	1.763	1.754	1.764
Fe-C(O1)	1.753(2)	1.748(6)	1.753(3)
Fe-C(O2)	1.930(1)	1.910(5)	1.922(2)
Fe-C(O2')	1.939(1)	1.918(5)	1.936(2)
Average C(ring)-C(ring), [Range]	1.433(2) [1.425(2)-1.445(2)]	1.371(11) [1.346(11)-1.405(10)]	1.427(3) [1.422(3)-1.431(3)]
Average C(ring)-C(substituent), [Range]	1.499(2) [1.479(2)-1.509(2)]	-	1.498(4) [1.491(3)-1.505(4)]
C(O1)-O1	1.154(2)	1.157(7)	1.154(3)
C(O2)-O2	1.179(2)	1.188(6)	1.172(3)
Fe'-Fe-C(O1)	95.86(5)	95.29(2)	96.8(1)
Fe-C(O2)-Fe'	82.64(6)	82.9(2)	83.1(1)
Fe-C(O1)-O1	175.20(14)	178.4(8)	175.8(2)
Fe-C(O2)-O2	139.22(12)	138.8(4)	139.0(2)
Fe'-C(O2)-O2	138.14(11)	138.4(4)	137.89(2)

Table 2.5 Selected data extracted from the molecular structure of **2.4** and comparative data for **2.e** and **2.g**.

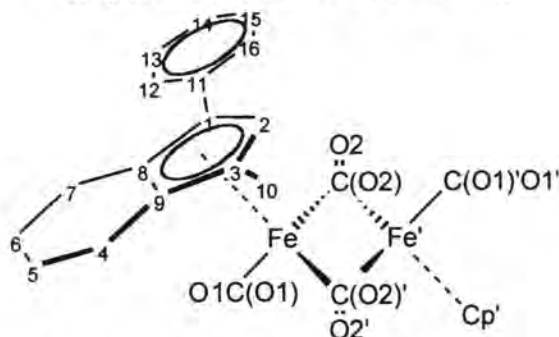


Fig 2.27 Key to Tables 2.5 and 2.7.

(Cp' is the symmetry generated tetrahydroindenyl ligand, which has been omitted for the sake of clarity.)

Care must be taken is assigning too great an importance to small differences between the values given in Table 2.5 for the various bond-lengths and angles of **2.4**, **2.e**, and **2.g**. The primary reason for this is the enormous difference in precision with which it was possible to find atoms using X-ray diffraction at the time of structure determination (1970 for **2.g**, 1980 for **2.e** and 1997 for **2.4**); this is shown clearly by the relative e.s.d.'s of the Fe-Fe' interatomic distances as shown in Table 2.5. Increased precision in more recently determined structures is due to several factors including advances in instrumentation and computing, as well as the ability to collect data at lower temperatures, reducing atomic vibration and resulting positional uncertainty.

The Fe-Fe interatomic distance is in accord with those frequently assigned as metal-metal single bonds in compounds of this sort (mainly due to its similarity to the Fe-Fe distance in $\text{Fe}_3(\text{CO})_9$, 2.560(6) Å)²⁴. However, Mitschler and co-workers have observed little or no electron density between the iron atoms in differential density maps obtained from crystallographic studies of **2.g**.²⁵ Benard has performed *ab initio* calculations of the deformation density distribution in **2.g** and found them in agreement with the experimentally observed density maps, displaying a large region of residual electron density close to zero located along the Fe-Fe line.²⁶ A feature of both the experimentally and theoretically determined maps is an area of density accumulation around the Fe_2C_2 bridged system, possibly suggesting a multi-centred delocalized bond as the metal-metal interaction in this complex. Hoffmann and co-workers have used extended Hückel type calculations to show the preference of doubly bridged structures like **2.g** for a d^7-d^7 configuration, due to the presence of seven molecular orbitals for occupation, with the HOMO being anti-bonding with respect to a direct Fe-Fe bond.²⁷ In light of these reports it is highly unlikely that there is a Fe-Fe bond present in **2.4**.

As has been discussed with respect to the oxidation potentials of ferrocenes in chapter one, substituents on a coordinated cyclopentadienyl ring alter the electronic character of the ligand and, therefore, the electron density on the metal atom. The inductive effect of alkyl substituents would increase the electron density on the atom, whereas phenyl groups, with their opposite influence on the electronic nature of the ligand, would cause a decrease in the electron density on the atom. An increase in electron density on the iron in dimers such as **2.4** would potentially alter metal-carbonyl and C-O distances by changing the magnitude of back-donation to carbonyl anti-bonding orbitals. If this occurred the resulting back-donation to carbonyl anti-bonding orbitals would cause an increase in Fe-CO bond strength and a decrease in C-O bond strength. One widely used relationship between bond-length (d) and bond strength, or rather bond enthalpy (E , the total enthalpy change associated with cleavage of the bond in question), is $E \propto d^x$; consequently increased back-donation to carbonyl anti-bonding orbitals should result in a decrease in iron-carbonyl carbon bond lengths and an increase in carbonyl carbon-carbonyl oxygen bond lengths.²⁸ Due to the magnitude of the errors in determination of atomic positions for carbonyl ligands, any trends in the data in Table 2.5 which might

support or counter this expectation are rendered effectively meaningless, e.g. the C(O2)-O2 bond length is apparently longer in **2.g** than in **2.e** with the value for **2.4** adopting the expected in-between position because of contrasting effects of the phenyl and alkyl substituents.

Change in bond enthalpy also causes a change in the frequency of the carbonyl stretches. The frequency of bond stretching (ν) is proportional to the square-root of the force constant of the bond (k), which is related to the strength of the bond, ($\nu \propto k^{1/2}$, from Hooke's law, $\nu = \{[1/(2\pi c)](k/\mu)^{1/2}\}$). The magnitude of the change in frequency is sufficient that it can be detected using infra-red spectroscopy. Hence, alkyl substitution as in **2.e** would be expected to cause a decrease in carbonyl stretching frequency due to increased electron density on the iron being back-bonded into the anti-bonding orbitals of the carbonyl ligands. With its three alkyl substituents and one phenyl substituent, the stretching frequencies of **2.4** would be predicted to lie between those of **2.e** and **2.g**. Indeed when the values of the A_u and B_u symmetry stretches are compared, Table 2.6 (all solution infra-red spectra used dichloromethane as the solvent), this is observed to be the case.

Dimer	B_u symmetric stretch (cm^{-1}).	A_u symmetric stretch (cm^{-1}).
2.g	1959	1775
2.4	1933	1757
2.e	1922	1727

Table 2.6 B_u and A_u stretching frequencies for **2.g**, **2.e** and **2.4**.

As was also seen in **2.3**, the C(ring)-C(phenyl) distance in **2.4**, 1.479(2) Å, is significantly shorter than the C(ring)-C(methyl) distance, 1.501(2). The iron atom-cyclopentadienyl centroid distance, 1.763 Å, is not any longer than in **2.e** or **2.g**; the distance is significantly longer, however, than in the ferrocenes, **2.3**, 1.672 Å, **2.a**, 1.657 Å, **2.b**, 1.657 Å, **2.c**, 1.662 Å, and **2.d**, 1.669 Å (structures in section 2.3.2b). This is not unexpected and reflects the ability of carbonyl ligands to bond more strongly to transition metals than cyclopentadienyl ligands, resulting in weaker iron-cyclopentadienyl ring interactions in the dimers than in the ferrocenes and lengthening the iron atom-ring centroid distance accordingly.

The tetrahydroindenyl ligands in **2.3** and **2.4** show very similar behaviour. In both cases the carbons of the cyclopentadienyl ring and the carbons of the substituents deviate away from the mean plane of the five membered ring; the deviations for **2.4** are given in Table 2.7 (positive deviation indicates deviation away from the iron atom). The cyclohexyl ring is puckered with an average C-C bond distance of 1.533 (2) Å, the deviations from the mean cyclopentadienyl plane are also given in Table 2.7.

Carbon atom	Deviation from C ₅ -plane (Å)
1	0.005
2	0.004
3	0.002
4	0.090
5	0.594
6	-0.132
7	0.1569
8	-0.004
9	0.001
10	0.142
11	0.140

Table 2.7 Carbon atom deviation from the mean plane of the cyclopentadienyl ring in **2.4**.

The iron atom-cyclopentadienyl centroid axis is not normal to the mean plane of the five membered ring in **2.4**; this means that the ring "tilts" in **2.4**, a feature also seen in **2.3**. The iron atom-cyclopentadienyl ring carbon distances are (Å): C(1) 2.123 (1); C(2) 2.146 (1); C(3) 2.188; C(8) 2.104 (1); C(9) 2.153 (1). As in **2.3**, the ring tilts "towards" the iron atom on the phenyl-substituted side of the ligand. However, in **2.4**, the deviation of the methyl group carbon away from the mean plane of the five-membered ring is no longer nearly the same, as in **2.3**, but greater than that of the *ipso*-carbon of the phenyl group. Both of these facts indicate that the phenyl ring is relieving its steric presence in the system more efficiently than the methyl group.

Earlier in the chapter the idea of the phenyl ring twisting to reduce steric demand was discussed; in **2.4** the dihedral angle between the phenyl and cyclopentadienyl rings is 39.4°. This is more than twice that of the analogous angle in **2.3**. As there is no appreciable change in the C(ring)-C(phenyl) distance between **2.3** and **2.4** it is unlikely that a twist of 39.4° has any major effect on the overlap of the π -systems of the two rings.

The greater twist-angle in **2.4** as compared to **2.3** may not be due solely to sterics; with the dihedral angle of 39.4°, the hydrogen on C(12), in the *ortho*-position on the phenyl ring, is now only ~2.8 Å away from the O1, the oxygen of the nearest terminal carbonyl, potentially close enough for some form of intramolecular interaction. However, as the deviations from the plane of the five membered ring are almost twice that observed in **2.3** for both the phenyl group and the methyl group, one hydrogen of which is only



~2.7 Å away from the oxygen of the nearest bridging carbonyl, it is unlikely that any stabilising intramolecular interactions are occurring and that the twist of the phenyl ring is only due to steric interactions between the tetrahydroindenyl ligand and the rest of the molecule.

2.4.3 Summary.

The dimer **2.4** was prepared in low to moderate yields (typically 25%). With difficulty samples were obtained for spectroscopic and X-ray diffraction analysis. Following literature assignments, the solution state infra-red spectrum of **2.4** indicates the ligand system is not sufficiently bulky to prevent formation of the *cis*-isomer in solution. The reason for poor NMR spectra is unclear, the presence of paramagnetic material due to decomposition or equilibria has been suggested. The solid state molecular structure for the *meso*-stereoisomer of **2.4** has been determined, in the space group $P2_1/c$. The molecular inversion centre is coincident with a crystallographic inversion centre. Indications of system steric strain are present in the molecular structure of **2.4** via deviations from ligand planarity by the cyclopentadienyl ring substituents. The phenyl substituent possesses an extra mode of steric relief to the methyl and cyclohexyl substituents, that of rotation about the cyclopentadienyl-phenyl bond. There is a possible correlation between the infra-red stretching frequencies (and hence their bond enthalpies and lengths) of the carbonyl ligands of **2.g**, **2.e** and **2.4** and the electronic properties of the three different cyclopentadienyl ligands. Although substituted-cyclopentadienyl iron dicarbonyl dimers are extensively studied, there are none in the literature which possess both alkyl and aryl substituents on the cyclopentadienyl rings.

2.5 1-Phenyl-3-methyl-4,5,6,7-tetrahydroindenyl methyl dicarbonyl iron(II).

2.5.1 Introduction.

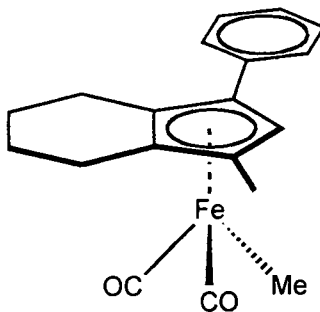
Dicarbonyl iron "half-sandwich" species with organic ligands are of use in a wide variety of applications, including organic asymmetric synthesis, organometallic synthesis, solid state conformational studies and solution conformational studies.²⁹

2.5.2 Discussion.

2.5.2a Synthesis.

The complex, 1-phenyl-3-methyl-4,5,6,7-tetrahydroindenyl methyl dicarbonyl iron(II), **2.5**, was prepared via the addition of **2.4** to sodium amalgam and, after separation from the amalgam, reaction of the sodium salt generated with iodomethane. Upon workup, **2.5** was obtained as an oily orange solid in moderate yield (45%). Compound **2.5** is a low melting solid and was purified by sublimation onto a liquid nitrogen cooled probe;

the sublimed material melted to a red oil on most occasions (distillation), but a dark red solid was obtained by careful, slow sublimation and provided suitable single crystals for a structural determination.



2.5

2.5.2b Characterization.

Characterization was by ^1H NMR, $^{13}\text{C}\{^1\text{H}\}$ NMR and infra-red spectroscopy, CHN analysis, mass spectrometry ($m/z = 336$ [M^+]) and single crystal X-ray diffraction. None of the problems involved with obtaining good quality spectra for **2.4** were encountered in the characterization of **2.5**.

2.5.2b(i) Infra-red spectroscopy.

The solution state (in hexanes) infra-red spectrum of **2.5** has two bands at 1997 cm^{-1} and 1944 cm^{-1} (Fig. 2.28); there is no sign of the four bands associated with the carbonyl stretches of **2.4** (Fig. 2.17). If it is assumed that the tetrahydroindenyl ligand is rotating rapidly about the metal-ligand axis, then the molecule has time averaged C_s symmetry and two bands would be expected, the band due to the A' symmetry stretch and the band due to the A'' symmetry stretch. The frequencies of the two bands in **2.5** are comparable with those in the solution state (in methylcyclohexane) infra-red spectrum bands of $(\eta\text{-C}_5\text{H}_5)\text{Fe}(\text{CO})_2\text{Me}$, 1992 cm^{-1} and 1938 cm^{-1} .

2.5.2b(ii) Nuclear magnetic resonance spectroscopy.

There are two possible stereoisomers of **2.5**, the R-isomer and the S-isomer. The synthetic route will have generated both in equal amounts, i.e. no resolution step has been used. The two differ only with respect to which face of the ligand is coordinated to the iron atom. As with the *rac*-isomers of **2.3** and **2.4**, these stereoisomers are indistinguishable by spectroscopic means.

There are several distinctive features in the ^1H NMR and $^{13}\text{C}\{^1\text{H}\}$ NMR spectra of **2.5** (Fig. 2.29).

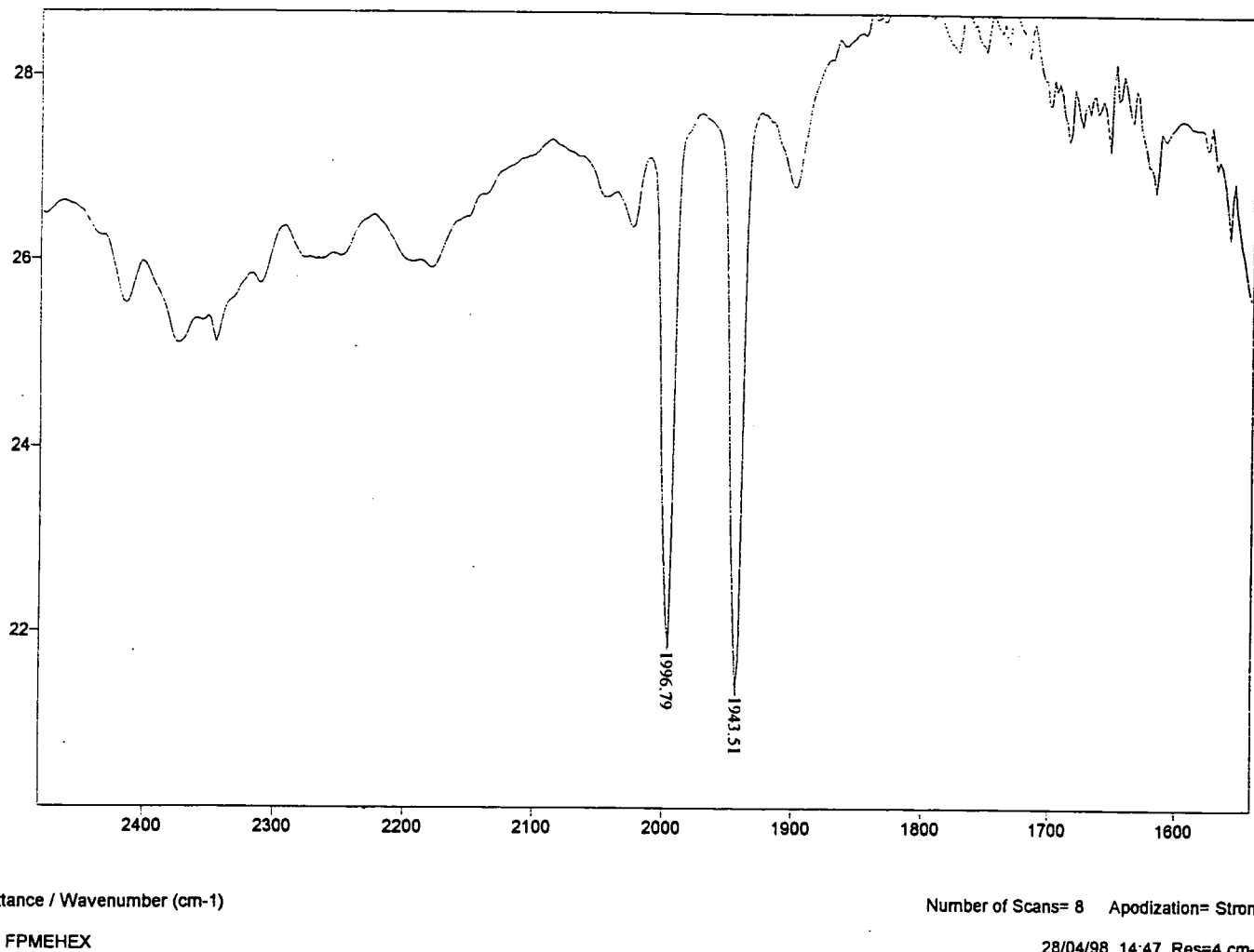


Fig. 2.28 Solution state infra-red spectrum of 2.5.

- A singlet at $\delta = 0.01$ ppm, which is assigned to the protons of the methyl group bonded directly to the iron atom; the resonance in the ^{13}C NMR spectrum at $\delta = -13.4$ ppm is assigned to the carbon of the methyl group bonded directly to the iron atom.
- A singlet at $\delta = 1.81$ ppm, which is assigned to the protons of the methyl group in the tetrahydroindenyl ligand; the resonance in the ^{13}C NMR spectrum at $\delta = 10.6$ ppm is assigned to the carbon of the methyl group in the tetrahydroindenyl ligand.
- A singlet at $\delta = 4.85$ ppm, which is assigned to the proton of the CH group in the cyclopentadienyl ring; the resonance in the ^{13}C NMR spectrum at $\delta = 84.0$ ppm is assigned to the carbon of the CH group in the cyclopentadienyl ring.

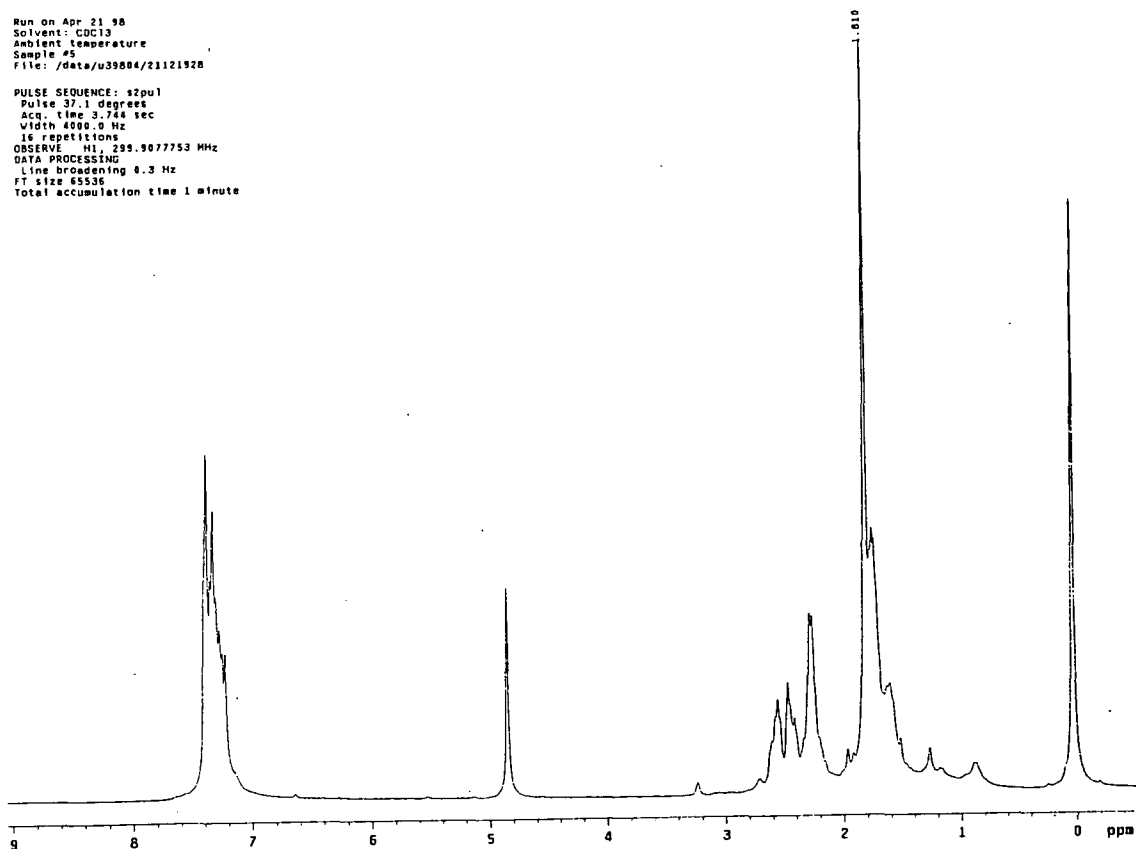
Unlike the ^{13}C NMR spectra for 2.4, the resonances due to the carbonyl ligands are visible in the ^{13}C NMR spectrum of 2.5; the resonances are at $\delta = 218.0$ ppm and 218.1 ppm.

Fig. 2.29 The ^1H NMR and $^{13}\text{C}\{^1\text{H}\}$ NMR spectra of 2.5

STANDARD 1H OBSERVE

Run on Apr 21 98
 Solvent: CDCl3
 Ambient temperature
 Sample 45
 File: /data/u39804/21121928

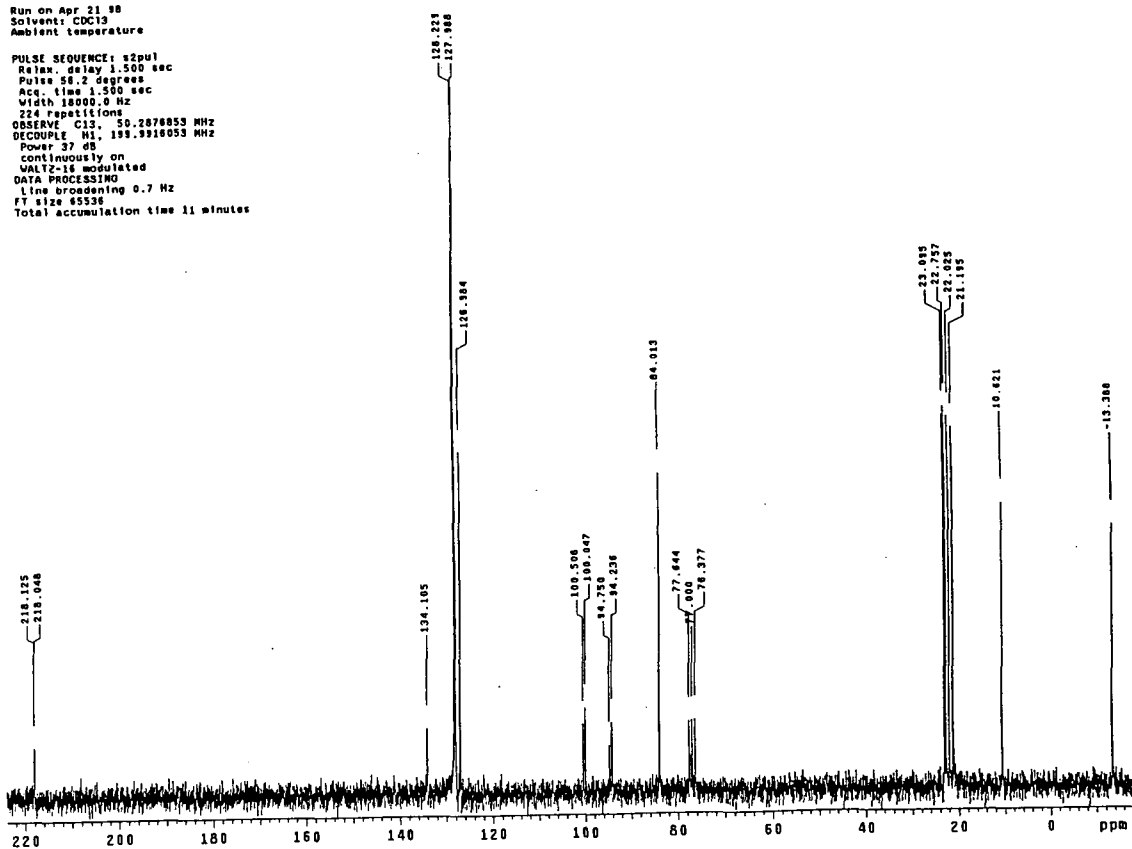
PULSE SEQUENCE: s2pu1
 Pulse 37.1 degrees
 Acq. time 3.744 sec
 Width 4000.0 Hz
 16 repetitions
 OBSERVE M1, 299.9077753 MHz
 DATA PROCESSING
 Line broadening 4.3 Hz
 FT size 65536
 Total accumulation time 1 minute



PhMeTHiF CO2 Me resublimed

Run on Apr 21 98
 Solvent: CDCl3
 Ambient temperature

PULSE SEQUENCE: s2pu1
 Relax. delay 1.500 sec
 Pulse 58.2 degrees
 Acq. time 1.500 sec
 Width 18000.0 Hz
 224 repetitions
 OBSERVE C13, 50.2878053 MHz
 DECOUPLE M1, 199.9918053 MHz
 Power 37 dB
 continuously on
 WALTZ-16 modulated
 DATA PROCESSING
 Line broadening 0.7 Hz
 FT size 65536
 Total accumulation time 11 minutes



2.5.2b(iii) Single crystal X-ray diffraction solid state molecular structure determination.

A crystal of sufficient crystallinity and size for a single crystal X-ray diffraction experiment was obtained. Data were collected (11265 reflections collected, 3711 independent, 3702 used for structure solution) at -123 °C and solved using the SHELXTL software suite. The iron alkyl crystallizes in the space group $P2_1/n$.

It is of interest to note that **2.5** crystallizes in a space group that contains an inversion centre. Therefore, both the R- and the S-isomers must be present in the crystal.

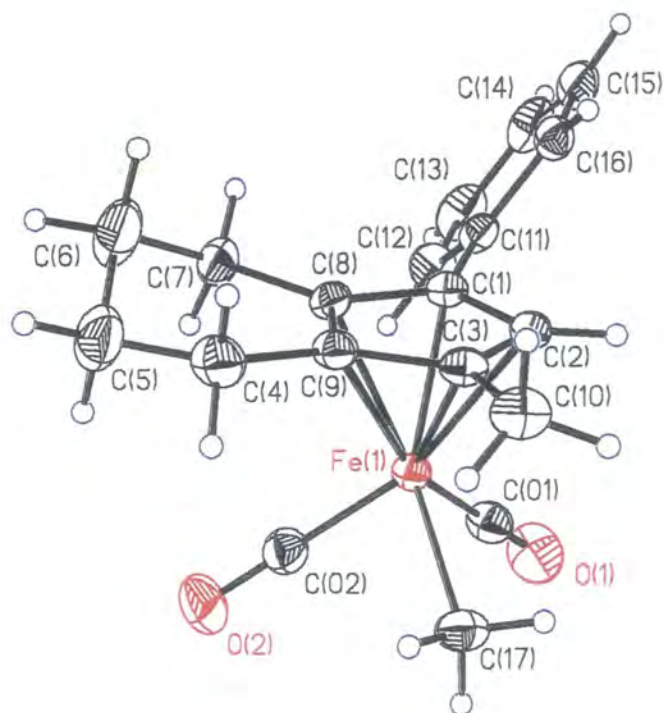
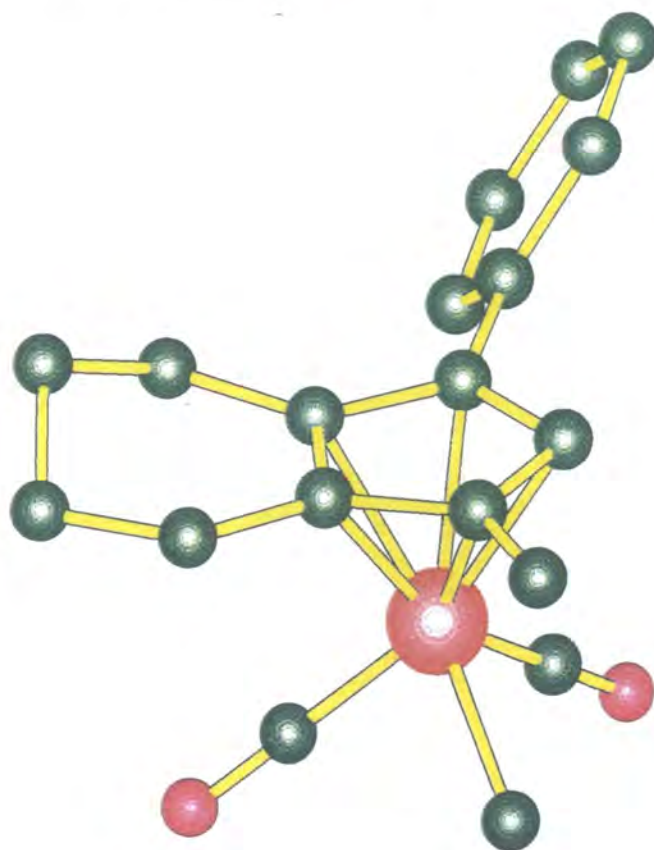
The compound **2.5** will be primarily compared with **2.3** and **2.5**, due to the lack of structures available on the Cambridge Structural Database (CSD) which contain a $\text{Cp}(\text{CO})_2\text{Fe}(\text{alkyl})$ moiety. Those few which are on the CSD, are presented in Table 2.8. It is worth noting that all of the structures in Table 2.8 were determined using room temperature single crystal X-ray diffraction, so their validity in terms of comparing structural data is dubious.

Cp	R	Centroid-Fe (Å)	R-Fe (Å)	Ref.
$(\eta\text{-C}_5\text{H}_5)$	$\text{-(CH}_2\text{)}_4\text{-}$	1.736	2.083 (20)	30
$(\eta\text{-C}_5\text{H}_4)\text{-FeCp}(\text{CO})_2$	Me	1.732	2.070 (40)	31
$(\eta\text{-C}_5\text{H}_4)\text{-P}(\text{Ph})_2\text{W}(\text{Cp})$ $(\text{CH}_3)(\text{CO})_2$	Me	1.725	2.056 (10)	32
$(\eta\text{-C}_5\text{H}_5)$	$\text{-(CH}_2\text{)}_3\text{-}$	1.737	2.082 (20)	30
$(\eta\text{-C}_5\text{H}_4)\text{-Si}(\text{CH}_3)_2\text{-)}_2\text{-}$	Me	1.721	2.039 (6)	33
$(\eta\text{-C}_5\text{H}_4)\text{-)}_3\text{-SiMe}$	Et	1.745	2.086(5)	34

Table 2.8 Cyclopentadienyl dicarbonyl alkyl compounds present on CSD.

Various data can be extracted from the molecular structure determined for **2.5**. A selection of these are tabulated in Table 2.9, along with comparative data for **2.3** and **2.4**.

Fig 2.30 Solid state molecular structure of 2.5.



Distance (Å)	2.3	2.4	2.5
Average	2.067(5)	2.106(7)	2.124(2)
Fe-C(ring), [Range]	[2.054(5) - 2.087(5)]	[2.104(1) - 2.188(1)]	[2.109(2) - 2.153(2)]
Fe-Centroid	1.672	1.763	1.742
Fe-C(O1)	-	1.753(2) (terminal)	1.757(2) (terminal)
Fe-C(O2)	-	1.930(1) (bridging)	1.748(2) (terminal)
Fe-C(methyl)	-	-	2.062(2)
Average	1.428(7)	1.433(2)	1.430(3)
C(ring)-C(ring), [Range]	[1.397(8) - 1.452(7)]	[1.425(2) - 1.445(2)]	[1.419(3) - 1.445(3)]
Average	1.503(7)	1.499(2)	1.500(3)
C(ring)-C(substituent), [Range]	[1.397(8) - 1.517(7)]	[1.479(2) - 1.509(2)]	[1.487(3)-1.509(3)]
C(ring)-C(phenyl)	1.474(7)	1.479(2)	1.487(3)
C(O1)-O1	-	1.154(2) (terminal)	1.149(3) (terminal)
C(O2)-O2	-	1.179(2) (bridging)	1.155(3) (terminal)

Table 2.9 Selected bond lengths for **2.3**, **2.4** and **2.5**.

Initially the cyclopentadienyl ring in **2.5** may appear to be further from the iron atom than in **2.4** due to the longer average Fe-C(ring) distances. This is misleading, and simply due to the tilt of the cyclopentadienyl ring, which is clearly observed when the Fe-C(ring) distances are considered individually (Å): Fe-C(1) 2.113(2); Fe-C(2) 2.109(2); Fe-C(3) 2.153(2); Fe-C(8) 2.118(2); Fe-C(9) 2.129(2). A much better indication of how close the cyclopentadienyl ring is to the iron atom, is the iron atom-cyclopentadienyl centroid distance; in **2.5** this is substantially longer than in **2.3** and shorter than in **2.4**. The shorter length in **2.3** is readily explained by the absence of strongly bonding carbonyl ligands. Carbonyl ligands are much better π -acceptor ligands than cyclopentadienyls, and are far more successful in competing for iron *d*-electrons in **2.5**, thus weakening the iron atom-cyclopentadienyl ring bond and lengthening it relative to **2.3** where competition is equal between the two tetrahydroindenyl ligands. In **2.4** the iron atom is bonded to three carbonyl ligands (one terminal and two bridging), whereas in **2.5** one of the bridging carbonyls is replaced by a methyl group (solely σ -donating with no π -accepting ability). Therefore, the competition between carbonyl and cyclopentadienyl *d*- π^* bonding is slightly reduced in **2.5** with respect to **2.4**, thus strengthening the iron atom-cyclopentadienyl ring bond and shortening it.

The dihedral angle between the mean plane of the phenyl and cyclopentadienyl rings is 54.4° in **2.5**, much bigger than in **2.3**, 17.4° , and **2.4**, 39.6° . The C(ring)-C(phenyl) bond distance is longer in **2.5** than in the other two tetrahydroindenyl-iron complexes. This may be due to the excessive twisting of the phenyl ring reducing the efficiency of the π -cloud overlap and conjugation between the phenyl and cyclopentadienyl rings.

The methyl group of the tetrahydroindenyl ligand and the methyl group bonded to the iron are eclipsed (Fig. 2.31). This presumably unfavourable configuration, sterically, is probably due to there being sufficient steric pressure in the molecule already, so as to force the two methyl groups close to one another. As Fig. 2.31 shows, the carbonyls sit in what are effectively gaps in the steric presence of the tetrahydroindenyl ligand "above" them. A configuration in which the two methyl groups are not eclipsed would cause steric interaction between the carbonyls and the substituents on the five membered ring, as well as bringing the methyl bonded to the iron nearer to something more bulky than the tetrahydroindenyl-methyl group.

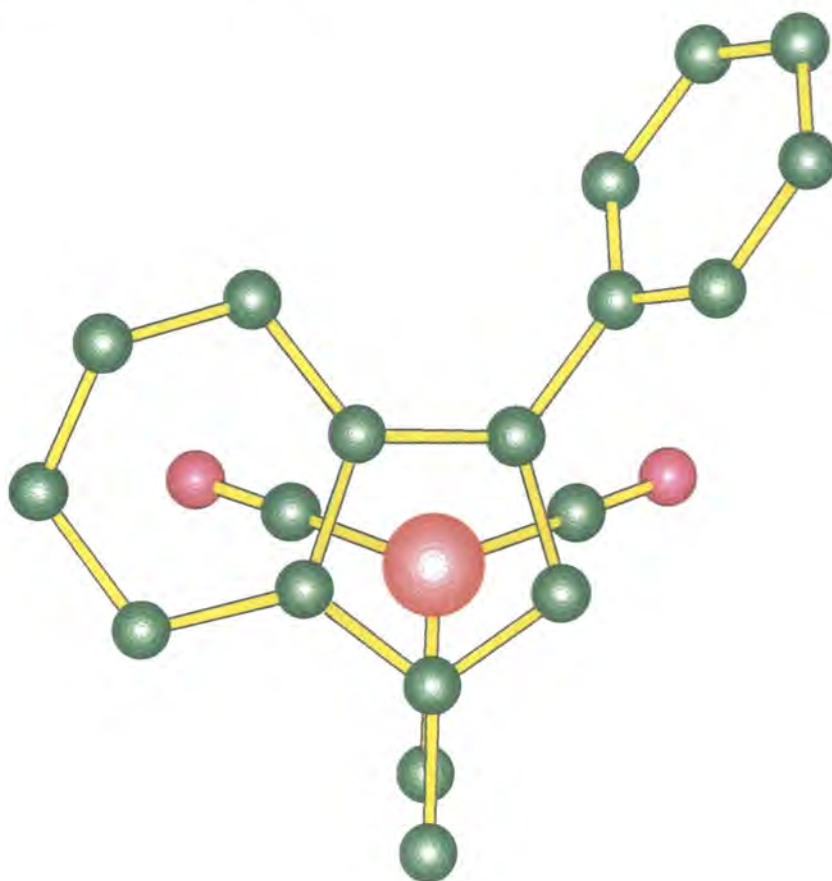


Fig. 2.31 View of **2.5** showing the eclipsed methyl groups.

The apparently greater steric pressure in **2.5**, compared with that in **2.3** or **2.4**, is also shown in the deviation of the substituents of the cyclopentadienyl ring away from the mean plane of the five membered ring. The deviations of the substituents and the ring carbons are tabulated in Table 2.10. No longer is the ring twisting of the phenyl group

sufficient to ease the steric burden of its environment; the deviation of the phenyl ring *ipso*-carbon relative to that of the methyl group carbon is no longer similar, as in **2.3**, or less, as in **2.4**, but much more. There is evidence of steric crowding in the molecule in the excessive puckering of C(4) of the cyclohexyl ring; the deviation of C(4) from the mean plane of the five-membered ring, 0.158 Å, is substantially greater than in both **2.3**, 0.013 Å, and **2.4**, 0.090 Å.

Carbon atom	Deviation from C ₅ -plane (Å)
1	0.004
2	0.009
3	0.010
4	0.158
5	0.039
6	0.742
7	0.130
8	-0.003
9	-0.008
10	0.096
11	0.188

Table 2.10 Carbon atom deviation from the mean plane of the cyclopentadienyl ring in **2.5**.

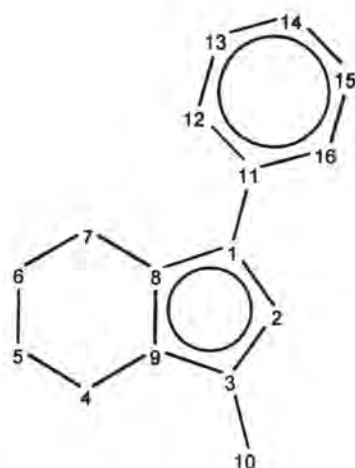


Fig. 2.32 Key to Table 2.10.

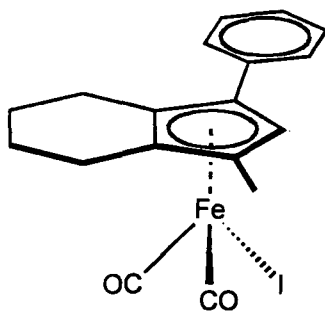
2.5.3 Summary.

The half-sandwich compound, **2.5** was synthesized, pure crystalline samples were difficult to prepare. Both the ^1H and ^{13}C NMR spectra have resonances at low frequencies, assigned to the methyl group bonded directly to the iron atom. The compound **2.5** crystallizes in the space group $P2_1/n$, which permits both stereoisomers to be in the same crystal. There are few similar structures to that of **2.5** on the Cambridge Structural Database, none of which were determined at low temperatures, unlike the molecular structure of **2.5**. The two methyl groups in **2.5** are forced into an unfavourable eclipsed conformation, presumably due to increased steric strain in the system, which is probably the same reason the dihedral angle between the planes of the phenyl and cyclopentadienyl rings in **2.5** is greater than in any of the other iron(II) compounds described in this chapter.

2.6 Further work.

2.6.1 Reaction of **2.4** with I_2 .

The synthesis of the iodide derivative, **2.6**, was attempted. Addition of iodine to cyclopentadienyl dicarbonyl iron dimers has been reported to yield the iodide of the monomer.¹ Various purification techniques were attempted (column chromatography, sublimation onto a liquid-nitrogen cooled probe, crystallization from polar and apolar solvents) to isolate a product from the addition of I_2 to **2.4**, with no success.



2.6

Solution state infra-red spectroscopy of the reaction mixture shows the disappearance of the four indicative carbonyl stretching bands for **2.4**, and the appearance of two bands at 2025 cm^{-1} and 1978 cm^{-1} (Fig. 2.33).

If **2.6** is present in solution and it is assumed that the tetrahydroindenyl ligand is rotating rapidly about the metal-ligand axis, the molecule has time averaged C_s symmetry and two bands would be expected, the A' symmetry and the A'' symmetry.

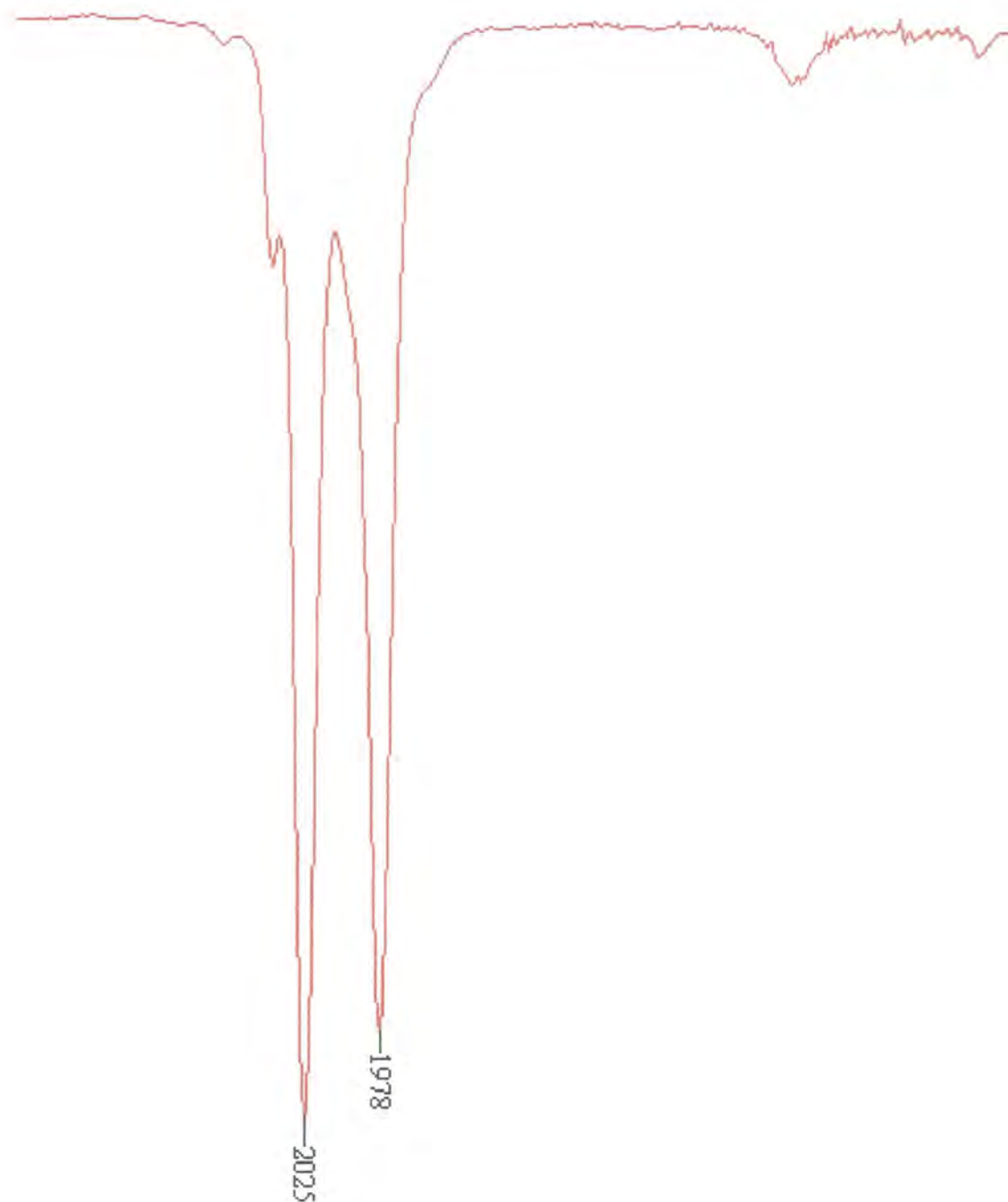
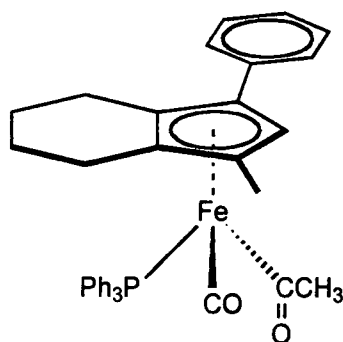


Fig. 2.33 Solution state infra-red spectrum of the product from the addition of I_2 to 2.4.

2.6.2 Reaction of 2.5 with PPh_3 .

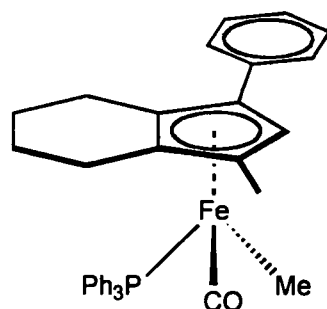
The reaction of 2.5 with PPh_3 was attempted. It was hoped that coordination of a phosphine ligand would cause insertion of a carbonyl into the iron-methyl bond to generate the acetyl complex, 2.7. This compound would have two stereogenic centres and exist as a mixture of two stereoisomers, the SS-/RR-isomer and the RS-/SR-isomer. The iron-methyl compound proved inert to phosphine coordination; NMR spectroscopic

analysis revealed predominantly **2.5** and PPh_3 after the reagents had been refluxed in THF for 48 h.



2.7

The ^1H NMR spectrum of the reaction mixture did show two very small doublets at $\delta = 4.67$ ppm ($J_{\text{H-P}} = 5.4$ Hz) and $\delta = 4.58$ ppm ($J_{\text{H-P}} = 5.4$ Hz), which may potentially be assigned to two CH protons on the cyclopentadienyl ring in two different environments to that of the CH proton in **2.5** (Fig. 2.34). Similar doublet resonances are observed in the region of the ^1H NMR spectrum assigned to the protons of a methyl group bonded directly to the iron, at $\delta = 0.58$ ppm ($J_{\text{H-P}} = 4.2$ Hz) and $\delta = 0.42$ ppm ($J_{\text{H-P}} = 6.2$ Hz), which may potentially be assigned to CH_3 protons on iron bonded methyl groups in two different environments to that of the iron bonded methyl group in **2.5**. If the resonances observed are due to the cyclopentadienyl ring CH protons and the iron bonded methyls of the two diastereoisomers of **2.7**, then the coupling would be due to the three-bond coupling between the phosphorus atom and the protons in both cases. This would suggest the presence of an alternative product to **2.7**, possibly that of **2.8**



2.8

STANDARD 1H OBSERVE
Run on Apr 23 98
Solvent: Benzene
Ambient temperature
File: /data/m29804/23090301

PULSE SEQUENCE: s2pu1
Pulse 61.2 degrees
Acq. time 2.992 sec
Width 6000.0 Hz
16 repetitions
OBSERVE H1, 199.9905580 MHz
DATA PROCESSING
Line broadening 0.3 Hz
FT size 65536
Total accumulation time 1 minute

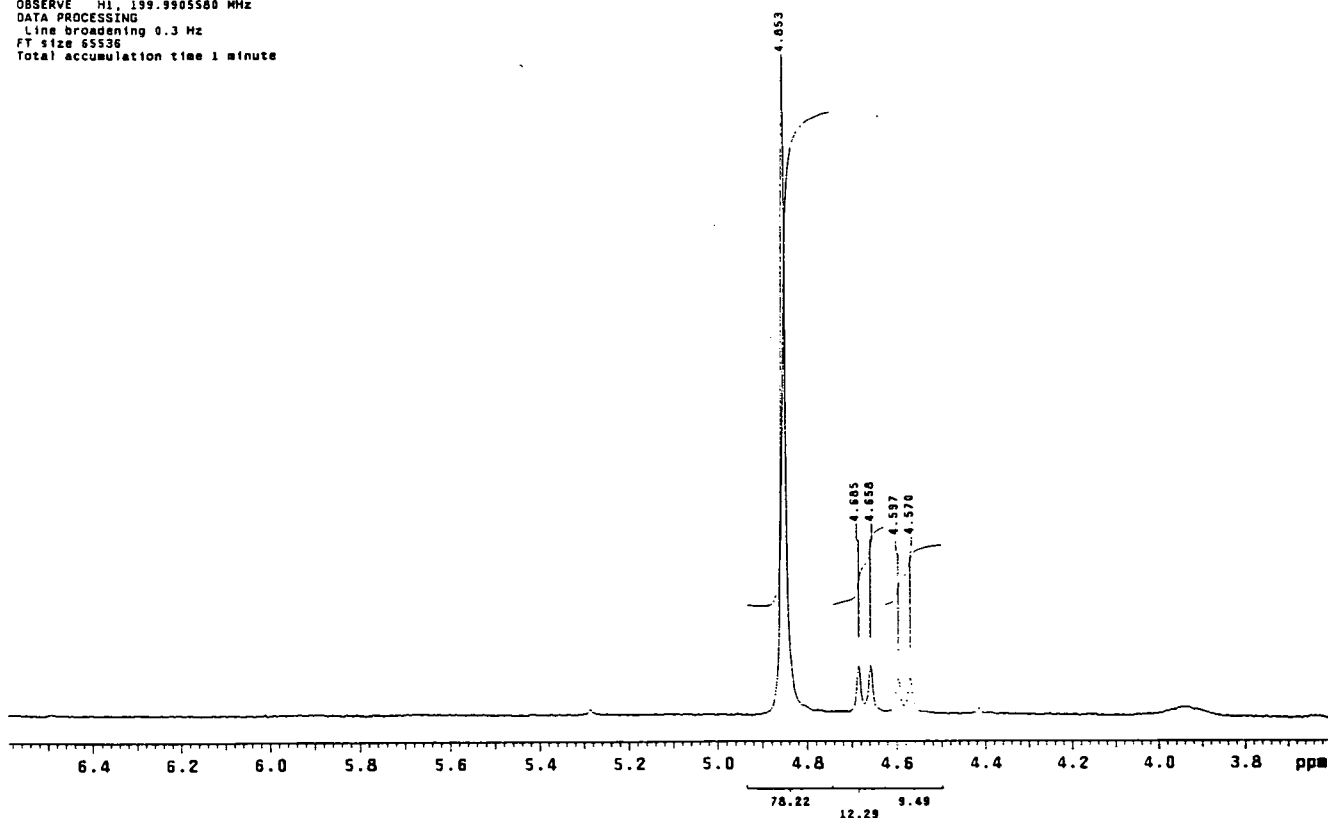
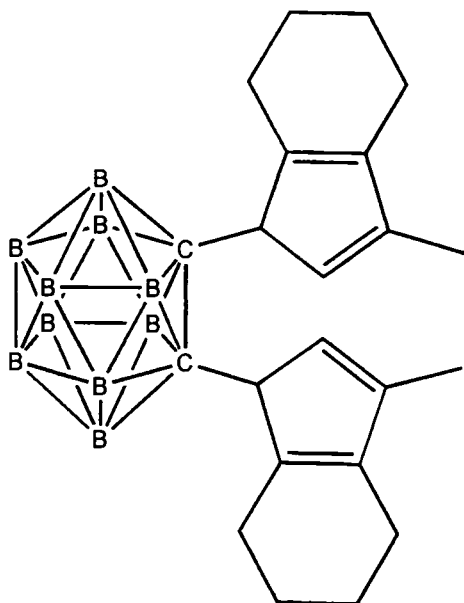


Fig. 2.34 Portion of ¹H NMR spectrum of product from the reaction of 2.5 with PPh₃.

2.6.3 The reaction of 1.12 with Li₂C₂B₁₀H₁₀.

The reaction of 1.12 with 1,2-Li₂C₂B₁₀H₁₀, dilithio-*ortho*-carborane, was attempted. It was hoped that, after aqueous acidic workup, the *ortho*-carborane linked bis-tetrahydroindenyl analogue of 2.1, compound 2.9, would be formed. NMR spectroscopic and GC-MS analysis of the post-workup reaction mixture indicated the presence of 1.12 and 1,2-C₂B₁₀H₁₂, *ortho*-carborane. 1,2-Li₂C₂B₁₀H₁₀ was used because the reaction might have resulted in a linked bis-tetrahydroindenyl system with a linker substantially more bulky and rigid than the ethano-linkers of systems such as Brintzinger's ethylene-bis(4,5,6,7-tetrahydroindene) discussed in chapter one, a desirable property in enantioselective reagents and/or catalysts. Another desirable property of the carborane reagent is that, relative to 1,2-dinucleophile derivatives of alky and aryl systems, which preferentially form alkynes and arynes respectively, it is a stable 1,2-dinucleophile.



2.9

Reactions of **1.12** with other nucleophile reagents, mostly as Grignards of alkyl and aryl species, have also been investigated in the hope of generating linked bis-tetrahydroindenyl systems, but with no success (a selection of nucleophile reagents investigated are in Fig. 2.35). The reason for this, as with the dilithio-*ortho*-carborane reaction, is probably the bulk of the tetrahydroindenone reagent, and the congestion formed at the carbon in the 1-position of the intermediate in the reaction. As might be expected in light of this, reactions of the lithium salt **2.1A** with dielectrophilic reagents has also met with little success (a selection of electrophilic reagents investigated are in Fig. 2.35).

2.7 Conclusions.

The tetrahydroindenone, **1.12**, is an easily prepared starting material for tetrahydroindenes like **2.1**. Substituents capable of extended conjugation out of the five-membered ring are not conducive to endocyclic double bond formation, as shown by the preparation of **2.2**.

The ferrocene **2.3** was prepared and the solid state structure of the *meso*-isomer was determined. Crystallizing in the space group $P2_1/c$, the molecular inversion centre and the crystallographic inversion centre are coincident. Cyclic voltammetric measurements have shown **2.3** to be more easily oxidized than $(\eta-C_5H_5)_2Fe$, as expected.

The dimer **2.4** was prepared, characterization was difficult by NMR spectroscopy. Infra-red spectroscopy revealed the presence of the *cis*- and *trans*-isomers in solution. Crystallizing in the space group $P2_1/c$, the molecular inversion centre of the *meso*-isomer was coincident with the crystallographic inversion centre. The dimer, **2.4**, has the longest centroid-iron distance of the iron(II) compounds discussed here.

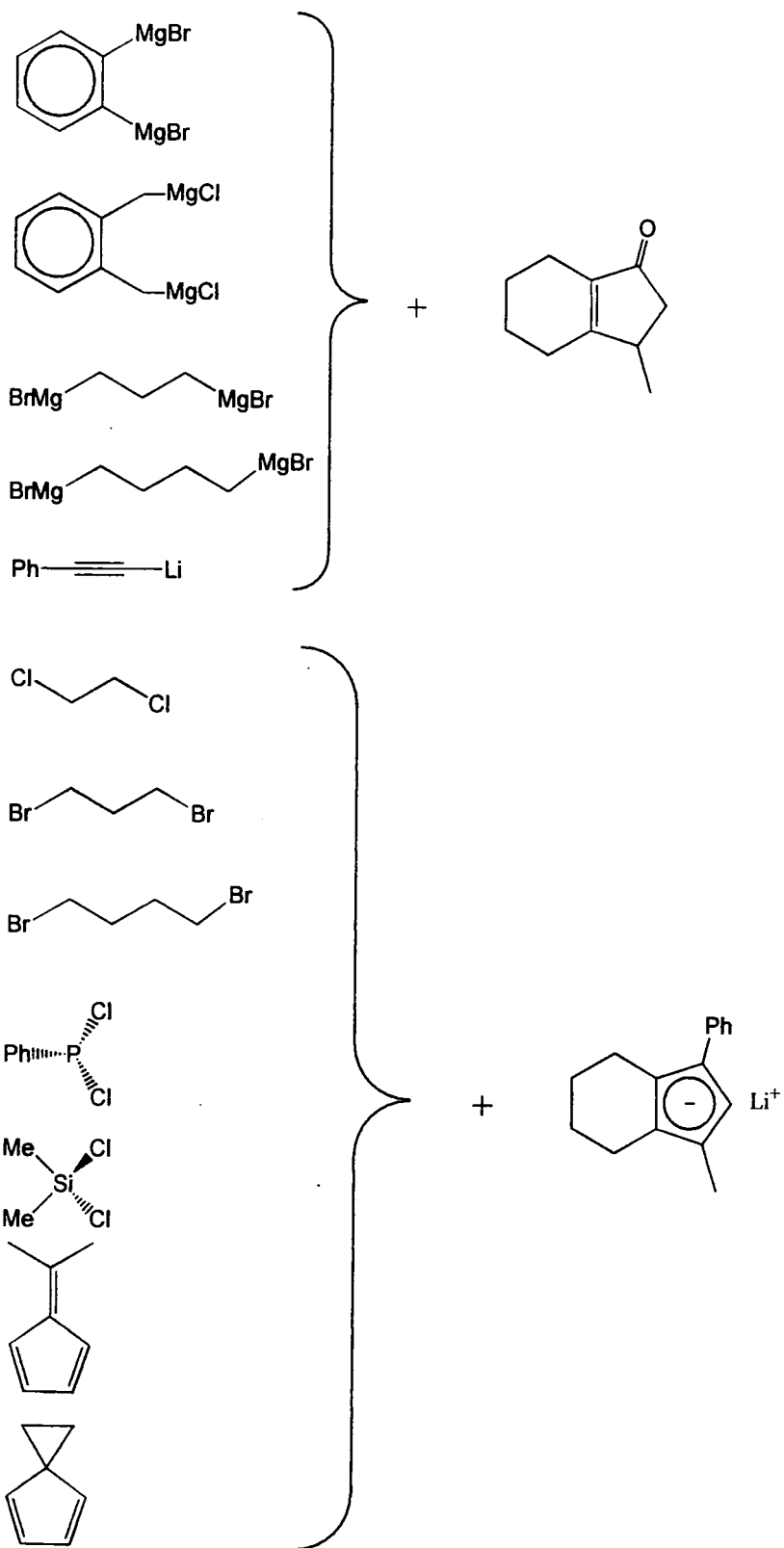
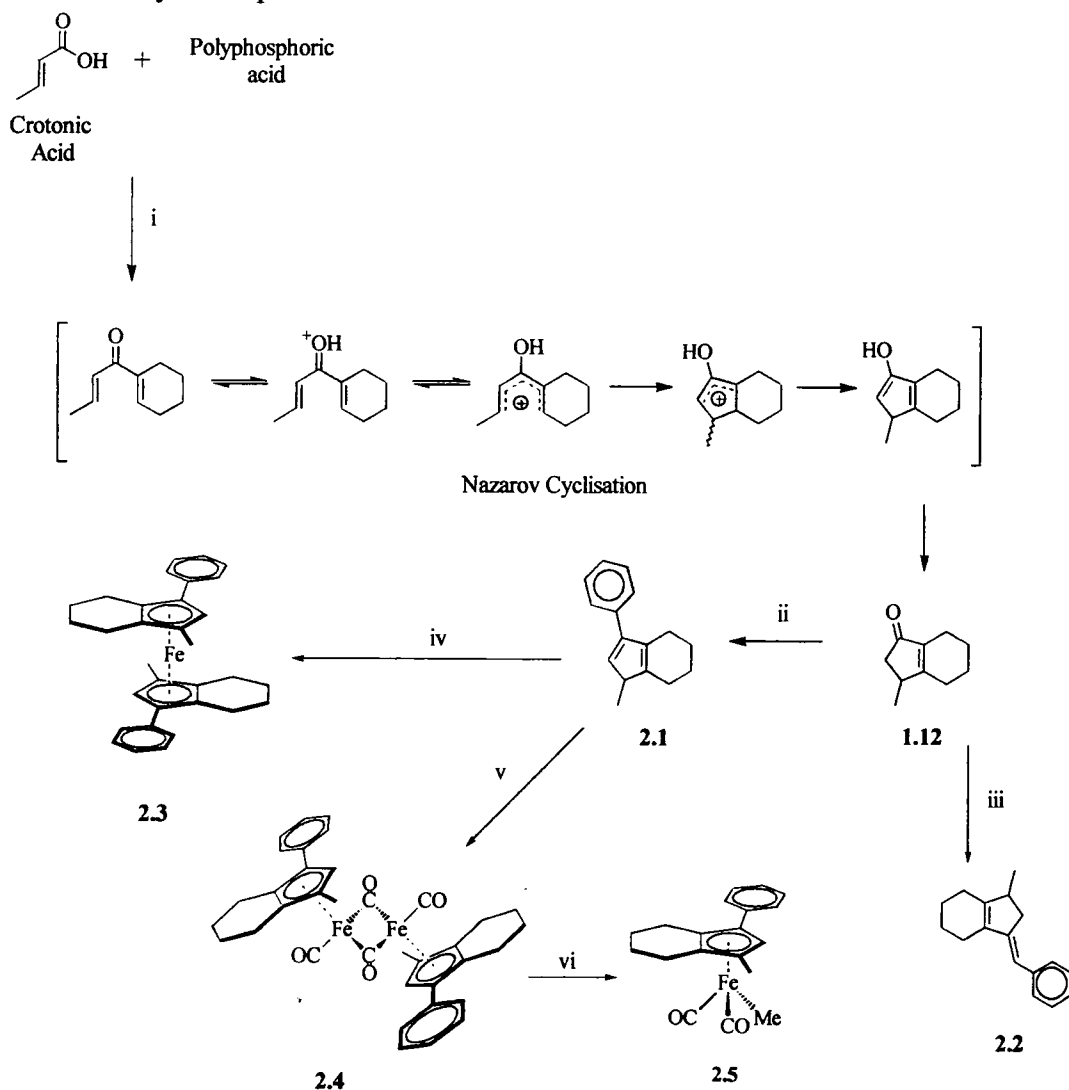


Fig. 2.35 Nucleophilic and electrophilic systems investigated as reagents in the synthesis of bis-tetrahydroindenyls.

The half-sandwich, iron methyl **2.5** was prepared, characterization was very straightforward. Determination of the solid state structure revealed one enantiomer present to be the R-isomer. Crystallizing in the space group $P2_1/n$, both enantiomers are present due to the presence of crystallographic inversion centres. The iron methyl, **2.5**, has the greatest phenyl ring-cyclopentadienyl ring dihedral angle of the iron compounds discussed here.

There are no reported compounds in the literature analogous to the compounds in this chapter with alkyl and aryl substituents on the cyclopentadienyl rings.

The chemistry of chapter two is summarized in Scheme 2.6.



Scheme 2.6 Summary of chemistry in chapter two.

(Reagents and conditions: i, cyclohexene, 60 °C; ii, PhMgBr, H₃O⁺; iii, PhCH₂MgBr, H₃O⁺; iv, BuLi, FeCl₂; v, Fe₂(CO)₉, toluene, reflux, 24 h; vi, sodium amalgam, CH₃I.)

2.8 References.

- 1 K. E. du Plooy, J. du Toit, D. C. Leventis and N. J. Coville, *J. Organomet. Chem.*, 1996, **508**, 231.
- 2 R. N. Austin, T. J. Clark, T. E. Dickson, C. M. Kilian, T. A. Nile, A. T. McPhail and D. J. Schabacker, *J. Organomet. Chem.*, 1995, **491**, 11.

- 3 K. L. Habermas, S. E. Denmark and T. K. Jones, *Organic reactions*, 1994, **45**, 1.
- 4 D. W. Brown, A. J. Floyd and M. Sainsbury, *Organic Spectroscopy*, Wiley, 1988, ch. 3, pp. 44-45
- 5 G. Schlosser, G. Katsoulos and S. Takagishi, *Synlett*, 1990, 747.
- 6 W. Kemp, *NMR in Chemistry*, Macmillan, 1986, Ch. 4, p. 63.
- 7 R. S. Cahn, C. K. Ingold and V. Prelog, *Angew. Chem., Int. Ed. Engl.*, 1966, **5**, 385.
- 8 T. J. Kealy and P. L. Pauson, *Nature (London)*, 1951, **168**, 1039.
- 9 a) B. X. Wang, X. Y. Li and S. J. Dong, *J. Electroanal. Chem.*, 1997, **435**, 23;
 b) I. R. Butler, U. Griesbach, P. Zanello, M. Fontani, D. Hibbs, M. B. Hursthouse and K. L. M. A. Malik, *J. Organomet. Chem.*, 1998, **565**, 243;
 c) A. S. AbdElAziz, C. R. deDenus, M. J. Zaworotko and C. V. K. Sharma, *J. Chem. Soc., Chem. Commun.*, 1998, 265;
 d) P. Carty and S. White, *Polymers and Poly. Comp.*, 1998, **6**, 33;
 e) J. Katrlík, J. Svorc, M. Stredansky and S. Miertus, *Biosensors and Bioelectronics*, 1998, **13**, 181;
 f) P. J. Swarts, M. Immelman, G. J. Lamprecht, S. E. Greyling and J. C. Swarts, *South African J. Chem.*, 1997, **50**, 208;
 g) I. H. Hall, A. E. Warren, C. C. Lee, M. D. Wasczacak and L. G. Sneddon, *Anticancer Research*, 1998, **18**, 951;
 h) T. Seshadri and H. J. Haupt, *J. Materials Chem.*, 1998, **8**, 1345;
 i) J. M. Lloris, R. MartinezManez, T. Pardo, J. Soto and M. E. PadillaTosta, *J. Chem. Soc., Dalton Trans.*, 1998, 2635.
- 10 D. W. Brown, A. J. Floyd and M. Sainsbury, *Organic Spectroscopy*, Wiley, New York, 1988, Ch. 3, pp.38-39.
- 11 G. Wilkinson, *Comprehensive Organometallic Chemistry: the Synthesis, Structures and Reactions of Organometallic Compounds*, Pergamon, Oxford, 1982, vol. 4, p. 478
- 12 L.A. Paquette, M.R. Sivik, E.I. Bzowej and K.J. Stanton, *Organometallics*, 1995, **14**, 4865.
- 13 a) D. P. Freyberg, J. L. Robbins, K. N. Raymond, and J. C. Smart, *J. Am. Chem. Soc.*, 1973, **60**, 287;
 b) Y. T. Struchkov, V. G. Andrianov, T. N. Sal'nikova, I. R. Lyatifov and R. R. Materikova, *J. Organomet. Chem.*, 1973, **60**, 287.
- 14 T. S. Piper, F. A. Cotton and G. Wilkinson, *J. Inorg. Nucl. Chem.*, 1955, **1**, 165.
- 15 a) P. Wang and J. D. Atwood, *J. Am. Chem. Soc.*, 1992, **114**, 6424;
 b) K. E. du Plooy, J. du Toit, D. C. Levendis and N. J. Coville, *J. Organomet. Chem.*, 1996, **508**, 231.
- 16 a) S. Zhang and T. L. Brown, *J. Am. Chem. Soc.*, 1993, **115**, 1779;
 b) A. J. Dixon, M. W. George, C. Hughes, M. Poliakoff and J. J. Turner, *J. Am. Chem. Soc.*, 1992, **114**, 1719;
 c) J. P. Blaha, B. E. Bursten, J. C. Dewan, R. B. Frankel, C. L. Randolph, B. A. Wilson and M. S. Wrighton, *J. Am. Chem. Soc.*, 1985, **107**, 4561;

- d) J. V. Caspar and T. J. Meyer, *J. Am. Chem. Soc.*, 1980, **102**, 7795.
- 17 A. R. Manning, *J. Chem. Soc. A.*, 1969, 1319.
- 18 P. McArdle, L. O'Neill and D. Cunningham, *Organometallics*, 1997, **16**, 1335.
- 19 O. A. Gansow, A. R. Burke and W. D. Vernon, *J. Am. Chem. Soc.*, 1972, **94**, 2550.
- 20 a) J. R. Pugh and T. J. Meyer, *J. Am. Chem. Soc.*, 1992, **114**, 3784;
b) S. L. Scott, J. H. Espenson and Z. Zhu, *J. Am. Chem. Soc.*, 1993, **115**, 1789.
- 21 a) S. Zhang and T. L. Brown, *J. Am. Chem. Soc.*, 1993, **115**, 1779;
b) A. J. Dixon, M. W. George, C. Hughes, M. Poliakoff and J. J. Turner, *J. Am. Chem. Soc.*, 1992, **114**, 1719.
- 22 a) J. V. Caspar and T. J. Meyer, *J. Am. Chem. Soc.*, 1980, **102**, 7794;
b) I. Kuksis and M. C. Baird, *Organometallics*, 1996, **15**, 4755;
c) I. Kuksis, I. Kovács and M. C. Baird, *Organometallics*, 1996, **15**, 4991;
d) H. Sitzmann, T. Dezember, W. Kaim, F. Baumann, D. Stalke, J. Kärcher, E. Dormann, H. Winter, C. Wachter and M. Keleman, *Angew. Chem., Int. Ed. Engl.*, 1996, **35**, 2872.
- 23 a) R. F. Bryan and P. T. Greene, *J. Chem. Soc.*, 1970, 3064;
b) R. G. Teller and J. M. Williams, *Inorg. Chem.*, 1980, **19**, 2770.
- 24 C. H. Wei and L. F. Dahl, *J. Am. Chem. Soc.*, 1969, **91**, 1351.
- 25 A. Mitschler, B. Rees and M. S. Lehmann, *J. Am. Chem. Soc.*, 1978, **100**, 3390.
- 26 M. Benard, *Inorg. Chem.*, 1979, **18**, 2782.
- 27 a) R. Hoffmann, *J. Chem. Phys.*, 1963, **39**, 1397;
b) R. Hoffmann and W. N. Lipscomb, *J. Chem. Phys.*, 1962, **36**, 2179;
c) E. D. Jemmis, A. R. Pinhas and R. Hoffmann, *J. Am. Chem. Soc.*, 1980, **102**, 2576.
- 28 a) A. K. Hughes, K. L. Peat and K. Wade, *J. Chem. Soc., Dalton Trans.*, 1997, 2139;
b) A. K. Hughes, K. L. Peat and K. Wade, *J. Chem. Soc., Dalton Trans.*, 1996, 4639;
c) C. E. Housecroft, K. Wade and B. C. Smith, *J. Chem. Soc., Chem. Commun.*, 1978, 765.
- 29 a) N. J. Coville, K. E. du Plooy and W. Pickl, *Coord. Chem. Rev.*, 1992, **116**, 1;
b) K. E. du Plooy, C. F. Marais, L. Carlton, R. Hunter, J. C. A. Boeyens and N. J. Coville, *Inorg. Chem.*, 1989, **28**, 3855;
c) Y. Morimoto, K. Ando, M. Uno and S. Takahashi, *Chem. Lett.*, 1996, 887;
d) S. C. Case-Green, J. F. Costello, S. G. Davies, N. Heaton, C. J. R. Hedgecock, V. M. Humphreys, M. R. Metzler and J. C. Prime, *J. Chem. Soc., Perkin Trans.*, 1994, 933;
e) J. Y. Thépot, V. Guerschais, L. Toupet and C. Lapinte, *Organometallics*, 1993, **12**, 4843;
f) L. Liebeskind, M. E. Welker and R. Fengl, *J. Am. Chem. Soc.*, 1986, **108**, 6328.

- 30 L. Pope, P. Somerville, M. Laing, K. J. Hindson and J. R. Moss, *J. Organomet. Chem.*, 1976, **112**, 309.
- 31 T. Yu. Orlova, V. N. Setkina, V. G. Andrianov and Yu. T. Struchkov, *Izv. Akad. Nauk SSSR, Ser. Khim.*, 1986, 437.
- 32 J. K. Stille, C. Smith, O. P. Anderson and M. M. Miller, *Organometallics*, 1989, **8**, 1040.
- 33 K. H. Pannell, J. Cervantes, L. Parkanyi and F. Cervantes-Lee, *Organometallics*, 1990, **9**, 859.
- 34 M. E. Wright and V. W. Day, *J. Organomet. Chem.*, 1987, **329**, 43.

Chapter Three
Zirconium(IV) Complexes Incorporating the Ligand
1-Phenyl-3-Methyl-4,5,6,7-Tetrahydroindenyl.

3.1 Introduction.

An important series of metallocenes are the bent metallocenes of group 4. These are capable of binding two ligands in addition to the two cyclopentadienyl groups. In doing so the two cyclopentadienyls bend back away from the additional ligands; this bending rehybridizes the d_{z^2} , $d_{x^2-y^2}$ and d_{xy} orbitals so that they point out of the open side of the metallocene away from the rings and towards the additional ligands. As they only have four valence electrons, group 4 metals have a maximum oxidation state of M(IV) and can only bind two X ligands in addition to the two cyclopentadienyl groups, e.g. $(\eta\text{-C}_5\text{H}_5)_2\text{TiCl}_2$. This leaves the 16e metallocenes with an empty orbital, which gives them the ability to act as Lewis acids and the tendency to bind π -basic ligands.¹

In the field of Ziegler-Natta catalysis, group 4 metallocenes have proved to be useful olefin polymerization catalyst systems. The active species has been identified as the coordinatively unsaturated cationic $[(\eta\text{-C}_5\text{H}_5)_2\text{MR}]^+$ system which mimics the catalytic sites of surface-alkylated TiCl_3 of the classical Ziegler-Natta process. These cationic species can be obtained by using the metallocene dichlorides in the presence of methylaluminoxane (MAO) or via R^- abstraction of the dialkyl using CPh_3^+ and a non-coordinating anion.²

In this chapter the syntheses, characterization and structural properties of a bulky zirconocene dichloride and dimethyl are discussed. As with the bis-tetrahydroindenyl iron(II) complexes in chapter two, the bent metallocenes in this chapter have two stereogenic centres. They can, therefore, potentially form four isomers (the number of stereoisomers that a molecule possessing one or more stereogenic centres can form is equal to two to the power of the number of stereogenic centres). Two of the isomers are commonly referred to collectively as the *rac*-isomer; these are the RR- and the SS-forms, which are interconvertible via the operation of an intermolecular mirror plane. In the case of 2.3, 2.4 and the complexes discussed in this chapter, there are effectively only three isomers, the *meso*-isomer exists in a single form, the RS-form (the SR-form, the theoretical fourth isomer, is rendered equivalent by the intramolecular mirror plane present).

3.2 Bis (1-phenyl-3-methyl-4,5,6,7-tetrahydroindenyl) zirconium(IV) dichloride.

3.2.1 Introduction.

Initially prepared in 1962 by Samuel, $(\eta\text{-C}_5\text{H}_5)_2\text{ZrCl}_2$, is commonly used as a reagent in cyclization reactions for the synthesis of polycyclic compounds and has been observed to possess antitumour activity.^{3,4,5}

Dicyclopentadienyl metal halides are ideal starting materials for ligand exchange and redox reactions. Only the non-cyclopentadienyl ligands participate in the reactions and the major reaction types observed are: alkylations; reductions; exchange reactions with donor ligands.⁶

In this section the synthesis and characterization of a sterically hindered zirconocene dichloride with two stereogenic centres as well as some of its properties are discussed.

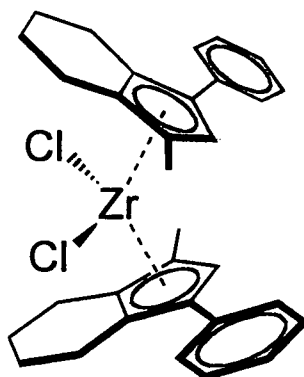
3.2.2 Discussion.

3.2.2a Synthesis.

The zirconocene dichloride, **3.1**, was prepared via the addition of freshly sublimed zirconium tetrachloride to lithium 1-phenyl-3-methyl-4,5,6,7-tetrahydroindenide, **2.1A**. Crystallization from toluene followed by recrystallization from dichloromethane gave yellow crystals of **3.1** in high yield (72%).

3.2.2b Characterization.

Characterization was by one-dimensional (1-D) ^1H and ^{13}C NMR spectroscopy, two-dimensional (2-D) ^1H - ^1H NMR correlation spectroscopy (COSY) and ^1H - ^{13}C NMR correlation spectroscopy (heteronuclear correlation, HETCOR), and CHN analysis. The crystals of **3.1** were of sufficient size and crystallinity for solid state structural analysis by single crystal X-ray diffraction.



3.1

As previously mentioned, three isomers of **3.1** are possible (Fig. 3.1). The enantiomers that collectively form the *rac*-isomer in these types of complexes are rarely discussed individually due to their indistinguishability via spectroscopic means.

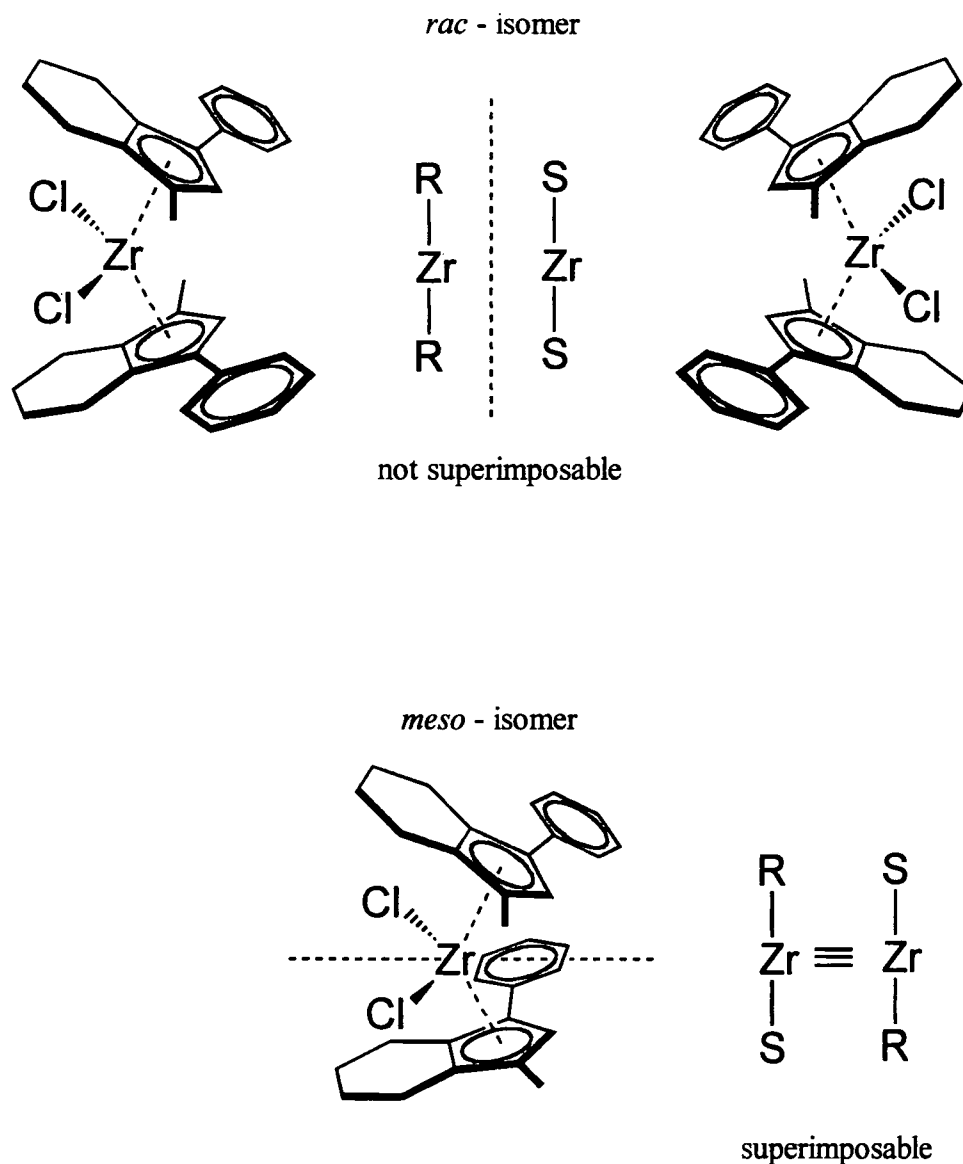


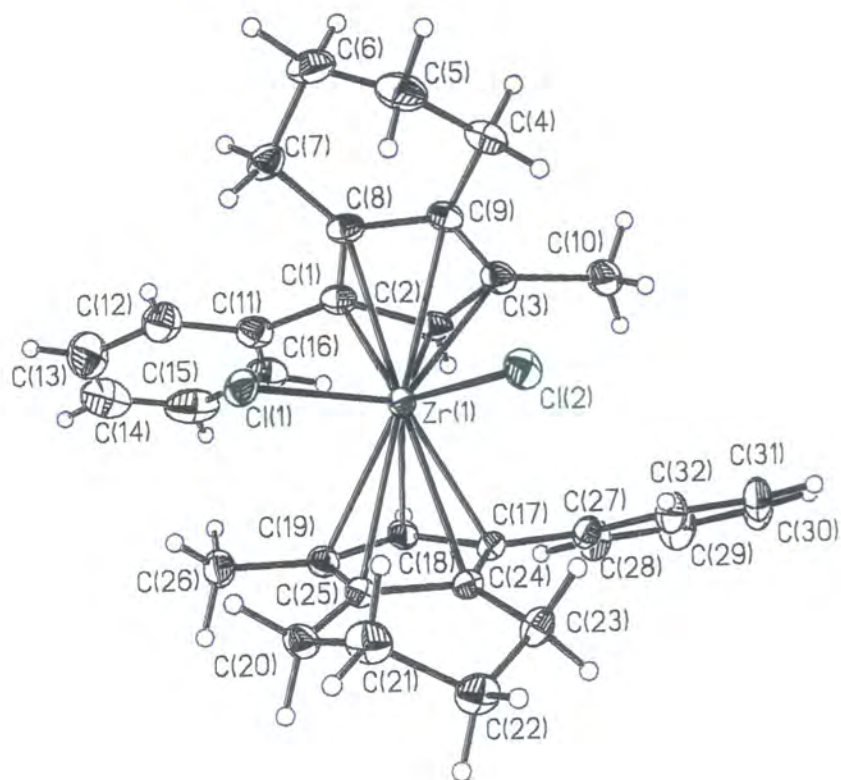
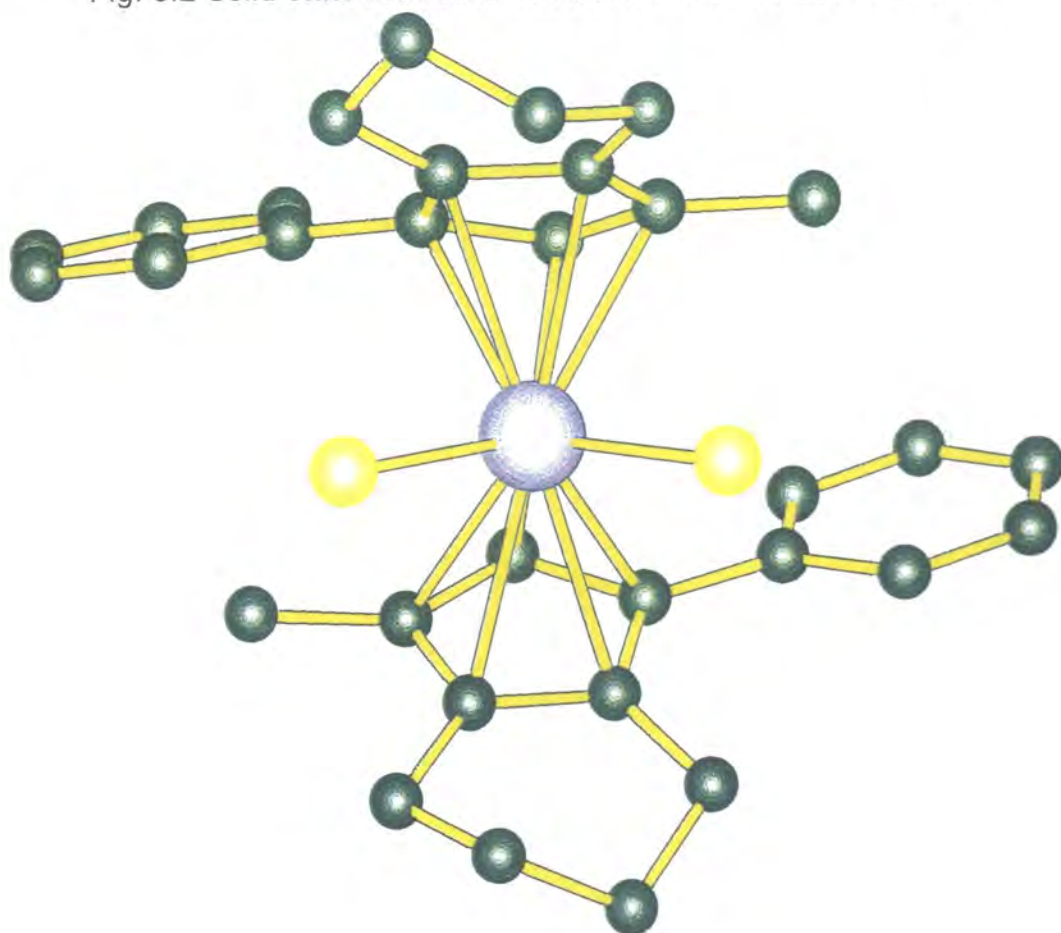
Fig 3.1 Stereoisomers of **3.1**.

3.2.2b(i) Single crystal X-ray diffraction molecular structure determination.

Upon data collection (21504 reflections collected, 6091 independent, 6088 used for structure solution) and solution (using the SHELXTL software suite) of the single crystal X-ray diffraction experiment, **3.1** was found to crystallize in the space group $P2_12_12_1$. As $P2_12_12_1$ possesses no symmetry elements capable of transforming a chiral centre in a R-configuration into a S-configuration, and *vice versa*, this means **3.1** is either present as a single enantiomer of the *rac*-isomer, or as the *meso*-isomer. In the cases of **2.3** and **2.4**, it was immediately apparent that the *meso*-isomer was present in both cases due to the coincidence of the iron atom, in **2.3**, and the midpoint of the iron-iron vector, in **2.4**, with a crystallographic inversion centre, thus generating the required molecular inversion centre of the *meso*-isomer. Unfortunately, the reverse is not true;

the absence of crystallographic inversion centres does not prohibit the presence of molecular inversion centres.

Fig. 3.2 Solid state molecular structure of the RR-isomer of 3.1.



Applying the conventions described earlier in assigning chiral configurations, it is immediately apparent that both tetrahydroindenyl rings have the same configuration, the R-configuration. There are no metal-ligand sites of S-configuration present in the crystal, due to the absence of inversion centres or mirror planes. Hence, only a single isomer of the *rac*-isomer is present, the RR-enantiomer (Fig. 3.2). This spontaneous resolution of enantiomers upon crystallization is not new, the most famous example of it is Pasteur's separation of the enantiomers of *rac*-tartaric acid⁷.

The physical morphologies of the crystals obtained were identical, rendering "crystal picking", to obtain the solid state structure of the other SS-enantiomer, futile.

Various data can be extracted from the molecular structure obtained for **3.1**; a selection is tabulated in Table 3.1, along with comparative data for $(\eta\text{-C}_5\text{H}_5)_2\text{ZrCl}_2$, **3.a** (Fig. 3.3), and the *rac*-isomer of bis(1-cyclohexyltetrahydroindenyl) zirconium dichloride, **3.b** (Fig. 3.4).⁸

There is a definite trend in Zr-centroid distances; this is probably due to sterics, with the relatively small $(\eta\text{-C}_5\text{H}_5)$ ring in **3.a** being able to get closer to the Zr than the cyclohexyl-substituted tetrahydroindenyl in **3.b**, which in turn can get closer than the relatively big tetrahydroindenyl ring in **3.1**. The centroid-Zr-centroid angle is smallest for **3.a** and largest for **3.1**, this is probably due to the inability of the tetrahydroindenyl rings in **3.1**, and to a lesser extent in **3.b**, to fit as closely together in space as the $(\eta\text{-C}_5\text{H}_5)$ rings in **3.a**. These angles are typical for non-bridged Group 4 metallocenes, the angle is larger than that observed in **3.1** by *ca.* 4° for ethylene-bridged *ansa*-metallocenes.⁹ The average C(ring)-C(ring) distance is curiously longer in **3.1** than in **3.a**. Corey and co-workers report the short C(ring)-C(ring) distances in **3.a** as being due to large anisotropic displacement parameters of the ring C atoms, this is commonly observed the $(\eta\text{-C}_5\text{H}_5)$ ligand, and can be seen in **2.g**, $[(\eta\text{-C}_5\text{H}_5)\text{Fe}(\text{CO})_2]_2$, in chapter two.^{7a} Substituting the cyclopentadienyl ring holds the carbons of the ring more rigidly in place, reducing the anisotropic displacement parameters and allowing more precise C(ring)-C(ring) distances to be determined.

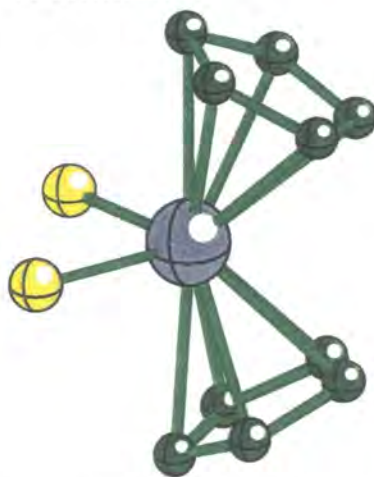


Fig. 3.3 Solid state molecular structure of $(\eta\text{-C}_5\text{H}_5)_2\text{ZrCl}_2$.

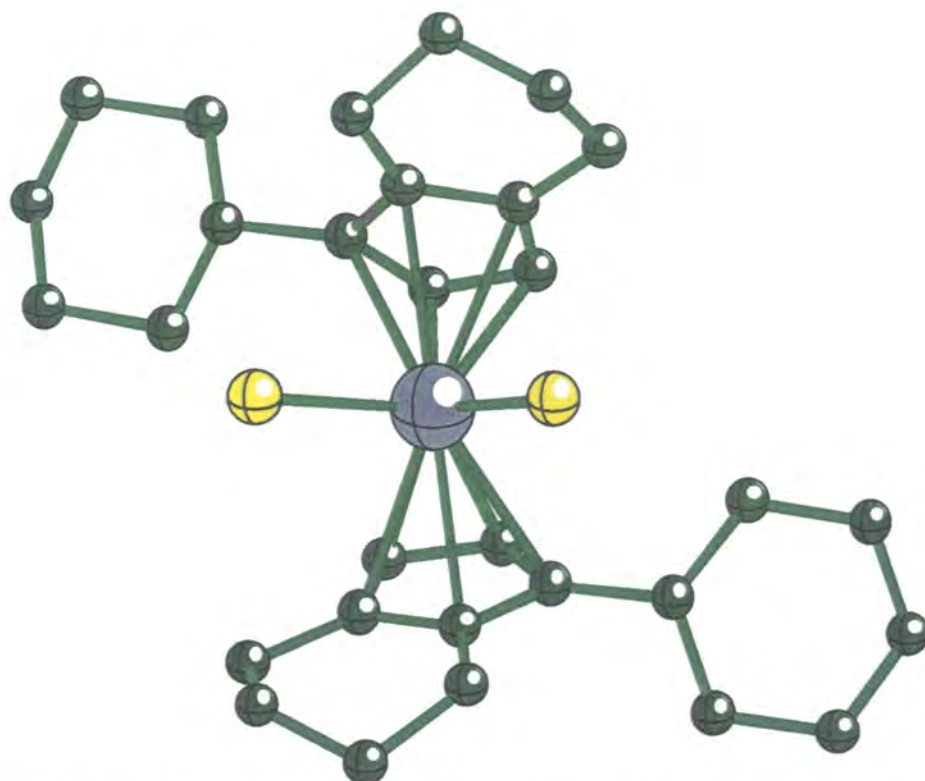


Fig. 3.4 Solid state molecular structure of the R,R-isomer of *rac*-bis(1-cyclohexyltetrahydroindenyl) zirconium dichloride

Distance (Å) or Angle (°)	3.1	3.a	3.b
Zr-Cl(1)	2.4470 (5)	2.444(1)	2.443(1)
Zr-Cl(2)	2.4477 (5)	2.450(1)	2.443(1)
Zr-Centroid(1)	2.250	2.200	2.228
Zr-Centroid(2)	2.237	2.201	2.228
Average C(ring)-C(ring), [Range]	1.424(3) [1.406(3) - 1.442(3)]	1.383(7) [1.325 - 1.408]	Data not provided
Average C(ring)-C(alkyl-substituent), [Range]	1.505(3) [1.497(3) - 1.513(3)]	-	1.506(3)
Cl(1)-Zr-Cl(2)	97.78(2)	97.0(1)	95.8(1)
Centroid(1)-Zr-Centroid(2)	131.8	129.5	130.8

Table 3.1 Selected data extracted from the molecular structure of **3.1** and comparative data for **3.a** and **3.b**.

The cyclopentadienyl ring is not perfectly planar and has the following deviations from the mean plane (Å): C(1) -0.011; C(2) 0.006; C(3) 0.002; C(8) 0.012; C(9) -0.009. The steric bulk of the substituents causes the carbons of the methyl group, the phenyl group and cyclohexyl ring adjacent to the five membered ring to deviate away from the mean plane of the cyclopentadienyl ring away from the zirconium. The cyclohexyl ring is

puckered with an average for the C-C bond distances of 1.526 (4) Å and with the following deviations from the mean cyclopentadienyl plane (Å, positive deviation indicates deviation away from the zirconium atom): C(4) 0.098; C(5) -0.153; C(6) 0.649; C(7) 0.187. The *ipso*-carbon of the phenyl group and the carbon of the methyl group deviate by 0.043 Å and 0.133 Å from the mean plane of the cyclopentadienyl ring respectively. Carbon atom deviations from the mean plane of the cyclopentadienyl ring in **3.1** are summarized in Table 3.2, along with comparative values for the ferrocene **2.3**.

Carbon atom	Deviation from C ₅ -plane (Å)	
	3.1	2.3
1 (ring C)	-0.011	-0.006
2 (ring C)	0.006	0.004
3 (ring C)	0.002	0.000
8 (ring C)	0.012	0.006
9 (ring C)	-0.009	-0.004
4 (C9-CH ₂)	0.098	0.013
7 (C8-CH ₂)	0.187	0.143
10 (methyl C)	0.133	0.076
11 (<i>ipso</i> -phenyl C)	0.043	0.082

Table 3.2 Carbon atom deviation from the mean plane of the cyclopentadienyl ring in **3.1** and **2.3**.

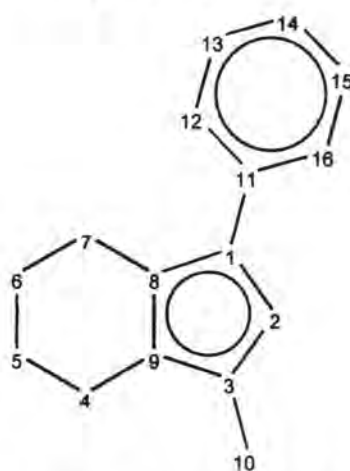


Fig. 3.5 Key to Table 3.2.

The dihedral angle between the phenyl ring and the cyclopentadienyl ring is 15.9°, effectively identical to that for **2.3**, 15.1°, as are the C(ring)-C(phenyl) bond distances, 1.478(3) in **3.1** and 1.474(7) in **2.3**. However, the structure determined for **3.1** is the *rac*-isomer whereas the structure for **2.3** is the *meso*-isomer. As described in chapter two, the *meso*-configuration of a bis-tetrahydroindenyl system can adopt a distal

configuration due to its centrosymmetric nature, allowing the bulky substituents to be as far away as possible from each other. This is not true in the case of the *rac*-isomer of **3.1**, as shown in Fig. 3.6, the tetrahydroindenyl ligands do not adopt a distal configuration, rather the bulky cyclohexyl groups of both ligands are directed in the same direction, and the phenyl groups nearly eclipse the methyl groups.

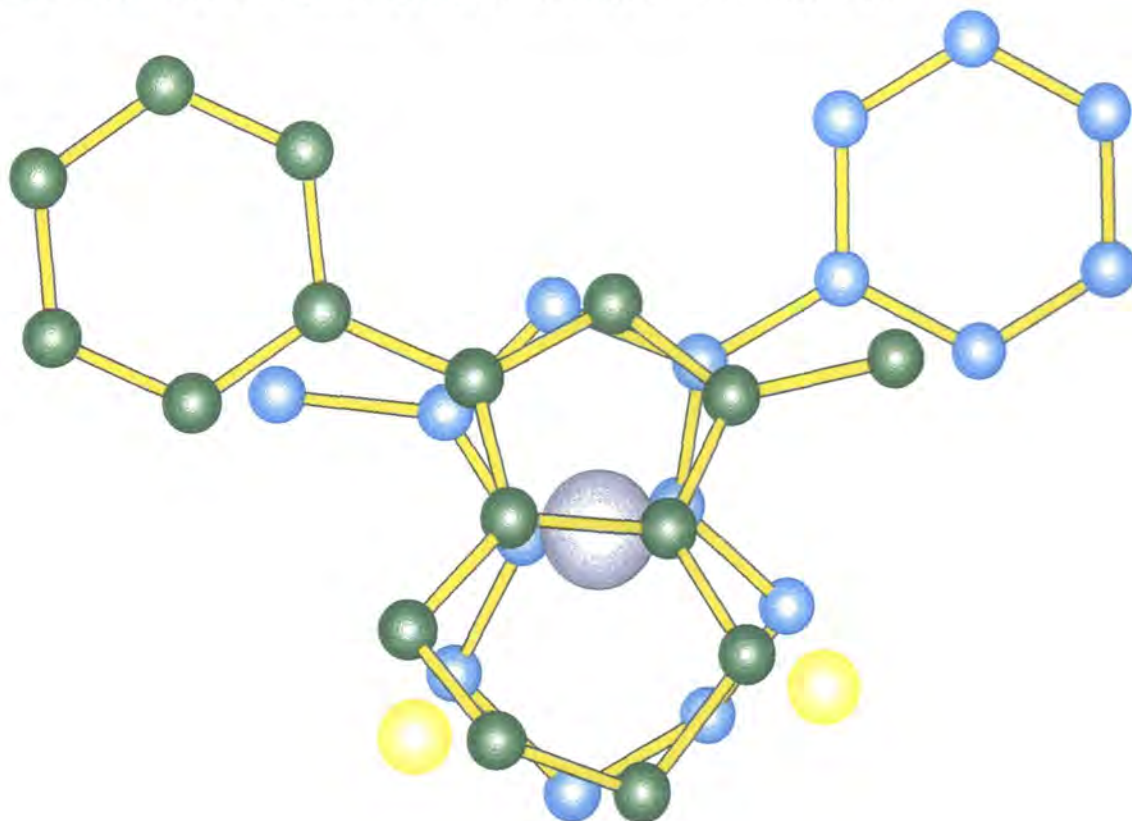


Fig. 3.6 View of molecular structure of **3.1** along centroid-centroid axis.

(Bonds to the zirconium have been removed for clarity).

The increased strain of this configuration is obvious from the greater deviations from the mean plane of the cyclopentadienyl ring in **3.1** for the alkyl substituents of the cyclopentadienyl ring, compared with those in **2.3**. The behaviour of the phenyl ring is strange, it twists the same amount in **3.1** as in **2.3**, the bond lengths are the same, yet the rest of the molecule appears strained whilst the deviation of the *ipso*-carbon of the phenyl ring from the cyclopentadienyl ring mean plane in **3.1** is half of that in **2.3**. One possible explanation may be that in this configuration the phenyl ring can rotate "around" the methyl group in the other ligand which it is almost eclipsing, "into" the space generated by the CH group of the opposite ligand. In the distal configuration of **2.3** whichever way the phenyl ring rotated, it either interacted with the methyl group or the cyclohexyl group of the opposite ligand. If this is true, in **3.1** the presence of a "gap" means greater steric strain is relieved for smaller ring rotation, allowing the two π -clouds of the ligand to maintain efficient overlap. This conjugation is probably of even more importance in **3.1** than in the iron compounds of chapter two, due to greater electron

density donation from the cyclopentadienyl ring to the electron deficient 16-electron zirconium centre. The conjugation with the phenyl ring can possibly be thought of as "topping-up" the electron density in the π -system of the cyclopentadienyl ring. It is interesting to note that, in the structure of **3.b**, where the isomer is also the *rac*-isomer and the substituent present is a cyclohexyl ring on the 1-carbon, incapable of π -conjugation with the cyclopentadienyl ring, the dihedral angle between the mean planes of the cyclopentadienyl ring and the substituent is almost 90° (Fig. 3.7).

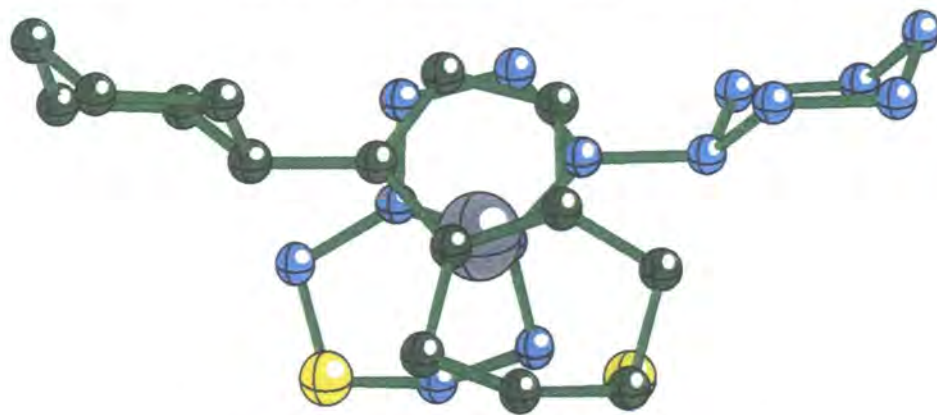


Fig. 3.7 Cyclohexyl substituent ring twist in **3.b**.

As the structures of **3.1** and **3.b** are, in other respects very similar, this enhances the argument for increased strain on the ligands in the *rac*-isomer of **3.1** compared with that on the ligands in the *meso*-configuration seen for **2.3**, and the probability that in some manner the apparently insufficient phenyl ring twist in **3.1** is due to interactions between the cyclopentadienyl ring and the phenyl ring, namely conjugation between the adjacent π -clouds.

Comparisons between **3.1** and **2.3** can only be taken so far as the systems have different structures, different metal centres, are different stereoisomers, and are generally very different environments for the ligand. It is with these considerations in mind that the earlier discussions must be held.

3.2.2b(ii) Nuclear magnetic resonance spectroscopy.

The ^1H NMR spectrum of the crude reaction mixture shows two sharp resonances at $\delta = 6.32$ ppm and 5.88 ppm, which are assigned to the CH hydrogens of the five membered rings in the *rac*- and *meso*-isomers. The NMR spectra of the recrystallized product indicates the presence of the *rac*-isomer alone, as ascertained by single crystal X-ray diffraction structural analysis. Attempts to fractionally recrystallize the isomers led to either the *rac*-isomer alone or a mixture of the two isomers.

Using the ^1H - ^1H COSY and ^{13}C - ^1H HETCOR 2-D spectra of the *rac*-isomer of **3.1** (Fig. 3.8 and Fig. 3.9 respectively), the ^1H and ^{13}C NMR spectra of the *rac*-isomer of **3.1** were readily assigned. Selected ^{13}C NMR spectra assignments are tabulated in Table 3.3 along with comparative assignments for the ferrocene **2.3**.

Fig 3.8 ^1H - ^1H COSY spectrum of 3.1.

0001

P4 PULSE SEQUENCE: COSY
TE 02-09-96
SOLVENT CDCl3
P4 LE COSY

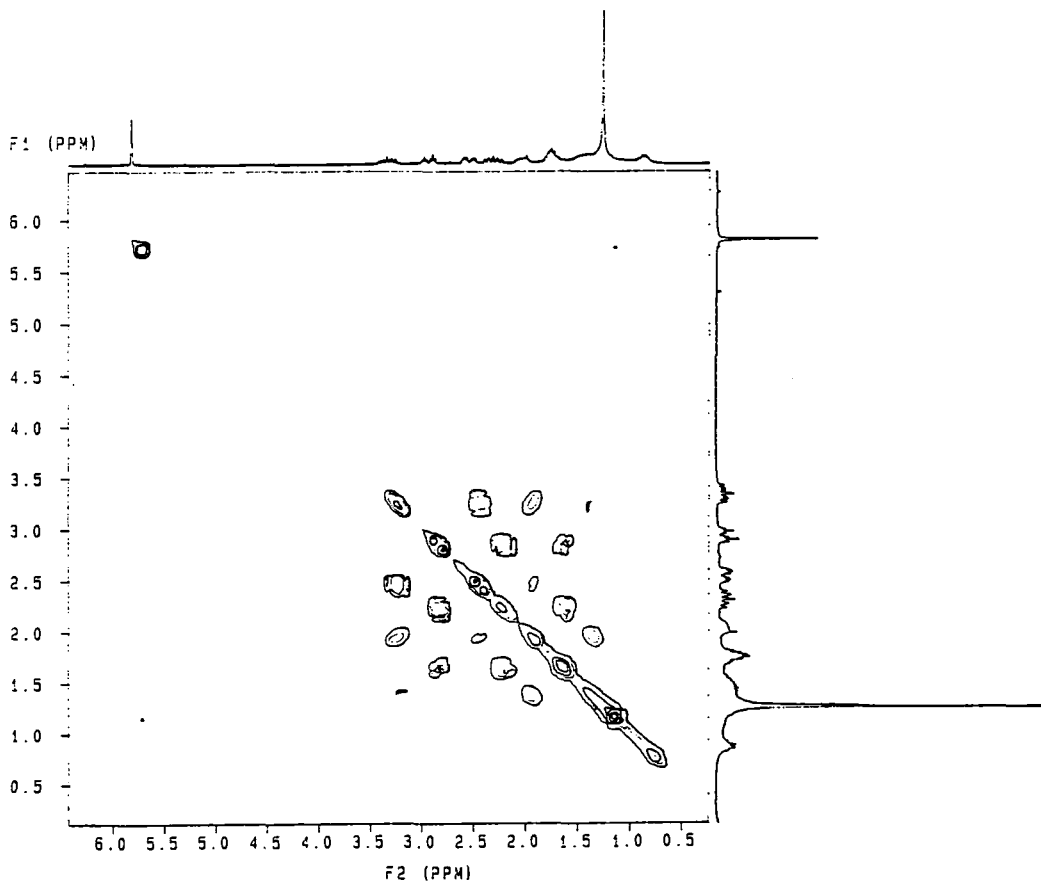
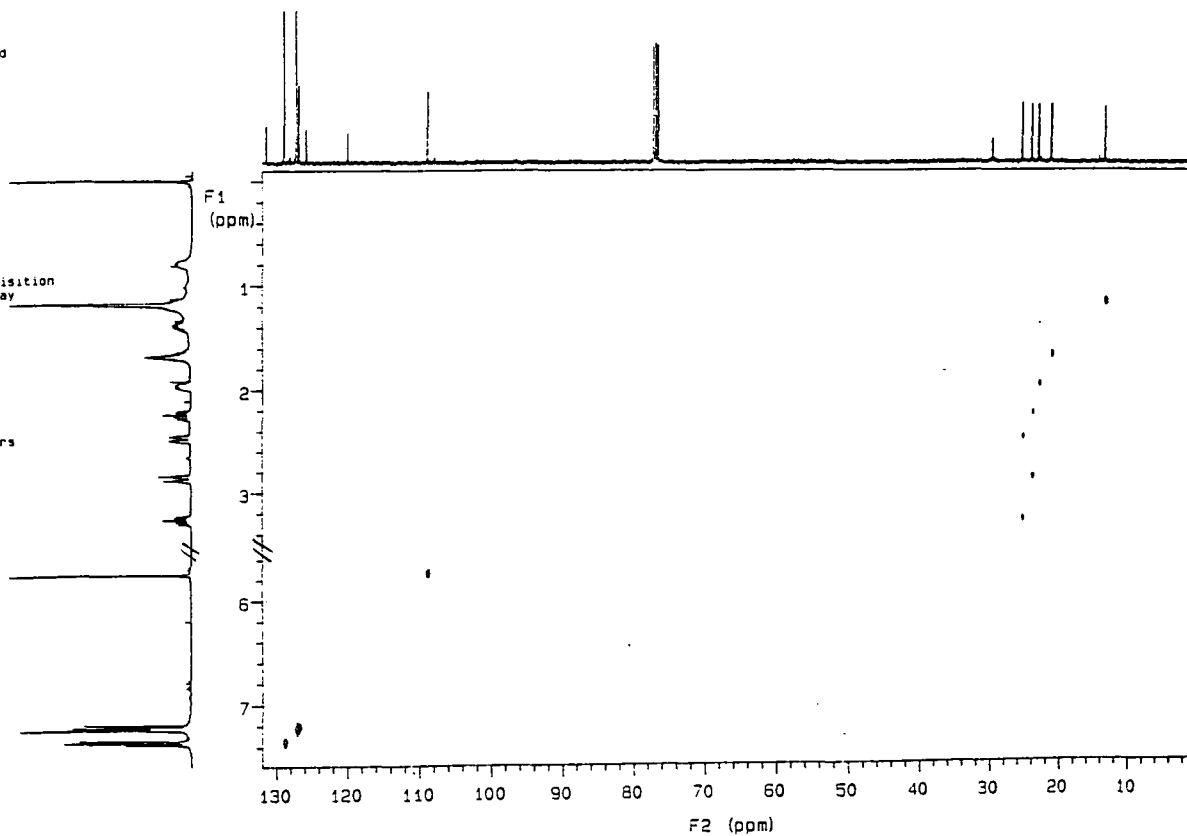


Fig. 3.9 ^{13}C - ^1H HETCOR spectrum of 3.1.

BMB 051
FILE /data/curdat/bmb26seppc.fid
RUN ON Sep 25 97
SOLVENT CDCl3
Pulse sequence xncord
OBSERVE C13
Frequency 100.576 MHz
Spectral width 14445.6 Hz
2D Spectral width 3099.8 Hz
Acquisition time 0.071 sec
Relaxation delay 1.000 sec
Pulse width 15.5 usec
Ambient temperature
No. repetitions 128
No. increments 256
DECOUPLE H1
High power 40
Decoupler gated on during acquisition
Decoupler gated off during delay
Double precision acquisition
DATA PROCESSING
Sine bell squared 0.053 sec
Shifted by -0.025 sec
FT size 2048
F1 DATA PROCESSING
Sine bell square 0.062 sec
Shifted by -0.041 sec
FT size 1024
Total acquisition time 10.5 hours



Chemical shift, δ (ppm)		Assignment
3.1	2.3	
13.3	11.2	CH ₃
21.2 - 25.4	21.9 - 24.7	CH ₂
108.9	70.3	C(Cp)-H
119.9 - 134.1	81.3 - 86.2	quat. C

Table 3.3 Selected ¹³C NMR spectra data for 3.1 and 2.3.

The chemical shifts, δ , are at higher frequencies in 3.1 than in 2.3, with the effect being more noticeable for nuclei closer to the metal.

There are several obvious differences between 3.1 and 2.3 which could all cause, either individually or in combination, the observed variations in chemical shift. These include, amongst others, the different sizes of the two metals, their different electropositivities, the different structures of the two metallocenes, the presence of extra ligands in 3.1, and the 16-electron nature of the zirconium centre as opposed to the 18-electron nature of the iron centre (although this may be partially compensated by the chlorine ligands behaving as partial π -donors).

Literature discussions concentrate mainly on the difference in ¹³C NMR chemical shifts between metal-complexed and free organic species or electronic shielding of the transition metal nuclei.^{10,11} Where the different chemical shifts of identical ligands in different complexation environments are discussed, arguments usually resort to generalisations about electronic shielding of the nuclei in question. Shielding, as will be discussed here, consists of several components, each potentially affected by various parameters of organometallic molecules; inconsistencies and variations from apparently proven trends, which have been associated with one particular shielding component, in ¹³C NMR chemical shifts are usually explained as being due to an unknown/additional parameter affecting another shielding component or the same component in the same way. This is clearly not satisfactory, but the large number of factors that influence chemical shifts combined with the wide variation in organometallic compounds studied by ¹³C NMR spectroscopy, may render it impossible to quantitatively relate changes on going from one organometallic molecule to another with ¹³C NMR chemical shifts.

The brief discussion here will concentrate on the possible effects of some of the differences between 3.1 and 2.3 on the shielding (σ) of the carbon nuclei in the tetrahydroindenyl ligands. It is important to remember that this does not exhaustively examine all of the differences between the two systems, but simply suggests a possible reason for the different chemical shifts. The discussion also suffers from the obvious disadvantage of only considering two systems, it does, however, highlight an important

difference between the two systems which is directly related to a parameter in one of the components of the shielding of the carbon nuclei.

The chemical shift (δ) is related to the shielding constant (σ) by

$$\delta = 10^6(\sigma_{\text{ref}} - \sigma)$$

where σ_{ref} is that for tetramethyl silane (TMS), which is quite strongly shielded (large σ) resulting in most ^{13}C NMR chemical shifts being positive ($\delta > 0$). It is important to note, therefore, that, by convention, chemical shifts (δ) and shielding (σ) have different signs.

The overall shielding of a carbon nucleus, i , consists of several components, the two major components are the diamagnetic shielding term, σ_i^{diam} , and the paramagnetic shielding term, σ_i^{para} . Although there are smaller shielding terms which may be considered in certain systems, the total shielding can effectively be thought of as the sum of the diamagnetic and paramagnetic terms.

$$\sigma = \sigma_i^{\text{diam}} + \sigma_i^{\text{para}}$$

The diamagnetic term involves the free rotation of electrons about the nucleus in question and the paramagnetic term describes the hindrance to this rotation caused by the other electrons and nuclei in the molecule. The total shielding is positive if the diamagnetic contribution dominates and is negative if the paramagnetic contribution dominates.

The diamagnetic shielding term is approximately proportional to the electron density of the atom. It follows that the shielding is greater if the electron density on the atom is increased as a result of the influence of an electropositive atom nearby. However, this cannot be the factor causing the differences in chemical shifts between 3.1 and 2.3, as iron is less electropositive than zirconium. The more electropositive zirconium would cause an increase in the shielding constant which would give chemical shifts at lower frequencies, not higher as observed. Therefore the chemical shift change must be due to something else, one possibility lies in the effect on the paramagnetic shielding term upon bending of a metallocene and coordination of extra ligands.

The paramagnetic shielding term may be evaluated as follows,

$$\sigma_i^{\text{para}} = -\left\{ \left[\frac{\mu_0 \mu_B}{2\pi} \right] (r^{-3})_{np} \left[(Q_i + \sum_{r,j} Q_j) / \Delta E \right] \right\} \quad \text{Eqn 3.1}$$

μ_0 = permeability (vacuum)

μ_B = Bohr magneton

where r is the mean radius of the $2p$ orbital of carbon i , Q_i is the electron density at carbon i , Q_j is the bond order between atoms i and j , and ΔE is the mean electronic excitation energy for the molecule (usually approximated to the energy gap between the HOMO and LUMO of the molecule).¹²

Due to the minus sign at the start of Eqn 3.1, an increase in Q_i , Q_j or a decrease in ΔE , results in a decrease in σ_i^{para} .

Lauher and Hoffmann have shown how the energy gap between HOMO and LUMO orbitals in a bent transition-metalocene fragment decreases dramatically as a function of dihedral angle between the rings, due to orbital rehybridization upon bending. This means that, after some small rehybridization upon coordination of two X ligands, the frontier orbitals are closer in Cp_2MX_2 , e.g. **3.1**, than Cp_2M , e.g. **2.3**, resulting in a lower mean electronic excitation energy. A lower ΔE results in a more negative σ_i^{para} , which in turn causes the overall shielding to be smaller, leading to higher chemical shifts.

One potential flaw in this argument is that the value ΔE is usually applied to all carbons in the molecule, so the effect of decreasing it should be seen equally in all carbons, but it is not. However, the concept of a mean electronic excitation energy is usually applied to simpler organic molecules, where all or nearly all carbon atomic orbitals play a significant role in the formation of the molecular orbital set that forms the frontier orbitals. In the case of **3.1** and **2.3**, atomic orbitals of carbons like the CH_2 carbons of the cyclohexyl ring play less role in the makeup of the frontier orbital set of the whole molecule than those of the cyclopentadienyl ring carbons. It is possible that the chemical shifts of carbons further from the metal have electronic excitation energies significantly different to that of the mean due to their atomic orbitals playing a less important role in the makeup of the molecular orbital set that form the frontier orbitals.

3.2.3 Summary.

The zirconocene dichloride, **3.1**, was prepared in high yield and characterized using both 1-D and 2-D NMR spectroscopy. Upon crystallization, the *rac*-isomer of **3.1** was shown to spontaneously resolve into separate crystals of the RR- and SS-forms, the structure of the RR-form was determined, and found to be in the space group $\text{P2}_1\text{2}_1\text{2}_1$ (which contains no symmetry elements capable of transforming a R-centre into a S-centre). The Zr-centroid distance was found to be longer than that in $(\eta\text{-C}_5\text{H}_5)_2\text{ZrCl}_2$. The cyclopentadienyl rings of the tetrahydroindenyl ligands in **3.1** form a nearly eclipsing configuration, with the cyclohexyl rings pointing in the same direction, out over the chlorine ligands. Comparisons have been made between the NMR spectroscopic data of **3.1** and the ferrocene **2.3**, a possible reason for similarities and differences has been proposed involving relative energies of the frontier orbital sets.

3.3 Bis (1-phenyl-3-methyl-4,5,6,7-tetrahydroindenyl) dimethyl zirconium(IV).

3.3.1 Introduction.

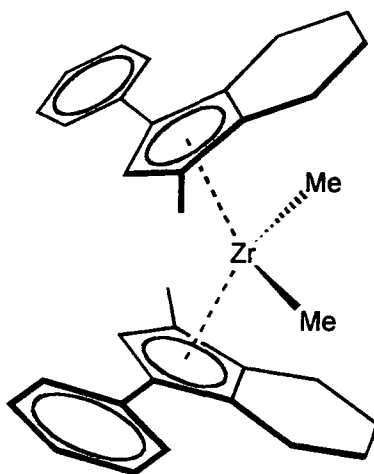
Used in the study of cocatalyst systems for metathesis reactions, $(\eta\text{-C}_5\text{H}_5)_2\text{ZrMe}_2$, was first prepared in 1973 by Samuel.¹³

In this section the synthesis and characterization of a sterically hindered dimethyl zirconocene with two stereogenic centres as well as some of its properties are discussed.

3.3.2 Discussion.

3.3.2a Synthesis.

The dimethyl zirconocene, **3.2**, was readily prepared via the addition of methyllithium to *rac*-**3.1**. Recrystallization from hexanes at $-20\text{ }^{\circ}\text{C}$ gave colourless crystals of **3.2** in high yield (86%).



3.2

3.3.2b Characterization.

Characterization was by ^1H and ^{13}C NMR spectroscopy and CHN analysis. The large (*ca.* 2 mm x 2 mm x 2 mm) crystals of **3.2** were suitable for single crystal X-ray diffraction solid state structure determination.

3.3.2b(i) Nuclear magnetic resonance spectroscopy.

The ^1H NMR spectrum of the crude reaction mixture possesses a single sharp resonance in the cyclopentadienyl-CH region at $\delta = 4.96$ ppm. This indicates the presence of only one isomer in solution, this is not unexpected as only a single isomer of **3.1** was used in the synthesis of **3.2**. Harsher reaction conditions are usually required for isomerization of a coordinated tetrahydroindenyl group, due to the necessary breaking and reforming of the metal-cyclopentadienyl bond, Collins and co-workers have effected *meso*- to *rac*-isomerization via recrystallization from boiling toluene.¹⁴ For this reason the predicted isomer of **3.2** in solution is the *rac*-isomer.

The singlet at $\delta = -0.20$ ppm in the ^1H NMR spectrum of **3.2** is assigned to the hydrogens of the methyl groups bonded directly to the zirconium centre. These low frequency chemical shifts are characteristic for metal alkyl ^1H NMR spectra.¹⁵ A similar shift is observed in the ^1H NMR spectrum of the iron-alkyl species **2.5**, $\delta = 0.01$ ppm.

In ^1H NMR spectra the diamagnetic shielding term dominates as the paramagnetic term is effectively zero for nuclei with electrons in spherically symmetrical orbitals, e.g. hydrogen. As the diamagnetic shielding term is approximately proportional to the electron density of the atom, it follows that the shielding is greater if the electron density on the atom is increased as a result of the influence of an electropositive atom nearby. The more electropositive zirconium causes a greater increase in the shielding constant which gives a chemical shift at lower frequencies than those observed in the case of the iron alkyl, **2.5**.

As explained earlier, in the case of ^{13}C NMR spectra the paramagnetic contribution to the overall shielding is a significant term. If the hypothesis in section 3.2 regarding the difference in frontier orbital energies affecting a significant change in ^{13}C NMR spectra are correct, the resonance in the ^{13}C NMR spectrum of **3.2** assigned to the carbons of the directly bonded methyl groups is expected at a higher frequency than assigned to the analogous carbon in **2.5**.

- In the case of **3.2** the resonance in the ^{13}C NMR spectrum assigned to the directly bonded methyl carbon is at $\delta = 39.8$ ppm, in the case of **2.5**, the analogous resonance is at $\delta = -13.4$ ppm.

The substantial change in chemical shift between the two alkyls lends further credence to the idea that the shift change is related to differing energies in frontier orbital sets and the ^{13}C NMR chemical shifts of carbons playing a more important role in the formation of these sets are affected proportionally.

It is necessary to observe, however, that the half-sandwich molecule **2.5** is obviously different from the "full-sandwich" ferrocene, **2.3**, so care must be taken in drawing comparisons between those arguments used in discussing **2.3** and **3.1**, and the observed metal-alkyl spectroscopic shifts between **2.5** and **3.2**. If the three η^1 -ligands of **2.5** are thought of as being collectively co-planar with the cyclopentadienyl ring of the tetrahydroindenyl ligand, then it is not unreasonable to suggest that theories based on changes due to bending of co-planar ligands, as in the case of **2.3** and **3.1**, may be applied to the case of **2.5** and **3.2**.

With the obvious exception of the resonance due to the methyl group bonded directly to the zirconium, the ^{13}C NMR spectra of **3.1** and **3.2** are almost identical. This is not true for the ^1H NMR spectra, where observed differences in chemical shifts are probably due to the influence of the more electronegative chlorine ligands on the dominating diamagnetic shielding term reducing the overall shielding at the hydrogen nuclei and subsequently moving chemical shifts to higher frequencies. The effect disappears as the number of bonds separating the chlorine from the hydrogen increase. The change is only noticeable in the chemical shift for the singlets assigned to the cyclopentadienyl CH hydrogens, $\delta = 4.96$ ppm for **3.2** and $\delta = 5.76$ ppm for **3.1**, but is not a contributing

factor at all in the chemical shifts of singlets assigned to the tetrahydroindenyl methyl groups hydrogens, $\delta = 1.46$ ppm for **3.2** and $\delta = 1.20$ ppm for **3.1**.

3.3.2b(ii) Single crystal X-ray diffraction solid state molecular structure determination.

Upon data collection (10043 reflections collected, 6888 independent, 6882 used for structure solution) and solution (using the SHELXTL software suite) of the single crystal X-ray diffraction experiment, **3.2** was found to crystallize in the space group P-1. Applying the conventions described in chapter two in assigning chiral configurations, it is immediately apparent that both tetrahydroindenyl rings have the same configuration, the S-configuration (Fig. 3.11). As P-1 possesses an inversion centre (its only symmetry element), capable of transforming a chiral centre in a R-configuration into a S-configuration, and *vice versa*, this means **3.2** is present as a 1:1 mixture of both enantiomers.

Various data can be extracted from the molecular structure obtained for **3.2**; a selection is tabulated in Table 3.4, along with comparative data for **3.1**, and $(\eta\text{-C}_5\text{H}_5)_2\text{ZrMe}_2$, **3.c** (Fig. 3.10).¹⁶

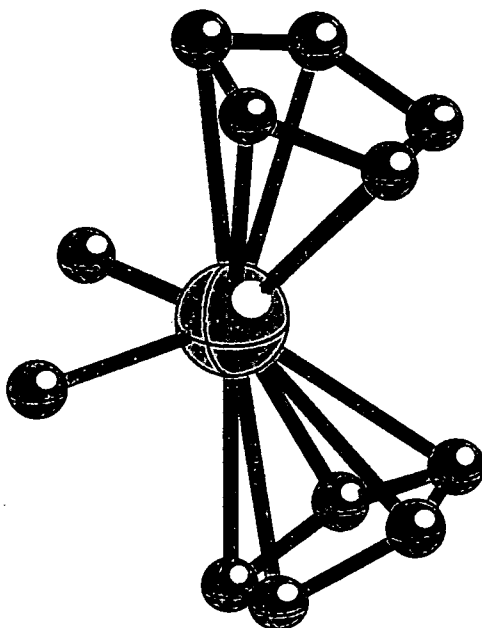
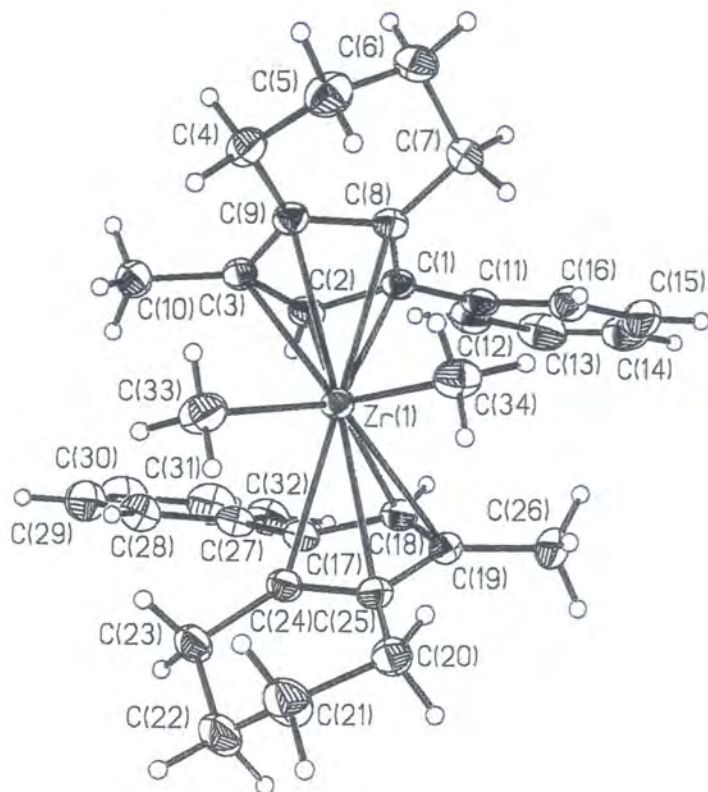
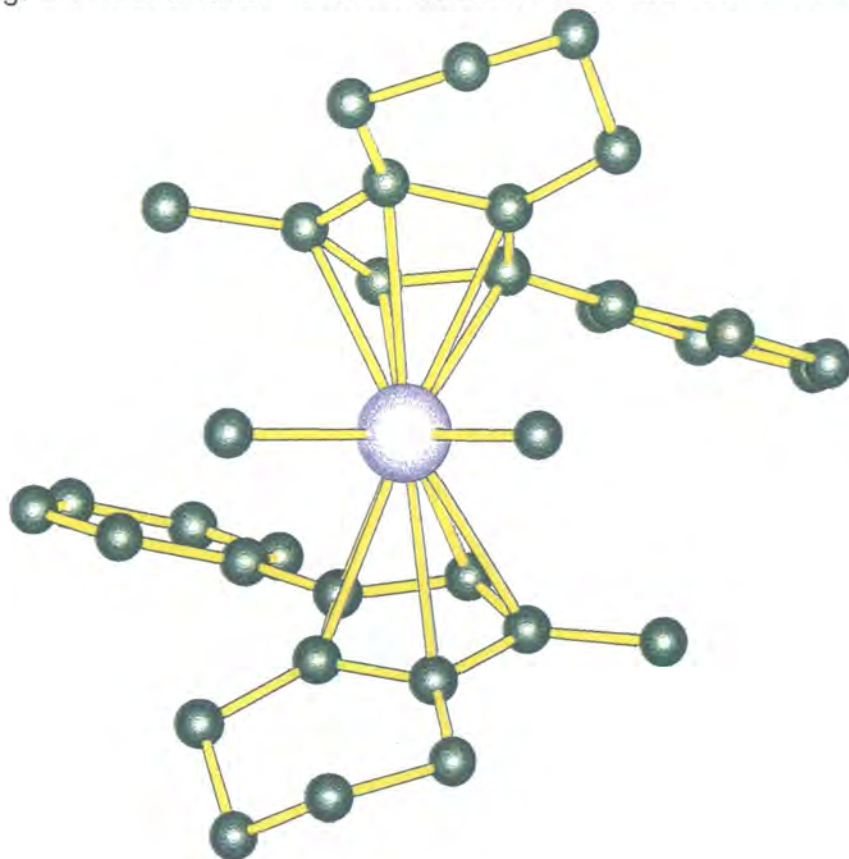


Fig. 3.10 Solid state molecular structure of $(\eta\text{-C}_5\text{H}_5)_2\text{ZrMe}_2$.

There are no significant differences between the structures of **3.2** and **3.c**; initially a possibly smaller steric interaction between the tetrahydroindenyl ligand and the methyl ligand (approximating to the interaction between the cyclopentadienyl ligand and the methyl ligand in **3.c**) with respect to the chlorine ligand in **3.1** might be thought to account for this. However, there are no substantial differences between the structures of **3.1** and **3.2** when the bond lengths and bond angles in Table 3.4 are compared, but when **3.2** is viewed along the cyclopentadienyl centroid-cyclopentadienyl centroid axis, it can be seen that the ligand rings are more staggered in **3.2** than in **3.1** (Fig. 3.12, compare with Fig. 3.6, the view of the molecular structure of **3.1** along centroid-centroid axis).

This may explain the greater dihedral angle in 3.2, as the phenyl ring now has more room to rotate in compared with the phenyl rings in 3.1 (due to the carbon of the cyclopentadienyl ring which the *ipso*-carbon is bonded to eclipsing the CH carbon of the cyclopentadienyl ring of the other ligand).

Fig. 3.11 Solid state molecular structure of the SS-isomer of 3.2.



Distance (Å) or Angle (°)	3.2	3.1	3.c
Zr-Me(1)	2.264(2)	-	2.280(5)
Zr-Me(2)	2.270(2)	-	2.273(5)
Zr-Centroid(1)	2.264	2.250	2.23
Zr-Centroid(2)	2.260	2.237	2.23
Average C(ring)-C(ring), [Range]	1.423(2) [1.409(2) - 1.435(2)]	1.424(3) [1.406(3) - 1.442(3)]	{not provided}
Average C(ring)-C(alkyl- substituent), [Range]	1.505(2) [1.500(2) - 1.508(2)]	1.505(3) [1.497(3) - 1.513(3)]	-
Me(1)-Zr-Me(2)	96.64(8)	-	95.6
Centroid(1)-Zr-Centroid(2)	132.2	131.8	132.5
C(ring)-C(phenyl)	1.479(2)	1.478(3)	-
Cp-Ph dihedral	27.7	15.9	-

Table 3.4 Selected data extracted from the molecular structure of **3.2** and comparative data for **3.1** and **3.c**.

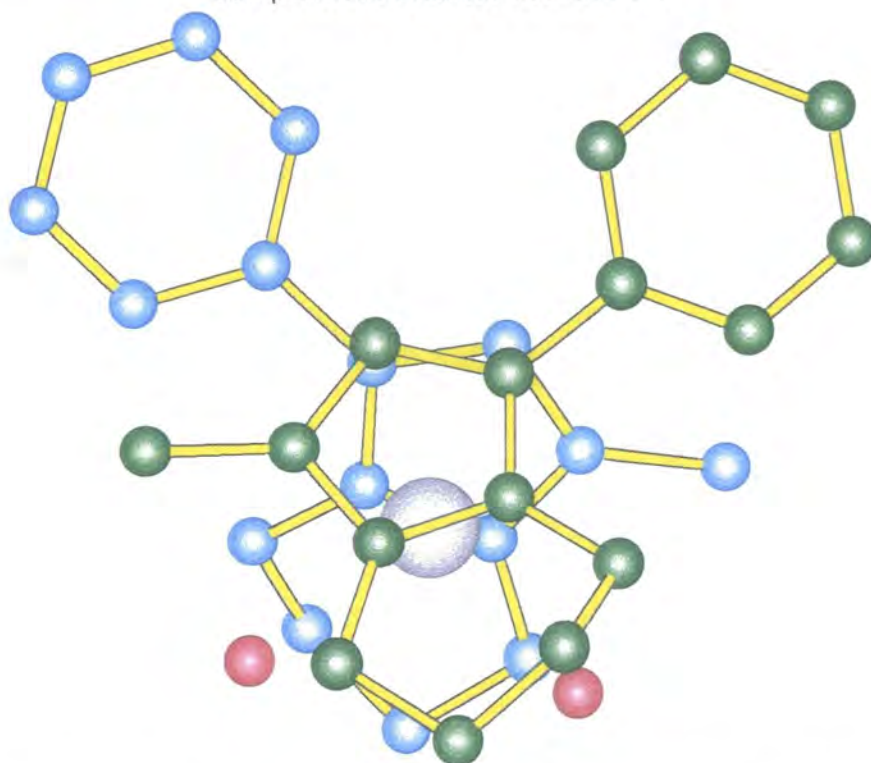


Fig. 3.12 View of molecular structure of **3.2** along centroid-centroid axis. (Bonds to the zirconium have been removed and methyl carbons bonded directly to the zirconium rendered in red-purple for clarity.)

Care must be taken in comparing values for distances and angles in **3.c** with **3.1** or **3.2**, as little detail is given in the report by Hunter and co-workers and their X-ray diffraction experiment was performed at room temperature, as opposed to -123 °C in the cases of **3.1** and **3.2**.

The cyclopentadienyl ring is not perfectly planar and has the following deviations from the mean plane (Å, positive deviation indicates deviation away from the zirconium atom): C(1) -0.005; C(2) 0.002; C(3) 0.002; C(8) 0.007; C(9) -0.005. The steric bulk of the substituents causes the carbons of the methyl group, the phenyl group and cyclohexyl ring adjacent to the five membered ring to deviate away from the mean plane of the cyclopentadienyl ring away from the zirconium. The cyclohexyl ring is puckered with an average for the C-C bond distances of 1.530 (3) Å and with the following deviations from the mean cyclopentadienyl plane (Å): C(4) 0.182; C(5) 0.108; C(6) 0.886; C(7) 0.262. These values are all slightly larger than for **3.1**. It is possible that the tetrahydroindenyl ligand can use its fused cyclohexyl ring component as another means of relieving steric pressure when coordinated to a metal. Although in the cases of **3.1** and **3.2**, with the cyclohexyl rings adopting positions "over" the two X ligands, so as to effectively occupy the least sterically influential position in each molecular structure, it is unlikely that the greater deviations of the cyclohexyl ring from the mean plane of the five-membered ring in **3.2** are significant. This is especially true when it is considered that the X ligands in **3.1** (chlorines) are smaller than those in **3.2** (methyls), so smaller deviations due to less steric pressure would be predicted.

The *ipso*-carbon of the phenyl group and the carbon of the methyl group deviate by 0.114 Å and 0.117 Å from the mean plane of the cyclopentadienyl ring respectively. Carbon atom deviations from the mean plane of the cyclopentadienyl ring in **3.2** are summarised in Table 3.5, along with comparative values for the zirconocene **3.1**.

Carbon atom	Deviation from C ₅ -plane (Å)	
	3.1	3.2
1 (ring C)	-0.011	-0.005
2 (ring C)	0.006	0.002
3 (ring C)	0.002	0.002
8 (ring C)	0.012	0.007
9 (ring C)	-0.009	-0.005
4 (C9-CH ₂)	0.098	0.182
7 (C8-CH ₂)	0.187	0.261
10 (methyl C)	0.133	0.117
11 (<i>ipso</i> -phenyl C)	0.043	0.114

Table 3.5 Carbon atom deviation from the mean plane of the cyclopentadienyl ring in **3.1** and **3.2**.

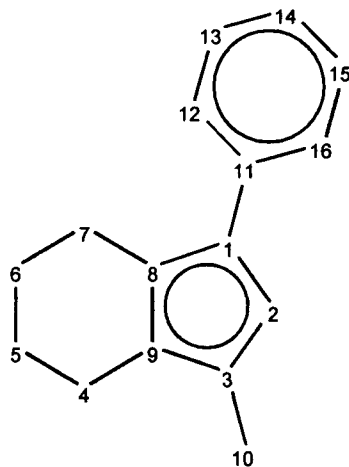


Fig. 3.13 Key to Table 3.5.

3.3.2b(iii) CHN analysis.

One more thing remains to be said about the determined crystal structure of **3.2**: for every two molecules of **3.2** present there exists a disordered (over two sites) molecule of n-hexane from crystallization. This accounts exactly for the CHN analysis. Analysis found: C, 76.5; H, 8.1. Calculated for $ZrC_{34}H_{40}$: C, 91.0; H, 9.0. Calculated for $ZrC_{34}H_{40} \cdot (C_6H_{14})_{1/2}$: C, 76.2; H, 8.1.

3.3.3 Summary.

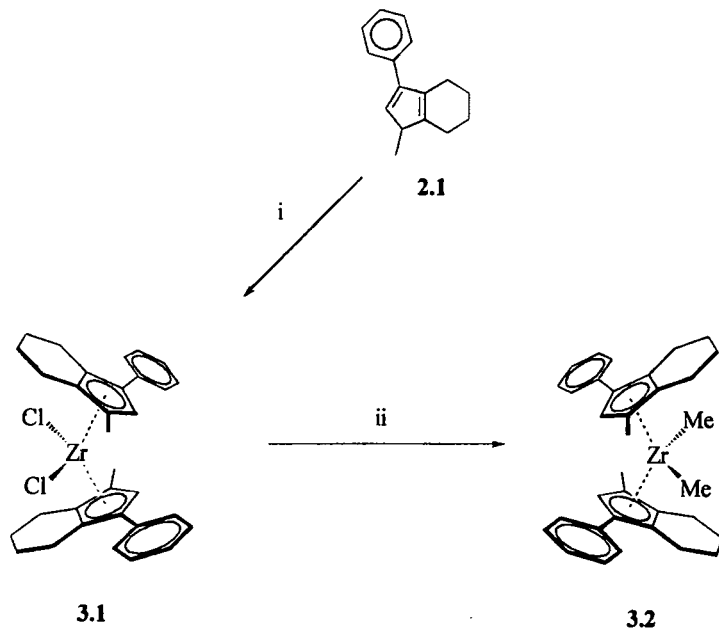
The *rac*-isomer of the dimethyl zirconocene **3.2** has been prepared from the *rac*-isomer of the **3.1**. Crystallizing in space group P-1, **3.2** possesses one molecule of n-hexane with half occupancy in the asymmetric unit and adopts a different orientation of the tetrahydroindenyl rings to that seen in the structure of **3.1**. The NMR spectroscopic assignments of the resonances for the methyl groups bonded directly to the metal resemble that for the analogous methyl group of the half-sandwich iron-alkyl compound, **2.5**, in the 1H NMR spectrum, but not in the ^{13}C NMR spectrum. Possible reasons associated with effects on various components of the overall shielding have been suggested.

3.4 Conclusions.

Although possible explanations for the similarities and differences of the NMR spectroscopic data for 1-phenyl-3-methyl-4,5,6,7-tetrahydroindenyl in the different environments described in chapters two and three have been suggested, the number of parameters left untouched in the discussion renders these explanations far from definite. One way of testing the relationship between frontier orbital energy separation and observed spectroscopic shifts would be to model the orbital structures of various bent and parallel metallocenes and see if they relate sensibly to known NMR spectroscopic data. Modelling packages such as "IGLO", which can use NMR spectroscopic data to aid structure prediction or use structural data to predict spectroscopic information, are

not yet capable of dealing with systems involving transition metals.^{17,18} However, Green has recently investigated the orbital structures of various bent-metallocenes using the Cerius² package of Molecular Simulations Inc., and related her findings to properties of the systems studied.¹⁹ This may be an alternative route to obtaining comparative data between parallel and bent metallocenes, for correlation with spectroscopic properties.

The chemistry of chapter three is summarized in Scheme 3.1.



Scheme 3.1 Summary of chemistry in chapter three.

(Reagents and conditions: i, BuLi, ZrCl₄; ii, MeLi.)

3.5 References.

- 1 J. W. Lauher and R. Hoffmann, *J. Am. Chem. Soc.*, 1976, **98**, 1729.
- 2 a) H. H. Brintzinger, D. Fischer, R. Müllhaupt, B. Rieger and R. M. Waymouth, *Angew. Chem., Int. Ed. Engl.*, 1995, **34**, 1143;
b) P. C. Mohring and N. J. Coville, *J. Organomet. Chem.*, 1994, **28**, 1.
- 3 E. Samuel, *Hebd. Seances Acad. Sci. Ser. C*, 1962, **254**, 308.
- 4 a) L. F. Fieser and M. Fieser, *Fieser and Fieser's Reagents for Organic Synthesis*, Wiley, 1982, vol. 10, p. 131;
b) L. F. Fieser and M. Fieser, *Fieser and Fieser's Reagents for Organic Synthesis*, Wiley, 1982, vol. 11, p. 51.
- 5 P. Kopf-Maiser, *J. Cancer Res. Clin. Oncol.*, 1984, **108**, 254.
- 6 N. J. Long, *Metallocenes*, Blackwell, London, 1st edn., 1998, ch.4, p. 148.
- 7 G. B. Kauffman, *J. Chem. Edu.*, 1975, **52**, 777.
- 8 a) J. Y. Corey, X. -H. Zhu, L. Brammer and N. P. Rath, *Acta Cryst.*, 1995, **C51**, 565;
b) C. Krüger, F. Lutz, M. Nolte, G. Erker and M. Aulbach, *J. Organomet. Chem.*, 1993, **452**, 79.
- 9 D. J. Cardin, M. F. Lappert, and C. L. Raston, *Chemistry of Organo-Zirconium and -Hafnium Compounds*, Ellis Horwood, Chichester, 1986.

- 10 a) E. A. LaLancette and R. E. Benson, *J. Am. Chem. Soc.*, 1965, **87**, 1941;
b) H. Spiesecke and W. G. Schneider, *Tetrahedron Letts.*, 1961, 468;
c) B. E. Mann and B. F. Taylor, *¹³C NMR Data for Organometallic Compounds*, Academic Press, New York, 1981;
d) J. Mason, *Chem. Rev.*, 1987, **87**, 1299.
- 11 a) P. W. Jolly and R. Mynott, *Adv. Organomet. Chem.*, 1981, **19**, 257;
b) B. E. Mann, *Adv. Organomet. Chem.*, 1988, **28**, 397.
- 12 Ch. Elschenbroich and A. Salzer, *Organometallics*, VCH, New York, 1989, 1st ed., p 296.
- 13 a) E. Samuel, *J. Am. Chem. Soc.*, 1973, **95**, 6263;
b) *Ger. Pat.*, 3 007 725, 1981.
- 14 S. Collins, B. A. Kuntz, N. J. Taylor, and D. G. Ward, *J. Organomet. Chem.*, 1988, **342**, 21.
- 15 M. A. Giardello, M. S. Eisen, C. L. Stern and T. J. Marks, *J. Am. Chem. Soc.*, 1995, **117**, 12114.
- 16 W. E. Hunter, D. C. Hrnčir, R. V. Bynum, R. A. Penttila and J. L. Atwood, *Organometallics*, 1983, **2**, 750.
- 17 M. Fox, private communication, 1998.
- 18 For an initial paper on IGLO see: J. C. Facelli, A. M. Orendt, D. M. Grandt and J. Michl, *Chem. Phys. Lett.*, 1984, **112**, 147.
- 19 J. C. Green, *Chem. Soc. Rev.*, 1998, **27**, 263.

Chapter Four
Experimental Details.

4.1 Experimental equipment and conditions.

4.1.1 General experimental details.

Air sensitive compounds were manipulated under a nitrogen atmosphere using standard Schlenk line and glovebox techniques. Schlenk line inert atmosphere manifolds were supplied with dinitrogen at 1.2 bar and vacuum manifolds were connected to Edwards two-stage pumps capable of evacuating the lines to pressures of ~1 mmHg. The glovebox used was a Braun "Labstar 50". Solvents were pre-dried over sodium wire or, in the case of dichloromethane and acetonitrile, 4 Å molecular sieves, and distilled from appropriate drying agents under an inert atmosphere of dinitrogen: toluene from sodium; diethyl ether from sodium-potassium alloy; dichloromethane from calcium hydride; tetrahydrofuran (THF) from potassium; hexane from potassium; acetonitrile from calcium hydride; pentane from sodium hydride. Solvents were degassed using a freeze-pump-thaw process. Unless indicated otherwise all reagents were used as received. The reaction of **2.4** with I₂, and the reaction of **2.5** with PPh₃ were performed according to literature methods.¹ All preparations were performed in a fume-hood.

4.1.2 Instrumental methods.

4.1.2a Spectroscopy, spectrometry and CHN analysis.

Nuclear Magnetic Resonance (NMR) spectra were recorded on Varian XL-200 (¹H), Varian Gemini-200 (¹H and ¹³C), Bruker AC-250 (¹H and ¹³C) or Varian VXR-400 (¹H-¹H COSY and ¹H-¹³C HETCOR) instruments. Per-deutero benzene and deutero chloroform were dried over 4 Å molecular sieves for 2 d and degassed using a freeze-pump-thaw process. Infrared spectra were obtained as liquid films on a Perkin-Elmer 1615 FTIR spectrometer or as solid samples on a Graseby Specac 10500 Golden Gate coupled to a Perkin Elmer 1000 series "Paragon" spectrometer. Mass spectrometry was undertaken on a VG Micromass 7070E instrument operating in EI mode. Gas chromatography-mass spectrometry was performed using a Hewlett Packard 5890 Series II gas chromatograph coupled to a Finnegan Mass Lab Trio 1000 mass spectrometer operating in EI mode, using a 1.25 metre HP methyl silicone column; column temperature 40 °C for 1 min, then 10 °C/min to 270 °C. CHN analyses were performed by an on-site analytical service using an EAI CE-440 Elemental Analyser.

4.1.2b Cyclic voltammetry.

Cyclic voltammetry was carried out with an EG&G PAR Potentiostat/Galvanostat Model 263 using a platinum bead electrode, an Ag/AgCl non-aqueous (acetonitrile) reference electrode, lithium perchlorate as the supporting electrolyte and acetonitrile as the solvent.

4.1.2c X-ray diffraction crystallography.

4.1.2c(i) Microcrystalline powder X-ray diffraction.

Powder X-ray diffraction patterns were recorded at room temperature on a Philips powder diffractometer; details of the data collection are given in Table 4.1.

Start angle (°)	4.00
End angle (°)	60.00
Step size (°)	0.02
Speed (s step ⁻¹)	2.00
Total steps	2800
Tube	Cu
Wavelength, λ (Å)	1.5418
Generator settings (kV, mA)	40, 25

The powder was finely ground to guarantee a random distribution of crystallites. The sample was placed in a sample holder, care was taken to achieve a smooth surface which was level with the sample holder. The sample holder was mounted in the centre of the powder diffractometer sample chamber. Engagement of bayonet locking systems of the sample chamber lid permitted the opening of the X-ray shutter tube via an interlock system. The experiment was then started via a computer link.

4.1.2c(ii) Single crystal X-ray diffraction.

For each compound structurally analysed using single crystal X-ray diffraction a suitable crystal was selected by ensuring that all dimensions were in the order of 0.05 mm - 0.5 mm (if not the crystal was cut with a sharp scalpel blade so as to leave as many natural faces as possible) and testing that the crystals extinguished sharply and completely when rotated under polarized light.

The crystal was then mounted onto the end of a glass fibre using an oil-drop method in which the crystal is encapsulated in a viscous perfluoroether oil which acts as a protective film and which solidifies when placed onto the diffractometer under a 150 K liquid nitrogen flow;² the diffractometer is equipped with an Oxford Cryostreams Cryostream unit which allows experiments to be carried out at any temperature in the range 85-300 K.³ By means of a brass-pip and goniometer head the crystal was placed in the diffractometer; the goniometer head allows crystal translation in three perpendicular directions, so that, once the goniometer head is secured in the diffractometer, the position of the crystal can be adjusted such that it lies in the centre of the oncoming beam. The diffractometer used was a Siemens SMART-CCD diffractometer, pictured in Fig. 4.1. Once the crystal is centred using the built-in microscope, diffraction is measured using a 512 x 512 pixel scintillation area detector

that uses a charged-couple-device (CCD) to amplify the output. A lead beam-stop is fixed in the direct line of the incident X-ray beam and a 'glass-panelled' interlock prevents user intervention when the X-ray shutter is open.

Lattice parameters were obtained by least squares refinement of 25 high angle reflections.⁴ Data were collected using graphite monochromated Mo K α radiation, $\lambda = 0.71073\text{\AA}$. Other data for each structure are presented in appendix A. All computations used SHELXTL, data reduction, corrections and analysis were by SAINT and XPREP.⁵ Structures were solved by direct methods using XS and subsequently refined by Fourier and least squares using XL.⁶ Hydrogen atoms were freely refined in all cases.

Molecular structure diagrams were rendered using XP in SHELXTL or Ball and Stick,⁷ file conversion for Ball and Stick used Babel.⁸

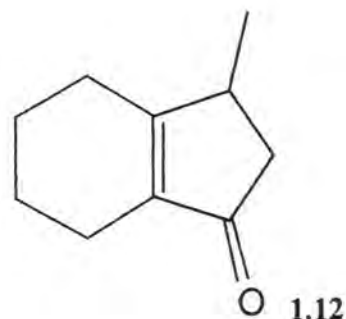


Fig. 4.1 A Siemens SMART-CCD diffractometer.

4.2 Preparations.

4.2.1 Preparation of 3-methyl-2,3,4,5,6,7-hexahydroind-8(9)-en-1-one, 1.12.

Cyclohexene (27.3 g, 0.332 mol) was added dropwise to a mechanically stirred mixture of crotonic acid (28.7 g, 0.333 mol) and polyphosphoric acid (200 g) maintained at 60 °C. The mixture was stirred at 60 °C for 2 h. A solution of NaOH (10% by mass, 100 cm³) was added and the slurry was stirred for 16 h to facilitate decomposition of the polyphosphoric acid. The mixture was extracted with 40-60 °C petroleum ether (3x100 cm³), and the combined organic extracts were washed with 5% ammonia

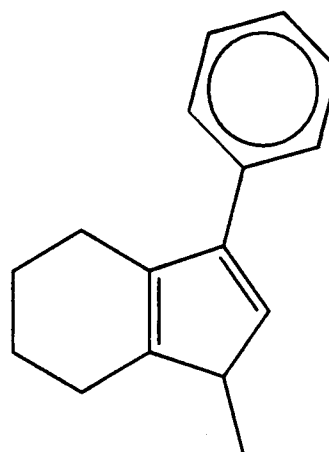


solution in water (50 cm³), followed by saturated sodium chloride solution (2x50 cm³). The solution was dried over magnesium sulphate and the solvent removed under reduced pressure. Distillation under reduced pressure (b.p. = 58-60 °C, ~1 mmHg) afforded **1.12** as a colourless oil. Yield 27.4 g, 55%.

4.2.2 Preparation of 1-phenyl -3-methyl-4,5,6,7-tetrahydroindene, **2.1**.

4.2.2a Grignard method.

Phenyl magnesium bromide was prepared from bromobenzene (5.50 g, 35 mmol) and magnesium turnings (0.97 g, 40 mmol) in diethyl ether (100 cm³). The Grignard solution was cooled to 0 °C and **1.12** (5.00 g, 33 mmol) was slowly added with stirring. The mixture was allowed to warm to room temperature and was stirred for 15 h. After filtration from the excess Mg the solution was quenched with water (50 cm³) and the organic layer was extracted with diethyl ether (2x50 cm³). The combined organic extracts were dried over magnesium sulphate and then filtered. Aqueous HCl (6 M, 0.5 cm³) was then added and the solution was stirred for 2 h. After washing with water and drying with magnesium sulphate the solution was concentrated on a rotary evaporator. Distillation at reduced pressure (b.p. = 80-81 °C, ~1 mmHg) provided **2.1** as an orange-red oil. Yield 3.6 g, 52%.



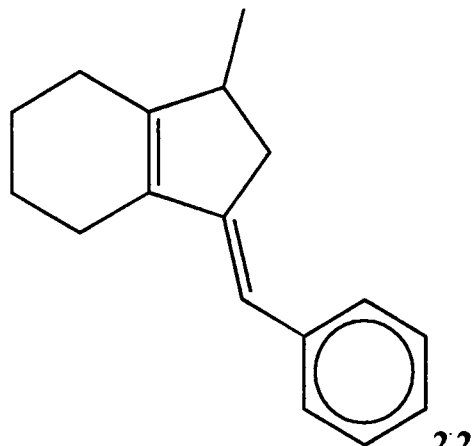
2.1

4.2.2b Phenyl lithium method.

A diethyl ether solution (100 ml) of **1.12** (3.54 g, 23.6 mmol) was cooled to 0 °C and phenyl lithium (11.8 ml, 23.6 mmol, 2M in 70:30 cyclohexane:diethyl ether) was slowly added with stirring. The mixture was allowed to warm to room temperature and then was stirred for 15 h. The solution was quenched with water (50 cm³) and the organic layer was extracted with diethyl ether (2x50 cm³). The combined organic extracts were dried over magnesium sulphate and filtered. Aqueous HCl (6-M, 0.5 cm³) was then added and the solution was stirred for 2h. After washing with water and drying with magnesium sulphate the solution was concentrated on a rotary evaporator. Distillation at reduced pressure (b.p. = 80-81 °C, ~1 mmHg) provided **2.1** as an orange-red oil. Yield 1.7 g, 25%.

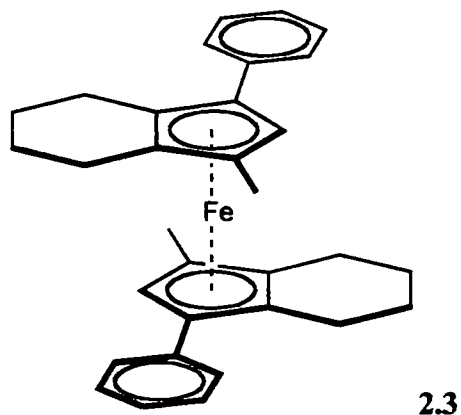
4.2.3 Preparation of 1-benzylidene-3-methyl-2,3,4,5,6,7-hexahydroind-8(9)-ene, 2.2.

Benzyl magnesium chloride was prepared from benzylchloride (4.43 g, 35 mmol) and magnesium turnings (0.97 g, 40 mmol) in diethyl ether (100 cm³). The Grignard solution was cooled to 0 °C and 1.12 (5.00 g, 33.3 mmol) was slowly added with stirring. The mixture was allowed to warm to room temperature and was stirred for 15 h. After filtration from the excess Mg the solution was quenched with water (50 cm³) and the organic layer was extracted with diethyl ether (2x50 cm³). The combined organic extracts were dried over magnesium sulphate and then filtered. Aqueous HCl (6 M, 0.5 cm³) was then added and the solution was stirred for 2 h. After washing with water and drying with magnesium sulphate the solution was concentrated on a rotary evaporator. Distillation at reduced pressure (b.p. = 105-107 °C, ~1 mmHg) provided 2.2 as an orange-red oil. Yield 4.8 g, 64%.



4.2.4 Preparation of bis(1-phenyl-3-methyl-4,5,6,7-tetrahydroindenyl) iron(II), 2.3.

Butyllithium (1.65 M in hexanes, 2.41 ml, 3.91 mmol) was added at 0 °C to a solution of 2.1 (0.83 g, 3.91 mmol) in diethyl ether (30 cm³) and the solution was stirred for 4 h at 0 °C. The resulting lithium 1-phenyl-3-methyl-4,5,6,7-tetrahydro-indenide, was isolated on a porosity-3 frit and washed with diethyl ether (3x10 cm³) to remove excess butyllithium and organic impurities. The solid was then dissolved in THF (40 cm³) and the resulting solution was added to a slurry of anhydrous

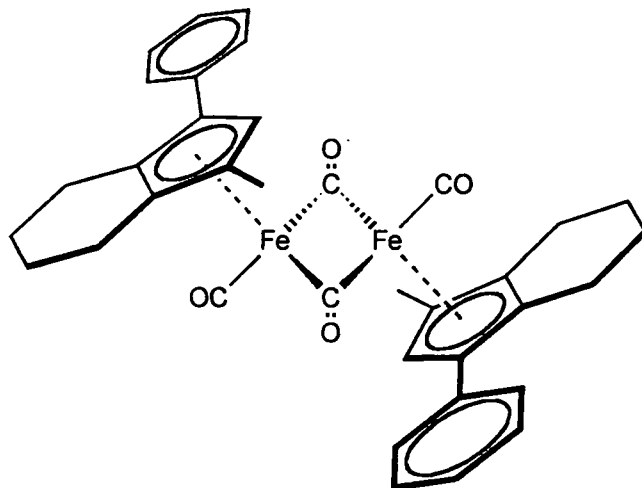


FeCl₂ (0.25 g, 1.96 mmol) in THF (10 cm³) at 0 °C. The mixture was allowed to warm to room temperature and was then stirred for 14 h. After quenching with water (50 cm³), the organic layer was extracted with diethyl ether (2x20 cm³) and dried over magnesium sulphate. After filtration the solution was concentrated and recrystallized from low boiling petroleum ether to give orange crystals of 2.3. Yield 0.10 g, 10%.

Further concentration and cooling to $-20\text{ }^{\circ}\text{C}$, gave an orange microcrystalline powder. Yield 0.20 g, 20%. Total yield 0.30g, 30%.

4.2.5 Preparation of 1-phenyl-3-methyl-4,5,6,7-tetrahydroindenyl dicarbonyl iron(II) dimer, 2.4.

Diiron nonacarbonyl, $\text{Fe}_2(\text{CO})_9$, was purified by washing under N_2 with, in order, 25% hydrochloric acid in water, water, ethanol, and diethyl ether. It was then dried under reduced pressure. A toluene (250 cm^3) solution of **2.1** (6.3 g, 30 mmol) and $\text{Fe}_2(\text{CO})_9$ (5.0 g, 13.7 mmol) was refluxed under nitrogen for 24 h.

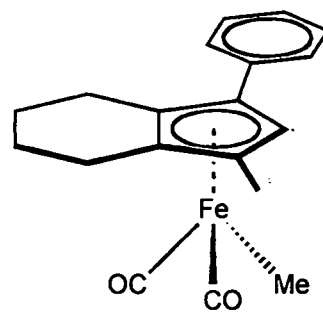


2.4

The solvent was removed under reduced pressure and hexanes (100 cm^3) were added. The resulting suspension was filtered through celite and the residue was washed with hexanes (20 cm^3) to remove any remaining ligand. The product was extracted from the black residue with toluene ($3 \times 50\text{ cm}^3$). Reduction of the volume to ca. 25 cm^3 under reduced pressure followed by filtration gave **2.4** as a black powder. Yield 2.16g, 25%.

4.2.6 Preparation of 1-phenyl-3-methyl-4,5,6,7-tetrahydroindenyl methyl iron(II) dicarbonyl, 2.5.

A solution of **2.4** (1.5 g, 2.34 mmol) in THF (20 cm^3) was added dropwise to sodium amalgam (0.2 g of Na) under THF (20 cm^3) and stirred at room temperature for 2 h. The THF solution was decanted away from the amalgam, the amalgam was washed with portions of THF ($2 \times 20\text{ cm}^3$) and the THF portions were combined. The solution was cooled to $0\text{ }^{\circ}\text{C}$, and iodomethane (0.65 cm^3 , 1.4 g, 10 mmol) was added and the reaction mixture was allowed to warm to room temperature and

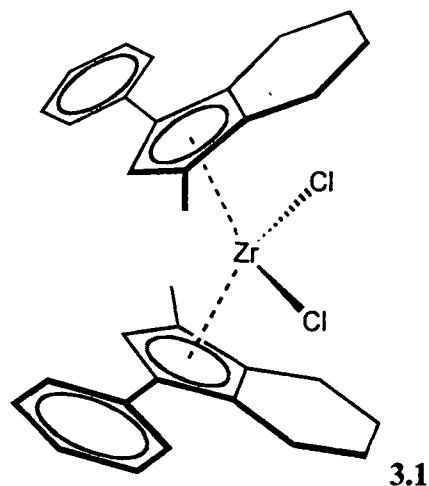


2.5

was stirred for 1 h. Volatiles were removed under reduced pressure and the residue was extracted with hexanes (20 cm^3). The mixture was filtered and the volatiles removed under reduced pressure to leave an orange oily residue. Sublimation at $100\text{ }^{\circ}\text{C}$ onto a liquid nitrogen cooled probe gave **2.5** as an oily orange solid; alternatively sublimation at $85\text{ }^{\circ}\text{C}$ over a 10 h period gave crystalline **2.5**. Yield 0.67 g, 45%.

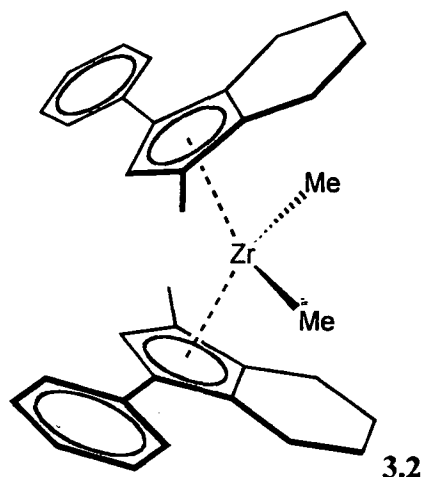
4.2.7 Preparation of bis(1-phenyl-3-methyl-4,5,6,7-tetrahydroindenyl) zirconium(IV) dichloride, 3.1.

(Lithium 1-phenyl-3-methyl-4,5,6,7-tetrahydroindenide was prepared the same way as for the preparation of 2.3.) A slurry of freshly sublimed zirconium tetrachloride (0.55 g, 2.4 mmol) in Et₂O (20 ml) was added to a slurry of lithium 1-phenyl-3-methyl-4,5,6,7-tetrahydroindenide (1.0 g, 4.6 mmol) in Et₂O (20 ml) at 0 °C under N₂. The reaction mixture was slowly warmed to room temperature and was stirred for 13 h. The Et₂O was removed under reduced pressure and toluene (20 ml) was added. The reaction mixture was filtered to remove LiCl and reduced in volume to ca. 5 ml. Cooling to -20 °C for 20 h gave yellow-brown semi-crystalline material, further recrystallization from CH₂Cl₂ at -20 °C gave 3.1 as a yellow crystalline solid. Yield 1.0 g, 72%.



4.2.7 Preparation of *rac*-bis(1-phenyl-3-methyl-4,5,6,7-tetrahydroindenyl) dimethyl zirconium(IV), 3.2.

Methyl lithium (1.6 M in Et₂O, 1.25 ml, 2.0 mmol) was added to a diethyl ether (10 ml) solution of *rac*-3.1 (0.23 g, 0.4 mmol) at 0 °C. The solution was warmed to room temperature and stirred for 24 h. The Et₂O was removed under reduced pressure and hexanes (20 ml) added. The solution was filtered to remove LiCl and reduced in volume to ca. 5 ml. Cooling to -20 °C for 48h gave colourless crystals of 3.2. Yield 0.19 g, 86%.



4.3 References.

- 1 a) K. E. duPlooy, J. duToit, D. C. Levendis and N. J. Coville, *J. Organomet. Chem.*, 1996, **508**, 231;
b) M. Green and D. J. Westlake, *J. Chem. Soc.*, 1971, 367.
- 2 D. S. Stalke and T. Kottke, *J. Appl. Cryst.*, 1993, **26**, 615.
- 3 J. Cosier and A. M. Glazer, *J. Appl. Cryst.*, 1986, **19**, 105.
- 4 a) Siemens Analytical X-ray Instruments, *SMART*, Version 4.050, Siemens Analytical X-ray Instruments, Inc., Madison, Wisconsin, U.S.A, 1995;

- b) W. Kabsch, *J. Appl. Cryst.*, 1993, **26**, 795.
- 5 a) Siemens Analytical X-ray Instruments, *SAINTE*, Version 4.050, Siemens Analytical X-ray Instruments, Inc., Madison, Wisconsin, U.S.A, 1995;
- b) W. Kabsch, *J. Appl. Cryst.*, 1988, **21**, 916;
- c) G. M. Sheldrick, *XPREP in SHELXTL*, Version 5.03/VMS, Siemens Analytical X-ray Instruments, Inc., Madison, Wisconsin, U.S.A, 1995.
- 6 a) G. M. Sheldrick, *Acta Crystallogr.*, 1990, **A46**, 467;
- b) G. M. Sheldrick, *SHELXL-93, Program for the Refinement of Crystal Structures using Single Crystal Diffraction Data*, University of Göttingen, Germany, 1993.
- 7 N. Müller, *Ball and Stick 3.5*, Cherwell Scientific, Oxford, 1993.
- 8 P. Walters and M. Stahl, *BABEL*, Department of Chemistry, University of Arizona, 1994.

Chapter Five
Characterizing Data.

5.1 Data characterizing 3-methyl-2,3,4,5,6,7-hexahydroind-8(9)-en-1-one.

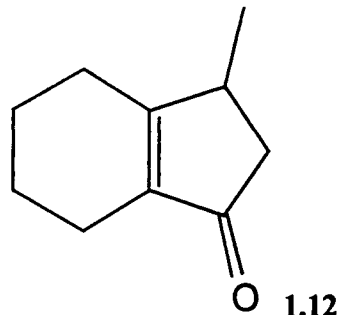
$^1\text{H NMR}$: δ (ppm, CDCl_3) 1.11 (d, 3H, $J = 6.2$ Hz, CH_3);

1.30-2.80 (series of overlapping m, 11H).

$^{13}\text{C}\{^1\text{H}\}$ NMR: δ (ppm, CDCl_3) 19.2 (CH_3); 20.4, 22.1, 22.6, 26.4 (CH_2); 36.7 (CH_2); 43.9 (CH); 138.3, 177.9, 208.7 (quat. C).

MS (EI): m/z 150 [M^+].

IR: ν (cm^{-1}) 1700 (vs) (CO), 1647 (vs) (C=C).



5.2 Data characterizing 1-phenyl-3-methyl-4,5,6,7-tetrahydroindene, 2.1.

$^1\text{H NMR}$, $^{13}\text{C}\{^1\text{H}\}$ NMR and GC-MS: indicated the presence of several isomers.

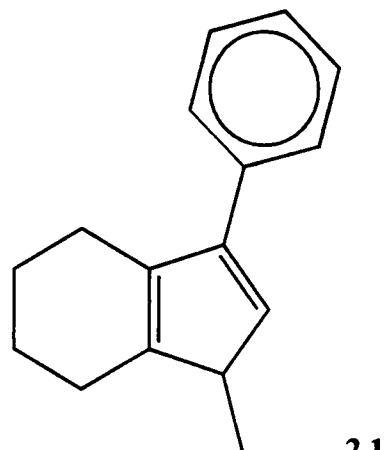
MS (EI): m/z 210 [M^+].

CHN Analysis: Best Anal. Found: C, 85.7; H, 8.1.
 $\text{C}_{16}\text{H}_{18}$ Calc.: C, 91.3; H, 8.6 %.

GC-MS:

Summary

Retention time (min)	Base peak m/z [M^+]
15:785	210
16:351	210
17:201	210
17:651	210

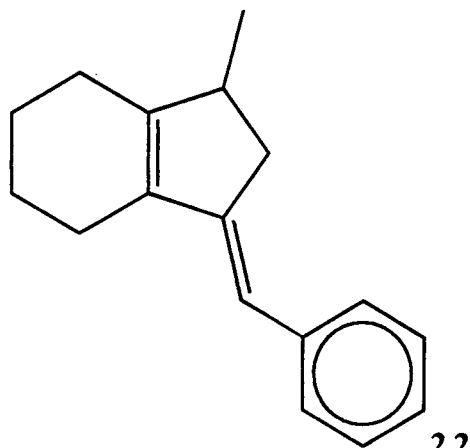


5.3 Data characterizing 1-benzylidene-3-methyl-2,3,4,5,6,7-hexahydroind-8(9)-ene, 2.2.

$^1\text{H NMR}$: δ (ppm, CDCl_3) 1.14 (d, 3H, CH_3); 1.60 - 2.60 (series of br m, 8H, CH_2); 2.45 (m, 1H, CHH); 2.80 (br m, 1H, $\text{C}(\text{Me})\text{H}$); 3.18 (m, 1H, CHH); 6.16 (s, 1H, $=\text{C}(\text{Ph})\text{H}$); 7.10-7.5 (series of m, 5H, phenyl CH's).

$^{13}\text{C}\{^1\text{H}\}$ NMR: δ (ppm, CDCl_3) 20.2 (CH_3); 22.8, 23.1, 23.5, 25.3 (CH_2); 39.4 ($\text{C}(\text{Me})\text{H}$ or cyclopentenyl CH_2); 41.6 (cyclopentenyl CH_2 or $\text{C}(\text{Me})\text{H}$); 114.9 ($=\text{C}(\text{Ph})\text{H}$); 125.7 (*para*-CH); 128.4 (*meta*-CH or *ortho*-CH); 128.8 (*ortho*-CH or *meta*-CH); 137.0, 139.8, 149.3, 151.4 (quat. C and *ipso*-C).

MS (EI): m/z 224 [M^+].



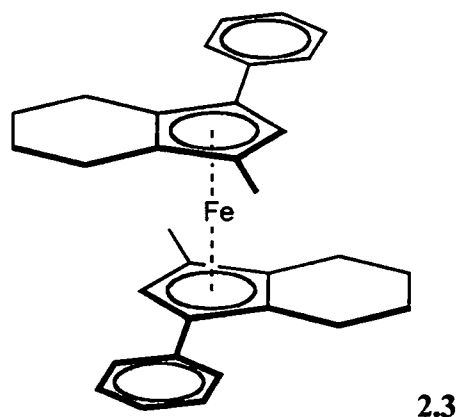
5.4 Data characterizing bis(1-phenyl-3-methyl-4,5,6,7-tetrahydroindenyl) iron(II), 2.3.

$^1\text{H NMR}$: δ (ppm, C_6D_6) 1.31 (m, 1H, CH_2); 1.37 (m, 1H, CH_2); 1.54-1.72 (overlapping m, 2H, CH_2); 1.58 (s, 3H, CH_3); 1.91 (m, 1H, CH_2); 2.15 (m, 1H, CH_2); 2.27 (m, 1H, CH_2); 2.58 (m, 1H, CH_2); 3.79 (s, 1H, CH); 7.09-7.47 (series of m, 5H, phenyl CH's).

$^{13}\text{C}\{^1\text{H}\}$ NMR: δ (ppm, C_6D_6) 11.2 (CH_3); 21.9, 23.1, 24.1, 24.7 (CH_2); 70.3 (CH); 81.3, 81.4, 82.6, 86.2 (quat. C); 125.4 (*para*-CH); 127.5 (*meta*-CH); 128.6 (*ortho*-CH); 139.2 (*ipso*-C).

IR: ν (cm^{-1} , solid state) 1949 (w), 1881 (w), 1812 (w), 1751 (w) (summation bands of phenyl ring).

M.p.: 163-165 °C.



MS (EI): m/z 474 [M+].

CHN Analysis: Anal. Found: C, 80.8; H, 7.2. $C_{32}H_{34}Fe$ Calc.: C, 81.0; H, 7.2 %.

Powder X-ray diffraction:

Fig. 5.1 Experimentally obtained powder diffraction pattern of **2.3**.

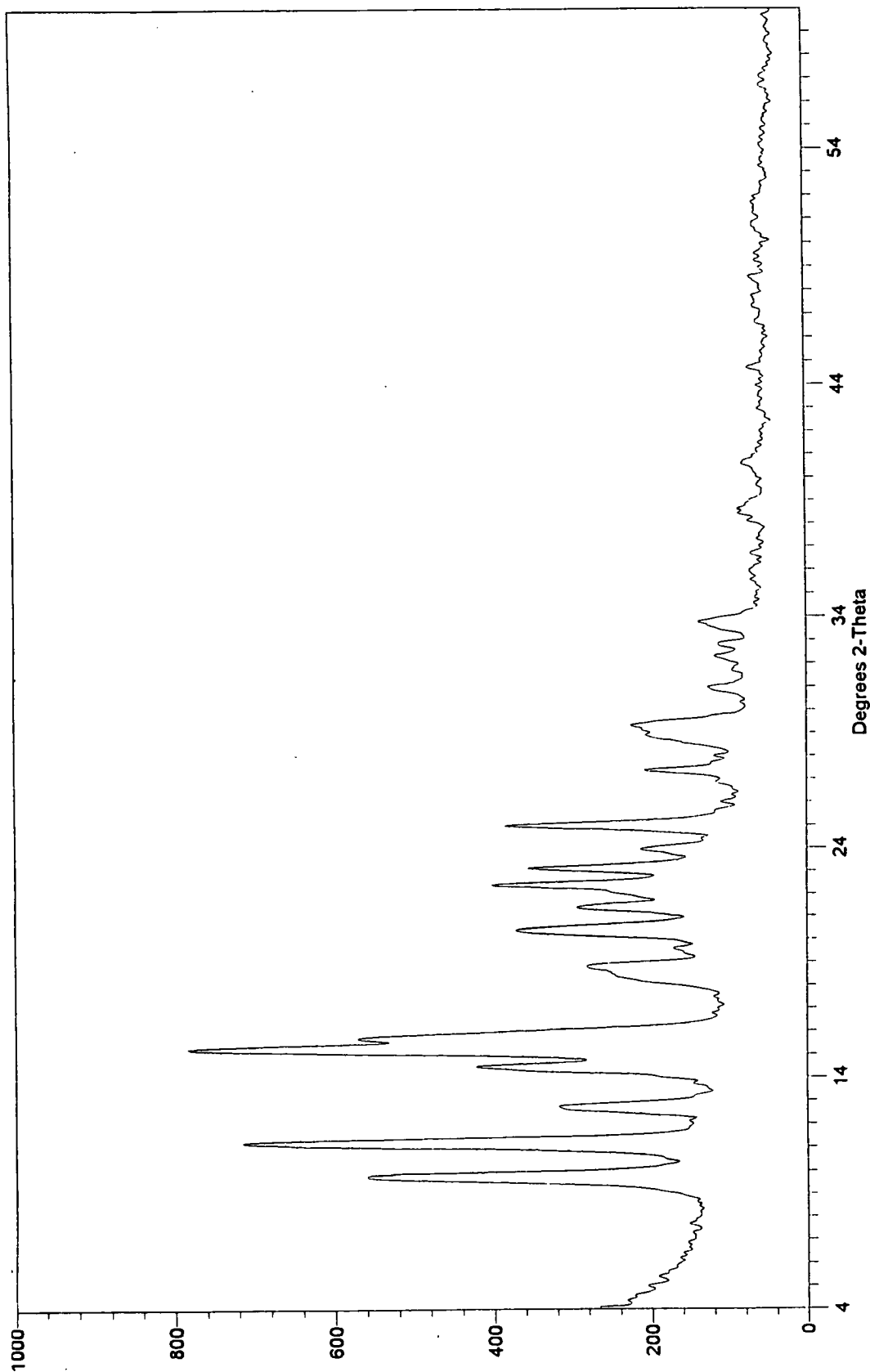
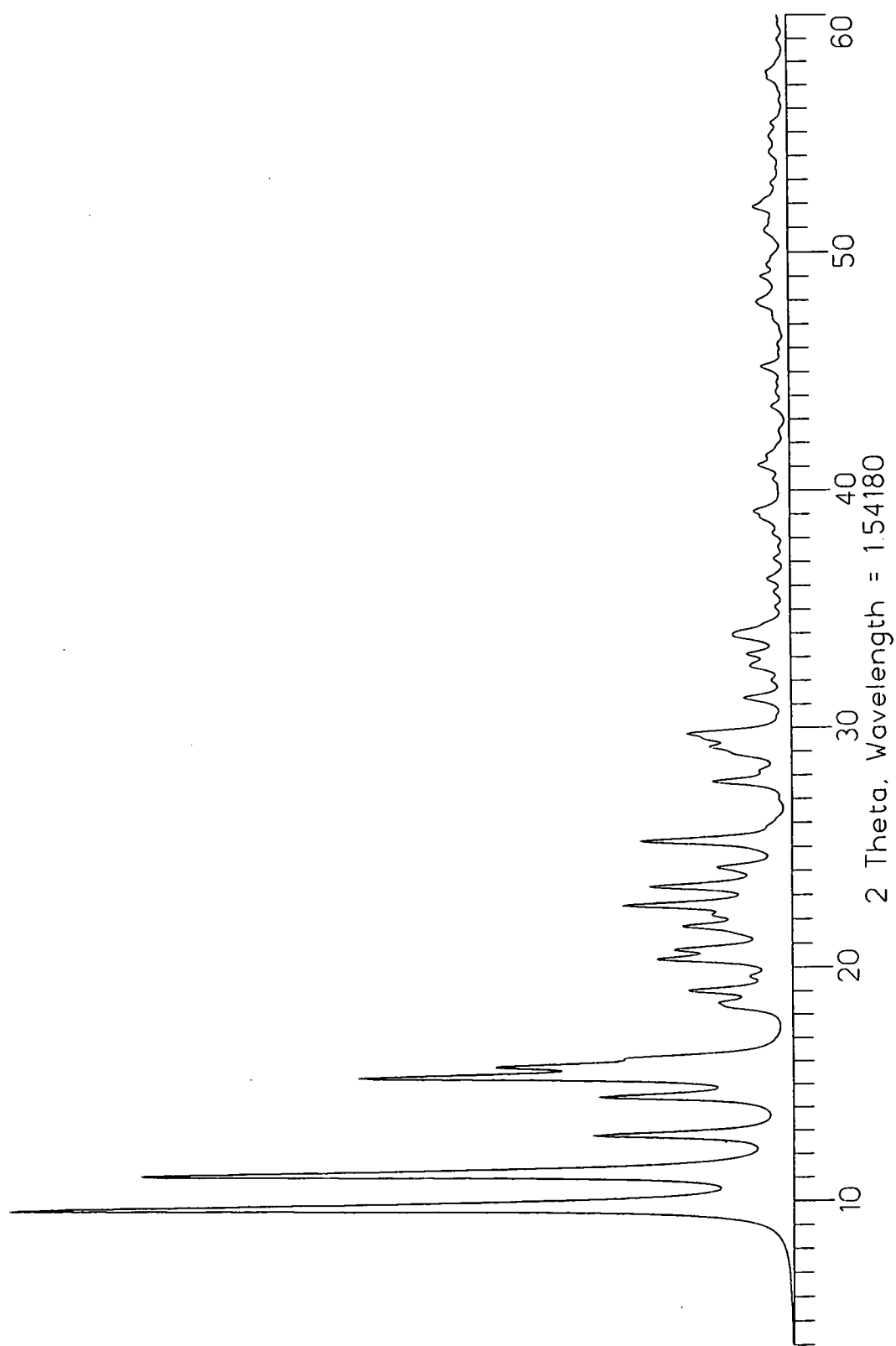


Fig. 5.2 Calculated X-ray powder diffraction pattern of 2.3.

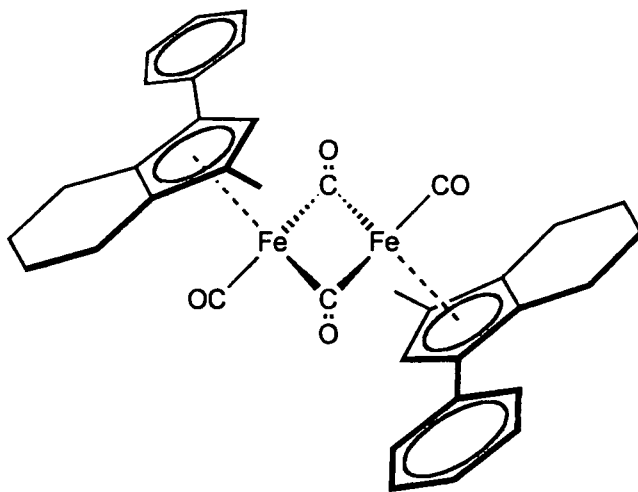


5.5 Data characterizing 1-phenyl-3-methyl-4,5,6,7-tetrahydroindenyl iron dicarbonyl dimer, 2.4.

$^1\text{H NMR}$: δ (ppm, C_6D_6)

1.14-3.00 (series of m, 7H, CH_2); 1.65 (s, 3H, CH_3); 2.74 (m, 1H, CH_2); 3.75 (br. s, 1H, CH); 7.11-7.43 (series of m, 5H, phenyl CH's).

$^{13}\text{C}\{^1\text{H}\}$ NMR: δ (ppm, C_6D_6) 10.0 (CH_3); 21.1, 22.1, 22.4, 22.9 (CH_2); 91.8, 99.5, 100.3, 101.9 (quat. C); 127.3 (*para*-CH); 128.0 (*meta*-CH or *ortho*-CH); 129.5 (*ortho*-CH or *meta*-CH); 133.5 (*ipso*-C).



2.4

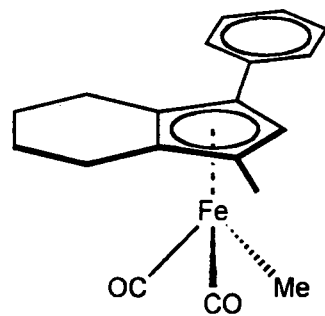
IR: ν (cm^{-1} , dichloromethane) 1974 (vs) (A_1 -symmetry CO stretch of the *cis*-isomer), 1933 (vs) (B_u -symmetry CO stretch of the *trans*-isomer and B_2 -symmetry CO stretch of the *cis*-isomer), 1796 (w, sh) (A_1 -symmetry CO stretch of the *cis*-isomer), 1759 (vs) (A_u -symmetry CO stretch of the *trans*-isomer and B_1 -symmetry CO stretch of the *cis*-isomer).

MS (EI): m/z 642 [M^+].

CHN Analysis: Anal. Found: C, 66.8; H, 5.8. $\text{C}_{36}\text{H}_{34}\text{O}_4\text{Fe}_2$ Calc.: C, 67.3; H, 5.3.

5.6 Data characterizing 1-phenyl-3-methyl-4,5,6,7-tetrahydroindenyl methyl iron(II) dicarbonyl, 2.5.

$^1\text{H NMR}$: δ (ppm, CDCl_3) 0.01 (s, 3H, Fe- CH_3); 1.40-2.80 (series of m, 8H, CH_2); 1.81 (s, 3H, CH_3); 4.85 (s,



2.5

^1H , *CH*); 7.28-7.39 (series of m, 5H, phenyl *CH*'s).

$^{13}\text{C}\{^1\text{H}\}$ NMR: (ppm, CDCl_3) -13.4 (Fe-CH_3); 10.6 (CH_3); 21.2, 22.0, 22.8, 23.1 (CH_2); 84.0 (*CH*); 94.2, 94.8, 100.0, 100.5 (quat. *C*); 127.0 (*para-CH*); 128.0 (*ortho-/meta-CH*); 128.2 (*meta-/ortho-CH*); 134.1 (*ipso-C*); 218.0, 218.1 (*CO*).

IR: ν (cm^{-1} , hexanes) 1996 (vs) (*CO*), 1943 (vs) (*CO*).

MS (EI): m/z 336 [M^+].

CHN Analysis: Anal. Found: C, 67.0; H, 5.9. $\text{C}_{19}\text{H}_{20}\text{O}_2\text{Fe}$ Calc.: C, 67.8; H, 6.0.

5.7 Data characterizing bis(1-phenyl-3-methyl-4,5,6,7-tetrahydroindenyl) zirconium dichloride, 3.1.

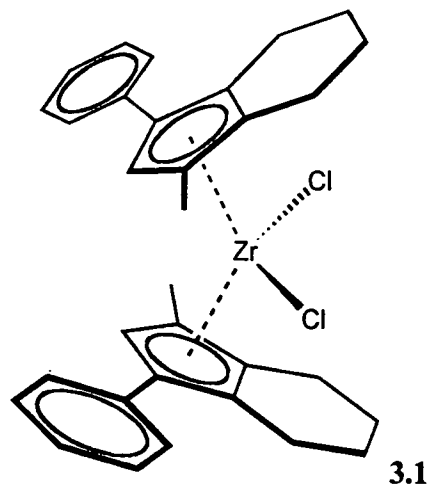
^1H NMR: δ (ppm, CDCl_3) 1.24 (s, 3H, CH_3); 1.44 (m, 1H, $-\text{CH}_2\text{CH}_2\text{CH}_2\text{CH}_2-$); 1.75 (overlapping m, 2H, $-\text{CH}_2\text{CH}_2\text{CH}_2\text{CH}_2-$); 2.03 (m, 1H, $-\text{CH}_2\text{CH}_2\text{CH}_2\text{CH}_2-$); 2.30 (m, 1H, $-\text{CH}_2\text{CH}_2\text{CH}_2\text{CH}_2-$); 2.54 (m, 1H, $-\text{CH}_2\text{CH}_2\text{CH}_2\text{CH}_2-$); 2.92 (m, 1H, $-\text{CH}_2\text{CH}_2\text{CH}_2\text{CH}_2-$); 3.33 (m, 1H, $-\text{CH}_2\text{CH}_2\text{CH}_2\text{CH}_2-$). 5.81 (s, 1H, *CH*); 7.27 (overlapping m, 3H, *ortho-CH* and *para-CH*); 7.43 (t, 2H, *meta-CH*).

$^{13}\text{C}\{^1\text{H}\}$ NMR: δ (ppm, CDCl_3) 13.3 (CH_3); 21.2 ($-\text{CH}_2\text{CH}_2\text{CH}_2\text{CH}_2-$); 23.0 ($-\text{CH}_2\text{CH}_2\text{CH}_2\text{CH}_2-$); 24.0 ($-\text{CH}_2\text{CH}_2\text{CH}_2\text{CH}_2-$); 25.4 ($-\text{CH}_2\text{CH}_2\text{CH}_2\text{CH}_2-$); 108.9 (*CH*); 119.9, 125.7, 131.3, 132.5, 134.1 (quat. *C* or *ipso-C*); 126.8 (*para-CH*); 127.1 (*ortho-CH*); 128.8 (*meta-CH*).

CHN Analysis: Anal. Found: C, 66.0; H, 5.9. $\text{C}_{32}\text{H}_{34}\text{Cl}_2\text{Zr}$ Calc.: C, 66.2; H, 5.9.

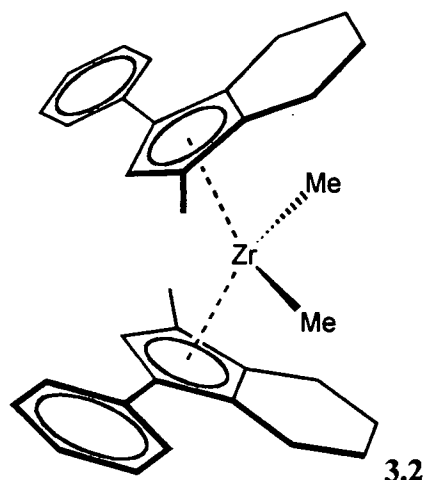
5.7 Data characterizing bis(1-phenyl-3-methyl-4,5,6,7-tetrahydroindenyl) dimethyl zirconium(IV), 3.2.

^1H NMR: δ (ppm, C_6D_6) -0.20 (s, 3H, Zr-CH_3); 1.46 (s, 3H, CH_3); 1.40, 1.70, 1.85, 2.43, 2.63, 2.78, 2.95 (series of m, 8H, CH_2); 4.96 (s, 1H, *CH*); 7.27 (overlapping m, 3H, *ortho-CH* and *para-CH*); 7.03 (m, 2H, *meta-CH*).



$^{13}\text{C}\{^1\text{H}\}$ NMR: δ (ppm, C_6D_6) 39.8 (Fe- CH_3); 12.6 (CH_3); 22.3, 23.7, 24.2, 25.0 (CH_2); 104.5 (CH); 119.0, 120.0, 123.3, 126.0 (quat. C); 125.9 (*para*-CH); 126.7 (*ortho*-CH); 128.7 (*meta*-CH); 136.3 (*ipso*-C).

CHN Analysis: Anal. Found: C, 76.5; H, 8.1.
 $\text{C}_{34}\text{H}_{40}\text{Zr}(\text{C}_6\text{H}_{14})_{1/2}$ Calc.: C, 76.2; H, 8.1.



5.8 Data obtained for reaction of 2.4 with I_2 .

IR: ν (cm^{-1} , dichloromethane) 2025, 1979.

Appendix A
Crystallographic Data.

A1 Crystallographic data for bis(1-phenyl-3-methyl-4,5,6,7-tetrahydroindenyl) iron(II), 2.3.

Empirical formula	C ₃₂ H ₃₄ Fe
Formula weight	474.44
Temperature	150(2) K
Wavelength	0.71073 Å
Crystal system	Monoclinic
Space group	P2(1)/c
Unit cell dimensions	a = 9.021(1) Å alpha = 90° b = 13.778(1) Å beta = 94.19(1)° c = 9.600(1) Å gamma = 90°
Volume, Z	1190.0(2) Å ³ , 2
Density (calculated)	1.324 Mg/m ³
Absorption coefficient	0.652 mm ⁻¹
F(000)	504
Crystal size	0.30 x 0.30 x 0.15 mm
Theta range for data collection	2.26 to 25.47°
Limiting indices	-10 ≤ h ≤ 8, -16 ≤ k ≤ 16, -11 ≤ l ≤ 10
Reflections collected	5882
Independent reflections	1974 [R(int) = 0.0679]
Absorption correction	Semi-empirical from psi-scans
Max. and min. transmission	0.9099 and 0.7742
Refinement method	Full-matrix least-squares on F ²
Data / restraints / parameters	1935 / 0 / 167
Goodness-of-fit on F ²	1.222
Final R indices [I > 2σ(I)]	R1 = 0.0669, wR2 = 0.1308
R indices (all data)	R1 = 0.0980, wR2 = 0.1891
Largest diff. peak and hole	0.734 and -0.524 e.Å ⁻³

Atomic coordinates ($\times 10^4$) and equivalent isotropic displacement parameters ($\text{\AA}^2 \times 10^3$) for **2.3**. U(eq) is defined as one third of the trace of the orthogonalized Uij tensor.

	x	y	z	U(eq)
Fe	0	5000	0	35(1)
C(1)	-307(5)	4246(3)	1801(5)	31(1)
C(2)	703(5)	5050(4)	2100(5)	37(1)
C(3)	1946(6)	4941(4)	1314(5)	43(1)
C(4)	2822(6)	3653(5)	-465(6)	52(2)
C(5)	2068(6)	2819(5)	-1293(6)	51(2)
C(6)	1293(7)	2144(5)	-336(6)	51(2)
C(7)	-53(6)	2651(4)	238(6)	42(1)
C(8)	383(6)	3626(4)	810(5)	35(1)
C(9)	1759(5)	4089(4)	531(5)	34(1)
C(10)	3294(7)	5601(5)	1379(7)	60(2)
C(11)	-1689(5)	4073(4)	2495(5)	34(1)
C(12)	-2767(6)	3385(4)	2019(6)	42(1)
C(13)	-4016(6)	3218(5)	2748(6)	49(2)
C(14)	-4217(7)	3720(5)	3970(7)	60(2)
C(15)	-3175(7)	4386(5)	4461(7)	60(2)
C(16)	-1933(6)	4562(4)	3727(6)	45(1)

Bond lengths [\AA] and angles [$^\circ$] for **2.3**.

Fe-C(1)	2.054(5)	C(1)-C(8)	1.452(7)
Fe-C(9)	2.058(5)	C(1)-C(11)	1.474(7)
Fe-C(8)	2.066(5)	C(3)-C(10)	1.517(7)
Fe-C(2)	2.070(5)	C(4)-C(9)	1.526(7)
Fe-C(3)	2.087(5)	C(7)-C(8)	1.493(7)
C(1)-C(2)	1.450(7)	C(4)-C(5)	1.528(8)
C(2)-C(3)	1.405(7)	C(5)-C(6)	1.514(8)
C(3)-C(9)	1.397(8)	C(6)-C(7)	1.538(8)
C(8)-C(9)	1.438(7)	C(11)-C(12)	1.411(7)

Appendix A: Crystallographic Data.

C(12)-C(13)	1.388(7)	C(9)-C(3)-Fe	69.2(3)
C(13)-C(14)	1.386(9)	C(2)-C(3)-Fe	69.6(3)
C(14)-C(15)	1.372(9)	C(10)-C(3)-Fe	129.6(4)
C(15)-C(16)	1.388(8)	C(9)-C(4)-C(5)	110.2(5)
C(11)-C(16)	1.392(7)	C(6)-C(5)-C(4)	110.8(5)
C(1)-Fe-C(9)	68.4(2)	C(5)-C(6)-C(7)	110.5(5)
C(1)-Fe-C(8)	41.3(2)	C(8)-C(7)-C(6)	110.3(5)
C(9)-Fe-C(8)	40.8(2)	C(9)-C(8)-C(1)	106.2(4)
C(1)-Fe-C(2)	41.2(2)	C(9)-C(8)-C(7)	122.6(5)
C(9)-Fe-C(2)	66.6(2)	C(1)-C(8)-C(7)	131.0(5)
C(8)-Fe-C(2)	68.5(2)	C(9)-C(8)-Fe	69.3(3)
C(1)-Fe-C(3)	68.3(2)	C(1)-C(8)-Fe	68.9(3)
C(9)-Fe-C(3)	39.4(2)	C(7)-C(8)-Fe	130.8(4)
C(8)-Fe-C(3)	68.1(2)	C(3)-C(9)-C(8)	110.1(4)
C(2)-Fe-C(3)	39.5(2)	C(3)-C(9)-C(4)	127.7(5)
C(2)-C(1)-C(8)	106.6(4)	C(8)-C(9)-C(4)	122.2(5)
C(2)-C(1)-C(11)	125.0(4)	C(3)-C(9)-Fe	71.4(3)
C(8)-C(1)-C(11)	128.2(5)	C(8)-C(9)-Fe	69.9(3)
C(2)-C(1)-Fe	70.0(3)	C(4)-C(9)-Fe	126.4(4)
C(8)-C(1)-Fe	69.8(3)	C(16)-C(11)-C(12)	116.9(5)
C(11)-C(1)-Fe	129.2(3)	C(16)-C(11)-C(1)	119.8(5)
C(3)-C(2)-C(1)	109.1(5)	C(12)-C(11)-C(1)	123.2(5)
C(3)-C(2)-Fe	70.9(3)	C(13)-C(12)-C(11)	121.0(5)
C(1)-C(2)-Fe	68.8(3)	C(14)-C(13)-C(12)	120.3(6)
C(9)-C(3)-C(2)	108.0(5)	C(15)-C(14)-C(13)	119.8(6)
C(9)-C(3)-C(10)	126.3(5)	C(14)-C(15)-C(16)	120.1(6)
C(2)-C(3)-C(10)	125.6(6)	C(15)-C(16)-C(11)	122.0(6)

Symmetry transformations used to generate equivalent atoms: **2.3** $-x, -y+1, -z$

Anisotropic displacement parameters ($\text{\AA}^2 \times 10^3$) for **2.3**. The anisotropic displacement factor exponent takes the form: $-2 \pi^2 [h^2 a^{*2} U_{11} + \dots + 2 h k a^* b^* U_{12}]$

	U11	U22	U33	U23	U13	U12
Fe	30(1)	42(1)	35(1)	13(1)	6(1)	3(1)
C(1)	33(3)	31(3)	29(3)	8(2)	2(2)	8(2)
C(2)	39(3)	35(3)	37(3)	8(3)	0(2)	0(3)
C(3)	37(3)	45(3)	44(3)	16(3)	-5(2)	-7(3)
C(4)	32(3)	75(5)	50(4)	19(3)	10(3)	13(3)
C(5)	46(3)	73(4)	33(3)	-3(3)	7(3)	21(3)
C(6)	55(4)	59(4)	40(3)	-9(3)	3(3)	12(3)
C(7)	43(3)	46(3)	36(3)	-6(3)	-1(3)	-1(3)
C(8)	35(3)	39(3)	30(3)	8(2)	3(2)	3(2)
C(9)	28(3)	43(3)	32(3)	12(2)	3(2)	5(2)
C(10)	46(3)	67(4)	67(4)	19(4)	-3(3)	-19(3)
C(11)	32(3)	36(3)	36(3)	7(2)	12(2)	4(2)
C(12)	39(3)	47(3)	41(3)	6(3)	11(3)	0(3)
C(13)	36(3)	57(4)	56(4)	13(3)	6(3)	-7(3)
C(14)	46(4)	70(5)	67(4)	12(4)	29(3)	5(3)
C(15)	64(4)	72(5)	48(4)	-9(3)	24(3)	15(4)
C(16)	45(3)	45(3)	47(3)	-7(3)	17(3)	-2(3)

Hydrogen coordinates ($\times 10^4$) and isotropic displacement parameters ($\text{\AA}^2 \times 10^3$) for **2.3**.

	x	y	z	U(eq)
H(2)	542(5)	5570(4)	2720(5)	21(12)
H(4A)	3727(6)	3413(5)	72(6)	68(20)
H(4B)	3125(6)	4158(5)	-1120(6)	77(22)
H(5A)	1339(6)	3081(5)	-2018(6)	48(16)
H(5B)	2826(6)	2451(5)	-1768(6)	48(16)
H(6A)	1997(7)	1941(5)	448(6)	57(18)
H(6B)	958(7)	1555(5)	-860(6)	53(17)
H(7A)	-856(6)	2726(4)	-514(6)	31(13)

Appendix A: Crystallographic Data.

H(7B)	-435(6)	2249(4)	987(6)	72(21)
H(10A)	3681(26)	5631(22)	452(12)	72(12)
H(10B)	4066(17)	5350(16)	2055(30)	72(12)
H(10C)	3002(11)	6253(8)	1660(38)	72(12)
H(12)	-2640(6)	3036(4)	1184(6)	53(17)
H(13)	-4729(6)	2752(5)	2406(6)	66(20)
H(14)	-5078(7)	3606(5)	4458(7)	58(18)
H(15)	-3301(7)	4723(5)	5307(7)	65(19)
H(16)	-1231(6)	5033(4)	4073(6)	34(13)

A2 Crystallographic data for 1-phenyl-3-methyl-4,5,6,7-tetrahydroindenyl iron dicarbonyl dimer, 2.4.

Empirical formula	C ₃₆ H ₃₄ Fe ₂ O ₄
Formula weight	642.33
Temperature	150(2) K
Wavelength	0.71073 Å
Crystal system	Monoclinic
Space group	P2(1)/c
Unit cell dimensions	a = 11.4440(10) Å alpha = 90° b = 11.2110(10) Å beta = 103.050(10)° c = 11.5270(10) Å gamma = 90°
Volume, Z	1440.7(2) Å ³ , 2
Density (calculated)	1.481 Mg/m ³
Absorption coefficient	1.047 mm ⁻¹
F(000)	668
Crystal size	0.58 x 0.48 x 0.20 mm
Theta range for data collection	1.83 to 30.12°
Limiting indices	-15<=h<=15, -15<=k<=15, -15<=l<=16
Reflections collected	14599
Independent reflections	3961 [R(int) = 0.0360]
Refinement method	Full-matrix least-squares on F ²
Data / restraints / parameters	3949 / 0 / 258
Goodness-of-fit on F ²	1.103
Final R indices [I>2sigma(I)]	R1 = 0.0271, wR2 = 0.0686
R indices (all data)	R1 = 0.0318, wR2 = 0.0754
Largest diff. peak and hole	0.406 and -0.400 e.Å ⁻³

Atomic coordinates ($\times 10^4$) and equivalent isotropic displacement parameters ($\text{\AA}^2 \times 10^3$) for 2.4. $U(\text{eq})$ is defined as one third of the trace of the orthogonalized U_{ij} tensor.

	x	y	z	$U(\text{eq})$
Fe	1097(1)	5103(1)	547(1)	17(1)
O(1)	2175(1)	4313(1)	-1373(1)	37(1)
O(2)	-16(1)	2789(1)	763(1)	34(1)
C(O1)	1700(1)	4618(1)	-641(1)	24(1)
C(O2)	-1(1)	3779(1)	421(1)	23(1)
C(1)	2280(1)	6426(1)	1468(1)	17(1)
C(2)	1273(1)	6326(1)	2009(1)	19(1)
C(3)	1226(1)	5150(1)	2470(1)	21(1)
C(9)	2204(1)	4498(1)	2208(1)	21(1)
C(8)	2855(1)	5271(1)	1587(1)	20(1)
C(4)	2589(1)	3242(1)	2572(2)	29(1)
C(5)	3908(2)	3047(2)	2542(2)	35(1)
C(6)	4183(2)	3536(2)	1397(2)	36(1)
C(7)	4028(1)	4898(1)	1307(2)	27(1)
C(10)	390(2)	4721(2)	3214(2)	31(1)
C(11)	2683(1)	7547(1)	1005(1)	18(1)
C(16)	2601(1)	8616(1)	1608(1)	22(1)
C(15)	2984(1)	9692(1)	1208(2)	26(1)
C(14)	3473(1)	9708(1)	207(2)	28(1)
C(13)	3560(1)	8654(1)	-400(1)	27(1)
C(12)	3163(1)	7584(1)	-14(1)	23(1)

Bond lengths [\AA] and angles [$^\circ$] for 2.4.

Fe-C(O1)	1.753(2)	Fe-C(9)	2.1525(14)
Fe-C(O2)	1.9295(14)	O(1)-C(O1)	1.154(2)
Fe-C(1)	2.1231(13)	O(2)-C(O2)	1.179(2)
Fe-C(2)	2.1460(13)	C(1)-C(2)	1.434(2)
Fe-C(3)	2.1882(14)	C(2)-C(3)	1.426(2)
Fe-C(8)	2.1044(13)	C(3)-C(9)	1.425(2)

Appendix A: Crystallographic Data.

C(1)-C(8)	1.445(2)	C(O2-Fe-C(3))	89.33(6)
C(9)-C(8)	1.435(2)	C(8)-Fe-C(3)	65.41(5)
C(1)-C(11)	1.479(2)	C(1)-Fe-C(3)	65.65(5)
C(3)-C(10)	1.501(2)	C(2)-Fe-C(3)	38.41(5)
C(9)-C(4)	1.506(2)	C(9)-Fe-C(3)	38.32(5)
C(8)-C(7)	1.509(2)	O(1)-C(O1-Fe)	175.20(14)
C(4)-C(5)	1.533(2)	O(2)-C(O2-Fe)	139.22(12)
C(5)-C(6)	1.527(3)	C(2)-C(1)-C(8)	106.36(11)
C(6)-C(7)	1.538(2)	C(2)-C(1)-C(11)	124.75(12)
C(11)-C(16)	1.398(2)	C(8)-C(1)-C(11)	128.60(11)
C(16)-C(15)	1.397(2)	C(2)-C(1)-Fe	71.24(7)
C(15)-C(14)	1.392(2)	C(8)-C(1)-Fe	69.32(7)
C(14)-C(13)	1.388(2)	C(11)-C(1)-Fe	128.99(9)
C(13)-C(12)	1.391(2)	C(3)-C(2)-C(1)	109.61(12)
C(11)-C(12)	1.406(2)	C(3)-C(2)-Fe	72.39(8)
C(O1-Fe-C(O2	93.86(7)	C(1)-C(2)-Fe	69.51(7)
C(O1-Fe-C(8)	88.80(6)	C(9)-C(3)-C(2)	107.35(12)
C(O2-Fe-C(8)	129.37(6)	C(9)-C(3)-C(10)	126.07(13)
C(O1-Fe-C(1)	106.75(6)	C(2)-C(3)-C(10)	126.24(14)
C(O2-Fe-C(1)	154.95(6)	C(9)-C(3)-Fe	69.48(8)
C(8)-Fe-C(1)	39.97(5)	C(2)-C(3)-Fe	69.19(8)
C(O1-Fe-C(2)	145.90(6)	C(10)-C(3)-Fe	131.69(10)
C(O2-Fe-C(2)	119.61(6)	C(3)-C(9)-C(8)	108.47(12)
C(8)-Fe-C(2)	65.67(5)	C(3)-C(9)-C(4)	127.98(13)
C(1)-Fe-C(2)	39.25(5)	C(8)-C(9)-C(4)	123.42(13)
C(O1-Fe-C(9)	109.95(6)	C(3)-C(9)-Fe	72.20(8)
C(O2-Fe-C(9)	93.83(6)	C(8)-C(9)-Fe	68.51(8)
C(8)-Fe-C(9)	39.37(5)	C(4)-C(9)-Fe	128.22(10)
C(1)-Fe-C(9)	66.13(5)	C(9)-C(8)-C(1)	108.20(11)
C(2)-Fe-C(9)	64.61(5)	C(9)-C(8)-C(7)	121.82(13)
C(O1-Fe-C(3)	148.27(6)	C(1)-C(8)-C(7)	129.44(12)

C(9)-C(8)-Fe	72.12(7)	C(16)-C(11)-C(1)	119.20(12)
C(1)-C(8)-Fe	70.71(7)	C(12)-C(11)-C(1)	122.60(12)
C(7)-C(8)-Fe	129.44(10)	C(15)-C(16)-C(11)	120.97(13)
C(9)-C(4)-C(5)	110.79(13)	C(14)-C(15)-C(16)	119.97(14)
C(6)-C(5)-C(4)	111.36(13)	C(13)-C(14)-C(15)	119.68(14)
C(5)-C(6)-C(7)	111.83(14)	C(14)-C(13)-C(12)	120.45(14)
C(8)-C(7)-C(6)	110.78(13)	C(13)-C(12)-C(11)	120.71(13)
C(16)-C(11)-C(12)	118.19(12)		

Symmetry transformations used to generate equivalent atoms: 1 -x,-y+1,-z

Anisotropic displacement parameters ($\text{\AA}^2 \times 10^3$) for 2.4. The anisotropic displacement factor exponent takes the form: $-2 \pi^2 [h^2 a^{*2} U_{11} + \dots + 2 h k a^* b^* U_{12}]$

	U11	U22	U33	U23	U13	U12
Fe	15(1)	15(1)	20(1)	-2(1)	1(1)	-2(1)
O(1)	42(1)	39(1)	33(1)	-7(1)	14(1)	6(1)
O(2)	31(1)	21(1)	43(1)	8(1)	-8(1)	-7(1)
C(O1)	23(1)	21(1)	26(1)	-3(1)	2(1)	-1(1)
C(O2)	20(1)	20(1)	24(1)	-1(1)	-2(1)	-4(1)
C(1)	15(1)	16(1)	20(1)	-2(1)	2(1)	-2(1)
C(2)	17(1)	19(1)	21(1)	-3(1)	4(1)	-2(1)
C(3)	20(1)	22(1)	20(1)	0(1)	1(1)	-5(1)
C(9)	20(1)	18(1)	22(1)	0(1)	-2(1)	-2(1)
C(8)	16(1)	19(1)	22(1)	-3(1)	0(1)	-1(1)
C(4)	29(1)	19(1)	35(1)	3(1)	-6(1)	-2(1)
C(5)	30(1)	22(1)	47(1)	0(1)	-6(1)	7(1)
C(6)	28(1)	30(1)	47(1)	-7(1)	3(1)	11(1)
C(7)	17(1)	27(1)	36(1)	-4(1)	4(1)	3(1)
C(10)	29(1)	36(1)	28(1)	4(1)	7(1)	-9(1)
C(11)	14(1)	18(1)	21(1)	0(1)	1(1)	-2(1)
C(16)	20(1)	19(1)	26(1)	-2(1)	6(1)	-1(1)

C(15)	26(1)	17(1)	36(1)	-1(1)	5(1)	-2(1)
C(14)	23(1)	24(1)	35(1)	9(1)	3(1)	-3(1)
C(13)	24(1)	32(1)	24(1)	6(1)	5(1)	-3(1)
C(12)	23(1)	24(1)	22(1)	-2(1)	4(1)	-3(1)

Hydrogen coordinates ($\times 10^4$) and isotropic parameters ($\text{\AA}^2 \times 10^3$) for 2.4.

	x	y	z	U(eq)
H(2)	707(17)	6945(17)	2050(16)	26(5)
H(41)	2448(18)	3094(18)	3406(18)	33(5)
H(42)	2067(19)	2716(19)	2059(19)	37(5)
H(51)	4480(18)	3452(18)	3253(18)	33(5)
H(52)	4141(22)	2166(22)	2663(22)	53(7)
H(61)	5052(21)	3344(20)	1389(20)	45(6)
H(62)	3634(19)	3134(19)	679(19)	38(5)
H(71)	4665(20)	5243(19)	1884(19)	36(5)
H(72)	4083(19)	5200(18)	526(20)	34(5)
H(101)	-270(24)	5243(23)	3189(23)	54(7)
H(102)	96(22)	3995(24)	2970(22)	56(7)
H(103)	810(23)	4648(23)	4025(24)	56(7)
H(16)	2286(16)	8590(16)	2305(16)	25(4)
H(15)	2932(18)	10386(19)	1655(18)	33(5)
H(14)	3710(20)	10405(21)	-100(20)	41(6)
H(13)	3887(19)	8659(19)	-1104(20)	38(5)
H(12)	3196(17)	6857(18)	-445(17)	30(5)

A3 Crystallographic data for 1-phenyl-3-methyl-4,5,6,7-tetrahydroindenyl methyl iron(II) dicarbonyl, 2.5.

Empirical formula	C ₁₉ H ₂₀ Fe O ₂
Formula weight	336.20
Temperature	150(2) K
Wavelength	0.71073 Å
Crystal system	Monoclinic
Space group	P2(1)/n
Unit cell dimensions	a = 10.3593(8) Å alpha = 90° b = 9.3123(6) Å beta = 106.95(1)° c = 17.6347(13) Å gamma = 90°
Volume, Z	1627.3(2) Å ³ , 4
Density (calculated)	1.372 g/cm ³
Absorption coefficient	0.931 mm ⁻¹
F(000)	704
Crystal size	0.34 x 0.26 x 0.20 mm
Theta range for data collection	2.06 to 27.49°
Limiting indices	-13<=h<=12, -11<=k<=12, -22<=l<=22
Reflections collected	11260
Independent reflections	3711 [R(int) = 0.0268]
Absorption correction	Multiscan
Max. and min. transmission	0.8311 and 0.7586
Refinement method	Full-matrix least-squares on F ²
Data / restraints / parameters	3702 / 0 / 279
Goodness-of-fit on F ²	1.086
Final R indices [I>2sigma(I)]	R1 = 0.0352, wR2 = 0.0804
R indices (all data)	R1 = 0.0544, wR2 = 0.0947
Largest diff. peak and hole	0.792 and -0.346 e.Å ⁻³

Atomic coordinates ($\times 10^4$) and equivalent isotropic displacement parameters ($\text{\AA}^2 \times 10^4$) for **2.5**. U(eq) is defined as one third of the trace of the orthogonalized Uij tensor.

	x	y	z	U(eq)
Fe	2266.3(3)	2507.7(3)	331.6(2)	193(1)
C(1)	4367(2)	2695(2)	869(1)	202(4)
C(2)	4093(2)	2386(2)	34(1)	206(4)
C(3)	3450(2)	1027(2)	-127(1)	217(4)
C(4)	2795(3)	-962(3)	759(2)	324(6)
C(5)	2727(3)	-1076(4)	1615(2)	470(8)
C(6)	3922(4)	-376(3)	2219(2)	472(8)
C(7)	3985(3)	1240(3)	2075(1)	295(5)
C(8)	3861(2)	1525(2)	1214(1)	210(4)
C(9)	3281(2)	501(2)	599(1)	223(4)
C(10)	3072(3)	253(3)	-906(2)	299(5)
C(11)	5203(2)	3902(2)	1303(1)	220(4)
C(12)	4793(3)	4795(3)	1824(2)	326(6)
C(13)	5652(3)	5873(3)	2239(2)	385(6)
C(14)	6918(3)	6050(3)	2147(2)	376(6)
C(15)	7343(3)	5165(3)	1635(2)	337(6)
C(16)	6490(2)	4100(3)	1213(1)	260(5)
C(17)	749(3)	2176(3)	-709(2)	299(5)
C(01)	1959(2)	4361(3)	208(1)	281(5)
O(1)	1756(2)	5575(2)	139(1)	455(5)
C(02)	1025(2)	2263(2)	812(1)	285(5)
O(2)	191(2)	2097(2)	1118(1)	453(5)

Bond lengths [\AA] and angles [$^\circ$] for **2.5**.

Fe-C(02)	1.748(2)	Fe-C(3)	2.153(2)
Fe-C(01)	1.757(2)	Fe-C(8)	2.118(2)
Fe-C(17)	2.062(2)	Fe-C(9)	2.129(2)
Fe-C(1)	2.113(2)	C(1)-C(2)	1.445(3)
Fe-C(2)	2.109(2)	C(2)-C(3)	1.419(3)

Appendix A: Crystallographic Data.

C(3)-C(9)	1.428(3)	C(3)-C(2)-C(1)	108.8(2)
C(1)-C(8)	1.421(3)	C(2)-C(3)-C(9)	107.4(2)
C(8)-C(9)	1.438(3)	C(2)-C(3)-C(10)	126.5(2)
C(1)-C(11)	1.487(3)	C(9)-C(3)-C(10)	126.0(2)
C(3)-C(10)	1.498(3)	C(9)-C(4)-C(5)	111.1(2)
C(4)-C(9)	1.507(3)	C(6)-C(5)-C(4)	113.3(2)
C(4)-C(5)	1.535(4)	C(5)-C(6)-C(7)	111.7(2)
C(5)-C(6)	1.524(4)	C(8)-C(7)-C(6)	110.2(2)
C(6)-C(7)	1.531(4)	C(1)-C(8)-C(9)	108.1(2)
C(7)-C(8)	1.509(3)	C(1)-C(8)-C(7)	129.2(2)
C(11)-C(12)	1.395(3)	C(9)-C(8)-C(7)	122.4(2)
C(11)-C(16)	1.400(3)	C(3)-C(9)-C(8)	108.3(2)
C(12)-C(13)	1.398(4)	C(3)-C(9)-C(4)	127.8(2)
C(13)-C(14)	1.378(4)	C(8)-C(9)-C(4)	123.1(2)
C(14)-C(15)	1.385(4)	C(12)-C(11)-C(16)	118.7(2)
C(15)-C(16)	1.392(3)	C(12)-C(11)-C(1)	123.1(2)
C(01)-O(1)	1.149(3)	C(16)-C(11)-C(1)	118.1(2)
C(02)-O(2)	1.155(3)	C(11)-C(12)-C(13)	120.2(3)
C(02)-Fe-C(01)	93.18(11)	C(14)-C(13)-C(12)	120.5(3)
C(02)-Fe-C(17)	86.22(11)	C(13)-C(14)-C(15)	120.0(2)
C(01)-Fe-C(17)	88.46(11)	C(14)-C(15)-C(16)	120.0(3)
C(8)-C(1)-C(2)	107.2(2)	C(15)-C(16)-C(11)	120.7(2)
C(8)-C(1)-C(11)	126.3(2)	O(1)-C(01)-Fe	179.0(2)
C(2)-C(1)-C(11)	125.9(2)	O(2)-C(02)-Fe	178.9(2)

Anisotropic displacement parameters ($\text{\AA}^2 \times 10^4$) for **2.5**. The anisotropic displacement factor exponent takes the form: $-2 \pi^2 [h^2 a^{*2} U_{11} + \dots + 2 h k a^* b^* U_{12}]$

	U11	U22	U33	U23	U13	U12
Fe	174(2)	196(2)	208(2)	-1(1)	56(1)	11(1)
C(1)	167(10)	208(11)	221(10)	-5(8)	39(8)	17(8)
C(2)	180(10)	223(10)	221(10)	7(9)	67(8)	24(9)
C(3)	179(10)	219(10)	239(11)	-31(8)	41(8)	24(8)
C(4)	295(13)	233(12)	424(15)	-3(11)	71(11)	-58(10)

Appendix A: Crystallographic Data.

C(5)	520(20)	410(20)	430(20)	150(13)	48(14)	-149(15)
C(6)	590(20)	420(20)	360(20)	138(13)	63(14)	-89(15)
C(7)	311(13)	324(13)	234(12)	56(10)	56(10)	-13(11)
C(8)	193(11)	206(10)	217(11)	14(8)	36(8)	18(8)
C(9)	185(10)	195(10)	274(11)	6(9)	44(9)	6(8)
C(10)	286(13)	305(13)	291(13)	-95(10)	63(10)	22(11)
C(11)	234(11)	189(10)	206(10)	24(8)	15(8)	-8(9)
C(12)	332(14)	341(14)	308(13)	-57(10)	99(11)	-24(11)
C(13)	560(20)	297(14)	252(13)	-63(10)	55(12)	7(12)
C(14)	490(20)	292(13)	248(12)	5(10)	-41(11)	-149(12)
C(15)	315(14)	342(14)	299(13)	74(10)	2(11)	-124(11)
C(16)	266(12)	247(12)	254(11)	21(9)	57(9)	-41(9)
C(17)	213(12)	370(20)	280(12)	-26(10)	19(9)	12(10)
C(01)	228(12)	296(13)	326(13)	-5(10)	92(10)	20(10)
O(1)	503(12)	255(10)	668(14)	38(9)	266(11)	82(9)
C(02)	290(12)	279(13)	292(12)	24(9)	95(10)	26(10)
O(2)	410(11)	568(12)	482(12)	59(10)	286(10)	1(9)

Hydrogen coordinates ($\times 10^4$) and isotropic displacement parameters ($\text{\AA}^2 \times 10^3$) for **2.5**.

	x	y	z	U(eq)
H(2)	4298(25)	3013(28)	-342(15)	27(7)
H(41)	3430(31)	-1683(33)	646(17)	45(8)
H(42)	1934(31)	-1192(31)	401(17)	41(8)
H(51)	2661(32)	-2092(36)	1739(19)	50(9)
H(52)	1934(38)	-451(39)	1717(21)	70(11)
H(61)	4799(43)	-987(44)	2126(22)	84(13)
H(62)	3858(32)	-579(34)	2797(20)	57(9)
H(71)	4886(30)	1660(30)	2429(17)	41(8)
H(72)	3251(31)	1705(32)	2228(17)	44(8)
H(101)	3762(36)	-365(38)	-893(20)	61(10)
H(102)	2294(34)	-298(34)	-991(18)	51(9)
H(103)	2992(31)	917(34)	-1334(19)	49(9)
H(12)	3973(29)	4672(29)	1886(16)	33(7)

Appendix A: Crystallographic Data.

H(13)	5349(27)	6475(30)	2580(17)	35(7)
H(14)	7449(32)	6730(33)	2411(18)	45(8)
H(15)	8181(32)	5247(33)	1606(18)	47(9)
H(16)	6779(25)	3487(27)	870(15)	23(6)
H(171)	473(28)	1203(32)	-736(16)	36(8)
H(172)	-27(26)	2821(26)	-776(14)	23(6)
H(173)	1089(29)	2346(29)	-1138(18)	38(8)

A4 Crystallographic data for bis(1-phenyl-3-methyl-4,5,6,7-tetrahydroindenyl) zirconium dichloride, 3.1.

Empirical formula	C ₃₂ H ₃₄ Cl ₂ Zr
Formula weight	580.71
Temperature	150(2) K
Wavelength	0.71073 Å
Crystal system	Orthorhombic
Space group	P2(1)2(1)2(1)
Unit cell dimensions	a = 11.34250(10) Å alpha = 90° b = 14.7866(2) Å beta = 90° c = 15.81420(10) Å gamma = 90°
Volume, Z	2652.31(5) Å ³ , 4
Density (calculated)	1.454 Mg/m ³
Absorption coefficient	0.636 mm ⁻¹
F(000)	1200
Crystal size	0.38 x 0.18 x 0.16 mm
Theta range for data collection	1.89 to 27.50°
Limiting indices	-14<=h<=14, -19<=k<=16, -20<=l<=20
Reflections collected	21504
Independent reflections	6091 [R(int) = 0.0347]
Absorption correction	Multiscan
Max. and min. transmission	0.805261 and 0.894391
Refinement method	Full-matrix least-squares on F ²
Data / restraints / parameters	6088 / 0 / 453
Goodness-of-fit on F ²	1.039
Final R indices [I>2sigma(I)]	R1 = 0.0236, wR2 = 0.0453
R indices (all data)	R1 = 0.0346, wR2 = 0.0497
Largest diff. peak and hole	0.298 and -0.285 e.Å ⁻³

Atomic coordinates ($\times 10^4$) and equivalent isotropic displacement parameters ($\text{\AA}^2 \times 10^3$) for 3.1. $U(\text{eq})$ is defined as one third of the trace of the orthogonalized U_{ij} tensor.

	x	y	z	$U(\text{eq})$
Zr(1)	6279(1)	4681(1)	1154(1)	15(1)
Cl(1)	4400(1)	4474(1)	420(1)	22(1)
Cl(2)	7572(1)	4574(1)	-81(1)	25(1)
C(1)	5710(2)	3579(2)	2284(1)	21(1)
C(2)	6883(2)	3892(2)	2478(2)	22(1)
C(3)	7677(2)	3551(2)	1874(1)	23(1)
C(4)	7491(2)	2448(2)	582(2)	28(1)
C(5)	6487(2)	2085(2)	34(2)	34(1)
C(6)	5522(2)	1687(2)	587(2)	33(1)
C(7)	4923(2)	2407(2)	1134(2)	25(1)
C(8)	5820(2)	3010(2)	1549(1)	20(1)
C(9)	7013(2)	3017(1)	1299(1)	20(1)
C(11)	4646(2)	3764(2)	2795(1)	24(1)
C(12)	3506(2)	3619(2)	2486(2)	32(1)
C(13)	2520(3)	3821(2)	2977(2)	44(1)
C(14)	2652(3)	4189(2)	3779(2)	46(1)
C(15)	3761(3)	4331(2)	4095(2)	41(1)
C(16)	4751(2)	4117(2)	3619(2)	31(1)
C(10)	8992(2)	3642(2)	1876(2)	30(1)
C(17)	7277(2)	6053(1)	1740(1)	16(1)
C(18)	6257(2)	5865(1)	2253(1)	18(1)
C(19)	5234(2)	6046(2)	1780(1)	19(1)
C(20)	4852(2)	6704(2)	263(1)	22(1)
C(21)	5559(2)	6748(2)	-561(2)	28(1)
C(22)	6709(2)	7259(2)	-418(2)	27(1)
C(23)	7528(2)	6779(2)	218(2)	23(1)
C(24)	6858(2)	6371(2)	943(1)	17(1)
C(25)	5598(2)	6351(1)	966(1)	18(1)
C(27)	8514(2)	6013(2)	2033(1)	18(1)

C(28)	8768(2)	6090(2)	2898(1)	26(1)
C(29)	9917(2)	6044(2)	3192(2)	33(1)
C(30)	10846(2)	5947(2)	2632(2)	30(1)
C(31)	10612(2)	5873(2)	1773(2)	28(1)
C(32)	9463(2)	5913(2)	1476(2)	24(1)
C(26)	3973(2)	6015(2)	2075(2)	24(1)

Selected bond lengths [Å] and angles [°] for 3.1.

Zr(1)-Cl(1)	2.4470(5)	C(11)-C(12)	1.398(4)
Zr(1)-Cl(2)	2.4477(5)	C(12)-C(13)	1.394(4)
Zr(1)-C(1)	2.504(2)	C(13)-C(14)	1.389(4)
Zr(1)-C(2)	2.492(2)	C(14)-C(15)	1.370(4)
Zr(1)-C(3)	2.569(2)	C(15)-C(16)	1.389(4)
Zr(1)-C(8)	2.601(2)	C(11)-C(16)	1.409(3)
Zr(1)-C(9)	2.607(2)	C(17)-C(18)	1.440(3)
Zr(1)-C(17)	2.501(2)	C(18)-C(19)	1.407(3)
Zr(1)-C(18)	2.467(2)	C(19)-C(25)	1.424(3)
Zr(1)-C(19)	2.543(2)	C(24)-C(25)	1.429(3)
Zr(1)-C(24)	2.605(2)	C(17)-C(24)	1.426(3)
Zr(1)-C(25)	2.604(2)	C(17)-C(27)	1.480(3)
C(1)-C(2)	1.442(3)	C(19)-C(26)	1.505(3)
C(2)-C(3)	1.406(3)	C(20)-C(25)	1.492(3)
C(3)-C(9)	1.421(3)	C(23)-C(24)	1.502(3)
C(8)-C(9)	1.410(3)		
C(1)-C(8)	1.441(3)	C(20)-C(21)	1.532(3)
C(1)-C(11)	1.478(3)	C(21)-C(22)	1.524(3)
C(3)-C(10)	1.497(3)	C(22)-C(23)	1.543(3)
C(4)-C(9)	1.513(3)	C(27)-C(28)	1.402(3)
C(7)-C(8)	1.503(3)	C(28)-C(29)	1.385(3)
C(4)-C(5)	1.528(4)	C(29)-C(30)	1.384(3)
C(5)-C(6)	1.519(4)	C(30)-C(31)	1.388(3)
C(6)-C(7)	1.530(4)	C(31)-C(32)	1.387(3)

Appendix A: Crystallographic Data.

C(27)-C(32)	1.398(3)	C(18)-Zr(1)-C(9)	127.67(7)
Cl(1)-Zr(1)-Cl(2)	97.78(2)	C(18)-Zr(1)-C(17)	33.68(7)
Cl(1)-Zr(1)-C(1)	91.88(5)	C(18)-Zr(1)-C(1)	87.49(7)
Cl(1)-Zr(1)-C(2)	125.42(6)	C(18)-Zr(1)-C(19)	32.58(7)
Cl(1)-Zr(1)-C(3)	131.82(5)	C(18)-Zr(1)-C(3)	98.94(7)
Cl(1)-Zr(1)-C(8)	79.66(5)	C(2)-Zr(1)-C(3)	32.20(7)
Cl(1)-Zr(1)-C(9)	101.65(5)	C(17)-Zr(1)-C(3)	94.83(8)
Cl(1)-Zr(1)-C(17)	132.15(5)	C(1)-Zr(1)-C(3)	54.51(8)
Cl(1)-Zr(1)-C(18)	114.45(6)	C(19)-Zr(1)-C(3)	129.18(7)
Cl(1)-Zr(1)-C(19)	82.96(5)	C(18)-Zr(1)-C(8)	120.19(7)
Cl(1)-Zr(1)-C(24)	106.18(5)	C(2)-Zr(1)-C(8)	53.78(7)
Cl(1)-Zr(1)-C(25)	78.81(5)	C(17)-Zr(1)-C(8)	140.57(7)
Cl(2)-Zr(1)-C(1)	133.05(5)	C(1)-Zr(1)-C(8)	32.72(7)
Cl(2)-Zr(1)-C(2)	118.40(6)	C(19)-Zr(1)-C(8)	124.57(7)
Cl(2)-Zr(1)-C(3)	86.70(5)	C(3)-Zr(1)-C(8)	53.11(7)
Cl(2)-Zr(1)-C(8)	104.53(5)	C(18)-Zr(1)-C(25)	53.43(7)
Cl(2)-Zr(1)-C(9)	79.54(5)	C(2)-Zr(1)-C(25)	128.37(7)
Cl(2)-Zr(1)-C(17)	94.40(5)	C(17)-Zr(1)-C(25)	53.63(7)
Cl(2)-Zr(1)-C(18)	127.87(5)	C(19)-Zr(1)-C(25)	32.09(7)
Cl(2)-Zr(1)-C(19)	129.87(5)	C(3)-Zr(1)-C(25)	148.21(7)
Cl(2)-Zr(1)-C(24)	78.96(5)	C(8)-Zr(1)-C(25)	150.28(7)
Cl(2)-Zr(1)-C(25)	98.49(5)	C(2)-Zr(1)-C(24)	119.15(7)
C(1)-Zr(1)-C(19)	96.82(7)	C(17)-Zr(1)-C(24)	32.35(7)
C(1)-Zr(1)-C(25)	128.46(7)	C(1)-Zr(1)-C(24)	141.32(7)
C(2)-Zr(1)-C(17)	86.80(7)	C(19)-Zr(1)-C(24)	53.51(7)
C(2)-Zr(1)-C(19)	99.96(7)	C(3)-Zr(1)-C(24)	121.67(7)
C(2)-Zr(1)-C(1)	33.54(7)	C(8)-Zr(1)-C(24)	172.91(7)
C(17)-Zr(1)-C(19)	54.71(6)	C(25)-Zr(1)-C(24)	31.85(6)
C(17)-Zr(1)-C(1)	112.34(7)	C(2)-Zr(1)-C(9)	52.91(7)
C(18)-Zr(1)-C(2)	75.12(7)	C(17)-Zr(1)-C(9)	126.07(7)
C(18)-Zr(1)-C(24)	53.98(7)	C(1)-Zr(1)-C(9)	53.52(7)

Appendix A: Crystallographic Data.

C(19)-Zr(1)-C(9)	149.79(7)	C(8)-C(9)-C(4)	123.3(2)
C(3)-Zr(1)-C(9)	31.85(7)	C(3)-C(9)-C(4)	126.8(2)
C(8)-Zr(1)-C(9)	31.42(7)	C(8)-C(9)-Zr(1)	74.07(13)
C(25)-Zr(1)-C(9)	178.01(7)	C(3)-C(9)-Zr(1)	72.61(12)
C(24)-Zr(1)-C(9)	146.72(7)	C(4)-C(9)-Zr(1)	125.0(2)
C(8)-C(1)-C(2)	106.2(2)	C(12)-C(11)-C(16)	117.2(2)
C(8)-C(1)-C(11)	128.3(2)	C(12)-C(11)-C(1)	122.4(2)
C(2)-C(1)-C(11)	125.3(2)	C(16)-C(11)-C(1)	120.3(2)
C(8)-C(1)-Zr(1)	77.37(12)	C(13)-C(12)-C(11)	121.0(3)
C(2)-C(1)-Zr(1)	72.80(13)	C(14)-C(13)-C(12)	120.4(3)
C(11)-C(1)-Zr(1)	118.7(2)	C(15)-C(14)-C(13)	119.5(3)
C(3)-C(2)-C(1)	109.4(2)	C(14)-C(15)-C(16)	120.6(3)
C(3)-C(2)-Zr(1)	76.90(13)	C(15)-C(16)-C(11)	121.2(3)
C(1)-C(2)-Zr(1)	73.66(13)	C(24)-C(17)-C(18)	107.1(2)
C(2)-C(3)-C(9)	107.1(2)	C(24)-C(17)-C(27)	127.3(2)
C(2)-C(3)-C(10)	127.1(2)	C(18)-C(17)-C(27)	125.3(2)
C(9)-C(3)-C(10)	125.4(2)	C(24)-C(17)-Zr(1)	77.84(13)
C(2)-C(3)-Zr(1)	70.89(13)	C(18)-C(17)-Zr(1)	71.85(12)
C(9)-C(3)-Zr(1)	75.54(12)	C(27)-C(17)-Zr(1)	120.8(2)
C(10)-C(3)-Zr(1)	123.9(2)	C(19)-C(18)-C(17)	109.0(2)
C(9)-C(4)-C(5)	110.7(2)	C(19)-C(18)-Zr(1)	76.66(12)
C(6)-C(5)-C(4)	110.3(2)	C(17)-C(18)-Zr(1)	74.47(12)
C(5)-C(6)-C(7)	112.1(2)	C(18)-C(19)-C(25)	107.5(2)
C(8)-C(7)-C(6)	111.0(2)	C(18)-C(19)-C(26)	127.8(2)
C(9)-C(8)-C(1)	107.7(2)	C(25)-C(19)-C(26)	124.5(2)
C(9)-C(8)-C(7)	122.1(2)	C(18)-C(19)-Zr(1)	70.76(11)
C(1)-C(8)-C(7)	129.8(2)	C(25)-C(19)-Zr(1)	76.34(12)
C(9)-C(8)-Zr(1)	74.51(13)	C(26)-C(19)-Zr(1)	122.6(2)
C(1)-C(8)-Zr(1)	69.91(12)	C(25)-C(20)-C(21)	110.6(2)
C(7)-C(8)-Zr(1)	126.4(2)	C(22)-C(21)-C(20)	110.0(2)
C(8)-C(9)-C(3)	109.5(2)	C(21)-C(22)-C(23)	112.5(2)

Appendix A: Crystallographic Data.

C(24)-C(23)-C(22)	112.3(2)	C(24)-C(25)-Zr(1)	74.11(13)
C(17)-C(24)-C(25)	107.7(2)	C(20)-C(25)-Zr(1)	125.8(2)
C(17)-C(24)-C(23)	129.7(2)	C(32)-C(27)-C(28)	117.7(2)
C(25)-C(24)-C(23)	122.2(2)	C(32)-C(27)-C(17)	122.4(2)
C(17)-C(24)-Zr(1)	69.81(12)	C(28)-C(27)-C(17)	119.8(2)
C(25)-C(24)-Zr(1)	74.04(13)	C(29)-C(28)-C(27)	121.1(2)
C(23)-C(24)-Zr(1)	127.7(2)	C(30)-C(29)-C(28)	120.4(2)
C(19)-C(25)-C(24)	108.7(2)	C(29)-C(30)-C(31)	119.3(2)
C(19)-C(25)-C(20)	128.2(2)	C(32)-C(31)-C(30)	120.5(2)
C(24)-C(25)-C(20)	122.7(2)	C(31)-C(32)-C(27)	120.9(2)
C(19)-C(25)-Zr(1)	71.57(12)		

Anisotropic displacement parameters ($\text{\AA}^2 \times 10^3$) for **3.1**. The anisotropic displacement factor exponent takes the form: $-2 \pi^2 [h^2 a^{*2} U_{11} + \dots + 2 h k a^* b^* U_{12}]$

	U11	U22	U33	U23	U13	U12
Zr(1)	15(1)	16(1)	15(1)	0(1)	-1(1)	0(1)
Cl(1)	21(1)	23(1)	23(1)	0(1)	-6(1)	-2(1)
Cl(2)	27(1)	28(1)	21(1)	-2(1)	6(1)	3(1)
C(1)	27(1)	17(1)	17(1)	4(1)	-2(1)	2(1)
C(2)	30(1)	17(1)	20(1)	1(1)	-6(1)	3(1)
C(3)	25(1)	20(1)	25(1)	3(1)	-6(1)	5(1)
C(4)	32(1)	21(1)	30(1)	-3(1)	-1(1)	8(1)
C(5)	45(2)	29(1)	27(1)	-9(1)	-3(1)	8(1)
C(6)	42(2)	21(1)	36(2)	-6(1)	-11(1)	-2(1)
C(7)	27(1)	20(1)	28(1)	6(1)	-3(1)	-5(1)
C(8)	27(1)	14(1)	19(1)	5(1)	-4(1)	1(1)
C(9)	25(1)	16(1)	18(1)	2(1)	-1(1)	4(1)
C(11)	30(1)	20(1)	23(1)	6(1)	6(1)	2(1)
C(12)	33(2)	32(1)	32(2)	3(1)	6(1)	-2(1)
C(13)	34(2)	44(2)	53(2)	9(2)	19(2)	-1(1)
C(14)	55(2)	35(2)	48(2)	12(1)	35(2)	7(1)

Appendix A: Crystallographic Data.

C(15)	70(2)	26(1)	29(1)	6(1)	19(2)	0(2)
C(16)	46(2)	24(1)	24(1)	8(1)	8(1)	0(1)
C(10)	22(1)	26(1)	42(2)	-1(1)	-9(1)	5(1)
C(17)	16(1)	15(1)	16(1)	0(1)	0(1)	-2(1)
C(18)	20(1)	17(1)	17(1)	-4(1)	1(1)	1(1)
C(19)	19(1)	18(1)	20(1)	-3(1)	1(1)	1(1)
C(20)	21(1)	20(1)	25(1)	2(1)	-6(1)	3(1)
C(21)	34(1)	28(1)	21(1)	6(1)	-9(1)	4(1)
C(22)	35(1)	26(1)	22(1)	8(1)	2(1)	0(1)
C(23)	22(1)	24(1)	22(1)	3(1)	2(1)	-6(1)
C(24)	19(1)	14(1)	17(1)	0(1)	1(1)	-1(1)
C(25)	17(1)	16(1)	22(1)	-1(1)	-1(1)	1(1)
C(27)	16(1)	19(1)	20(1)	3(1)	-1(1)	-3(1)
C(28)	23(1)	34(1)	20(1)	-1(1)	-1(1)	-3(1)
C(29)	28(1)	46(2)	25(1)	2(1)	-8(1)	-2(1)
C(30)	16(1)	40(2)	34(1)	6(1)	-8(1)	-3(1)
C(31)	17(1)	37(2)	30(1)	6(1)	3(1)	0(1)
C(32)	20(1)	32(1)	21(1)	2(1)	1(1)	-2(1)
C(26)	18(1)	27(1)	27(1)	-4(1)	1(1)	1(1)

Hydrogen coordinates ($\times 10^4$) and isotropic displacement parameters ($\text{\AA}^2 \times 10^3$) for 3.1.

	x	y	z	U(eq)
H(2)	7076(22)	4239(17)	2925(16)	32(7)
H(4B)	7908(21)	1947(17)	819(15)	25(6)
H(4A)	8025(21)	2818(16)	224(14)	22(6)
H(5A)	6246(26)	2617(19)	-315(17)	47(8)
H(5B)	6754(25)	1629(19)	-378(17)	44(8)
H(6B)	5883(21)	1233(17)	949(16)	33(7)
H(6A)	4851(23)	1376(17)	186(16)	39(7)
H(7B)	4451(22)	2139(16)	1538(15)	25(6)
H(7A)	4433(22)	2748(16)	809(15)	25(7)
H(12)	3383(22)	3374(17)	1938(17)	33(8)

Appendix A: Crystallographic Data.

H(13)	1816(25)	3718(18)	2739(17)	36(8)
H(14)	2060(28)	4332(22)	4104(20)	69(11)
H(15)	3889(23)	4596(19)	4640(17)	46(8)
H(16)	5497(23)	4237(17)	3849(16)	38(7)
H(10A)	9209(22)	4063(19)	2248(16)	32(7)
H(10C)	9371(20)	3802(15)	1336(16)	25(6)
H(10B)	9340(26)	3093(22)	2033(18)	5 1(9)
H(18)	6341(21)	5672(15)	2872(15)	30(6)
H(20B)	4602(21)	7318(17)	446(15)	25(6)
H(20A)	4123(24)	6330(18)	216(16)	39(8)
H(21A)	5732(19)	6132(17)	-783(14)	22(6)
H(21B)	5099(21)	7036(17)	-1012(16)	32(7)
H(22A)	7085(21)	7292(16)	-959(16)	33(7)
H(22B)	6488(19)	7892(15)	-196(13)	17(6)
H(23B)	8107(22)	7200(17)	410(15)	28(7)
H(23A)	7978(23)	6310(17)	-157(16)	33(7)
H(28)	8129(20)	6161(15)	3320(14)	21(6)
H(29)	10080(22)	6024(17)	3804(18)	42(7)
H(30)	11591(25)	5849(19)	2865(17)	41(8)
H(31)	11223(22)	5791(17)	1405(16)	40(7)
H(32)	9289(20)	5818(16)	905(15)	23(6)
H(26C)	3472(20)	5740(16)	1681(14)	27(7)
H(26B)	3730(25)	624(18)	2197(16)	35(7)
H(26A)	3945(22)	5627(17)	2566(15)	33(7)

A5 Crystallographic data for bis(1-phenyl-3-methyl-4,5,6,7-tetrahydroindenyl) dimethyl zirconium(IV), 3.2.

Empirical formula	C ₃₇ H ₄₇ Zr
Formula weight	582.97
Temperature	150(2) K
Wavelength	0.71073 Å
Crystal system	Triclinic
Space group	P-1
Unit cell dimensions	a = 11.446(3) Å alpha = 106.088(4)° b = 11.451(3) Å beta = 107.572(4)° c = 13.609(4) Å gamma = 103.996(3)°
Volume, Z	1527(1) Å ³ , 2
Density (calculated)	1.268 Mg/m ³
Absorption coefficient	0.383 mm ⁻¹
F(000)	618
Crystal size	0.3 x 0.24 x 0.2 mm
Theta range for data collection	1.70 to 27.48°
Limiting indices	-14<=h<=13, -14<=k<=11, -15<=l<=17
Reflections collected	10043
Independent reflections	6888 [R(int) = 0.0116]
Absorption correction	Multi-scan
Max. and min. transmission	0.93 and 0.82
Refinement method	Full-matrix least-squares on F ²
Data / restraints / parameters	6882 / 0 / 502
Goodness-of-fit on F ²	1.146
Final R indices [I>2sigma(I)]	R1 = 0.0268, wR2 = 0.0580
R indices (all data)	R1 = 0.0320, wR2 = 0.0607
Largest diff. peak and hole	0.741 and -0.379 e.Å ⁻³

Atomic coordinates ($\times 10^4$) and equivalent isotropic displacement parameters ($\text{\AA}^2 \times 10^3$) for 3.2. $U(\text{eq})$ is defined as one third of the trace of the orthogonalized U_{ij} tensor.

	x	y	z	$U(\text{eq})$
Zr(1)	2525(1)	-3121(1)	-1258(1)	20(1)
C(1)	122(2)	-3767(2)	-1616(1)	22(1)
C(2)	531(2)	-4820(2)	-1480(1)	23(1)
C(3)	1365(2)	-4446(2)	-359(1)	24(1)
C(4)	2122(2)	-2412(2)	1459(1)	29(1)
C(5)	2062(2)	-1045(2)	1764(2)	36(1)
C(6)	715(2)	-1068(2)	1097(2)	34(1)
C(7)	426(2)	-1504(2)	-154(2)	27(1)
C(8)	714(2)	-2731(2)	-540(1)	22(1)
C(9)	1484(2)	-3154(2)	218(1)	23(1)
C(11)	-850(2)	-3819(2)	-2647(1)	26(1)
C(16)	-876(2)	-2703(2)	-2872(2)	32(1)
C(15)	-1815(2)	-2783(2)	-3841(2)	41(1)
C(14)	-2735(2)	-3975(3)	-4612(2)	46(1)
C(13)	-2725(2)	-5089(2)	-4410(2)	43(1)
C(12)	-1796(2)	-5017(2)	-3436(2)	34(1)
C(10)	1940(2)	-5267(2)	183(2)	31(1)
C(34)	2955(2)	-967(2)	-892(2)	33(1)
C(33)	4351(2)	-2893(2)	142(2)	38(1)
C(17)	2433(2)	-4992(2)	-2828(1)	23(1)
C(18)	1662(2)	-4318(2)	-3303(1)	25(1)
C(19)	2503(2)	-3087(2)	-3136(1)	25(1)
C(20)	5057(2)	-1923(2)	-2305(2)	29(1)
C(21)	6281(2)	-2205(2)	-1713(2)	42(1)
C(22)	6096(2)	-3624(2)	-2172(2)	42(1)
C(23)	5006(2)	-4457(2)	-1967(2)	29(1)
C(24)	3772(2)	-4152(2)	-2374(1)	24(1)
C(25)	3808(2)	-2986(2)	-2553(1)	24(1)
C(27)	1931(2)	-6352(2)	-2921(1)	26(1)

C(32)	747(2)	-7222(2)	-3797(2)	33(1)
C(31)	245(2)	-8504(2)	-3903(2)	43(1)
C(30)	918(2)	-8952(2)	-3147(2)	44(1)
C(29)	2097(2)	-8108(2)	-2278(2)	39(1)
C(28)	2595(2)	-6821(2)	-2163(2)	31(1)
C(26)	2122(2)	-2114(2)	-3587(2)	34(1)
C(1S)	5613(9)	-2055(9)	3845(7)	106(3)
C(2S)	6117(10)	-708(9)	4686(8)	112(3)
C(3S)	5131(7)	-128(7)	4628(6)	83(2)
C(4S)	4335(8)	-1157(8)	4564(7)	100(2)
C(5S)	5330(8)	-1789(8)	4545(7)	93(2)
C(6S)	6411(9)	-1238(9)	4216(8)	99(2)

Bond lengths [Å] and angles [°] for 3.2.

Zr(1)-C(1)	2.521(2)	C(3)-C(10)	1.500(2)
Zr(1)-C(2)	2.488(2)	C(4)-C(9)	1.506(2)
Zr(1)-C(3)	2.570(2)	C(7)-C(8)	1.508(2)
Zr(1)-C(8)	2.623(2)	C(4)-C(5)	1.528(3)
Zr(1)-C(9)	2.631(2)	C(5)-C(6)	1.524(3)
Zr(1)-C(17)	2.527(2)	C(6)-C(7)	1.537(2)
Zr(1)-C(18)	2.483(2)	C(11)-C(16)	1.399(3)
Zr(1)-C(19)	2.560(2)	C(16)-C(15)	1.391(3)
Zr(1)-C(24)	2.621(2)	C(15)-C(14)	1.384(3)
Zr(1)-C(25)	2.625(2)	C(14)-C(13)	1.380(3)
Zr(1)-C(33)	2.264(2)	C(13)-C(12)	1.392(3)
Zr(1)-C(34)	2.270(2)	C(11)-C(12)	1.403(2)
C(1)-C(2)	1.432(2)	C(17)-C(18)	1.433(2)
C(2)-C(3)	1.409(2)	C(18)-C(19)	1.414(2)
C(3)-C(9)	1.420(2)	C(19)-C(25)	1.423(2)
C(8)-C(9)	1.418(2)	C(24)-C(25)	1.416(2)
C(1)-C(8)	1.435(2)	C(17)-C(24)	1.429(2)
C(1)-C(11)	1.479(2)	C(19)-C(26)	1.504(2)

Appendix A: Crystallographic Data.

C(20)-C(25)	1.509(2)	C(2)-Zr(1)-C(17)	80.79(5)
C(23)-C(24)	1.515(2)	C(1)-Zr(1)-C(17)	99.48(5)
C(17)-C(27)	1.478(2)	C(33)-Zr(1)-C(19)	122.82(6)
C(20)-C(21)	1.548(3)	C(34)-Zr(1)-C(19)	80.64(6)
C(21)-C(22)	1.505(3)	C(18)-Zr(1)-C(19)	32.52(5)
C(22)-C(23)	1.526(3)	C(2)-Zr(1)-C(19)	111.92(5)
C(27)-C(28)	1.401(3)	C(1)-Zr(1)-C(19)	102.02(5)
C(27)-C(32)	1.401(2)	C(17)-Zr(1)-C(19)	54.29(5)
C(32)-C(31)	1.389(3)	C(33)-Zr(1)-C(3)	82.85(7)
C(31)-C(30)	1.385(3)	C(34)-Zr(1)-C(3)	125.92(6)
C(30)-C(29)	1.388(3)	C(18)-Zr(1)-C(3)	110.92(5)
C(29)-C(28)	1.391(3)	C(2)-Zr(1)-C(3)	32.30(5)
C(1S)-C(2S)	1.487(12)	C(1)-Zr(1)-C(3)	54.10(5)
C(2S)-C(3S)	1.434(11)	C(17)-Zr(1)-C(3)	98.34(5)
C(3S)-C(4S)#1	1.418(10)	C(19)-Zr(1)-C(3)	143.08(5)
C(4S)-C(3S)#1	1.418(10)	C(33)-Zr(1)-C(24)	78.74(7)
C(4S)-C(5S)	1.492(10)	C(34)-Zr(1)-C(24)	114.47(6)
C(5S)-C(6S)	1.498(11)	C(18)-Zr(1)-C(24)	53.36(5)
C(33)-Zr(1)-C(34)	96.64(8)	C(2)-Zr(1)-C(24)	110.80(5)
C(33)-Zr(1)-C(18)	131.43(7)	C(1)-Zr(1)-C(24)	131.36(5)
C(34)-Zr(1)-C(18)	109.11(7)	C(17)-Zr(1)-C(24)	32.16(5)
C(33)-Zr(1)-C(2)	112.63(7)	C(19)-Zr(1)-C(24)	52.87(5)
C(34)-Zr(1)-C(2)	129.78(6)	C(3)-Zr(1)-C(24)	118.28(5)
C(18)-Zr(1)-C(2)	81.50(5)	C(33)-Zr(1)-C(8)	111.49(6)
C(33)-Zr(1)-C(1)	134.53(6)	C(34)-Zr(1)-C(8)	78.50(6)
C(34)-Zr(1)-C(1)	97.75(6)	C(18)-Zr(1)-C(8)	113.55(5)
C(18)-Zr(1)-C(1)	82.83(5)	C(2)-Zr(1)-C(8)	53.47(5)
C(2)-Zr(1)-C(1)	33.21(5)	C(1)-Zr(1)-C(8)	32.32(5)
C(33)-Zr(1)-C(17)	100.72(7)	C(17)-Zr(1)-C(8)	131.06(5)
C(34)-Zr(1)-C(17)	134.11(6)	C(19)-Zr(1)-C(8)	123.40(5)
C(18)-Zr(1)-C(17)	33.24(5)	C(3)-Zr(1)-C(8)	52.85(5)

Appendix A: Crystallographic Data.

C(24)-Zr(1)-C(8)	163.20(5)	C(2)-C(3)-C(9)	107.32(14)
C(33)-Zr(1)-C(25)	91.03(6)	C(2)-C(3)-C(10)	127.8(2)
C(34)-Zr(1)-C(25)	84.65(6)	C(9)-C(3)-C(10)	124.7(2)
C(18)-Zr(1)-C(25)	53.00(5)	C(2)-C(3)-Zr(1)	70.66(9)
C(2)-Zr(1)-C(25)	131.90(5)	C(9)-C(3)-Zr(1)	76.54(9)
C(1)-Zr(1)-C(25)	133.09(5)	C(10)-C(3)-Zr(1)	122.63(11)
C(17)-Zr(1)-C(25)	53.11(5)	C(9)-C(4)-C(5)	111.2(2)
C(19)-Zr(1)-C(25)	31.82(5)	C(6)-C(5)-C(4)	111.2(2)
C(3)-Zr(1)-C(25)	149.24(5)	C(5)-C(6)-C(7)	111.5(2)
C(24)-Zr(1)-C(25)	31.31(5)	C(8)-C(7)-C(6)	110.07(14)
C(8)-Zr(1)-C(25)	153.10(5)	C(9)-C(8)-C(1)	107.59(14)
C(33)-Zr(1)-C(9)	83.06(6)	C(9)-C(8)-C(7)	122.07(14)
C(34)-Zr(1)-C(9)	94.34(6)	C(1)-C(8)-C(7)	129.3(2)
C(18)-Zr(1)-C(9)	132.76(5)	C(9)-C(8)-Zr(1)	74.65(9)
C(2)-Zr(1)-C(9)	52.78(5)	C(1)-C(8)-Zr(1)	69.92(8)
C(1)-Zr(1)-C(9)	53.04(5)	C(7)-C(8)-Zr(1)	130.01(11)
C(17)-Zr(1)-C(9)	129.60(5)	C(8)-C(9)-C(3)	109.05(14)
C(19)-Zr(1)-C(9)	153.95(5)	C(8)-C(9)-C(4)	123.7(2)
C(3)-Zr(1)-C(9)	31.66(5)	C(3)-C(9)-C(4)	126.5(2)
C(24)-Zr(1)-C(9)	147.30(5)	C(8)-C(9)-Zr(1)	74.03(9)
C(8)-Zr(1)-C(9)	31.32(5)	C(3)-C(9)-Zr(1)	71.80(9)
C(25)-Zr(1)-C(9)	173.86(5)	C(4)-C(9)-Zr(1)	128.27(11)
C(2)-C(1)-C(8)	106.85(14)	C(16)-C(11)-C(12)	117.7(2)
C(2)-C(1)-C(11)	125.5(2)	C(16)-C(11)-C(1)	122.3(2)
C(8)-C(1)-C(11)	127.3(2)	C(12)-C(11)-C(1)	120.0(2)
C(2)-C(1)-Zr(1)	72.15(9)	C(15)-C(16)-C(11)	120.9(2)
C(8)-C(1)-Zr(1)	77.75(9)	C(14)-C(15)-C(16)	120.5(2)
C(11)-C(1)-Zr(1)	120.99(10)	C(13)-C(14)-C(15)	119.6(2)
C(3)-C(2)-C(1)	109.18(14)	C(14)-C(13)-C(12)	120.3(2)
C(3)-C(2)-Zr(1)	77.03(9)	C(13)-C(12)-C(11)	121.0(2)
C(1)-C(2)-Zr(1)	74.64(9)	C(24)-C(17)-C(18)	106.63(14)

C(24)-C(17)-C(27)	127.3(2)	C(25)-C(24)-Zr(1)	74.50(9)
C(18)-C(17)-C(27)	125.7(2)	C(17)-C(24)-Zr(1)	70.27(9)
C(24)-C(17)-Zr(1)	77.57(9)	C(23)-C(24)-Zr(1)	130.01(12)
C(18)-C(17)-Zr(1)	71.72(9)	C(24)-C(25)-C(19)	108.74(14)
C(27)-C(17)-Zr(1)	121.56(11)	C(24)-C(25)-C(20)	123.8(2)
C(19)-C(18)-C(17)	109.19(14)	C(19)-C(25)-C(20)	126.9(2)
C(19)-C(18)-Zr(1)	76.74(9)	C(24)-C(25)-Zr(1)	74.19(9)
C(17)-C(18)-Zr(1)	75.05(9)	C(19)-C(25)-Zr(1)	71.57(9)
C(18)-C(19)-C(25)	107.17(14)	C(20)-C(25)-Zr(1)	127.27(12)
C(18)-C(19)-C(26)	127.0(2)	C(28)-C(27)-C(32)	117.8(2)
C(25)-C(19)-C(26)	125.6(2)	C(28)-C(27)-C(17)	122.6(2)
C(18)-C(19)-Zr(1)	70.75(9)	C(32)-C(27)-C(17)	119.6(2)
C(25)-C(19)-Zr(1)	76.62(9)	C(31)-C(32)-C(27)	120.9(2)
C(26)-C(19)-Zr(1)	122.87(12)	C(30)-C(31)-C(32)	120.5(2)
C(25)-C(20)-C(21)	111.3(2)	C(31)-C(30)-C(29)	119.5(2)
C(22)-C(21)-C(20)	112.2(2)	C(30)-C(29)-C(28)	120.2(2)
C(21)-C(22)-C(23)	111.6(2)	C(29)-C(28)-C(27)	121.1(2)
C(24)-C(23)-C(22)	110.0(2)	C(3S)-C(2S)-C(1S)	113.2(8)
C(25)-C(24)-C(17)	108.26(14)	C(4S)#1-C(3S)-C(2S)	110.8(7)
C(25)-C(24)-C(23)	121.71(14)	C(3S)#1-C(4S)-C(5S)	113.3(7)
C(17)-C(24)-C(23)	129.0(2)	C(4S)-C(5S)-C(6S)	119.1(7)

Symmetry transformations used to generate equivalent atoms: #1 -x+1,-y,-z+1

Anisotropic displacement parameters ($\text{\AA}^2 \times 10^3$) for 3.2. The anisotropic displacement factor exponent takes the form: $-2 \pi^2 [h^2 a^{*2} U_{11} + \dots + 2 h k a^* b^* U_{12}]$

	U11	U22	U33	U23	U13	U12
Zr(1)	17(1)	22(1)	20(1)	8(1)	8(1)	6(1)
C(1)	18(1)	26(1)	24(1)	9(1)	10(1)	7(1)
C(2)	20(1)	21(1)	28(1)	7(1)	13(1)	5(1)
C(3)	22(1)	26(1)	29(1)	14(1)	14(1)	9(1)
C(4)	29(1)	34(1)	24(1)	12(1)	11(1)	10(1)
C(5)	42(1)	32(1)	25(1)	5(1)	11(1)	8(1)
C(6)	44(1)	31(1)	31(1)	8(1)	20(1)	18(1)

Appendix A: Crystallographic Data.

C(7)	28(1)	28(1)	29(1)	11(1)	13(1)	13(1)
C(8)	20(1)	24(1)	24(1)	9(1)	12(1)	8(1)
C(9)	21(1)	26(1)	24(1)	11(1)	11(1)	7(1)
C(11)	20(1)	37(1)	24(1)	9(1)	12(1)	13(1)
C(16)	27(1)	43(1)	30(1)	15(1)	13(1)	15(1)
C(15)	39(1)	66(1)	36(1)	29(1)	19(1)	30(1)
C(14)	36(1)	79(2)	25(1)	17(1)	11(1)	28(1)
C(13)	30(1)	59(1)	26(1)	1(1)	6(1)	15(1)
C(12)	26(1)	41(1)	28(1)	5(1)	9(1)	12(1)
C(10)	32(1)	34(1)	40(1)	22(1)	20(1)	16(1)
C(34)	34(1)	26(1)	37(1)	8(1)	20(1)	5(1)
C(33)	24(1)	61(1)	29(1)	19(1)	10(1)	11(1)
C(17)	20(1)	26(1)	21(1)	6(1)	9(1)	8(1)
C(18)	20(1)	33(1)	19(1)	7(1)	7(1)	10(1)
C(19)	26(1)	34(1)	22(1)	13(1)	12(1)	15(1)
C(20)	26(1)	30(1)	38(1)	17(1)	17(1)	10(1)
C(21)	24(1)	42(1)	65(1)	25(1)	21(1)	11(1)
C(22)	28(1)	51(1)	66(2)	36(1)	27(1)	22(1)
C(23)	22(1)	31(1)	38(1)	16(1)	14(1)	13(1)
C(24)	21(1)	7(1)	24(1)	9(1)	11(1)	10(1)
C(25)	23(1)	29(1)	24(1)	11(1)	13(1)	10(1)
C(27)	23(1)	25(1)	28(1)	5(1)	13(1)	7(1)
C(32)	30(1)	30(1)	29(1)	1(1)	10(1)	7(1)
C(31)	37(1)	29(1)	43(1)	-2(1)	12(1)	1(1)
C(30)	50(1)	22(1)	55(1)	7(1)	27(1)	5(1)
C(29)	44(1)	30(1)	47(1)	16(1)	23(1)	14(1)
C(28)	29(1)	27(1)	34(1)	9(1)	13(1)	8(1)
C(26)	36(1)	45(1)	34(1)	24(1)	16(1)	21(1)

Hydrogen coordinates ($\times 10^4$) and isotropic displacement parameters ($\text{\AA}^2 \times 10^3$) for 3.2.

	x	y	z	U(eq)
H(18)	715(19)	-4645(17)	-3670(15)	22(4)
H(2)	295(19)	-5630(19)	-2063(16)	28(5)
H(5B)	2723(21)	-478(20)	1620(17)	34(5)
H(7)	-477(21)	-1670(19)	-561(17)	32(5)
H(12)	-1814(20)	-5783(21)	-3306(17)	35(6)
H(20A)	5095(20)	-1074(21)	-1840(17)	36(5)
H(4B)	3028(22)	-2381(20)	1755(17)	38(6)
H(4A)	1652(19)	-2914(19)	1794(16)	29(5)
H(26B)	1212(22)	-2184(21)	-3681(18)	41(6)
H(29)	2579(22)	-8397(21)	-1755(18)	40(6)
H(5A)	2289(22)	-640(21)	2570(19)	44(6)
H(26A)	2711(23)	-1220(23)	-3086(19)	45(6)
H(30)	611(23)	-9816(24)	-3212(19)	48(6)
H(23B)	5270(19)	-4347(19)	-1177(17)	31(5)
H(16)	-240(22)	-1882(22)	-2373(18)	40(6)
H(6)	51(22)	-1655(22)	1218(18)	42(6)
H(32)	278(22)	-6928(22)	-4334(19)	43(6)
H(23A)	4810(20)	-5392(21)	-2383(17)	36(5)
H(28)	3392(21)	-6252(20)	-1545(17)	36(5)
H(14)	-3408(25)	-4021(24)	-5306(21)	56(7)
H(6B)	657(21)	-178(21)	1367(17)	39(6)
H(13)	-3379(24)	-5908(23)	-4920(20)	50(7)
H(26C)	2137(23)	-2285(22)	-4328(20)	50(7)
H(33A)	4363(25)	-2440(25)	829(22)	61(8)
H(7B)	945(21)	-793(21)	-305(17)	37(6)
H(15)	-1789(23)	-2009(23)	-3969(19)	49(7)
H(34A)	2240(24)	-712(22)	-1334(19)	49(6)
H(10A)	2782(26)	-4820(24)	710(21)	54(7)
H(31)	-530(25)	-9069(24)	-4498(20)	53(7)

Appendix A: Crystallographic Data.

H(34C)	3145(23)	-540(23)	-123(21)	51(7)
H(20B)	5056(23)	-1882(22)	-3022(20)	50(7)
H(33C)	5113(25)	-2392(24)	72(20)	55(7)
H(10C)	1983(23)	-6018(24)	-335(20)	50(7)
H(34B)	3693(23)	-588(22)	-1013(19)	45(6)
H(33B)	4476(25)	-3714(26)	151(21)	59(8)
H(10B)	1429(25)	-5591(24)	522(21)	56(7)
H(22B)	6898(22)	-3752(21)	-1837(18)	40(6)
H(21B)	7028(24)	-1680(23)	-1851(19)	50(6)
H(21A)	6511(25)	-1960(25)	-819(22)	61(8)
H(22A)	5794(26)	-3895(26)	-3069(23)	68(8)
H(1S1)	6245(28)	-2463(22)	4027(30)	159
H(1S2)	5467(59)	-2027(9)	3121(10)	159
H(1S3)	4803(33)	-2544(20)	3845(37)	159
H(2S1)	6471(10)	-723(9)	5424(8)	135
H(2S2)	6826(10)	-173(9)	4576(8)	135
H(3S1)	4768(7)	-113(7)	3891(6)	100
H(3S2)	4425(7)	-648(7)	4753(6)	100
H(4S1)	3927(8)	-1139(8)	3834(7)	120
H(4S2)	3656(8)	-1679(8)	4714(7)	120
H(5S1)	4864(8)	-2691(8)	4041(7)	112
H(5S2)	5733(8)	-1787(8)	5283(7)	112
H(6S1)	6781(40)	-1883(21)	3994(48)	149
H(6S2)	7079(29)	-492(36)	4837(17)	149
H(6S3)	6066(14)	-985(54)	3605(33)	149

Appendix B

Courses, Lectures, Colloquia and

Conferences Attended.

B1 FIRST YEAR INDUCTION COURSES:
OCTOBER 1995

The course consists of one hour lectures on the services available in the department.

1. Department Safety
2. Safety Matters
3. Electrical Appliances and Infrared Spectroscopy
4. Chromatography and Microanalysis
5. Atomic Absorption and Inorganic Analysis
6. Library Facilities
7. Mass Spectroscopy
8. Nuclear Magnetic Resonance Spectroscopy
9. Glass Blowing Techniques
10. Introduction to Computing Facilities

B2 EXAMINED LECTURE COURSES:
OCTOBER 1995 TO APRIL 1996

Three courses were attended, consisting of 6 one hour lectures followed by a written examination in each.

1. "Diffraction and Scattering Methods", Prof. J. A. K. Howard
2. "Organometallic Chemistry", Prof. D. Parker
3. "NMR Techniques", Dr. A. Kenwright

B3 RESEARCH COLLOQUIA, SEMINARS AND LECTURES
ORGANISED BY THE DEPARTMENT OF CHEMISTRY

Only lectures attended by the author are shown.

1995

October 25 Dr. D. M. Davies, University of Northumbria.

Chemical reactions in organized systems.

November 15 Dr. A. Sella, UCL, London.

Chemistry of Lanthanides with Polypyrazoylborate Ligands.

November 17 Prof. D. Bergbreiter, Texas A&M, USA.

Design of Smart Catalysts, Substrates and Surfaces from Simple Polymers.

November 29 Prof. D. Tuck, University of Windsor, Ontario, Canada.

New Indium Coordination Chemistry.

1996

January 10 Dr. B. Henderson, Waikato University, NZ.

Electrospray Mass Spectrometry – a new sporting technique.

January 17 Prof. J. W. Emsley, Southampton University.

Liquid Crystals: More than Meets the Eye.

February 12 Dr. P. Pringle, University of Bristol.

Catalytic Self-Replication of Phosphines on Platinum(0)

February 21 Dr. C. R. Pulham, University of Edinburgh.

Heavy Metal Hydrides – an exploration of the chemistry of stannanes and plumbanes.

March 6 Dr. R. Whitby, University of Southampton.

New approaches to chiral catalysts: Induction of planar and metal centred asymmetry.

October 9 Professor G. Bowmaker, University of Auckland, NZ.

Appendix B: Courses, Lectures, Colloquia and Conferences Attended.

Coordination and Materials Chemistry of the Group 11 and Group 12
Metals: Some Recent Vibrational and Solid State NMR Studies.

October 29 Prof. D. M. Knight, Department of Philosophy, University of Durham.

The Purpose of Experiment – A Look at Davy and Faraday.

October 30 Dr. P. Mountford, Nottingham University.

Recent Developments in Group IV Imido Chemistry.

December 11 Dr. C. Richards, Cardiff University.

Stereochemical Games and Metallocenes.

1997

January 16 Dr. S. Brooker, University of Otago, NZ.

Macrocycles: Exciting Yet Controlled Thiolate Coordination Chemistry.

January 22 Dr. N. Cooley, BP Chemicals, Sunbury.

Synthesis and Properties of Alternating Polyketones.

February 4 Dr. A. J. Banister, University of Durham.

From Runways to Non-metallic Metals – A New Chemistry Based on
Sulphur.

February 5 Dr. A. Haynes, University of Sheffield.

Mechanism in Homogeneous Catalytic Carbonylation.

February 18 Prof. Sir James Black, Foundation/King's College London.

My Dialogues with Medicinal Chemists.

October 15 Dr. M. Ormerod, Department of Chemistry, Keele University.

Studying catalysts in action.

October 21 Prof. A. F. Johnson, IRC, Leeds.

Reactive processing of polymers: science and technology.

Appendix B: Courses, Lectures, Colloquia and Conferences Attended.

October 22 Prof. R. J. Puddephat (RSC Endowed Lecture), University of Western Ontario.

Organoplatinum chemistry and catalysis.

October 23 Prof. M. R. Bryce, University of Durham, Inaugural Lecture.

New Tetrathiafulvalene Derivatives in Molecular, Supramolecular and Macromolecular Chemistry: controlling the electronic properties of organic solids.

October 29 Prof. B. Peacock, University of Glasgow.

Probing chirality with circular dichroism.

November 11 Prof. V. Gibson, Imperial College, London.

Metallocene polymerisation.

November 26 Prof. R. W. Richards, University of Durham, Inaugural Lecture.

A random walk in polymer science.

December 2 Dr. C. J. Ludman, University of Durham.

Explosions.

1998

January 27 Prof. R. Jordan, Department of Chemistry, University of Iowa, USA.

Cationic transition metal and main group metal alkyl complexes in olefin polymerization.

February 25 Dr. C. Jones, Swansea University.

Low coordination arsenic and antimony chemistry.

March 18 Dr. J. Evans, Oxford University.

Materials which contract on heating (from shrinking ceramics to bullet proof vests).

B4 CONFERENCES AND SYMPOSIA ATTENDED

“The Royal Society of Chemistry Anglo-Dutch Symposium”, University of Sheffield, Sheffield, September 1996.

“The Royal Society of Chemistry Scottish Dalton Meeting”, University of Edinburgh, Edinburgh, February 1997.

“North East Universities Graduate Symposium”, University of Newcastle upon Tyne, Newcastle upon Tyne, April 1997.

“The Royal Society of Chemistry Autumn Meeting and Pre-Doctoral Symposium”, University of Aberdeen, Aberdeen, September 1997. (Poster presented.)

“Universities of Scotland Inorganic Club Conference”, University of Edinburgh, Edinburgh, September 1997. (Poster presented.)

“Main Group Symposium”, University of Durham, Durham, June 1998.

